WAVE FORCES ON OSCILLATING BODIES AT SMALL FORWARD SPEED

by

Chunsheng HU

A thesis submitted for the degree of

Doctor of Philosophy

in Ocean Engineering and Naval Architecture

in the Faculty of Engineering,

University of London

Department of Mechanical Engineering

University Colloege London

1989

To my family

Abstract

A theoretical investigation is carried out to study the interactions between waves and large offshore structures at small forward speed. First order added mass, radiation damping and exciting forces as well as dynamic responses of rigid structures at small forward speed are presented. Second order mean drift forces at forward speed and low frequency wave drift damping are also presented.

An asymptotic analysis of the mean drift force on a vertical cylinder at small forward speed in long waves is first carried out. The mean drift force is obtained analytically by using a far field method, and the wave drift damping is estimated and discussed.

For arbitrary bodies, a perturbation theory on the basis of a small forward speed parameter is proposed and developed. The fluid flow around the body is solved in terms of a zero forward speed problem and a forward speed correction problem. The latter is linearly proportional to the forward speed.

A novel multipole expansion is presented for the velocity potential of zero forward speed motion. The expressions are valid for both completely submerged bodies and surface piercing bodies.

A computer program is implemented, based on the small forward speed theory. Two coupled numerical methods are utilized. Solutions of the first order dynamic motions, second order mean drift forces and wave drift damping are presented for several floating and

submerged horizontal cylinders.

It is observed that the influence of the small forward speed on the second order hydrodynamic forces is larger than that on the first order hydrodynamic forces; and that among the first order forces, the influence on the exciting forces is larger than that on the added mass and radiation damping.

CONTENTS PAGE

List of tables PAGE

List of figures PAGE

Chapter 1

INTRODUCTION

1.1 The potential theory

Waves, currents, wind and ice are the four major factors which individually and interactively contribute to the environmental loading and the motions of offshore structures. Each of the factors is of complex nature and is internally subdivided into various physical phenomena. The present work is undertaken to address some aspects of dynamic interactions among waves, currents and offshore structures.

An offshore structure may be fixed, moored, tethered, dynamically positioned, or free floating. In ambient ocean waves a fixed structure will experience continuous loading; a compliant structure will be set to oscillatory motions in addition to the loading. For design and operation an accurate knowledge of the wave forces and motions of the structure is required. To fulfil this requirement, the fluid-structure interaction problem must be solved.

The exact problem of fluid-structure interaction is governed by the Navier-Stokes equations, since the water can be regarded as a Newtonian fluid. This generally combines viscosity dominated boundary layer flow, which is localized to the body, and the non-viscous flow in the remaining fluid domain. Practical solutions of this problem in

surface waves problem are literally impossible, and this is likely to remain so for many years. Theoretical simplifications are inevitable.

According to the role played by viscosity, offshore structures may be classified into two groups in hydrodynamic analysis: small bodies and large bodies.

It has been observed and widely confirmed that when the body is small compared with the wavelength, the viscous force is significant. In this case the wave field can be regarded as unmodified by the body and the force may be expressed by Morison's equation, attributed to Morison et al. (1950). The formula contains an inertial force and a drag force, and many uncertainties remain in determining the inertial coefficient and the drag coefficient.

When the dimension of the body is comparable with the wavelength, the viscous effect is usually negligible. The modification by the body of the fluid flow must be taken into account, and the flow can be accurately described by a velocity potential function governed by the Laplace equation. These considerations give rise to wave diffraction and radiation.

The velocity potential is subject to some non-linear conditions on the surrounding boundaries. For waves of moderate amplitude a perturbation method is commonly applied, which expresses the velocity potential as a series containing the first order potential, the second order potential, ..., etc. in the wave amplitude. Each potential is solved successively with the higher

order potentials depending on the lower order potentials. Different orders of solution indicate different degree of accuracy. For steep waves, other theories are more appropriate (Sarpkaya and Isaacson 1981, Mei 1982).

There are of course cases in which neither the potential theory nor the Morison's equation alone can describe the situation accurately. This happens for bodies of intermediate size, or arbitrary size, but in particular shape, orientation, surface roughness or mode of motion. A known example is the rolling motion of large volume ships, for example shown by Takagi (1974) and Brown et al. (1983). In such circumstances the theoretical results sometimes still give satisfactory results after some empirical adjustment (Takagi 1974).

The present work is concerned with the potential flow regime. It is aimed at predicting some second order phenomena, although the first order motion must be solved first.

1.2 Slow-drift motions

Many phenomena can be predicted by the linearized potential theory. For the zero Froude number problem, the theory has been well developed over the last few decades. General computer programs for three dimensional problems are available (for example, Eatock Taylor and Zietsman 1982, Faltinsen and Michelsen 1974, Garrison 1978), and many programs have been successfully used as a reliable tool in offshore design and operations .

However, there are some important phenomena for which linear theory does not give even a first approximation for prediction.

In regular waves, a compliant structure is observed to take a particular offset equilibrium attitude, or a particular displacement, with respect to its pre-located position and the pre-located angle of the incident wave. A sea-going ship in waves experiences an added resistance above its resistance in otherwise calm water. These phenomena are of second order in wave amplitude and can be explained by the theory of second order mean drift forces.

In bichromatic or random seas, the behaviour of a large compliant structure is known to be characterised by large amplitude horizontal motions of low frequency (Verhagen and Sluijs 1970). The significant response lies well below the primary frequency of waves. The phenomenon can be explained by the excitation of the second order slowly varying drift force originating from the difference frequency component of the second order force. Since the natural frequencies of the compliant structure are low, the small drift forces of low frequency can generate large amplitude motions due to resonance. Prediction of the magnitude of the slow drift motion is one of the most important topics in practice. To achieve this, both the low frequency drift force and the damping are required.

The slowly varying drift force has been extensively studied and progress has been made in numerical computations. Due to the difficulties imposed by the inhomogeneous free surface condition for the second order potential , earlier methods neglected or partially

approximated the contribution of the second order potential, e.g. Hsu and Blenkarn (1970), Marthinsen (1983), Newman (1974), Pinkster (1980). A breakthrough is marked by the work of of Lighthill (1979) and Molin (1979). Following their idea, Eatock Taylor and Hung[ ] have shown that, by applying the Green's second identity and introducing an auxiliary first order potential, the second order time harmonic force due to the second order potential can be computed "exactly" without actually determining the second order potential. Hung (1988) has further extended the method to compute the difference frequency second order force as well as the sum frequency second order force for arbitrary bodies in bichromatic waves. Extension to random seas has been discussed by Matsui (1986).

Alternatively, based on a boundary integral formulation suggested by Wehausen and Laitone (1960) for the general inhomogeneous free surface condition problem, direct calculation of the second order potential has been reported by Kim and Yue (1989) for axisymmetrical bodies and by Chau (1988) for arbitrary bodies.

Since the slow drift motion is a resonant phenomenon, it can only be predicted if adequate knowledge is available concerning the damping. There are three main sources of damping: radiation damping, viscous damping and wave drift damping. The subject is less well understood than the slow drift force.

Wave radiation damping is due to the oscillation of the body in an idealized fluid. It is associated with the scattering of the wave energy generated by the body. From experience of the linearized potential theory it is known that this damping is negligible compared

with viscous damping as the frequency approaches zero.

Viscous damping is due to the drag force arising from skin friction and vortex shedding. It may consist of a linear term and a quadratic term in the fluid velocity, corresponding to a laminar boundary layer and a turbulent boundary layer respectively. The quadratic term often predominates, because oscillatory flow tends to form turbulent boundary layers rather than laminar boundary layers, as pointed out by Faltinsen (1986), and also evident from the experiments of Wichers et al. (1984).

The concept of the wave drift damping, or wave damping as it is sometimes called, appears to have been initially introduced by Wichers and Sluijs (1979). From their free decaying tests of large amplitude low frequency motions, Wichers et al. (1979, 1984) found that the damping in waves differs significantly from the viscous damping measured in calm water. The difference can be of the same order of magnitude as the viscous damping and must be included in predicting the slow drift motion. Their experimental results have shown that this additional damping is independent of the frequency of the slowly varying oscillation, but dependent on the wave frequency; the magnitude is proportional to the square of the wave amplitude. This additional damping is attributed to the slow drift velocity dependent wave drift force and hence termed as "wave drift damping" or "wave damping" for short.

Wichers and Sluijs (1979) suggested that, for the surge motion, the wave drift damping may be predicted by the gradient of added resistance with respect to the forward speed, having

interpreted the slow drift velocity as a "quasi-steady" forward speed. This method of gradient of added resistance is further discussed by Wichers and Huijsmans (1984) from a mathematical point of view and followed by other investigators, for example, by Hearn et al. (1987), Zhao and Faltinsen (1988). An asymptotic solution of the wave drift damping based on the principle of gradient of added resistance is presented by Eatock Taylor, Hu and Nielsen (1990) for a vertical cylinder. The principle may be expected also applicable for the sway motion. Predicting the wave drift damping is a major task of the present work.

An alternative way of describing the slow drift motion is to use multi-scale analysis. The fundamental idea of the multi-scale analysis is illustrated in the text book of Nayfeh(1973). An application is made by Triantafyllou (1982). Triantafyllou (1982) proposed using two time scales to describe the motion, arguing that the slow drift motion contains a component of high frequency and a component of low frequency. The motion is explicitly expressed as a long time scale component and a short time scale component. He further argued that the ratio of the two time scales may be assumed to be the same order of magnitude as the wave slope. It is finally concluded that the short time scale problem appears to be identical to the zero-speed first order motion, except that it is now parametrically dependent on the long time scale motion. The long time scale motion may be solved in time domain with each time step long enough such that the time average can be taken for the short time scale motion. A simple illustration for the rolling motion of a vessel is given, but no numerical implementation is made. Agnon and Mei (1985) further extended Triantafyllou's multi-scale analysis to

both time and space, arguing that the slow modulation in time is usually accompanied by slow modulation in space. They attempted to solve the slow drift motion of a two dimensional block, but there seems to be an algebraic error in their analysis. Extension to three dimensions was attempted by Zhao and Liu (1987).

1.3 Present work

The subject of this thesis is prediction of wave drift damping from the gradient of added resistance. The major task is to solve a boundary value problem for the linearized diffraction and radiation potentials at forward speed, since the forward speed dependent mean drift forces can be determined from the first order potentials. As one part of the requirement for calculating the mean drift forces, the first order responses are also to be solved. Inclusion of a nonzero forward speed in the analysis effectively means that the interactions among waves, the structure and a uniform current are examined, because the effect of a forward speed is equivalent to the presence of a uniform current in the opposite direction. However, it must be emphasised that the potential assumption excludes the viscous effect, especially the skin friction and the vortex shedding associated with waves and the current. This sometimes is a severe restriction.

A small forward speed perturbation expansion is proposed and developed for solving the boundary value problem. The fundamental idea is to assume that the velocity potential can be expressed as a series of terms of different order in the forward speed. For small

forward speed, only the zero-speed solution and the first order speed correction term which is linearly proportional to the forward speed are retained and all higher order terms are neglected. Consequently, the boundary value problem is decomposed into two boundary value problems corresponding to the zero-speed potential and the forward speed correction potential with the latter depending on the former. After a careful analysis of the behaviour of the velocity potential at large distances, it is shown that the forward speed correction potential can be expressed as an integral over the body surface plus an integral over the free surface. The expression for the zero-speed potential is rather conventional, i.e. as an integral over the body surface. An important feature of the theory is that the pulsating source potential is used as the Green function for both the zero-speed problem and the forward speed correction problem. This is different to other theories which usually use a pulsating translating source potential as the Green function. The latter is known to be far more expensive to compute. The fact that the same Green function is used for both problems also proves to be advantageous in numerical discretization, since the final matrices only need to be evaluated once for both problems.

Although the integrand of the body surface condition contains the unknown potentials, the integrand of the free surface integral (which arises for the forward speed correction term only) is simply a functional of the zero-speed potential and the steady potential, which are known because the steady motion and the zero-speed motion will be solved prior to solving the forward speed correction term. The evaluation of the free surface integral is time consuming and is a major difficulty in the present theory. For the purpose of

evaluating it efficiently, a fast converging multipole expansion is developed such that the zero-speed potential and the steady potential can be expressed analytically. Subsequently, the slowly converging oscillatory part in the free surface integral can be integrated explicitly, which improves the efficiency of the computation.

In numerical implementation a coupled technique is used. The fluid domain is divided into an inner domain and an outer domain by an artificial control surface. A boundary integral formulation is used in the inner domain with the simple Rankine source Green function. For the zero-speed potential, the inner domain expression may be either matched with a similar integral formulation (BIE-BIE) but with the pulsating source potential Green function; or matched with the multipole expansion (BIE-BMP) developed in the thesis. For the forward speed correction, only the integral-integral coupling exists (BIE-BIE). The BIE-BMP coupling is very efficient and no irregular frequencies are encountered in the computation. The BIE-BIE coupling is superior to a uncoupled boundary integral formulation, because it can locate the irregular frequencies.

The thesis is organized as follows. After this introduction a brief literature review is presented in Chapter 2. In Chapter 3, after a general discussion about the boundary value problem, an asymptotic solution of the mean drift force is presented for a vertical cylinder at small forward speed. This asymptotic analysis is carried out to enhance the understanding of the wave drift damping phenomenon, and the analytical result obtained may be used for checking more general numerical solutions. Chapter 4 is the core of the thesis, in which a small forward speed perturbation theory is

presented, together with a novel multipole expansion for the zero-speed potential. Also presented in Chapter 4 are the details of numerical implementation, particularly concerning the second derivatives and evaluation of the free surface integrals. In Chapter 5, formulations for forces and rigid body motions are re-examined with the presence of small forward speed. Numerical results are presented and discussed in Chapter 6. The last chapter lists conclusions. Although numerical implementation is mainly in two dimensions, theoretical analyses are carried out for both two dimensional and three dimensional motions.

Chapter 1

LITERATURE SURVEY

2.1 Overview

Solving the velocity potential at forward speed is not a new subject for naval architects. The history may be traced back about a century ago. However, the problem has not yet been solved for blunt bodies. Certain difficulties can be identified.

Firstly, a steady potential usually needs to be solved prior to solving the unsteady potential. This steady potential is the solution for bodies moving in steady translation through otherwise calm water. In general, the problem is nonlinear and not easy to solve.

Secondly, the free surface condition for the unsteady potential contains the disturbance of the steady potential. This violates the most commonly used boundary integral method, since the free surface condition can no longer be taken into account by a properly chosen Green function.

Thirdly, the body surface condition for the unsteady potential contains the second derivatives of the steady potential, which demands excessive accuracy in numerical computation.

Most investigations circumvented these difficulties by imposing some genuine approximations. Noticeably, the steady potential is frequently neglected completely or partially. A study of the literature reveals that theories may be loosely classified into two categories: (i) those developed for bodies of particular geometries, such as thin, slender ship theories and strip theories; and (ii) those aimed at arbitrary bodies. The words "aimed at" are used for the reason that although there are some three dimensional methods existing, most of them can not properly deal with one or more of the aforementioned difficulties; therefore they can not really be applied for arbitrary bodies, unless the difficulty is overcome.

2.2 Development of the steady motion theory

The development of the steady motion theory has been slow and unsatisfactory.

Following the pioneering work of Michell (1898) for the wave resistance on a thin ship, the progress in this area has been more or less restricted to the refinement of the thin ship theory for a long period thereafter. Notable are a series of papers by Havelock, who studied various effects of systematic variations. Those works are summarized in Havelock (1926). Even long after appearance of more practical methods, the thin ship approximation still attracts certain attention, for example by Keller and Ahluwalia (1976), because of its simplicity in mathematics, particularly, the explicit expression for the wave resistance. About fifty years after Michell's work, a generation of slender ship theories appeared, taking advantage of

the fact that ships are usually enlongated, with the beam and draft of the same small order of magnitude compared with the length. The slender ship theory was firstly introduced by Cummins (1965) and also investigated by other authors. The linearized Neumann-Kelvin free surface condition is used. For broader applications, a more general solution is required. This is usually based on numerical methods.

For deeply submerged bodies, the linearized Neumann-Kelvin problem can be solved without geometrical approximation (although the linearization itself is a significant approximation) at present. In 1967, Giesing and Smith (1967) reported successful numerical solutions for deeply submerged hydrofoils. The results are obtained from a distribution of Kelvin source over the contours of the cylinder. A similar method was used by Chang and Pien (1975), but a dipole distribution was used instead, which was found more efficient. Bai (1975) solved the problem again, using a coupled method with a finite element fomulation imposed in an inner domain and an eigen series expansion in the outer domain. There are also many other coupled methods successfully applied for this problem, for example, by Mei and Chen (1976) also using a localized finite element method, by Yeung and Bouger (1977) using a simple logarithmic Rankine source coupled with an eigen series expansion, and by Eatock Taylor and Wu (1986) using a finite element formulation coupled with a boundary integral formulation. Extension to three dimensional submerged bodies has been successfully made by Bai (1977). However, it can not be certain how deep the submergency should be, unless the nonlinear effects are examined.

For surface-piercing bodies, the progress is less advanced.

Although the linearized Neumann-Kelvin problem may be solved, the physical meaning is questionable. It has been shown that for surface-piercing bodies, nonlinear effects should be considered. Nevertheless, it is worth mentioning the analytical work by Brard (1972) for the linearized Neumann-Kelvin problem. Brard pointed out that if a singularity distribution method is used, a line distribution along the intersection of the body with the mean free surface must be included in addition to the distribution over the body surface. He also showed that, for a vertical elliptical cylinder of infinite draft at low Froude number, a significant contribution of the line integral was found, when a dipole distribution was used.

One approach for nonlinear analysis is a perturbation theory about a thin ship. The zeroth solution is taken as zero. This method has been pursued by Wehausen (1973), Guilloton(1964). Some improvements are found but not in a consistent manner, as shown by Gadd (1976).

Another approach is to perturb about the "double body" flow, as shown by Baba and Hara (1977). The theory is actually a slow-ship theory. The zeroth solution is taken to be the flow of the double body consisting of the immersed hull and its image above the mean free surface in an unbounded fluid. This is equivalent to imposing a "rigid wall" condition on the free surface. The first order solution is a surface wave potential, subjected to the free surface condition imposed on the sum of the potential and the double body flow.

Noblesse (1983) examined both approaches from a slightly

different point of view. He first imposed the nonlinear free surface condition on the undisturbed free surface and derived an integral expression for the velocity potential. Then an iterative procedure was applied to solve the integral equation. He showed that if the initial guess is taken as zero, the procedure is essentially equivalent to the perturbation about a thin ship; otherwise if the initial solution is taken to be the double body solution, the procedure is equivalent to the slow-ship perturbation. Chen and Noblesse (1983) compared different methods with experiments and showed that large discrepancies exist not only between theories and experiments, but also among theories themselves, particularly at small Froude number.

The nonlinear problem can also be approached from a free surface source distribution. Gadd (1976) presented some successful results by distributing the Rankine source over the body surface and surrounding mean free surface. However, the success can not be guaranteed due to the undesirable termination of the region of free surface panels. A similar procedure is also applied by Musker (1988), who reported that some meshes are not convergent. There are also many other methods, such as the ray theory (Keller 1979) and methods developed to investigate the bow or stern flows (Faltinsen 1983). Most of them are developed for specific problems and are not discussed here.

To summarize, theoretical predictions are still at a primitive stage for surface-piercing or shallowly submerged bodies, and further investigation is required to solve the nonlinear free surface problem. The present work, however, is not aimed at that goal.

Instead, the author is content with the double body flow approximation, because the Froude number concerned here is small and only first order terms in Froude number are required. Corrections to the double body flow approximation would consist of higher order quantities, and can be neglected for the purpose of the present work.

2.3 Development of the unsteady motion theory

The progress of the unsteady motion theory kept about the same pace as that of the steady motion theory. It is universally accepted that the beginning of the study of ship motions is marked by the work of William Froude (1861) for the rolling motion of a ship and by the work of Krylov (Kriloff) (1896) for the pitching and heaving motions. Both works neglected the disturbance due to the presence of the ship. The subsequently predicted force is known as the Froude-Krylov force nowadays. Consideration of the disturbance of body was firstly made by Michell (1898) for wave resistance of a thin ship. After that a generation of thin ship theories appeared (see Peters and Stoker 1957, Newman 1961), and followed by a more applicable generation of slender ship theories (see Ursell 1962, Newman and Tuck 1964). Some details may be found in the review of Ogilvie (1977). A restriction of those theories is that the wavelength must be long compared with the beam and draft, which proves to be a severe restriction for ships in head seas.

The difficulty due to the forward speed forced many investigators to circumvent the problem. As a result, many studies are devoted to the zero-speed motions. An important family is the

study of two dimensional flow past horizontal cylinders in beam seas, which forms a fundamental part of the strip theory developed later. This type of problem was first solved by Ursell (1949) for the heaving motion of a circular cylinder floating on the free surface. The multipole expansion method was used, which may be extended for arbitrary cross sections by combining the conformal mapping technique (Lewis 1929) or some localized numerical method (Nestegard and Sclavounos 1984). Vugts (1968) and Frank (1967) presented many results for several floating cylinders and some submerged cylinders.

In two famous papers, Haskind (1953) examined the theoretical aspects of motions at forward speed in great detail. He pointed out how the linearized ship motion can be solved by decomposing the velocity potential into a canonical form consisting of a diffraction potential and six radiation potentials for the six modes of oscillation. He also derived the fundamental solution of a pulsating translating source potential, and studied its asymptotic behaviour. A source distribution formulation for the velocity potential is presented, but the numerical implementation utilized the thin ship approximation. Another remarkable theoretical achievement is the Haskind-Hanaoka theorem, discovered by Haskind (1957) and Hanaoka (1959) independently. This theorem gives the relation between the ith component of the generalized force and the ith radiation potential. Extension to forward speed case is made by Newman (1965).

One of the most significant advances for realistic ship motions was the development of the strip theory. The fundamental idea is to assume that the fluid flow corresponding to each section of the ship is two dimensional and the interaction among different

sections is negligible. Consequently the added mass, radiation damping and the exciting forces can be expressed in terms of the two dimensional solutions. The first strip theory appears to have been presented by Korvin-Kroukovsky and Jacobs (1957). After that, there were extensive modifications and the strip theory dominated ship hydrodynamics for many years. Even today the strip theory is still a very useful tool for analysis of ship motions at forward speed.

The strip theory presented by Korvin-Kroukovsky and Jacobs is based on intuitive analysis rather than on a rigorous mathematical derivation, but surprisingly satisfactory agreement with experiments was found in many cases. A noticeable feature of this strip theory is the inconsistent way the forward speed is dealt with. This inconsistence remains in most modified ship theories, such as in some of the popular ones by Grim (1960), Gerritsma (1976) and Salvesen, et al. (1970). To overcome this inconsistence, Ogilvie and Tuck (1969) proposed a "rational strip theory" for the heave and pitch motion. They retained terms of order $\epsilon^{1/2}$, where ϵ is the slenderness of the ship. Thus they managed to formulate the theory consistently. Although the rational theory is rigorous, it is difficult to use.

Salvesen et al. (1970) reported a very popular strip theory, known as STF theory later. It is a modified version of the strip theory of Korvin- Kroukovsky and Jacobs (1957). One obvious improvement is that the STF theory satisfies the Timman-Newman (1962) relation for the cross coupling added mass and damping terms, whereas the strip theory of Korvin-Kroukovsky and Jacobs does not. Added mass, radiation damping and exciting forces are presented for all modes of motion except surge. Although STF theory is less rigorous

than the rational theory, it has become a most popular strip theory, because it is simple and gives satisfactory results.

A common feature of strip theories is that they are not valid for low frequency or for high speed. The condition $\omega >> U\partial/\partial x$ is often required. This is why most strip theories fail to give satisfactory results in following seas and quartering seas. To remove the low frequency limitation, Newman (1978) developed a unified strip theory, which is claimed valid for all frequencies. The method of matched asymptotic expansions is used. In an inner domain close to the body, the flow is described by a localized two dimensional sectional potential with an undetermined "constant", which is a function of the longitudinal coordinate. The diffraction potential in the inner domain is governed by a Helmholtz equation resulting from the factorization of the space periodicity in the longitudinal direction of the slender ship. Radiation potentials are governed by the two dimensional Laplace equation. In the outer domain the flow is described by a three dimensional potential obtained from a singularity distribution along the axis of the ship with unknown strength. The strength and the "constant" are determined by matching the two expressions in an overlap domain. The theory is applied to the radiation problem by Newman and Sclavounos (1980), and application to the diffraction problem is made by Sclavounos (1981)(1984) for zero forward speed and small forward speed. Improvement is found for the heave and pitch added mass and damping at zero forward speed, but the results at forward speed are less convincing. Further evaluation of the unified theory is necessary. It should be noted that Newman and Sclavounos (1980) assumed that the steady potential satisfies the "rigid wall" condition on the free

surface. This implies that the theory shares the common deficiency of other strip theories for high Froude number. For ship motions at high Froude number, a complementary approach is proposed by Chapman (1975) and also discussed by Ogilvie (1977).

Because the strip theory has its inherent deficiencies, above all the slender geometrical restriction, a three dimensional analysis must be persued for motions of platforms or the surge motion of conventional ships.

Chang (1977) is the first person who obtained successful numerical solutions from a three dimensional analysis. Both the steady problem and the unsteady problem are linearized. She used a source distribution which contains a body surface integral and a water line integral. The latter was recognized by Brard (1972). The disturbance of the steady potential is neglected completely in the procedure for solving the unsteady motion, but retained in the pressure force. Results of added mass and damping are presented for a Series 60 ship in all modes of motion except surge. Agreement with experiments is improved over the strip theory, but still remains unsatisfactory for pitch and roll damping coefficients. Chang suspected that the omission of steady flow in the free surface condition is responsible for the discrepancies. A similar method is also applied by Guevel and Bougis (1982).They used a source distribution and a combination of source and dipole distribution. Satisfactory results are obtained using a small number of panels. They identified irregular frequencies in the mixed distribution, but rather surprisingly no irregular frequencies are encountered in the source distribution. Bougis and Vallier (1981) also reported

satisfactory results for a tug-barge system, using a source distribution method.

A similar method is also applied by Inglis and Price (1982), who also examined the effect of the steady potential disturbance in the body surface condition, and the effect of the forward speed introduced convective term $U\partial/\partial x$ in the free surface condition. As expected, computations for a Series 60 ship showed that the influence of the steady potential disturbance in the body surface condition is insignificant, since the hull is slender. Also in agreement with expectation, the influence of the longitudinal convective term is significant at higher forward speed and lower frequencies. The influence is mostly pronounced in the heave and pitch damping coefficients. These results confirm the limitations of the strip theory that neglects the convective term under the assumption $\omega >> U\partial/\partial x$.

Hearn et al. (1987) also examined the simplified three dimensional method that neglects the longitudinal convective term. Computations for a similar tanker to that studied by Inglis and Price showed good agreement with the experiments of Pinkster (1980) over the intermediate frequency range and at small Froude number. This is consistent with the conclusions of Inglis and Price. Hearn et al. also computed the wave drift damping and obtained a good agreement with the experiments of Wichers (1982) for the same tanker. The validity of the simplified three dimensional method, however, can not be generalized to blunt bodies. Computations for a semisubmersible by Hearn and Tong (1987) showed that only a qualitative agreement with experiments is obtained for the wave drift damping. It should be

pointed out that this simplified three dimensional theory is inconsistent and therefore should not be expected to do too much.

For deeply submerged bodies, like the steady motion case, the theory enjoys a better success than its counterpart for surface-piercing bodies. For such circumstances, the free surface condition for both the steady flow and unsteady flow may be linearized. It is commonly argued that the disturbance of the steady potential in the free surface condition may be neglected as well. Under such simplifications, Grue and Palm (1985) examined the two dimensional radiation and diffraction problems for a submerged circular cylinder. A source distribution method was used. The integral equation was solved by expanding the source strength into a Fourier series and then truncating the series after a finite number of terms. Ten terms were found sufficient, if the axis of the cylinder is two or more times the radius below the free surface. Mo and Palm (1987) studied similar problems for an elliptic cylinder. The source distribution method was also used, but the integral equation was solved directly by a numerical method. For arbitrary cross-sections, Wu and Eatock Taylor (1987) presented an efficient method by coupling the finite element formulation with a boundary integral formulation, which can be regarded as a straightforward extension of the earlier work of Eatock Taylor and Zietsman (1981) for the zero speed problem. They also showed how the second derivatives of the steady potential in the body surface condition can be reduced to the first derivatives by applying an integral theorem derived by Ogilvie and Tuck (1969). Their results for a submerged circular cylinder compared very well with the semi-analytical solutions obtained by Grue and Palm (1985). Extension to deeply submerged three dimensional bodies is made by Wu

(1986). Wu and Eatock Taylor (1988) also obtained a semi-analytical solution for a deeply submerged sphere. A similar procedure to that of Grue and Palm (1985) is used, but the source strength is expanded as a series of Legendre functions instead of Fourier series, since the problem is three dimensional.

The three dimensional analyses discussed so far are for finite Froude numbers. Those analyses are very time consuming. Besides, numerical calculations for small forward speed are not well behaved, because the Green function becomes highly oscillatory as the speed approaches zero. In offshore applications, the forward speed (or current speed) is usually small. Therefore, it seems desirable to develop an efficient method under a small forward speed condition.

Huijsmans and Hermans (1985) made such an attempt. They proposed a perturbation method for small forward speed problems. A conventional source distribution formulation is used to start with. They then assumed the solution can be expanded into a series according to the forward speed. After neglecting higher order terms, they expanded the Green function as the sum of a zero-speed term and a forward speed correction term, linearly proportional to the forward speed. The expansion procedure is also applied to the source strength, the velocity potential etc. The boundary integral equation is then decomposed into a zero-speed equation and a forward speed correction equation, and solved successively. Computations were carried out for a Series 60 ship. The presented results of the heave and pitch cross coupling added mass and damping showed reasonable agreement with the results obtained from another method by Grekas (1983). More computation and comparison are necessary to evaluate the

accuracy of the theory. One point which should be mentioned here is that the expansion of the Green function is not uniformly convergent, since it is not appropriate in the far field. It therefore requires considerable care in application. In another paper, Huijsmans (1986) applied the theory to a tanker and computed the wave drift damping. Satisfactory agreement with the experiments of Wichers (1986) is found only over an intermediate frequency range. Surprisingly, at higher frequencies, the theoretical results showed different trends from the experiments. The discrepancies may be due to some manipulation error rather than the theory itself, since it appears that the mean drift force expression in Huijsmans (1986) is incomplete. The complete neglect of the steady potential should also be suspected.

A common drawback of most theories is the neglect of the disturbance of the steady potential in the free surface condition. This severely limits the their application to surface-piercing blunt bodies and also leaves many uncertainties in the predicted ship motions.

Taking into account the disturbance in the free surface condition is by no means a simple modification over the existing theories. As a matter of fact, it is the most difficult task in this area. An immediate consequence of introducing the steady potential in the free surface condition is that the most commonly used boundary integral method can no longer be applied straightforwardly, since it is impractical, if not impossible, to derive an appropriate Green function which takes into account the full free surface condition such that the integral over the free surface can be eliminated. Zhao

and Faltinsen (1988) and Zhao et al. (1988) are perhaps the only people who have taken up this challenge. In two successive papers they attacked the two dimensional and three dimensional problems separately. The forward speed (or the current speed as they referred to it) is assumed small and a double body flow approximation is made about the steady potential. A coupled numerical method is developed, as described below. The fluid domain is divided into an inner domain and an outer domain, with the inner domain being bounded by the body surface the free surface and a cylindrical control surface (or two vertical lines in two dimensions). The steady potential is included in all boundary conditions in the inner domain, but neglected in the outer domain on the free surface. In the inner domain a Rankine source distribution is used, which is then matched with a multipole expansion in the outer domain. The multipole functions used are the family of the pulsating translating source potential and its derivatives, which can be found in the review of Wehausen and Laitone (1960). The coupling procedure in their two dimensional analysis is slightly different from that in their three dimensional analysis, but the fundamental idea is the same. Both first order and second order computed results are presented for a semicircle and a hemisphere floating on the free surface. Comparison with experiments for the hemisphere is made and satisfactory agreement is found. They found that the influence of the forward speed is more important for the mean drift force than for the first order quantities. One weak point of the method is that the disturbance of the steady potential is not taken into account over the complete free surface; instead it is only included in a portion of the free surface localized to the body. The outer bound of this portion can only be determined by trial and error in practice. This implies that the boundary value problem must be

solved several times before a sensible decision is made, which inevitably increases the computing effort. Despite this shortcoming the work of Zhao and Faltinsen is still very challenging and initiated a practical approach.

Hu and Eatock Taylor (1989) proposed a small forward speed perturbation theory and presented some succesful results. With the multipole expansion developed by them, their theory has the potential to incorporate the steady flow disturbance effectively. This is discussed in this thesis.

To summarize, an accurate and efficient method for predicting motions of arbitrary bodies at forward speed in waves is not yet available. Particularly, it has not become clear how the disturbance of the steady potential in the free surface condition should be dealt with. The present work is an attempt to challenge that problem under the small forward speed condition.

Chapter 3

AN ASYMPTOTIC SOLUTION FOR A VERTICAL CYLINDER

As an introductory investigation towards the understanding of wave drift damping, an isolated vertical circular cylinder moving in long waves is considered in this chapter. Studying a vertical cylinder is not only simple, but also rewarding because it is a common member of offshore structures. Although the draft will be assumed to be infinite, the solution sheds some light on realistic cylinders of large draft, because the lower part of a cylinder does not affect the solution much due to the exponential decaying of waves.

Without losing generality, the formulation of the boundary value problem is discussed first for arbitrary bodies. This serves the purpose of the present chapter and at the same time lays a solid foundation for the whole thesis. Special attention is given to the interactions between the steady potential and the unsteady potential, particularly on the free surface. The far field formulation for the mean drift forces on arbitrary bodies at forward speed is also examined. The geometrical simplicity of the vertical cylinder is exploited only in Section 3.3.

3.1 The boundary value problem

A large body moving at a constant forward speed in waves is considered. There are some basic assumptions as listed below. The viscous effect is assumed negligible. The fluid is assumed ideal and

the flow irrotational. The body surface and the sea bed are assumed rigid and impermeable. The surface tension on the free surface is also assumed negligible. The motion of the fluid can be accurately described by a velocity potential. It is further assumed that the amplitude of motion is moderate such that a perturbation analysis is permissible. The assumptions are generally justifiable in practice for large bodies.

The mathematical formulation for the boundary value problem has been widely discussed, and can be found in the text books of Newman (1977) and Mei (1982). A perturbation analysis is applied here and a linearized boundary value problem will be ultimately derived. Strictly speaking, a non-dimensional analysis is required, but since the perturbation method is well understood in water waves, we shall generally omit the procedure of non-dimensionalization, unless where necessary. The derivation follows closely that of Newman (1978).

3.1.1 Exact formulation

Three Cartesian coordinate systems are defined:

$O_0x_0y_0z_0$: fixed in space,

Oxyz: moving in steady translation at the forward speed of the body

O'x'y'z': fixed with respect to the body.

The axes are chosen such that z_0 and z measure vertically upwards from the undisturbed free surface, whereas x_0 and x point in the direction of advance. The origin of the Oxyz coordinate system is in the body and the two coordinate systems coincide at time t=0. The

transformation between the two coordinate systems is then given by $(x,y,z) = (x_0 - Ut, y_0, z_0)$, with with U the forward speed of the body. The body-fixed coordinate system is defined such that $(x,y,z) = (x',y',z')$ in steady state equilibrium. The relation between the body-fixed coordinate system and the steady translation coordinate system will be discussed in Section 3.3. We shall also denote position vectors by $\vec{x}_0$, $\vec{x}$, $\vec{x}'$ respectively, in the three coordinate systems.

The space-fixed coordinate is the simplest in which to start physical reasoning, while the steadily moving coordinate system is the most convenient in which to solve the boundary value problem. The body-fixed coordinate system is undoubtably the best in which to describe the geometry configuration and to describe the body surface condition.

Let $\tilde{\Phi}$ denote a velocity potential. The fluid velocity is given by $\vec{V} = \vec{\nabla}\tilde{\Phi}$, where $\vec{\nabla} = \vec{i}\frac{\partial}{\partial x} + \vec{j}\frac{\partial}{\partial y} + \vec{k}\frac{\partial}{\partial z}$. The fluid pressure in a potential flow field is given by Bernoulli's equation. In the space-fixed coordinate system this is

$$P - P_a = -\rho\left(\tilde{\Phi}_t + \frac{1}{2} \vec{\nabla}\tilde{\Phi}.\vec{\nabla}\tilde{\Phi} + gz_0 \right), \qquad \text{(in } (\vec{x}_0,t) \text{ space)} \tag{3.1}$$

which is valid in the whole fluid domain. Here ρ is the fluid density, g is the gravitational acceleration, and P_a is the atmospheric pressure which is assumed constant. P_a will be taken as zero without loosing generality. From the Lorentz transformation $\frac{\partial}{\partial t}\tilde{\Phi}(\vec{x}_0,t) = (\frac{\partial}{\partial t} - U\frac{\partial}{\partial x})\tilde{\Phi}(\vec{x},t)$, the expression for Bernoulli's equation in the moving coordinate system is

$$P - P_a = -\rho\left(\tilde{\Phi}_t - U\tilde{\Phi}_x + \frac{1}{2}\vec{\nabla}\tilde{\Phi}.\vec{\nabla}\tilde{\Phi} + gz \right). \qquad \text{(in } (\vec{x},t) \text{ space)} \tag{3.2}$$

In the whole fluid domain the velocity potential is required to satisfy the Laplace equation

$$\nabla^2\tilde{\Phi} = 0. \tag{3.3}$$

There is an infinite number of solutions for this governing equation. Since for an occurring physical problem there is only one solution, appropriate boundary conditions must be imposed.

The free surface can be defined by its elevation $z_0=\eta(x_0,y_0,t)$ and on this surface there are two conditions to be satisfied

$$0 = \frac{D}{Dt}(z_0 - \eta), \qquad \text{on } z_0 = \eta \tag{3.4}$$

$$0 = -\rho\left(\tilde{\Phi}_t + \frac{1}{2}\vec{\nabla}\tilde{\Phi}.\vec{\nabla}\tilde{\Phi} + gz_0 \right), \qquad \text{on } z_0 = \eta \tag{3.5}$$

where $\frac{D}{Dt}$ is the substantial derivative: $\frac{D}{Dt} = \frac{\partial}{\partial t} + \vec{V}.\vec{\nabla}$. The first condition is the kinematic condition which requires that the fluid particles on the free surface always stay on the surface. The second is the dynamic condition which follows from the Bernoulli's equation (3.1) by taking the fluid pressure equal to the atmospheric pressure on the free surface. This implies that the viscosity and surface tension are neglected. The second condition is necessary because the free surface elevation is unknown. These two conditions can be combined into a single one

$$\tilde{\Phi}_{tt} + 2\vec{\nabla}\tilde{\Phi}.\vec{\nabla}\tilde{\Phi}_t + \frac{1}{2}\vec{\nabla}\tilde{\Phi}.\vec{\nabla}(\vec{\nabla}\tilde{\Phi}.\vec{\nabla}\tilde{\Phi}) + g\tilde{\Phi}_{z_0} = 0, \qquad \text{on } z_0 = \eta. \tag{3.6}$$

This is obtained by carrying out the substantial differentiation and eliminating the explicit appearance of η. The penalty for eliminating

one variable is the increase of the order of the differentiation by one.

The boundary condition on the submerged portion of an impermeable body surface is

$$\frac{\partial\tilde{\Phi}}{\partial n} = \vec{V}_S.\vec{n}, \qquad \text{on } S_0. \tag{3.7}$$

Here S_0 is the instantaneous body surface; $\vec{V}_S$ is the local velocity of S_0 and $\vec{n}$ is the unit normal vector, pointing out of the fluid. The direction of the normal vector is a matter of choice. It is always defined out of the fluid domain throughout this thesis unless otherwise redefined. The condition is not as simple as it appears. For bodies which are allowed to respond to fluid loading, the surface S_0 usually changes with time and is unknown before the fluid flow and the body motion are solved.

The boundary condition on the sea bed follows the same principle for the body surface, but is much simpler. Because the sea bed is fixed, the impermeable condition is

$$\frac{\partial\tilde{\Phi}}{\partial n} = 0, \qquad \text{on } z = -h, \tag{3.8}$$

for finite water depth, where h is the water depth; or

$$\nabla\tilde{\Phi} \to 0, \qquad \text{on } z \to -\infty. \tag{3.9}$$

for infinite water depth. To complete the formulation an appropriate condition must be imposed at large distances, which will be discussed later.

The formulations are exact within the framework of potential flow and neglect of surface tension. The exact formulation is hardly solvable because of the non-linearity. Simplification must be made in practice. Linearized formulations of the steady and unsteady problems are given below.

3.1.2 Steady potential

To describe the motion of a body at forward speed in waves, the waves generated by the motion of the body in otherwise calm water should be understood first. In the simplest case of steady translation, the fluid motion would be of steady state with respect to an observer on the body. The steady motion alone is also of great interest to classical ship hydrodynamics, since it is associated with the wave resistance and lift of ships.

Let $U\bar{\phi}$ denote the steady velocity potential due to the disturbance of the body, and let the relative velocity of the fluid be denoted by $\vec{W} = U\vec{\nabla}(\bar{\phi}-x)$. Then the pressure in the steady flow field is given by

$$\bar{P} - P_a = -\rho \left[\frac{1}{2}(\vec{W}.\vec{W} - U^2) + gz \right]. \tag{3.10}$$

The steady free surface elevation is obtained in an implicit form of

$$\bar{\eta} = -\frac{1}{2g}(\vec{W}.\vec{W} - U^2)\Big|_{z=\bar{\eta}} . \tag{3.11}$$

The boundary condition imposed on the free surface is

$$\frac{1}{2}\vec{W}.\vec{\nabla}(\vec{W}.\vec{W}) + gU\bar{\phi}_z = 0, \qquad \text{on } z=\bar{\eta}. \tag{3.12}$$

This condition is fully nonlinear and imposed on a unknown surface. The difficulty of dealing with this condition is so enormous that almost all investigators took a simplified condition

$$U^2\bar{\phi}_{xx} + g\bar{\phi}_z = 0 , \qquad \text{on } z=0, \tag{3.13}$$

with

$$\bar{\eta} = \frac{U^2}{g}\bar{\phi}_x\Big|_{z=0}. \tag{3.14}$$

Equation (3.13) is obtained from the linearization of the exact condition, based on the assumption that the steady potential and its derivatives are small. It is usually argued that this assumption holds for slender bodies in longitudinal translation, and for deeply submerged bodies of arbitrary configurations. Since little is known about the consequences of neglecting the nonlinear terms, the question regarding how slender, or how deeply submerged, a body should be still remains to be answered. Besides, even for a slender surface piercing body, if the body has an appreciable forward speed, the validity of the linearized condition is doubtable at the bow and stern.

At small forward speed a different simplification may be made. It is known that the wavelength is inversely proportional to the forward speed. As the forward speed tends to zero, the wavelength becomes infinitesimally small. Because the surface elevation is proportional to the square of the forward speed, the amplitude of the steady waves also becomes very small. The free surface profile

can be approximated by the undisturbed free surface. Therefore, the free surface condition can be replaced by the "rigid wall" condition.

Taking into account the body surface condition, it can be shown that at small forward speed, the steady potential satisfies the following linear boundary conditions up to the order $O(F_n)$

$$\nabla^2\bar{\phi} = 0, \qquad \text{in fluid domain,} \tag{3.15}$$

$$\bar{\phi}_z = 0, \qquad \text{on } z=0, \tag{3.16}$$

$$\vec{W}.\vec{n} = 0, \qquad \text{on } S_B, \tag{3.17}$$

Here, F_n is the Froude number, defined by $F_n=U/\sqrt{gL}$ with L the characteristic length of the body. S_B is the mean body surface.

At the sea bed, an impermeable condition is imposed. To complete the formulation, it is also necessary to impose an appropriate condition at infinity. Otherwise, there would be more than one possible solution. For the small forward speed approximation, where the "rigid wall" condition is used, it is sufficient to specify that the disturbance due to the body is zero at infinity. For finite values of Froude number, the condition at infinity may be stated in terms of the velocity being zero far ahead of the body, and bounded far behind.

The potential subject to the "rigid wall" free surface condition is called the "double-body potential", because the solution actually represents the motion of a double-body that consists of the submerged portion of the prototype and its image above the mean free surface in an unbounded fluid. This double-body

solution will be used in our small forward speed theory.

3.1.3 Unsteady potential

Consider a body moving in ambient waves at a constant average forward speed, while oscillating about its mean position. The total velocity potential may be decomposed into two parts

$$\tilde{\Phi}(\vec{x}_0,t) = U\bar{\phi}(\vec{x}) + \Phi(\vec{x},t), \tag{3.18}$$

where the first term is the steady disturbance potential as defined before; the second term is the unsteady potential which includes the interaction between the body and the ambient waves, and also includes the interaction between the steady potential and ambient waves in general. This decomposition is customary. The pressure is given by

$$P = -\rho \left[\frac{1}{2}(\vec{W}.\vec{W} - U^2) + \Phi_t + \vec{W}.\vec{\nabla}\Phi + \frac{1}{2}\vec{\nabla}\Phi.\vec{\nabla}\Phi + gz \right]. \tag{3.19}$$

The perturbation analysis for the unsteady motion can be carried out on the basis of a small parameter ϵ. This parameter may be interpreted as the wave slope, i.e the ratio of the wave amplitude to the wavelength. However, its precise definition is not crucial because ϵ will be absorbed into the physical quantities in the final formulations. The basic assumptions are that the unsteady potential and its derivatives are small; and that the displacement and the rotation angle of the body are also small. The magnitudes of these quantities are assumed of order $O(\epsilon)$. Accordingly, the unsteady potential is of order O(1) as can be seen from the body surface condition.

From a Stokes' expansion, all quantities can be expressed in the following form

$$\begin{aligned}
\Phi &= \epsilon\Phi^{(1)} + \epsilon^2\Phi^{(2)} + \ldots, \\
\eta &= \eta^{(0)} + \epsilon\eta^{(1)} + \epsilon^2\eta^{(2)} + \ldots, \\
P &= P^{(0)} + \epsilon P^{(1)} + \epsilon^2 P^{(2)} + \ldots, \\
\vec{\alpha} &= \epsilon\vec{\alpha}^{(1)} + \epsilon^2\vec{\alpha}^{(2)} + \ldots, \\
\vec{n} &= \vec{n}^{(0)} + \epsilon\vec{n}^{(1)} + \epsilon^2\vec{n}^{(2)} + \ldots, \text{ etc.}
\end{aligned} \tag{3.20}$$

Substituting these equations into the governing equations and boundary conditions, and ordering with respect to ϵ, we obtain a series of boundary value formulations for the first order potential $\Phi^{(1)}$, second order potential $\Phi^{(2)}$, etc. Quantities at the instantaneous position will also be expanded to their mean position. For example, the potential on the free surface η is expressed in the following Taylor series

$$\Phi\Big|_{z=\eta} = \Phi\Big|_{z=\bar{\eta}} + (\eta-\bar{\eta})\frac{\partial\Phi}{\partial z}\Big|_{z=\bar{\eta}} + \ldots.$$

The leading term of those omitted is of order $O(\epsilon^3)$.

Because for the purposes of the present work the first order solution is sufficient, we shall generally neglect higher order potentials and the superscript "(1)" for the first order potential will also be omitted.

3.1.3.1 Free surface condition

The exact free surface condition (3.6) is now written in the form of

$$\frac{1}{2}\vec{W}.\vec{\nabla}(\vec{W}.\vec{W}) + gU\bar{\phi}_z$$

$$+ \Phi_{tt} + 2\vec{W}.\vec{\nabla}\Phi_t + g\Phi_z + \vec{W}.\vec{\nabla}(\vec{W}.\vec{\nabla}\Phi) + \frac{1}{2}\vec{\nabla}\Phi.\vec{\nabla}(\vec{W}.\vec{W})$$

$$+ 2\vec{\nabla}\Phi.\vec{\nabla}\Phi_t + \vec{\nabla}\Phi.\vec{\nabla}(\vec{W}.\vec{\nabla}\Phi) + \frac{1}{2}\vec{W}.\vec{\nabla}(\vec{\nabla}\Phi.\vec{\nabla}\Phi) + \frac{1}{2}\vec{\nabla}\Phi.\vec{\nabla}(\vec{\nabla}\Phi.\vec{\nabla}\Phi) = 0, \quad \text{on } z=\eta. \tag{3.21}$$

After linearization with respect to ϵ the free surface condition for the unsteady potential is

$$\Phi_{tt} + 2\vec{W}.\vec{\nabla}\Phi_t + g\Phi_z + \vec{W}.\vec{\nabla}(\vec{W}.\vec{\nabla}\Phi) + \frac{1}{2}\vec{\nabla}\Phi.\vec{\nabla}(\vec{W}.\vec{W})$$

$$- \frac{1}{g}(\Phi_t+\vec{W}.\vec{\nabla}\Phi)[\frac{1}{2}\frac{\partial}{\partial z}(\vec{W}.\vec{\nabla}(\vec{W}.\vec{W}))+gU\bar{\phi}_{zz}]/[1+\frac{1}{2g}\frac{\partial}{\partial z}(\vec{W}.\vec{W})] = 0, \quad \text{on } z=\bar{\eta}, \tag{3.22}$$

where $\Phi = \Phi^{(1)}$, and the superscript has been omitted for convenience. The steady flow condition (3.12) has been subtracted in the above equation. Up to first order of ϵ, the free surface elevation is given by

$$\eta = \bar{\eta} - \frac{1}{g}(\Phi_t + \vec{W}.\vec{\nabla}\Phi)/[1 + \frac{1}{2g}\frac{\partial}{\partial z}(\vec{W}.\vec{W})] \Big|_{z=\bar{\eta}}. \tag{3.23}$$

The unsteady quantities are of order $O(\epsilon)$ and it is understood that the subscript referring the order of magnitude is omitted for simplicity. The errors due to this approximation are of order $O(\epsilon^2)$. Equation (3.22) agrees with the equation (3.23) of Newman (1978). The boundary condition now is imposed on the mean free surface.

A major difficulty is caused by the steady flow in the free

surface condition. Further simplifications lead to diverse theories of marine hydrodynamics, based on different assumptions and arguments. However, despite the efforts of scientists and engineers for decades, the problem still remains unsolved for blunt surface piercing bodies.

For slender bodies or deeply submerged bodies, it is commonly argued that the steady disturbance potential $\bar{\phi}$ and its derivatives are small. The steady flow is therefore negligible in the free surface condition. Equation (3.22) reduces to

$$\Phi_{tt} - 2U\Phi_{xt} + g\Phi_z + U^2\Phi_{xx} = 0, \qquad \text{on } z=0. \tag{3.24}$$

This condition is almost exclusively used in marine hydrodynamics. It is clear that the omission of the steady flow is often inconsistent from a mathematical point of view; and numerical results are not completely satisfactory, as can be noted from the literature. A glance at sea-going ships suggests that at an appreciable forward speed the steady flow at the bow and stern are by no means negligible, even for slender bodies. However, because including the steady potential in the free surface condition complicates the problem to a formidable extent, the condition (3.24) is usually used regardless.

The linearized condition (3.24) is sometimes used in the far field, based on the argument that the steady waves will become negligible. This is not a strong argument, because it is not clear whether the steady waves decay faster than the unsteady waves in the far field. In particular, in two dimensional problems neither wave would decay at all.

At small forward speed, a sensible simplification can be pursued by neglecting terms of order $O(F_n^2)$ and higher. Up to order $O(F_n)$, we obtain

$$\Phi_{tt} + 2\vec{W}.\vec{\nabla}\Phi_t + g\Phi_z - U\Phi_t\tilde{\phi}_{zz} = 0, \qquad \text{on } z=0, \tag{3.25}$$

with

$$\eta \simeq -\frac{1}{g}(\Phi_t + \vec{W}.\vec{\nabla}\Phi)\Big|_{z=0}. \tag{3.26}$$

We may recall that up to this degree of accuracy, the counterpart of the free surface condition for the steady waves degenerates to the "rigid wall" condition. The steady potential is replaced by a solution in an unbounded fluid. In this case, we are sure that the steady flow is negligible in equation (3.25) in the far field due to the rapid decay of the steady disturbance in an unbounded fluid. Hence, in the far field

$$\Phi_{tt} - 2U\Phi_{xt} + g\Phi_z = 0, \qquad \text{on } z=0. \tag{3.27}$$

The small forward speed approximations will be used in the present study.

3.1.3.2 Body surface condition

Let a vector be denoted by a column matrix $\vec{a} = (a_1, a_2, a_3)^T$, where T denotes the transpose of a matrix, and make the following definitions:

$\vec{x} = (x, y, z)^T$: the position vector in Oxyz system;

$\vec{x}' = (x', y', z')^T$: the position vector in O'x'y'z' system;

$\vec{\xi} = (\xi_1,\xi_2,\xi_3)^T$: the displacement between O' and O;

$\vec{\Omega} = (\Omega_1,\Omega_2,\Omega_3)^T$

$= (\xi_4,\xi_5,\xi_6)^T$: the rotation angles of the body in Oxyz;

$\vec{n} = (n_1,n_2,n_3)^T$: the unit normal vector, pointing out of the fluid;

$\vec{x}x\vec{n} = (n_4,n_5,n_6)^T$: the generalised unit normal vector for rotations;

It can be shown that for small amplitude motion, the coordinate transformation is given by

$$\vec{x} = \vec{x}' + \vec{\xi} + \vec{\Omega}x\vec{x}', \tag{3.28}$$

$$\vec{n} = \vec{n}' + \vec{\Omega}x\vec{n}', \tag{3.29}$$

$$\vec{x}x\vec{n} = \vec{x}'x\vec{n}' + \vec{\xi}x\vec{n}' + \vec{\Omega}x(\vec{x}'x\vec{n}'), \tag{3.30}$$

up to the first order. Since the primed column vectors are time dependent, and in magnitude equal their corresponding counterparts at the mean position, we may omit the prime and reinterpret these vectors as evaluated on the mean body surface. In deriving the body surface conditions, some vector identies in Appendix A are found to be useful.

Let $\vec{\alpha}$ denote the displacement of the body surface S_0 from the mean body surface S_B, then: $\vec{\alpha} = (\vec{\xi}+\vec{\Omega}x\vec{x})_{S_B} + O(\epsilon^2)$. The velocity of the body is decomposed into $\vec{V} = U\vec{i} + \dot{\vec{\alpha}}$, where an overdot denotes time differentiation in the steadily moving coordinate system. The body surface condition is given by

$$\vec{\nabla}(\Phi + U\bar{\phi}).\vec{n} = \dot{\vec{\alpha}}.\vec{n} + \vec{U}.\vec{n}, \qquad \text{on } S_0, \tag{3.31}$$

or

$$\Phi_n = \dot{\vec{\alpha}}.\vec{n} - \vec{W}.\vec{n}, \qquad \text{on } S_0. \tag{3.32}$$

The last term is not zero, since it is evaluated on the instantaneous body surface.

From a Taylor series expansion, together with equation (3.29), it follows that

$$(\vec{W}.\vec{n})_{S_0} = (\vec{W} + \vec{\alpha}.\vec{\nabla}\vec{W})_{S_B}.(\vec{n} + \vec{\Omega}x\vec{n})_{S_B} + O(\epsilon^2)$$

$$- \vec{\xi}.(\vec{n}.\vec{\nabla}\vec{W})_{S_B} + \vec{\Omega}.[\vec{n}.\vec{\nabla}(\vec{x}x\vec{W})]_{S_B} + O(\epsilon^2). \tag{3.33}$$

Some vector identities have been used, including: $\vec{n}x(\vec{\nabla}x\vec{W}) = \vec{\nabla}\vec{W}.\vec{n} - \vec{n}.\vec{\nabla}\vec{W}$, and $\vec{\nabla}x\vec{W} = 0$. The body surface condition is obtained as

$$\Phi_n \simeq \dot{\vec{\xi}}.\vec{n} + \dot{\vec{\Omega}}.(\vec{x}x\vec{n}) - \vec{\xi}.(\vec{n}.\vec{\nabla}\vec{W}) - \vec{\Omega}.[\vec{n}.\vec{\nabla}(\vec{x}x\vec{W})], \qquad \text{on } S_B. \tag{3.34}$$

This is identical to the expression obtained by Newman (1978). In obtaining equation (3.34), it has been assumed that $\vec{W}$ and its first derivatives are bounded, which implies that the body surface is smooth.

3.1.3.3 Decomposition of the unsteady potential

Within the linearized framework, the motions of the body excited by a regular (sinusoidal) wave train will be sinusoidal too. Due to the steady translating motion, the incident wave arrives at

the body at a frequency of encounter. As a result, the body will oscillate at the frequency of encounter rather than at the wave frequency. The relation between the frequency of encounter ω and the wave frequency ω_0 is given by

$$\omega = |\omega_0 - Uk_0\cos\beta|. \tag{3.35}$$

where β is the angle of attack, i.e. the angle between the direction of incidence and the direction of the x-axis; k_0 is the wave number. ω_0 and k_0 satisfy the dispersive relation, i.e.

$$\omega_0^2 = gk_0, \tag{3.36}$$

for infinite water, or

$$\omega_0^2 = gk_0\tanh(k_0h), \tag{3.37}$$

for finite water, where h is the water depth. The frequency of encounter is reduced in following seas (β=0), whereas it is increased in head seas (β=π).

Let the translations and the rotations of the body be denoted by

$$\vec{\xi} = \mathrm{Re}[(\xi_1,\xi_2,\xi_3)e^{i\omega t}], \quad \vec{\Omega} = \mathrm{Re}[(\xi_4,\xi_5,\xi_6)e^{i\omega t}], \tag{3.38}$$

where ξ_i (i=1,2,..,6) are the complex amplitudes of the motions of the body. Then, the unsteady velocity potential can be decomposed into

$$\Phi = \mathrm{Re}\{[A(\phi_0 + \phi_7) + i\omega \sum_{j=1}^{6} \xi_j\phi_j]e^{i\omega t}\}, \tag{3.39}$$

where

$$\phi_0 = \frac{ig}{\omega_0} e^{k_0 z - ik_0(x\cos\beta + y\sin\beta)} . \tag{3.40}$$

A is the amplitude of the incident wave. ϕ_0 is the complex incident potential of unit amplitude; ϕ_7 is the diffraction potential due to the incidence of ϕ_0; and ϕ_j (j=1,2,...,6) are radiation potentials due to the forced oscillation of the body in the six modes of motion, corresponding to unit amplitude in the velocity.

From equations (3.34) and (3.39), the body surface condition can be written as follows

$$\frac{\partial \phi_7}{\partial n} = -\frac{\partial \phi_0}{\partial n}, \qquad \text{on } S_B, \tag{3.41}$$

$$\frac{\partial \phi_j}{\partial n} = n_j + \frac{U}{i\omega} m_j, \qquad \text{on } S_B, \qquad (j=1,2,\ldots,6) \tag{3.42}$$

where

$$U(m_1, m_2, m_3) = -(\vec{n}.\vec{\nabla})\vec{W}, \tag{3.43}$$

$$U(m_4, m_5, m_6) = -(\vec{n}.\vec{\nabla})(\vec{x}x\vec{W}). \tag{3.44}$$

These equations are essentially identical to those given by Newman (1978), except that the radiation potentials now are defined corresponding to unit velocity rather than unit displacement. The free surface condition (3.25) becomes

$$-\omega^2\phi + 2i\omega\vec{W}.\vec{\nabla}\phi + g\phi_z - i\omega U\phi\phi_{zz} = 0, \qquad \text{on } z=0. \tag{3.45}$$

Each of the six radiation potentials satisfies this free surface condition, whereas the diffraction potential does not. Instead, the sum $\phi_0+\phi_7$ satisfies this condition, because the incident potential

satisfies condition (3.24). All potentials satisfy the impermeable condition (3.8) at the sea bed or its asymptote (3.9) at great depth.

3.1.3.4 Discussion of uniqueness

The solution will not be unique if a proper condition is not imposed at infinity.

An unbounded ocean in the horizontal directions is an idealization of the real ocean. It is based on the argument that for a ship or a structure far away from the shore the effect of the coast is negligible. Mathematically, this simplifies a boundary value problem over a very large multi-connected domain into an exterior boundary value problem.

There are some mathematical ambiguities about what condition should be imposed at infinity. Obviously, the disturbance must be bounded (in a two dimensional problem) or tend to zero (in a three dimensional problem) at infinity. For initial value problems of transient waves, this condition appears to be sufficient. However, for steady-state oscillations this condition is not sufficient. A stronger condition is necessary. It is widely accepted that this condition may be generally stated as: at infinity the scattered waves due to disturbance by a body must propagate away from the body. This condition is called the radiation condition.

To find out the mathematical expressions for the radiation potential, it is usual to study the far field behaviour of a

fundamental solution first. A fundamental solution is often defined as the potential of a source, which may be pulsating, translating or both. Two approaches may be used. First, the steady-state oscillation problem may be taken as the limit of an initial value problem at $t \to +\infty$. The second approach is to consider the steady-state oscillation directly by introducing a small artificial viscosity in the momentum equation. Then, in the final expression the viscosity, often called Rayleigh viscosity, is made zero. Because the far field flow is not sensitive to the geometrical details, the behaviour of the disturbance potential of a body must be similar to that of a source in a similar motion.

For zero forward speed problems, it is widely accepted that a Sommerfeld type radiation condition is appropriate, which may be written as follows

$$\frac{\partial \phi}{\partial x} + ik_0\phi \to 0 \qquad \text{as} \quad x \to +\infty, \tag{3.46}$$

$$\frac{\partial \phi}{\partial x} - ik_0\phi \to 0 \qquad \text{as} \quad x \to -\infty, \tag{3.47}$$

for two dimensional problems; and

$$\sqrt{k_0 R}\left(\frac{\partial \phi}{\partial R} + ik_0\phi\right) \to 0 \qquad \text{as} \quad R \to +\infty, \qquad \left(R = \sqrt{x^2+y^2}\right) \tag{3.48}$$

for three dimensional problems.

For non-zero forward speed problems, however, the flow pattern is very complicated. Explicit expressions for the radiation condition can not be given in general. Due to the effect of the forward speed there is more than one scattered wave. Each of them travels at a different speed and direction. The value of the parameter $\tau = U\omega/g$ is

crucial in determining the wave patterns. In more detail, for supercritical motions, that is $\tau>1/4$, there are two waves. Both are located downstream. For subcritical waves, that is $\tau<1/4$, there are four waves, one being upstream and three downstream. One of these downstream waves has a phase velocity larger than the forward speed of the body, but its group velocity is smaller than the forward speed. Therefore, this wave is also located downstream.

At very low speed, as shown in Appendix B, the wavelengths of the two short waves downstream tend to be infinitesimal. Because their amplitudes depend on exponential decaying factors of the wave numbers, these two waves can be neglected. Following the asymptotic expressions given by Haskind (1953, 1954) in two separate papers for two dimensional problems and three dimensional problems respectively (N.B. Haskind's three dimensional asymptotic expression has an error, as shown in Appendix B), it can be derived in a straightforward way that, up to order of $O(\tau)$, the radiation condition can be written as follows

$$\frac{\partial\phi}{\partial x} + ik(1+2\tau)\phi \to 0 \qquad \text{as} \quad x \to +\infty, \tag{3.49}$$

$$\frac{\partial\phi}{\partial x} - ik(1-2\tau)\phi \to 0 \qquad \text{as} \quad x \to -\infty, \tag{3.50}$$

for two dimensional problems; and

$$\sqrt{kR}\ [\frac{\partial\phi}{\partial R} + ik(1+2\tau\cos\theta)\phi] \to 0 \qquad \text{as} \quad R \to +\infty, \quad (R=\sqrt{x^2+y^2}) \tag{3.51}$$

for three dimensional problems; where $k=\omega^2/g$.

The radiation condition is often not used explicitly in boundary integral methods. It is automatically satisfied due to the

properly chosen Green function. Other methods may require the explicit expressions of the radiation condition.

Because the radiation condition at infinity is somewhat artificial, a strict mathematical proof for the uniqueness of the prescribed boundary value problem should be provided. Apparently, this is not an easy task, and for a general problem a proof is not yet available. For the zero-speed problem, some special cases have been considered by John (1949, 1950) and Simons and Ursell (1984).

3.2 Far field formulation of mean drift forces

The time average component of the second order force and moment, or the mean drift force as commonly called, can be computed from the first order potential only. Some far field methods have been developed for computing at least some components of the mean drift force without necessarily integrating the pressure over the body surface.

In 1959, Newman (1959) derived expressions for the two horizontal components of the mean drift force from the energy conservation. At about the same time, Maruo (1960) derived the same expressions from a consideration of conservation of momentum. Later, Newman (1967) extended Maruo's procedure to include the vertical component of the mean drift moment, i.e. yaw moment. These expressions are given in terms of integrals over a control surface at infinity, thus called far field formulations. These far field formulations are tremendous simplifications, since both the behaviour

of the potential and the integration domain are much simpler than their counterparts in the near field. Ogilvie (1983) has given further consideration to this approach and expressed the formulae in a convenient way for computation.

The works described above are developed for zero forward speed motion. In extending this approach to the forward speed problem, care should be given to the disturbance of the steady potential. It is necessary to re-examine the formulae in a systematic manner.

3.2.1 Momentum conservation

In the space-fixed coordinate system, let us define a large fluid volume Ω enclosed by a surface S which consists of

S_0: the instantaneous wetted body surface,

S_C: a vertical cylindrical surface of large distances;

S_D: a horizontal closure surface at great depth,

S_F: the part of the free surface bounded by S_0 and S_C.

The surface S_C is chosen in such a way that it encloses the body and moves with the same steady velocity of the moving coordinate system. The normal velocity of the surface S is denoted by U_n, with the positive direction defined out of the fluid.

We consider the linear and angular momentum of the fluid with respect to an observer in the space-fixed coordinate system. (The alternative is to consider the momentum relative to an observer in the steadily moving coordinate system.) Let the fluid velocity be

denoted by $\vec{V}$. Then $\vec{V} = U\vec{V}\vec{\phi} + V\vec{\Phi}$. Furthermore, the angular momentum is taken with respect to the origin of the Oxyz coordinate system. Such defined linear and momentum can be written in the form of

$$\vec{I} = \rho \int_{\Omega} \vec{V} \, dS, \qquad \vec{L} = \rho \int_{\Omega} \vec{x}\vec{x}\vec{V} \, dS. \tag{3.52}$$

As derived in Appendix C the rate of change of the linear and angular momentum can be expressed in the form of

$$\frac{d\vec{I}}{dt} = -\rho \oint_{S} [\vec{V}(V_n - U_n) + (\frac{P}{\rho} + gz)\vec{n}] \, dS, \tag{3.53}$$

$$\frac{d\vec{L}}{dt} = -\rho\vec{U}x \int_{\Omega} \vec{V} \, dS - \rho \oint_{S} [(\vec{x}\vec{x}\vec{V})(V_n - U_n) + (\vec{x}\vec{x}\vec{n})(\frac{P}{\rho} + gz)] \, dS, \tag{3.54}$$

where the time derivatives are taken with respect to an observer in the fixed coordinate system $O_0x_0y_0z_0$. For convenience let us define the generalized velocity and the generalized momentum:

$$(V_1,V_2,V_3)=\vec{V}, \quad (V_4,V_5,V_6)=\vec{x}\vec{x}\vec{V}; \tag{3.55}$$

$$(v_1,v_2,v_3)=\vec{V}\Phi, \quad (v_4,v_5,v_6)=\vec{x}\vec{x}\vec{V}\Phi; \tag{3.56}$$

$$(\bar{v}_1,\bar{v}_2,\bar{v}_3)=U\vec{V}\bar{\phi}, \quad (\bar{v}_4,\bar{v}_5,\bar{v}_6)=\vec{x}\vec{x}U\vec{V}\bar{\phi}; \tag{3.57}$$

$$(I_1,I_2,I_3)=\vec{I}, \quad (I_4,I_5,I_6)=\vec{L}. \tag{3.58}$$

From these definitions together with the generalized normal defined in Section 3.1.3.2, we may write the the horizontal components for the linear momentum and the vertical component for the angular momentum in the form of

$$\frac{dI_i}{dt} = -\oint_S [\ \rho V_i(V_n-U_n) + Pn_i\ ]\ dS + \begin{cases} 0, & (i=1,2) \\ -\rho U\int_\Omega V_2\ d\Omega. & (i=6) \end{cases} \tag{3.59}$$

The ρgz dependent terms disappear because they do not contribute to the components concerned. The expressions can be simplified by utilizing the boundary conditions. On the horizontal closure S_D: $U_n=0$, $n_1=n_2=n_6=0$. For bodies localized to the free surface, the fluid velocity is also zero on S_D. If the body is an infinitely long vertical cylinder, the fluid motion at great depth reduces to a two dimensional flow in horizontal planes. The vertical component of the velocity is therefore also zero. Hence, there is no contribution from S_D. On the free surface S_F, since the normal velocity of the fluid is equal to that of the surface, i.e. $V_n = U_n$, and the fluid pressure on the free surface is zero, the integral on S_F does not contribute. Only the integral over the body surface and that on the control surface contribute. Further, noticing that $V_n=U_n$ on S_B and the integration of the fluid pressure over the body surface is just the desired force or moment, we finally obtain,

$$F_i = -\int_{S_C} [\ \rho V_i(V_n-U_n) + Pn_i\ ]\ dS - \frac{dI_i}{dt} + \begin{cases} 0, & (i=1,2) \\ -\rho U\int_\Omega V_2\ d\Omega. & (i=6) \end{cases} \tag{3.60}$$

The mean drift force and mean drift moment in a regular wave system can be obtained from the time average of the expressions. Since the whole motion is composed of a periodical oscillation superimposed on a steady motion, the momentum is also periodical. Thus their time derivatives are zero-mean periodical. Denote the time average by a superbar, then

$$\bar{F}_i = -\overline{\int_{S_C} [\ \rho V_i(V_n - U_n) + Pn_i\ ]\, dS} + \begin{cases} 0, & (i=1,2) \\ -\rho U^2 \int_{\bar{\Omega}} \bar{\phi}_y\, d\Omega. & (i=6) \end{cases} \tag{3.61}$$

Here $\bar{\Omega}$ denotes the time average of the volume Ω. The time average of the part of the volume integral associated with the oscillatory motion becomes zero due to periodicity.

To proceed further, it is convenient to separate the contributions due to the steady flow alone from the these associated with the oscillatory motion. Two adjustments are necessary. Firstly, the integrands should be separated into the part due to the steady flow alone and the remaining part. Secondly, the integration surface S_C should be divided into a mean surface $\bar{S}_C$ and a supplementary surface ΔS_C with z bounded between $\bar{\eta}$ and η . Then the integration is performed over each surface separately. Otherwise, it would be incorrect to simply take the time average over the integrands.

From a Taylor series, the integration of a function f over ΔS_C is approximated by

$$\int_{\Delta S_C} f\, dS = \oint_C dl \int_{\bar{\eta}}^{\eta} [\ f\Big|_{z=\bar{\eta}} + (z-\bar{\eta})\frac{\partial f}{\partial z}\Big|_{z=\bar{\eta}}\ ]\, dz \ + O(\epsilon^3)$$

$$= \oint_C [\ (\eta-\bar{\eta})f\Big|_{z=\bar{\eta}} + \frac{1}{2}(\eta-\bar{\eta})^2\frac{\partial f}{\partial z}\Big|_{z=\bar{\eta}}\ ]\, dl \ + O(\epsilon^3). \tag{3.62}$$

Here f is assumed of order O(1). In applying this approximation to the pressure integration in equation (3.61), only the first order relative free surface elevation is required; but for the integration

of the momentum flux term $V_i(V_n-U_n)$ the second order relative free surface elevation must be taken into account because the leading term of the momentum flux is of order O(1). The free surface elevation up to the second order of ϵ can be derived from the Bernoulli's equation

$$\eta - \bar{\eta} = \epsilon \frac{-\frac{1}{g}\left(\Phi_t^{(1)} + \vec{W}.\vec{\nabla}\Phi^{(1)} \right)}{1 + \frac{1}{2g}\frac{\partial}{\partial z}(\vec{W}.\vec{W})} \Bigg|_{z=\bar{\eta}}$$

$$+ \epsilon^2 \frac{\Phi_t^{(2)} + \vec{W}.\vec{\nabla}\Phi^{(2)} + \frac{1}{2}\vec{\nabla}\Phi^{(1)}.\vec{\nabla}\Phi^{(1)} - \frac{\left(\Phi_t^{(1)} + \vec{W}.\vec{\nabla}\Phi^{(1)}\right)\frac{\partial}{\partial z}\left(\Phi^{(1)} + \vec{W}.\vec{\nabla}\Phi^{(1)}\right)}{\frac{1}{2}\frac{\partial}{\partial z}(\vec{W}.\vec{W}) + g}}{\frac{1}{2}\frac{\partial}{\partial z}(\vec{W}.\vec{W}) + g}$$

$$+ O(\epsilon^3). \tag{3.63}$$

Here we have temporarily revived the superscripts (1) and (2) to denote the first order potential and the second order potential. The second order potential is included in the above expression because it is necessary to approximate the relative surface elevation up to the second order. These superscripts will be omitted again in the final expressions with the unsuperscribed variables representing their first order counterparts.

Following the approximation (3.62) together with the derived free surface elevation, it can be shown after some lengthy but straightforward algebra that the horizontal components of the mean force and the vertical component of the mean moment can be expressed as follows

$$\bar{F}_i = F_{Si} - \rho \int_{S_C} \overline{\left(v_i v_n - \frac{1}{2} v^2 n_i \right)} \, dS$$

$$- \rho \oint_C \{ \quad \frac{1}{2}\overline{(\eta-\bar{\eta})^2}[\ (g + \frac{1}{2}\frac{\partial}{\partial z}(\vec{W}.\vec{W}))n_i + \frac{\partial}{\partial z}(\bar{v}_i \vec{W}.\vec{n})\ ]$$

$$+ \overline{(\eta-\bar{\eta})(\ \vec{W}.\vec{n}v_i + v_n\bar{v}_i)}$$

$$+ \frac{\frac{1}{2}\vec{\nabla}\Phi.\vec{\nabla}\Phi - \frac{(\Phi_t + \vec{W}.\vec{\nabla}\Phi)\ \frac{\partial}{\partial z}(\Phi + \vec{W}.\vec{\nabla}\Phi)}{\frac{1}{2}\frac{\partial}{\partial z}(\vec{W}.\vec{W}) + g}}{\frac{1}{2}\frac{\partial}{\partial z}(\vec{W}.\vec{W}) + g} \bar{v}_i \vec{W}.\vec{n} \quad \} \ dl \tag{3.64}$$

where

$$F_{Si} = -\rho \int_{S_C} [\bar{v}_i(\bar{v}_n - U_n) - \frac{1}{2}(\vec{W}.\vec{W} - U^2)n_i]\ dS + \begin{cases} 0, & (i=1,2) \\ -\rho U^2 \int_{\bar{\Omega}} \bar{\phi}_y \ d\Omega, & (i=6) \end{cases} \tag{3.65}$$

Here the potential $\Phi=\Phi^{(1)}$ and $\eta-\bar{\eta}$ takes the first term in equation (3.63) etc. For simplicity the superscripts are omitted. The last term in the line integral comes from the contribution associated with the second order relative elevation of the free surface. The second order potential does not contribute to the mean force because of periodicity.

F_{Si} is the steady force on the body moving in otherwise calm water. The gz term in the pressure does not contribute to F_{Si} because its integration on the mean control surface is zero. The component of F_{Si} in the direction of advance is called "wave resistance", which is a primary concern in naval architecture. It is noted in equation (3.65) that the formula for the yaw moment is not feasible because of the volume integral. However, if the body is symmetrical about its middle plane y=0, then the the volume integral is zero and the formula for yaw moment also becomes easy for computation.

The remaining integral terms in equation (3.64) form the increased time average force, i.e. mean drift force, compared with the force on bodies moving in otherwise calm water. This mean drift force is proportional to the square of the incident waves. The corresponding component in the direction of advance is called "added resistance", which is the major concern here.

3.2.2 Small forward speed approximation

If the forward speed is small such that $F_n = U/\sqrt{gL} \ll 1$, then terms quadratic in F_n are negligible. Up to order $O(F_n)$ the steady free surface elevation is zero

$$\bar{\eta} = 0 \tag{3.66}$$

and the steady force and moment are also negligible: $F_{Si}=0$ $(i=1,2,6)$.

The horizontal components of the mean drift force and the vertical component of the mean drift moment are simplified to

$$\bar{F}_i = -\rho \int_{\bar{S}_C} \overline{\left(v_i v_n - \frac{1}{2} v^2 n_i \right)} \, dS$$

$$- \rho \oint_C \left[\frac{1}{2} \bar{\eta}^2 g n_i + \overline{\eta \left(\vec{W} \cdot \vec{n} v_i + v_n \bar{v}_i \right)} \right] dl + O(F_n^2, \epsilon^3), \quad (i=1,2,6) \tag{3.67}$$

To further simplify these expressions we shall study the asymptotic behaviour of the steady flow at far field. Up to order $O(F_n)$ the steady potential satisfies the "rigid wall" condition on the mean free surface z=0. Thus the steady flow can be approximated by the solution of the double-body moving in an unbounded fluid. The far field behaviour of a rigid body moving in an unbounded fluid is

similar to that of a dipole or a combination of dipoles (Newman 1977)

$$\bar{\phi} \simeq A_j \frac{\partial}{\partial x_j} \frac{1}{r} \sim O(\frac{1}{r^2}), \qquad \text{as} \quad r \to \infty. \tag{3.68}$$

Therefore, the steady flow is negligible in the line integral. It follows that

$$\bar{F}_i = -\rho \int_{S_C} (\overline{v_i v_n - \frac{1}{2} v^2 n_i}) \, dS$$
$$- \rho \oint_C \frac{1}{2} \bar{\eta^2} g n_i \, dl + O(F_n^2, \epsilon^3), \tag{3.69}$$

with

$$\eta = -\frac{1}{g}(\Phi_t - U\Phi_x). \tag{3.70}$$

Equation (3.69) is formally identical to that given by Ogilvie (1983) for zero forward speed case, but it should be emphasized that the velocity potential here depends on the forward speed and the similarity is restricted to the case of small forward speed.

3.3 The mean drift force on a vertical cylinder

Up to this point, the discussion has been quite general as far as the wavelength is concerned. The boundary value problems discussed in Section 3.1 is not easy to solve. Indeed, very little solutions are available. It is therefore useful to obtain solutions even under rather limiting conditions, if these may be used to validate more comprehensive numerical analyses for arbitrary bodies. The aim of the analysis in this section is to provide an asymptotic solution for a

vertical cylinder in regular waves at small forward speed.

As illustrated in Figure 3.1, the problem considered here is a vertical circular cylinder of infinite draft moving at a small forward speed U against incident waves of amplitude A. The cylinder is restrained from oscillations, so that only the diffraction problem is considered here. It is assumed that the water depth is infinite; the radius of the cylinder is small compared with the wavelength; and the Froude number is even smaller such that $F_n=U/\sqrt{(ga)} \ll \sqrt{(k_0 a)} \ll 1$. The last assumption is equivalent to $\omega \gg U\partial/\partial x$, which is necessary in simplifying the free surface condition.

The velocity potential is solved by the approach of matched asymptotic expansions. The mean drift force is calculated from the far field formulation derived in Section 3.2.

3.3.1 The use of matched asymptotic expansions for the cylinder

The basic ideas of the approach of matched asymptotic expansions are that first to divide the fluid domain into an inner domain close to the body and an outer domain outside; then to derive different expressions of the velocity potential in the two domains; and finally to match the two expressions over an overlap domain.

According to the approach of matched asymptotic expansions, it is necessary to consider the boundary conditions in more detail.

The steady potential in the present problem is quite simple.

Because of the infinite draft of the cylinder, the double-body steady flow field reduces to a two dimensional motion in the horizontal plane. Such a velocity potential can be obtained by distributing dipoles inside the body. The behaviour of the steady potential for the cylinder is therefore

$$\vec{\nabla}\bar{\phi}=O(\frac{a^2}{R^2}),$$

where $R=\sqrt{(x^2+y^2)}$.

The unsteady potential satisfies the free surface condition (3.25), which may be further simplified under the present conditions. It is noted that the variation of the diffraction potential along the vertical direction is characterised by variation of the incident potential, since the cylinder is infinitely long. Therefore the characteristic length in the z direction can be chosen as k_0^{-1}, which implies that $\partial/\partial z = O(k_0)$. In a horizontal direction the characteristic length is not so obvious because there are two lengths existing: the radius a and the wavelength $2\pi/k_0$. Arguably, the variation of the fluid flow in the domain within a wavelength around the body is characterised by the radius of the cylinder, and outside this domain the fluid flow is characterised by the wavelength. Therefore we may define the inner domain more clearly as the domain close to the cylinder, of which the distance from the outermost bound to the origin is no larger than a wavelength, and define the outer domain as the remaining fluid. Following these arguments and our present assumptions (i.e. $F_n \ll \sqrt{(k_0 a)} \ll 1$) equation (3.25) can be simplified to

$$\Phi_{tt} + g\Phi_z = 0 \quad \text{on} \quad z=0 \tag{3.71}$$

in the inner domain, where the omitted terms are of order $O(\Phi F_n/\sqrt{(k_0 a)})$. In the outer domain the steady potential decays rapidly and equation (3.25) reduces to

$$\Phi_{tt} - 2U\Phi_{xt} + g\Phi_z = 0 \quad \text{on } z=0. \tag{3.72}$$

The presence of the second term in equation (3.72) implies that terms of order $O(\Phi F_n\sqrt{(k_0 a)})$ have been retained. In the matching procedure presented below, the free surface conditions (3.71) and (3.72) are applied in the inner and outer domains respectively. The consistency of this procedure, in relation to the different free surface conditions, is discussed after the completion of the matching process.

3.3.2 Asymptotic expression of the diffraction potential

For the small cylinder the variation of the incident velocity over the cross section of the cylinder can be neglected. The diffraction potential may be approximated by distributing singularities along the axis of the cylinder. The three dimensional Laplace equation and the linearized free surface equation (3.72) are applied in the outer domain, together with a radiation condition and the requirement that the solution vanishes for $z\to\infty$. The inner domain solution, however, is found to be governed by the two dimensional Laplace equation (after extracting a slowly varying factor $e^{k_0 z}$). The outer solution is expressed in terms of a distribution of singularities, whose strengths are at first undetermined, and the inner solution includes an unknown additive constant. These two solutions are matched in an overlap domain such that the solution is

uniquely determined.

Because the present asymptotic analysis for the vertical cylinder is fairly independent from the rest of the thesis, use has been made here of ϕ_I and ϕ_D to represent the complex incident potential and the diffraction potential respectively. These correspond to $A\phi_0$ and $A\phi_7$ defined before. In the present problem, the incident wave potential is given by

$$\Phi_I = \mathrm{Re}\ [\ \phi_I\ e^{i\omega t}\ ], \qquad \text{with } \phi_I = \frac{igA}{\omega_0}\ e^{k_0(z+ix)}, \tag{3.73}$$

where as before ω_0 is the wave frequency, k_0 is the wave number given by $k_0=\omega_0^2/g$, and ω is the encounter frequency given by $\omega = \omega_0 + Uk_0$.

3.3.2.1 The inner solution

Let the diffraction be expressed in the form of $\Phi_D=\mathrm{Re}[\phi_D e^{i\omega t}]$. Then the body surface condition is written as

$$\frac{\partial \phi_D}{\partial n} = -\frac{\partial \phi_I}{\partial n} \qquad \text{on } R=a. \tag{3.74}$$

Expanding the incident potential into a Taylor series in the polar coordinates $x=R\cos\theta$ and $y=R\sin\theta$ yields

$$\frac{\partial \phi_D}{\partial R} = -\frac{\partial \phi_I}{\partial R} = \omega_0 A \frac{ik_0 a}{2}\ e^{k_0 z} + \omega_0 A\ e^{k_0 z}\cos\theta + \omega_0 A \frac{ik_0 a}{2}\ e^{k_0 z}\cos 2\theta + O[(k_0 a)^2] \qquad \text{on } R=a, \tag{3.75}$$

It can be seen that at a given depth z each term on the right

hand side in equation (3.75) corresponds to the velocity generated by a two dimensional singularity located at the axis of the cylinder. More specifically, the first term corresponds to a source, the second to a dipole, the third to a second derivative of the source etc. Guided by this condition, we may represent the diffraction potential by a superposition of multipoles with the strengths varying according to $e^{k_0 z}$ along the axis, i.e.

$$\psi = e^{k_0 z}(\psi_S + \psi_D + \psi_H + \ldots). \tag{3.76}$$

Here ψ represents the inner solution of the diffraction potential and ψ_S, ψ_D and ψ_H are the first three terms in the multipole expansion, corresponding to source, dipole and higher order singularity potentials. Substituting ψ into the Laplace equation and following the argument prior to equation (3.71), i.e. $(\partial/\partial x, \partial/\partial y, \partial/\partial z) = (O(1/a), O(1/a), O(k_0))$, we deduce that ψ_S, ψ_D, ψ_H etc. are governed by a two dimensional Laplace equation

$$\psi_{jxx} + \psi_{jyy} = O[(k_0 a)^2] , \tag{3.77}$$

where ψ_j represents ψ_S, ψ_D, ψ_H etc. Substituting equation (3.76) into the free surface condition (3.71) and taking the leading order terms, we obtain a "rigid wall" condition on the ψ_j on the free surface

$$\psi_{jz} = 0 \qquad \text{on } z=0. \tag{3.78}$$

These equations indicate that the ψ_j are two dimensional; they can be readily written as follows

2-D source $$\psi_S = \frac{q_S}{2\pi}(\ln k_0 R_1 - iC), \tag{3.79}$$

2-D dipole $$\psi_D = \frac{\partial \psi_S}{\partial \xi} = - \frac{q_D \cos\alpha}{2\pi R_1}, \tag{3.80}$$

2-D higher order multipole $$\psi_H = \frac{\partial \psi_D}{\partial \xi} = - \frac{q_H \cos 2\alpha}{2\pi R_1^2}, \tag{3.81}$$

where $\alpha = \text{arctg}[(y-\eta)/(x-\xi)]$ and $R_1 = \sqrt{[(x-\xi)^2+(y-\eta)^2]}$, evaluated here at $\xi=\eta=0$. The strengths are found by applying the boundary condition (3.75) with ϕ_D replaced by ψ. Substituting equation (3.76) with equations (3.79) to (3.81) into equation (3.75), we obtain

$$q_S = i\frac{\pi g A}{\omega_0}(k_0 a)^2, \tag{3.82}$$

$$q_D = 2\frac{\pi g A}{k_0 \omega_0}(k_0 a)^2, \tag{3.83}$$

$$q_H = i\frac{\pi g A}{2\omega_0 k_0^2}(k_0 a)^4. \tag{3.84}$$

In summary, the inner solution of the diffraction potential is written as follows

$$\psi \simeq \frac{gA}{2\omega}(k_0 a)^2 e^{k_0 z}\left(i\ln k_0 R - \frac{2\cos\theta}{k_0 R} - i\frac{(k_0 a)^2 \cos 2\theta}{2(k_0 R)^2} + C \right), \tag{3.85}$$

where the value of $\xi=\eta=0$ has been substituted and R, θ are the same as used in equation (3.75).

3.3.2.2 The outer solution

The outer solution for the diffraction potential may be

represented by a superposition of three dimensional multipoles distributed along the axis of the cylinder. In this way the diffraction solution can be expressed as the following summation

$$\phi_D = \phi_{DS} + \phi_{DD} + \phi_{DH} + \cdots \tag{3.86}$$

with the first three terms written as

$$\phi_{DS} = -\frac{1}{4\pi} \int_{-\infty}^{0} \sigma_S(\zeta)\, G_S(\vec{x},\vec{\xi})\, d\zeta, \tag{3.87}$$

$$\phi_{DD} = -\frac{1}{4\pi} \int_{-\infty}^{0} \sigma_D(\zeta)\, G_D(\vec{x},\vec{\xi})\, d\zeta, \tag{3.88}$$

$$\phi_{DH} = -\frac{1}{4\pi} \int_{-\infty}^{0} \sigma_H(\zeta)\, G_H(\vec{x},\vec{\xi})\, d\zeta. \tag{3.89}$$

Here G_S is a pulsating translating source potential which satisfies the three dimensional Laplace equation, the free surface condition (3.72) and the condition at the infinity; G_D is a corresponding dipole potential; and G_H is a higher order multipole potential. σ_S, σ_D and σ_H are the corresponding strengths. It is also assumed that equations (3.87) to (3.89) are evaluated at $\xi=\eta=0$.

G_S can be derived either directly from equation (3.72) or from the conventional pulsating translating source potential which satisfies the more complex free surface condition (3.24). Here we take the second method. As derived by Haskind (1954) such a conventional potential which satisfies the unsteady Neumann-Kelvin free surface condition is

$$G = \frac{1}{r} - \frac{1}{r'} - \frac{k}{\pi} \int_{-\pi}^{+\pi} \int_{0}^{\infty} \frac{\lambda e^{\lambda[z+\zeta+i(x-\xi)\cos\beta+i(y-\eta)\sin\beta]}}{(\tau\lambda\cos\beta - k(1-i\mu))^2 - k\lambda} \, d\beta d\lambda, \tag{3.90}$$

where $r = \sqrt{[(x-\xi)^2 + (y-\eta)^2 + (z-\zeta)^2]}$,

and $r' = \sqrt{[(x-\xi)^2 + (y-\eta)^2 + (z+\zeta)^2]}$.

The "artificial viscosity" μ is made to approach zero to ensure that G represents an outgoing wave at infinity. This is equivalent to defining the integration path to be an upper semicircle around the pole in equation (3.90). Haskind has also given the asymptotic expression at large distances from the body for small forward speed. However, it seems there is an error in his expression. As shown in Appendix B, we find the asymptotic term of G for small τ is

$$G_S = 2(1+2\tau\cos\alpha)\sqrt{2\pi k/R} \exp\{k(1+2\tau\cos\alpha)[z+\zeta - i(R-\xi\cos\theta-\eta\sin\theta)] - i\frac{\pi}{4}\} + O(\tau, \frac{1}{kr}), \tag{3.91}$$

where $\tau = \frac{U\omega}{g}$, $x = R\cos\theta$, $y = R\sin\theta$, $k = \omega^2/g = k_0(1+2\tau) + O(\tau^2)$.

α has been defined after equation (3.81), i.e. $\alpha = \text{arctg}[(y-\eta)/(x-\xi)]$. In Haskind's expression α is taken as θ. Although one can usually replace α by θ, this is not true for the term $R\cos\alpha$, since

$$R\cos\alpha = R\cos\theta - \xi\sin^2\theta + \eta\sin\theta\cos\theta + O(\frac{1}{R}).$$

Equation (3.91) satisfies the free surface condition (3.72) and therefore G may be replaced by G_S. The expression (3.91) is consistent with the asymptotic expression given by Newman (1959) if the small speed limit is taken there, as is shown in Appendix B.

The asymptotic expressions for the higher order singularities can be obtained from the derivatives of G_S as follows

$$G_D = \frac{\partial G_S}{\partial \xi} = k(1+2\tau\cos\theta)\ i\cos\theta\ G_S - i2k\tau R\frac{\partial \cos\alpha}{\partial \xi}\ G_S$$

$$= ik(\cos\theta+2\tau)G_S$$

$$= 2ik[\cos\theta+2\tau(1+\cos^2\theta)]\ \cos\theta\ \sqrt{2\pi k/R}$$

$$\exp\{k(1+2\tau\cos\alpha)[z+\zeta-i(R-\xi\cos\theta-\eta\sin\theta)]-i\tfrac{\pi}{4}\} + O(\tau^2, \frac{1}{kr}), \tag{3.92}$$

$$G_H = \frac{\partial G_D}{\partial \xi} = -[ik(\cos\theta+2\tau)]^2 G_S$$

$$= -2k^2\ [\cos^2\theta+\tau(4\cos\theta+2\cos^3\theta)\ \sqrt{2\pi k\ /R}$$

$$\exp\{k(1+2\tau\cos\theta)[z+\zeta-i(R-\xi\cos\theta-\eta\sin\theta)]-i\tfrac{\pi}{4}\}\ + O(\tau^2, \frac{1}{kr}). \tag{3.93}$$

These singularities G_S, G_D and G_H are Green functions. From these and equations (3.87) to (3.89) we can obtain the outer solution in terms of the unknown strengths σ_S, σ_D and σ_H.

3.3.2.3 Matching

To determine the strengths of the singularities in equations (3.87) to (3.89) it is necessary to examine the outer limit of the inner solution and the inner limit of the outer solution, and to match these two limits. For this reason let us first study the behaviour of equation (3.90) as kR→0 at small forward speed.

Huijsmans and Hermans (1985) have shown that the conventional pulsating translating source potential (3.90) can be expanded into a Taylor series in terms of the small parameter τ. In our present notation this expansion is written as

$$G \sim G_0 + \tau G_1 + \ldots \tag{3.94}$$

with the first two terms given by

$$G_0 = \frac{1}{r} - \frac{1}{r'} + 2\int_0^\infty \frac{\lambda e^{\lambda(z+\zeta)}}{\lambda - k(1-i\mu)} J_0(\lambda R_1)d\lambda, \tag{3.95}$$

$$G_1 = -4i\cos\alpha \int_0^\infty \frac{\lambda^2 e^{\lambda(z+\zeta)}}{(\lambda - k(1-i\mu))^2} J_1(\lambda R_1)d\lambda. \tag{3.96}$$

R_1 and α are the same as used in equations (3.79) to (3.81); $J_0(\lambda R_1)$ and $J_1(\lambda R_1)$ are the zeroth and first order Bessel functions of the first kind. Equation (3.96) differs from that derived by Huijsmans and Hermans by a sign: this is merely the result of the different time factors used, which also affects the integration paths.

Although the expansion in equation (3.94) is not uniformly convergent, it is valid in the matching domain. Since the summation of the first two terms satisfies the free surface condition (3.72), this is the Green function to be used in equation (3.87), that is

$$G_S = G_0 + \tau G_1 + O(\tau^2). \tag{3.97}$$

We recognise that G_0 is the conventional pulsating source potential, which can be expressed in an alternative form by using the following identity

$$\frac{1}{r'} = \int_0^\infty e^{\lambda(z+\zeta)} J_0(\lambda R_1)d\lambda.$$

Substitution into equation (3.95) yields

$$G_0 = \frac{1}{r} + \frac{1}{r'} + 2\int_0^\infty \frac{k\, e^{\lambda(z+\zeta)}}{\lambda - k(1-i\mu)} J_0(\lambda R_1)\, d\lambda. \tag{3.98}$$

To develop an inner expansion of the outer solution ϕ_{DS} we expand the Bessel functions $J_0(\lambda R_1)$ and $J_1(\lambda R_1)$ into ascending series and then integrate equations (3.96) and (3.98) term by term. Introducing a new variable $Y \equiv k|z+\zeta|$, we obtain

$$G_0 = \frac{1}{r} + \frac{1}{r'} - 2\pi i k e^{-Y} J_0(kR) + 2k \sum_{n=0}^{\infty} \frac{(kR)^{2n}}{(-4)^n (n!)^2} \left(\sum_{m=1}^{2n} \frac{(m-1)!}{Y^m} - e^{-Y} E_i(Y) \right), \tag{3.99}$$

$$G_1 = -2\pi i \cos\theta\, k^2 R \sum_{n=0}^{\infty} \frac{(kR)^{2n}}{(-4)^n n!(n+1)!} \left[-1 + (2n+3-Y) e^{-Y} E_1(-Y) + \sum_{m=1}^{2n+2} (2n+3-m) \frac{(m-1)!}{Y^m} \right]. \tag{3.100}$$

where $\xi = \eta = 0$ has been substituted. $E_i(Y)$ is the exponential integral function as defined in Abramowitz and Stegun (1965), and $E_1(-Y) = -(E_i(Y) + \pi i)$. The first term of the summation over n in equation (3.99) is defined as $-e^{-Y} E_i(Y)$. Details of the derivation can be found in Appendix D.

Substitution of equation (3.97) together with equations (3.99) and (3.100) into equation (3.87) leads to

$$\phi_{DS} = -\frac{1}{4\pi} \int_{-\infty}^{0} \sigma_S(\zeta) \left(\frac{1}{r} + \frac{1}{r'} \right) d\zeta + \frac{i}{2} J_0(kR) \int_{-\infty}^{0} \sigma_S(\zeta) e^{-Yk}\, d\zeta - \frac{1}{2\pi} \sum_{n=0}^{\infty} \frac{(kR)^{2n}}{(-4)^n (n!)^2} M_n(z, R, \theta), \tag{3.101}$$

where $M_n(z,R,\theta)$ is defined as

$$M_n(z,R,\theta) = k\int_{-\infty}^{0} \sigma_S(\zeta)\{\sum_{m=1}^{2n}\frac{(m-1)!}{Y^m} - e^{-Y}E_i(Y)$$

$$+ \tau\frac{i\pi\cos\theta kR}{n+1}[1-(2n+3-Y)e^{-Y}E_1(-Y) - \sum_{m=1}^{2n+2}(2n+3-m)\frac{(m-1)!}{Y^m}]\}\,d\zeta, \tag{3.102}$$

with

$$M_0(z,R,\theta) =$$

$$k\int_{-\infty}^{0}\sigma_S(\zeta)\{-e^{-Y}E_i(Y)+\tau i\pi\cos\theta k\, R[1-(3-Y)e^{-Y}E_1(-Y)-\sum_{m=1}^{2}(3-m)\frac{(m-1)!}{Y^m}]\}d\zeta. \tag{3.103}$$

The first two terms in equation (3.101) can be folded into one term by taking account of the symmetry about the Oxy plane:

$$-\frac{1}{4\pi}\int_{-\infty}^{0}\sigma_S(\zeta)(\frac{1}{r}+\frac{1}{r'})d\zeta = -\frac{1}{4\pi}\int_{-\infty}^{\infty}\sigma_S(\zeta)\frac{1}{r}d\zeta, \tag{3.104}$$

where we define $\sigma_S(-\zeta) = \sigma_S(\zeta)$. To derive the expression for small R the following relation is used

$$\frac{1}{\sqrt{(z-\zeta)^2+R^2}} = \frac{d}{d\zeta}\ln[\frac{\zeta-z}{R}+\sqrt{(\frac{\zeta-z}{R})^2+1}\,] \tag{3.105}$$

which can be justified directly by differentiation. Substituting equation (3.105) into equation (3.104) and integrating by parts, we obtain

$$-\frac{1}{4\pi}\int_{-\infty}^{0}\sigma_S(\zeta)(\frac{1}{r}+\frac{1}{r'})d\zeta = \frac{1}{4\pi}\int_{-\infty}^{\infty}\sigma_S'(\zeta)\ln[\frac{\zeta-z}{R}+\sqrt{(\frac{\zeta-z}{R})^2+1}\,]d\zeta \tag{3.106}$$

where the contribution from the infinite limits has been deleted on

the assumption that $\sigma_S(\zeta)\ln|\zeta| \to 0$ as $\zeta \to \pm\infty$. From a Taylor series expansion of the square-root function we can show that the limiting value of the argument of the logarithm is

$$\frac{\zeta-z}{R} + \sqrt{\left(\frac{\zeta-z}{R}\right)^2+1} \simeq \frac{2(\zeta-z)}{R}, \qquad (\zeta-z) > 0, \tag{3.107}$$

as $R\to 0$, or

$$\frac{\zeta-z}{R} + \sqrt{\left(\frac{\zeta-z}{R}\right)^2+1} \simeq \frac{R}{2|\zeta-z|}, \qquad (\zeta-z) < 0. \tag{3.108}$$

Substituting equations (3.107) and (3.108) into equation (3.106), it follows that

$$-\frac{1}{4\pi}\int_{-\infty}^{0} \sigma_S(\zeta)\left(\frac{1}{r} + \frac{1}{r'}\right)d\zeta \simeq \frac{1}{4\pi}\left[-\int_{-\infty}^{z} \sigma_S'(\zeta)\ln\frac{2(z-\zeta)}{R}d\zeta + \int_{z}^{\infty} \sigma_S'(\zeta)\ln\frac{2(\zeta-z)}{R}d\zeta\right]$$

$$= \frac{1}{2\pi}\sigma_S(z)\ln kR - \frac{1}{4\pi}\left[\int_{-\infty}^{z} \sigma_S'(\zeta)\ln 2k(z-\zeta)d\zeta - \int_{z}^{\infty} \sigma_S'(\zeta)\ln 2k(\zeta-z)d\zeta\right]. \tag{3.109}$$

Substituting equation (3.109) into equation (3.101), the inner expansion of the outer solution ϕ_{DS} is finally obtained as follows

$$\phi_{DS} \simeq \frac{1}{2\pi}\sigma_S(z)\ln k_0 R + s(z), \qquad R\to 0, \tag{3.110}$$

where

$$s(z) = -\frac{1}{4\pi}\left[\int_{-\infty}^{z} \sigma_S'(\zeta)\ln 2k(z-\zeta)d\zeta - \int_{z}^{\infty} \sigma_S'(\zeta)\ln 2k(\zeta-z)d\zeta\right]$$

$$+ \frac{i}{2}J_0(kR)\int_{-\infty}^{0} \sigma_S(\zeta)e^{-Yk}\,d\zeta - \frac{1}{2\pi}\sum_{n=0}^{\infty}\frac{(kR)^{2n}}{(-4)^n(n!)^2}M_n(z,R,\theta) + \frac{\tau}{\pi}\sigma_S(z); \tag{3.111}$$

or, approximately

$$s(z) \simeq -\frac{1}{4\pi}\left[\int_{-\infty}^{z} \sigma_S'(\zeta)\ln 2k(z-\zeta)\, d\zeta - \int_{z}^{\infty} \sigma_S'(\zeta)\ln 2k(\zeta-z)\, d\zeta\right]$$

$$+ \frac{1}{2\pi}\int_{-\infty}^{0} \sigma_S(\zeta)(E_1(Y)+i\pi)e^{-Y} k\, d\zeta + \frac{\tau}{\pi}\sigma_S(z) + O((kR)^2, \tau kR)\sigma_S. \tag{3.112}$$

Now let us develop the inner expansions of the outer solutions ϕ_{DD} and ϕ_{DH}. In principle this can be done by deriving the Green functions G_D and G_H first, and then following the procedures from equation (3.101) to equation (3.112). However there is a simpler way. We note that the derivatives of the Green functions G_D and G_H in equations (3.92) and (3.93) only involve differentiations with respect ξ. In view of this fact we may interchange the order of the ξ differentiations with the ζ integration in equations (3.88) and (3.89). Following this idea we can write

$$\phi_{DD}(\vec{x}) = \frac{\partial}{\partial \xi}\left[-\frac{1}{4\pi}\int_{-\infty}^{0} \sigma_D(\zeta)G_S(\vec{x},\vec{\xi})d\zeta\right]\Big|_{\xi=\eta=0}, \tag{3.113}$$

$$\phi_{DH}(\vec{x}) = \frac{\partial^2}{\partial \xi^2}\left[-\frac{1}{4\pi}\int_{-\infty}^{0} \sigma_H(\zeta)G_S(\vec{x},\vec{\xi})d\zeta\right]\Big|_{\xi=\eta=0}. \tag{3.114}$$

For convenience we define the functions in the square brackets in equations (3.113) and (3.114) as t_j:

$$t_j = -\frac{1}{4\pi}\int_{-\infty}^{0} \sigma_j(\zeta)G_S(\vec{x},\vec{\xi})d\zeta, \qquad j=1,2$$

with $\sigma_1(\zeta)=\sigma_D(\zeta)$ and $\sigma_2(\zeta)=\sigma_H(\zeta)$. As t_j is analogous to ϕ_{DS} we can obtain its expression by substituting equation (3.109) into equation

(3.101), interpreting R as R_1, and θ as α, and replacing σ_s by σ_j; hence

$$t_j = \frac{1}{4\pi}\int_{-\infty}^{\infty} \sigma_j'(\zeta)\ln[\frac{\zeta-z}{R_1}+\sqrt{(\frac{\zeta-z}{R_1})^2+1}]d\zeta + \frac{i}{2}J_0(kR_1)\int_{-\infty}^{0} \sigma_j(\zeta)e^{-Yk}\,d\zeta$$

$$- \frac{1}{2\pi}\sum_{n=0}^{\infty}\frac{(kR_1)^{2n}}{(-4)^n(n!)^2}M_{nj}(z,R_1,\alpha), \tag{3.115}$$

where M_{nj} has the same definition as M_n (equations (3.102) and (3.103)) with the extra subscript j indicating that σ_s should be replaced by σ_j. Differentiating equation (3.115) requires the derivatives of the logarithm function; evaluation of these at $\xi=\eta=0$ leads to

$$\frac{\partial}{\partial\xi}\ln[\frac{\zeta-z}{R_1}+\sqrt{(\frac{\zeta-z}{R_1})^2+1}] = -\frac{(\xi-x)(\zeta-z)}{R_1^2\,r} \simeq \frac{\cos\theta}{R}\mathrm{sgn}(\zeta-z) + O(\frac{R}{\zeta-z}), \tag{3.116}$$

$$\frac{\partial^2}{\partial\xi^2}\ln[\frac{\zeta-z}{R_1}+\sqrt{(\frac{\zeta-z}{R_1})^2+1}] = -\frac{(\xi-x)[R_1^2r^2-(\xi-x)^2R_1^2-2(\xi-x)^2r^2]}{R_1^4r^3}$$

$$\simeq \frac{\cos2\theta}{R^2}\mathrm{sgn}(\zeta-z) + \frac{\mathrm{sgn}(\zeta-z)}{2(\zeta-z)^2} + O[(\frac{R}{\zeta-z})^2], \tag{3.117}$$

where the last approximations hold as $R\to0$. The $\mathrm{sgn}(\zeta-z)$ is the sign function. Differentiating the remaining terms of (3.115) is a straightforward matter with the Bessel function being expanded into an ascending series

$$J_0(kR_1) = \sum_{n=0}^{\infty}\frac{(kR_1)^{2n}}{(-4)^n(n!)^2}.$$

Finally, we obtain the inner expansions of the outer solutions ϕ_{DD} and ϕ_{DH} in the following form

$$\phi_{DD} \simeq -\frac{\sigma_D(z)\cos\theta}{2\pi R} + O(k_0R,\tau)k_0\sigma_D, \tag{3.118}$$

$$\phi_{DH} \simeq -\frac{\sigma_H(z)\cos 2\theta}{2\pi R^2} + h(z), \tag{3.119}$$

where

$$h(z) \simeq -\frac{1}{4\pi}\int_{-\infty}^{\infty}\sigma_H'(\zeta)\frac{\mathrm{sgn}(\zeta-z)}{2(\zeta-z)^2}d\zeta - i\frac{k_0^3}{4}\int_{-\infty}^{0}\sigma_H(\zeta)e^{-Y}d\zeta$$
$$+\frac{k_0^3}{4\pi}\int_{-\infty}^{0}\sigma_H(\zeta)\left[\sum_{m=1}^{2}\frac{(m-1)!}{Y^m}-e^{-Y}E_i(Y)\right]d\zeta + O(k_0R,\tau k_0R)k_0^2\sigma_H. \tag{3.120}$$

Equations (3.118), (3.119) and (3.110) complete the inner expansion of the outer solution. As mentioned at the beginning of this section we now match the outer solution with the inner solution by requiring

$$\phi_D \sim \psi$$

in an overlap domain. Comparing equations (3.118), (3.119) and (3.110) with equation (3.85), we obtain the strengths of the outer solution as

$$\sigma_S = q_S e^{k_0 z} = i\frac{\pi gA}{\omega_0}(k_0a)^2 e^{k_0z}, \tag{3.121}$$

$$\sigma_D = q_D e^{k_0 z} = 2\frac{\pi gA}{k_0\omega_0}(k_0a)^2 e^{k_0z}, \tag{3.122}$$

$$\sigma_H = q_H e^{k_0 z} = i\frac{\pi g A}{2\omega_0 k_0^2}(k_0 a)^4 e^{k_0 z}, \tag{3.123}$$

and the "constant" in the inner solution as

$$C = [\frac{gA}{2\omega_0}(k_0 a)^2 e^{k_0 z}]^{-1}(h(z)+s(z)). \tag{3.124}$$

The matched asymptotic solution is thereby completed and the asymptotic solution of the diffraction potential is determined from equations (3.86) together with equations (3.87) to (3.89) and (3.121) to (3.123).

Substituting equations (3.90), (3.92) and (3.93), and equations (3.121) to (3.123) into equations (3.87) to (3.89), and neglecting terms of order τ^2 and higher, we obtain at large distances

$$\phi_{DS} \simeq -\frac{i\pi g A}{4\omega_0}(k_0 a)^2\sqrt{\frac{2}{\pi k_0 R}}(1+\tau\cos\theta)\exp\{k(1+2\tau\cos\theta)(z-iR)-i\frac{\pi}{4}\}, \tag{3.125}$$

$$\phi_{DD} \simeq -\frac{i\pi g A}{2\omega_0}(k_0 a)^2\sqrt{\frac{2}{\pi k_0 R}}[\cos\theta+\tau(2+2\cos\theta+\cos^2\theta)] \exp\{k(1+2\tau\cos\theta)(z-iR)-i\frac{\pi}{4}\}, \tag{3.126}$$

$$\phi_{DH} \simeq \frac{i\pi g A}{8\omega_0}(k_0 a)^4\sqrt{\frac{2}{\pi k_0 R}}[\cos^2\theta+\tau(4\cos\theta+4\cos^2\theta+\cos^3\theta)] \exp\{k(1+2\tau\cos\theta)(z-iR)-i\frac{\pi}{4}\}. \tag{3.127}$$

The potential ϕ_{DH} is of higher order in $k_0 a$ compared with ϕ_{DS} and ϕ_{DD}, and is therefore neglected hereafter.

The asymptotic expression for the diffraction potential can be finally written as follows

$$\phi_D \simeq -\frac{i\pi gA}{4\omega_0}(k_0a)^2\sqrt{\frac{2}{\pi k_0 R}}\,(\hat{\phi}_S+\hat{\phi}_D)\exp\{k(1+2\tau\cos\theta)(z-iR)-i\tfrac{\pi}{4}\}, \tag{3.128}$$

where $\hat{\phi}_S = 1+\tau\cos\theta$,

$\hat{\phi}_D = 2[\cos\theta+\tau(2+2\cos\theta+\cos^2\theta)]$.

It is appropriate to consider why ϕ_{DH} is of higher order than ϕ_{DS} in equations (3.125) to (3.127), despite the fact that their normal gradients ($\cos2\theta$ and θ independent terms) in equation (3.75) are of the same order. This can be explained by considering the strengths of the singularities. From equations (3.87) to (3.89) and the Green functions G_S,G_D and G_H in equations (3.90) to (3.93), we see that each potential ϕ_{DL} (L=S,D,H) consists of two parts: the first part is due to the singular term of the corresponding Green function and the second part is due to the harmonic term in that Green function. On the body surface the first part is dominant. The singularity (ψ_H) that generates the first part of ϕ_{DH} is much stronger than that (ψ_S) for ϕ_{DS}. Thus the same order conditions for ϕ_{DH} and ϕ_{DS} in equation (3.75) require the strengths of the corresponding singularities to be of different order, that is, the singularity strength for ϕ_{DH} is required to be much smaller than the strength for ϕ_{DS}. At large distances the first parts of both potentials decay rapidly, and there remains a spatially oscillating term from the second part of each Green function. These two oscillating terms decay at the same speed. The far field magnitude of each potential is therefore proportional to the singularity strength. This provides the necessary explanation, and a similar argument explains why ϕ_{DD} and ϕ_{DS} are of the same order of magnitude.

3.3.2.4 Discussion

At this stage it is appropriate to discuss the consistence of the procedure adopted. The outer solution has been required to satisfy the free surface condition (3.72), the second term of which is $O(\tau)$ smaller that the other two terms. This is consistent with equation (3.97). In the inner domain, the corresponding term has not been retained in the free surface condition (3.71), although this term is $O(k_0 a)$ larger than the corresponding term which has been retained in equation (3.72).[1] The consequences due to this inconsistence is discussed here.

Let ϕ_T denote the complete solution of the diffraction potential and ϕ_L denote the difference between ϕ_T and our approximate solution (3.128), i.e.

$$\phi_T = \phi_D + \phi_L. \tag{3.129}$$

Also define a differential operator $\Gamma \equiv -k + \frac{\partial}{\partial z} - 2i\tau\frac{\partial}{\partial x}$. Then up to the order proportional to the forward speed, the consistent free surface condition can be written in the form of

$$\Gamma(\phi_T+\phi_I) + 2i\tau\vec{\nabla}\phi.\vec{\nabla}(\phi_T+\phi_I) = 0 \qquad \text{on } z=0. \tag{3.130}$$

---

[1]. I am grateful to one of the referees for pointing this out during the preparation of the paper by Eatock Taylor, Hu and Neilsen (1990).

Since on the free surface (cf. equation (3.72))

$$\Gamma(\phi_D) = \Gamma(\phi_I) = 0, \tag{3.131}$$

we have

$$\Gamma(\phi_L) + 2i\tau\vec{\nabla}\tilde{\phi}.\vec{\nabla}\phi_L = -2i\tau\vec{\nabla}\phi.\vec{\nabla}(\phi_D+\phi_I)$$
$$= \kappa(R,\theta), \text{ say, on } z=0. \tag{3.132}$$

The body surface condition is

$$\frac{\partial\phi_L}{\partial n} = -\frac{\partial(\phi_D+\phi_I)}{\partial n} \qquad \text{on } R=a, \tag{3.133}$$

or

$$\frac{\partial\phi_L}{\partial n} \simeq 0 \qquad \text{on } R=a. \tag{3.134}$$

The error in equation (3.134) is proportional to order $O((k_0a)^2, \tau(k_0a)^2)$. Although the verification is fairly straightforward, it is helpful to note a few points. These are: $\sigma_S \sim \sigma_D \sim O((k_0a)^2)$, $\sigma_H \sim O((k_0a)^4)$, and in the inner domain the radial derivative is normally an order of $1/(k_0a)$ larger than the original quantity. However, the last statement does not hold for the leading term proportional to τ in equation (3.118). A careful analysis reveals that in equation (3.118) the τ-dependent leading term is, in fact, independent of R (cf. equations (3.113) and (3.115) together with equations (3.102) and (3.103)) and therefore does not contribute to the body surface condition (3.134) up to the order retained. Apart from that, the verification of equation (3.134) is trivial. At large distances ϕ_L and its derivatives are required to vanish.

Since all boundary conditions for ϕ_L are homogeneous, except on the free surface, the problem corresponding to the homogeneous part of equation (3.132) does not have a non-trivial solution. The solution for ϕ_L is analogous to a forced oscillation, which is determined by the forcing term $\kappa(R,\theta)$.

We can investigate the far field behaviour of ϕ_L as follows. As $R\to\infty$ we have

$$\phi' \sim \frac{\kappa_0(\theta)}{R}, \qquad \phi_I \sim \kappa_1(\theta,0)e^{ik_0R\cos\theta},$$

$$\phi_D \sim \frac{\kappa_2(\theta,0)}{\sqrt{k\,R}}\, e^{-i(1+2\tau\cos\theta)kR}.$$

Hence

$$\kappa(R,\theta) \sim \frac{\kappa_3(\theta,0)}{R^2}\, e^{ik_0R\cos\theta} + O(\frac{1}{R^{5/2}}). \tag{3.135}$$

Equation (3.132) then suggests that

$$\phi_L \sim \frac{\kappa_4(\theta,z)}{R^2}\, e^{ik_0R\cos\theta} + O(\frac{1}{R^{5/2}}). \tag{3.136}$$

But this term is negligible in the far field compared with ϕ_D. Thus ϕ_L is only a local disturbance, and the validity of the far field solution ϕ_D is justified.

As far as the purpose of this anlysis is concerned, the essential requirement is an asymptotic expression for the diffraction

potential (e.g. equation (3.128)), since this forms the basis for our evaluation of drift force. Therefore, the above discussion implies that any apparent inconsistence is not in fact significant in relation to the results obtained here.

3.3.3 Approximation of the mean drift force

The geometrical symmetry of the cylinder implies that the sway and yaw components of the mean drift force are zero: $\bar{F}_2=\bar{F}_6=0$. From the far field expression (3.69), the component in surge is written as

$$\bar{F}_1 = -\rho \int_{S_C} \left(\overline{\Phi_x \Phi_n - \frac{1}{2}\vec{\nabla}\Phi.\vec{\nabla}\Phi \; n_1} \right) dS - \frac{\rho}{2g} \oint_C \overline{\Phi_t^2} \; n_1 \; dl. \tag{3.137}$$

At this point the control surface S_C is further defined as a rectangular cylinder with two surfaces S_1, S_{-1} at $x \to \pm\infty$ and S_2, S_{-2} parallel to the x-axis at large distances $\pm y_c$. Since the fluid flow is symmetrical about $y=0$ and n_1 is anti-symmetrical about $y=0$, it immediately follows that the line integral is zero and that the surface integral of the second order mean pressure is also zero. Hence,

$$\bar{F}_1 = -\rho \iint_{S_2+S_{-2}} \overline{\Phi_x \Phi_n} \; dS = -2\rho \iint_{S_2} \overline{\Phi_x \Phi_y} \; dS. \tag{3.138}$$

From the relation

$$\overline{\mathrm{Re}[Ae^{i\omega t}] \; \mathrm{Re}[Be^{i\omega t}]} = \frac{1}{4}(A^*B + B^*A) = \frac{1}{2}\mathrm{Re}[AB^*] = \frac{1}{2}\mathrm{Re}[A^*B]$$

equation (3.138) can be rewritten as

$$\bar{F}_1 = -\mathrm{Re}[\rho \iint_{S_2} \phi_x \phi_y^* dS],$$

where an over bar denotes the time average and * denotes complex conjugate. We can therefore use the following results

$$\left.\begin{aligned} \phi_{Ix} &= ik_0\phi_I, \qquad \phi_{Iy} = 0, \\ \phi_{Dx} &= -ik(\cos\theta+2\tau)\phi_D, \qquad \phi_{Dy}^* = ik\sin\theta\phi_D^*, \end{aligned}\right\} \tag{3.139}$$

to obtain the far field expression

$$\bar{F}_1 = -\mathrm{Re}[\rho \iint_{S_2} (ik_0\phi_I - ik(\cos\theta+2\tau)\phi_D)\phi_{Dy}^* dS]. \tag{3.140}$$

Further simplification is possible by using an identity based on energy conservation. Maruo (1960) has shown that in the absence of current or forward speed the periodic potential Φ^0 satisfies

$$\overline{\iint_{S_C} \Phi_t^0 \Phi_n^0 dS} = 0, \tag{3.141}$$

where S_C is the outer cylindrical surface defined after equation (3.137). Newman (1959) had previously shown in a similar way that the average work done by the vertical force on a ship in waves combined with a current -Ux is

$$W_D = -\rho \overline{\iint_{S_C} \tilde{\Phi}_t \tilde{\Phi}_n dS}, \tag{3.142}$$

where the total velocity potential $\tilde{\Phi}$ is decomposed as

$$\tilde{\Phi}(\vec{x}_0,t) = \Phi_c(\vec{x},t)+U\tilde{\phi}_c(\vec{x})-Ux, \tag{3.143}$$

$\tilde{\phi}_c$ is the steady disturbance potential due to the existence of the body in the current, and Φ_c is the unsteady potential due to the incident and diffracted waves. It can be shown that $\tilde{\phi}_c$ and Φ_c satisfy the same boundary conditions as the corresponding potentials for the body at forward speed. In other words: $\tilde{\phi}_c = \tilde{\phi}$ and $\Phi_c = \Phi$.

From equation (3.142) we can derive a relation analogous to equation (3.141) for the unsteady potential. For the diffraction problem of the present cylinder the vertical work is zero; i.e. $W_D=0$. Substituting equation (3.143) into equation (3.142) and omitting the subscript, we obtain

$$\overline{\iint_{S_C}\Phi_t(\Phi_n-Un_1)dS} = 0$$

where $\tilde{\phi}_n$ has been neglected because $\tilde{\phi}$ is of order $O(\frac{1}{k_0R})$ in the far field. In a similar manner to equation (3.137), the preceding equation may be approximated up to $O(\tau\Phi^2)$ by

$$\iint_{S_C} \overline{\Phi_t\Phi_n}\, dS + \frac{U}{g}\int_C \overline{\Phi_t^2}n_1 dl = 0.$$

Again, the line integral vanishes due to symmetry. The equation can be further simplified to

$$\iint_{S_2} \overline{\Phi_t\Phi_n} dS = 0,$$

or

$$\mathrm{Re}\left[\iint_{S_2} i\omega(\phi_I+\phi_D)\phi_{Dy}^{*}\,dS\right] = 0. \tag{3.144}$$

Eliminating ϕ_I from equation (3.140) and equation (3.144) we have

$$\bar{F}_1 = -\,\mathrm{Re}\left[\rho\iint_{S_2}(-ik_0 - ik(\cos\theta+2\tau))\phi_D\phi_{Dy}^{*}\,dS\right]$$

$$= -\,\mathrm{Re}\left[\rho\int_{-\infty}^{+\infty}(k_0+k(\cos\theta+2\tau))k\sin\theta\,dx\int_{-\infty}^{0}\phi_D\phi_D^{*}\,dz\right]$$

$$= -\rho\int_{-\infty}^{+\infty}\frac{k_0+k(\cos\theta+2\tau)}{2(1+2\tau\cos\theta)}\sin\theta\;\phi_D\phi_D^{*}\Big|_{z=0}dx.$$

On S_2 $y=y_c$=constant, and $dx = -\frac{Rd\theta}{\sin\theta}$. Substitution of equation (3.128) yields

$$\bar{F}_1 \simeq -\frac{\rho\pi gA^2a}{16}(k_0a)^3\int_0^{\pi}(1+\cos\theta+\tau(1-\cos2\theta))(\hat{\phi}_S+\hat{\phi}_D)^2d\theta.$$

In order to distinguish the contributions from the source, the dipole and from their cross product the following variables are defined:

$$f_S \equiv \int_0^{\pi}(1+\cos\theta+\tau(1-\cos2\theta))\,\hat{\phi}_S^2d\theta = \pi(1+2\tau), \tag{3.145}$$

$$f_{SD} \equiv 2\int_0^{\pi}(1+\cos\theta+\tau(1-\cos2\theta))\,\hat{\phi}_S\hat{\phi}_Dd\theta = \pi(2+16\tau), \tag{3.146}$$

$$f_D \equiv \int_0^{\pi}(1+\cos\theta+\tau(1-\cos2\theta))\,\hat{\phi}_D^2d\theta = \pi(2+20\tau). \tag{3.147}$$

We thus finally obtain the mean drift force in the x-direction as

$$\bar{F}_1 \simeq -\frac{\rho\pi g A^2 a}{16}(k_0a)^3\ (\ f_S + f_{DS} + f_D),$$

or

$$\bar{F}_1 \simeq -\frac{\rho\pi^2 g A^2 a}{16}(k_0a)^3\ (5 + 38\tau). \tag{3.148}$$

This result can be easily verified under the condition $\tau=0$. From the well-known solution of the diffraction problem given by Havelock (1940) we integrate the pressure on the cylinder surface. After some algebra, the mean drift force can be written as

$$\bar{F}_0 = -\frac{2\rho g A\ a}{\pi(k_0a)^2}\sum_{m=0}^{\infty}\left(\frac{m(m+1)}{(k_0a)^2} - 1\right) f_m(k_0a), \tag{3.149}$$

where $f_m(k_0a) = \mathrm{Im}\left[\dfrac{1}{(H_m^{(2)'}(k_0a))^*\ H_{m+1}^{(2)'}(k_0a)}\right]$,

and $H_m^{(2)}(k_0a)$ is the mth order second kind of Hankel function; the $'$ denotes its derivative.

In the long wave limit $k_0a \to 0$; we obtain $f_0 = -\pi^3(k_0a)^5/8$ and $f_1 = \pi^3(k_0a)^7/64$. The mean drift force is then given by

$$\bar{F}_0 = -\frac{5\rho\pi^2 g A^2 a}{16}(k_0a)^3, \tag{3.150}$$

and equation (3.148) is therefore confirmed for the special case of $\tau=0$.

It can be seen from equations (3.145) to (3.147) that the contribution to the mean drift force from the source-dipole product term is of similar magnitude to the contribution from the dipole alone; indeed at zero forward speed these contributions are equal.

The contribution from the source alone is also significant. This behaviour may be contrasted with that of an infinitely long rigid circular cylinder moving perpendicular to its axis in an unbounded fluid, which may be modelled by a uniform axial distribution of dipoles. Furthermore, for such a cylinder arranged horizontally below a free surface, only dipoles and higher order singularities are required to model completely the diffraction problem. In the case of diffraction by a vertical surface piercing cylinder however, the source term is required to model the volume flow rate, associated with the rise and fall of the free surface at the waterline of the cylinder. It is not surprising, therefore, that this term has a significant influence on the mean drift force.

Expressions (3.148) to (3.150) are plotted in Figure 3.2. From a comparison with the exact solution it is found that the relative error of the long wave approximation at zero forward speed is less than 8.5% for $ka<0.3$. Results for the long wave asymptotic analysis are also given for forward speeds corresponding to $\tau=\pm 0.1$.

3.3.4 Approximation of wave drift damping

Weakly moored floating bodies in deep water have low natural frequencies in their horizontal modes, therefore slowly varying resonant responses can be excited. In such motions there are two main damping forces, ie. wave drift damping and viscous damping. As discussed by Wichers (1982), Wichers and Huijsmans(1984) the wave drift damping may be approximated from the gradient of the mean drift force with respect to the forward speed, evaluated at U=0. For the

circular cylinder in long waves we differentiate equation (3.148) with respect to U and obtain the wave drift damping as

$$B_{WD}=-\frac{\partial \bar{F}_1}{\partial U} = 2.375\pi^2(k_0a)^3\rho A^2 a\omega_0. \tag{3.151}$$

To assess the significance of the wave drift damping we compare B_{WD} with the viscous damping. The viscous damping force may be approximated by

$$F_V=\frac{1}{2} C_D\rho|\dot{x}|\dot{x}\ 2ad,$$

where d is the draft of the cylinder and C_D is the drag coefficient. We linearize F_V by equalizing the energy consumption during one cycle, and obtain the equivalent viscous damping coefficient as

$$B_V=\frac{8}{3\pi}C_D\rho ad\omega_n x_a,$$

where x_a is the amplitude of the low frequency oscillation at the natural frequency ω_n. The ratio of the wave drift damping to the viscous damping is then given by

$$\frac{B_{WD}}{B_V}= 0.8906\frac{\pi^3}{C_D}\frac{(k_0A)^2(k_0a)^2}{k_0d}\frac{\omega_0}{\omega_n}\frac{a}{x_a},$$

According to the assumptions it is required that k_0a and k_0A are small, and ω_0/ω_n is large. The wave drift damping in equation (3.151) has been obtained for the infinite draft cylinder. For a finite draft cylinder the error of using equation (3.148) is roughly proportional to $2e^{-2k_0d}$. Thus kd is required to be sufficiently large.

As an example we let the parameters be $k_0d=2$, $\omega_0/\omega_n=10$ and $x_a/a=4$, and take the drag coefficient $C_D= 0.7$. Table 3.1 shows the

ratio of the wave drift damping to the viscous damping, for different wave steepnesses and different radii of the cylinder. It is seen from Table 3.1 that the importance of wave drift damping increases rapidly with k_0a or k_0A. When $k_0a=k_0A=0.3$ the wave drift damping is about one third of the viscous damping. The value of τ in the table is defined as $k_0x_a\omega_n/\omega_0$; it is included as a guide to ensure that our discussion concerns the behaviour at small speeds.

To conclude this investigation, we discuss briefly the simplified 3-D method investigated by Hearn et al. (1987), which neglects the forward speed dependent terms in the free surface condition. In that method the diffraction problem for an advancing body is taken to be identical to the diffraction problem for a body at zero forward speed, except that the wave frequency is replaced by the encounter frequency. The wave drift damping is simply obtained from the gradient of the mean drift force with respect to frequency, evaluated at zero forward speed. From our result for the cylinder we can examine the error introduced by the omission of the forward speed dependent terms in the free surface condition, over the low frequency range.

By differentiating equation (3.149) and noticing that

$$-\frac{\partial}{\partial U} = -2k_0a(k_0/g)^{1/2}\frac{\partial}{\partial(k_0a)}$$

we obtain the approximation to the wave drift damping as

$$B_{WDO} = -2(ga)^{3/2}(ga)^{-1/2}\frac{\partial \bar{F}_0}{\partial(k_0a)}$$

$$\simeq \frac{15}{8}\pi^2(k_0a)^3\rho A^2 a\omega_0 \qquad \text{as } k_0a\to 0, \tag{3.152}$$

This is plotted in Figure 3.3 alongside the result given by equation (3.151) using our more complete analysis. Comparison of B_{WDO} with B_{WD} shows that B_{WDO} is about 20% underestimated. This suggests that the simplified method is not particularly a good approximation in the long wave limit for the cylinder.

3.4 Concluding remarks

In this chapter we have discussed the general boundary value formulation and the far field formulation of the mean drift force. As an example of application, a vertical cylinder moving in long waves is examined and the asymptotic solution for the mean drift force has been obtained from a matched asymptotic expansion method. From the analysis, it is found that when the wavelength is long the mean drift force is proportional to the sixth power of the wave frequency; and the wave drift damping coefficient is proportional to the seventh power of the wave frequency. In the low frequency range the viscous damping may be dominant, but the wave drift damping may be significant too. It is also found that a source distribution must be included as well as a dipole distribution on the axis of the cylinder in order to obtain the diffraction potential. The next task is to develop a numerical method applicable for arbitrary geometries.

Chapter 4

ANALYSIS FOR ARBITRARY BODIES

A new theory for unsteady motions of arbitrary bodies at small forward speed in waves is presented in this chapter.

The conventional approach to tackling the forward speed problem is to use a source distribution method. The approach has not become generally applicable because of some inherent limitations. A fundamental feature of the conventional approach is that the steady potential disturbance is negligible in the free surface condition for the unsteady potential. This is not normally acceptable, except, perhaps, for a few special cases such as a deeply submerged body. This inappropriate simplification is the major limitation in application. Besides, even where the steady potential disturbance is negligible on the free surface, the computing required by this approach is very time consuming. Futhermore, if the steady potential is neglected, the theory is inconsistent and the consequences of the inconsistence should be estimated, which can not be normally done. These limitations may explain why most publications concerned with forward speed problems are restricted to slender ships. Zhao and Faltinsen (1988) and Zhao et al. (1988) may be the only people who have tackled the disturbance of the steady potential on the free surface. However, as discussed in Chapter 2, their consideration of the steady potential disturbance is not performed in a rigorous manner.

The work presented in this chapter is an attempt to solve the unsteady forward speed problem, while at the same time taking into

account the steady potential disturbance in a consisten manner. A forward speed perturbation is proposed and examined. According to the present theory, the boundary value problem is expanded into a zero-speed problem and a forward speed correction problem, and then solved successively. Two possibilities of expansion are identified and both are investigated. The content is organized as follows. After a presentation of the proposed forward speed perturbation theory, a new multipole expansion for the zero-speed potential is given. This is followed by the details of numerical implementation for both zero and nonzero speed problems; the Chapter ends with a discussion of the convergence of the theory.

4.1 A small forward speed perturbation theory

The formulation of the boundary value problem has been discussed in detail in the previous chapter. Up to first order in forward speed, the linearized formulations may be summarized as follows.

The total velocity potential is expressed in the form

$$\tilde{\Phi} = U\bar{\phi} + \mathrm{Re}\{[A(\phi_0 + \phi_7) + \sum_{j=1}^{6} i\omega\xi_j\phi_j]e^{i\omega t}\}. \tag{4.1}$$

The steady potential is governed by

$$\nabla^2\bar{\phi} = 0, \qquad \text{in } \Omega, \tag{4.2}$$

$$\bar{\phi}_z = 0, \qquad \text{on } z=0, \tag{4.3}$$

$$\frac{\partial\bar{\phi}}{\partial n} = n_1, \qquad \text{on } S_B, \tag{4.4}$$

$$\nabla\bar{\phi} \to 0, \qquad \text{as } r \to \infty. \tag{4.5}$$

Let ϕ denote any of the seven unsteady disturbance potentials or their combination. The unsteady potential ϕ is governed by

$$\nabla^2\phi = 0, \qquad \text{in } \Omega, \tag{4.6}$$

$$-k\phi + 2i\tau\vec{\nabla}(\bar{\phi}-x).\vec{\nabla}\phi + \phi_z - i\tau\phi\bar{\phi}_{zz} = 0, \qquad \text{on } z=0, \tag{4.7}$$

$$\frac{\partial\phi_7}{\partial n} = -\frac{\partial\phi_0}{\partial n}, \qquad \text{on } S_B, \tag{4.8}$$

$$\frac{\partial\phi_j}{\partial n} = n_j + \frac{U}{i\omega}m_j, \qquad \text{on } S_B, \qquad (j=1,2,\ldots,6) \tag{4.9}$$

$$\nabla\phi \to 0, \qquad z \to -\infty, \tag{4.10}$$

$$\frac{\partial\phi}{\partial x} + ik(1+2\tau)\phi \to 0 \quad \text{as} \quad x \to +\infty, \qquad \text{(two dimensions)} \tag{4.11}$$

$$\frac{\partial\phi}{\partial x} - ik(1-2\tau)\phi \to 0 \quad \text{as} \quad x \to -\infty, \qquad \text{(two dimensions)} \tag{4.12}$$

$$\sqrt{kR}\left[\frac{\partial\phi}{\partial R} + ik(1+2\tau\cos\theta)\phi\right] \to 0 \quad \text{as } R \to +\infty, \qquad \text{(three dimensions)} \tag{4.13}$$

where $R=\sqrt{x^2+y^2}$, $\omega = \omega_0 - Uk_0\cos\beta = \omega_0(1-\tau_0\cos\beta)$, $k=\omega^2/g=k_0(1-\tau_0\cos\beta)^2$, and $\tau=U\omega/g=\tau_0(1-\tau_0\cos\beta)$, with $\tau_0=U\omega_0/g$ and $\omega_0^2=gk_0$. It should be emphasized that the free surface condition and radiation conditions are only valid for small forward speed.

At small forward speed, the solution may be expanded into a series according to the forward speed. Each term is then solved subsequently. Because the forward speed not only affects the magnitude of the unsteady motion , but also affects its periodicity, two possibilities of expansion exist: expansion at wave frequency and expansion at encounter frequency. Both possibilities are investigated

below.

4.1.1 Expansion at wave frequency

4.1.1.1 The boundary value problem

Suppose the velocity potential ϕ_j can be expanded into a series of the form

$$\phi_j = \phi_{j0} + \tau_0\phi_{j1} + \ldots,$$

where $\tau_0=U\omega_0/g$, and the second subscript denotes the order of dependence on the forward speed. According to this expansion (cf. equation (3.40)), th incident potential is of the form

$$\phi_{00} = \phi_0, \qquad \phi_{01} = 0. \tag{4.14}$$

The free surface condition (4.7) is expanded into

$$-k_0\phi_{j0} + \frac{\partial\phi_{j0}}{\partial z} = 0, \qquad \text{on } z=0, \tag{4.15}$$

$$-k_0\phi_{j1} + \frac{\partial\phi_{j1}}{\partial z} = 2i\frac{\partial\phi_{j0}}{\partial x} - 2k_0\cos\beta\phi_{j0} + 2iQ_j, \qquad \text{on } z=0, \tag{4.16}$$

where

$$Q_j = \begin{cases} -\vec{\nabla}\bar{\phi}.\vec{\nabla}\phi_{j0} - \frac{1}{2}(\bar{\phi}_{xx}+\bar{\phi}_{yy})\phi_{j0}, & j=1,2,\ldots,6, \\ -\vec{\nabla}\bar{\phi}.\vec{\nabla}(\phi_{j0}+\phi_{00}) - \frac{1}{2}(\bar{\phi}_{xx}+\bar{\phi}_{yy})(\phi_{j0}+\phi_{00}), & j=7. \end{cases} \tag{4.17}$$

Here for numerical reasons the Laplace equation has been used to replace the second derivatives in the vertical direction by derivatives in the horizontal direction, since the latter are easier

to calculate. For incident waves, there is no steady flow disturbance. Hence, Q_0=0. Besides, it can be easily verified that the right hand side of equation (4.16) is zero for incident waves. That would confirm that ϕ_{01}=0. For the disturbance potentials (j=1,2,...,7), Q_j tends to zero at infinity. The rate of decaying of Q_j is much faster than that of the other terms on the right hand side of equation (4.16) in three dimensions, whereas these other terms do not decay to zero in two dimensions in the direction where the incident waves come from.

The body surface condition is expanded into

$$\frac{\partial\phi_{70}}{\partial n} = -\frac{\partial\phi_{00}}{\partial n}, \qquad \frac{\partial\phi_{71}}{\partial n} = 0, \qquad \text{on } S_B, \tag{4.18}$$

$$\frac{\partial\phi_{j0}}{\partial n} = n_j, \qquad \frac{\partial\phi_{j1}}{\partial n} = -i\frac{m_j}{k_0} \qquad \text{on } S_B. \quad (j=1,2,\ldots,6) \tag{4.19}$$

At infinity the disturbance potential satisfies

$$\frac{\partial\phi_{j0}}{\partial R} = -ik_0\phi_{j0}, \qquad \text{as } R\to\infty, \tag{4.20}$$

$$\frac{\partial\phi_{j1}}{\partial R} = -ik_0\phi_{j1} - 2ik_0(\cos\theta-\cos\beta)\phi_{j0}, \qquad \text{as } R\to\infty, \tag{4.21}$$

for three dimensional problems, where $x=R\cos\theta$ $y=R\sin\theta$; or

$$\frac{\partial\phi_{j0}}{\partial x} = -ik_0\phi_{j0}, \qquad \frac{\partial\phi_{j1}}{\partial x} = -ik_0\phi_{j1} - 2ik_0(1-\cos\beta)\phi_{j0}, \quad \text{as } x\to\infty, \tag{4.22}$$

$$\frac{\partial\phi_{j0}}{\partial x} = ik_0\phi_{j0}, \qquad \frac{\partial\phi_{j1}}{\partial x} = ik_0\phi_{j1} - 2ik_0(1+\cos\beta)\phi_{j0}, \quad \text{as } x\to-\infty, \tag{4.23}$$

for two dimensional problems. β takes two values only: $\beta=\pi$ for head seas and β=0 for following seas for two dimensional problems.

4.1.1.2 Integral expressions of ϕ_{j0} and ϕ_{j1}

Three dimensions

Applying Green's second identity over a fluid domain Ω enclosed by a surface S, where S is defined by $S=S_B+S_R+S_D+S_F$, with

S_B: the wetted body surface,

S_R: a vertical circular cylindrical surface of large radius,

S_D: a horizontal closure surface at great depth,

S_F: the part of the free surface bounded by S_0 and S_R;

we obtain

$$\oint_S (\phi_j \frac{\partial G}{\partial n} - G\frac{\partial \phi_j}{\partial n})\, dS = \begin{cases} -4\pi\phi_j(\vec{x}), & \text{for } \vec{x} \text{ in } \Omega, \\ -2\pi\phi_j(\vec{x}), & \text{for } \vec{x} \text{ on } S, \\ 0, & \text{for } \vec{x} \text{ out of } \Omega, \end{cases} \tag{4.24}$$

(j=1,2,...,7), where the constant 2π is valid over smooth surface only, and the Green function is chosen in the form of $G = 1/r + H$ with H a harmonic function in the entire fluid. Instead of taking G as a translating pulsating source potential which is the conventional case, here a simpler Green function, i.e. a pulsating source potential, is used

$$\begin{aligned} G &= \frac{1}{r} - \frac{1}{r'} + 2\oint \frac{\lambda e^{\lambda(z+\zeta)}}{\lambda - k_0} J_0(\lambda R)\, d\lambda \\ &= \frac{1}{r} + \frac{1}{r'} + 2k\oint \frac{e^{\lambda(z+\zeta)}}{\lambda - k} J_0(\lambda R)\, d\lambda \end{aligned} \tag{4.25}$$

where the path of the integration is above the pole, and

$$r = [(x-\xi)^2 + (y-\eta)^2 + (z-\zeta)^2]^{1/2},$$

$$r' = [(x-\xi)^2 + (y-\eta)^2 + (z+\zeta)^2]^{1/2}.$$

After utilizing the boundary conditions, we obtain

$$\phi_j = \frac{1}{\alpha}\int_{S_B} (G\frac{\partial \phi_j}{\partial n} - \phi_j\frac{\partial G}{\partial n})\, dS + \frac{1}{\alpha}\int_{S_F} \tau_0 G(2i\frac{\partial \phi_j}{\partial x} - 2k_0\cos\beta\phi_j + 2iQ_j)\, dS$$
$$- \frac{1}{\alpha}\int_{S_R} 2\tau_0 ik_0(\cos\theta-\cos\beta)G\phi_j\, dS, \tag{4.26}$$

where α takes the value 2π if the field point is on the boundary surface and the surface is smooth. Ordering according to τ_0 yields

$$\phi_{j0} = \frac{1}{\alpha}\int_{S_B} (G\frac{\partial \phi_{j0}}{\partial n} - \phi_{j0}\frac{\partial G}{\partial n})\, dS, \tag{4.27}$$

$$\phi_{j1} = \frac{1}{\alpha}\int_{S_B} (G\frac{\partial \phi_{j1}}{\partial n} - \phi_{j1}\frac{\partial G}{\partial n})\, dS + \frac{1}{\alpha} J, \tag{4.28}$$

where J is defined by

$$J = 2i\int_{S_F} G(\frac{\partial \phi_{j0}}{\partial x} + ik_0\cos\beta\phi_{j0} + Q_j)\, dS - \int_{S_R} 2ik_0(\cos\theta-\cos\beta)G\phi_{j0}\, dS. \tag{4.29}$$

From the asymptotic expressions (i.e. $(\phi_j, G) \sim e^{k_0 z}$ as $R\to\infty$), the last integral can be integrated explicitly with respect to the z-coordinate. After integration the function J becomes

$$J = 2i\int_{S_F} G(\frac{\partial \phi_{j0}}{\partial x} + ik_0\cos\beta\phi_{j0} + Q_j)\, dS - \oint_{C_R} i(\cos\theta-\cos\beta)G\phi_{j0}\, dl. \tag{4.30}$$

where C_R is the intersection line (a circle) of the cylindrical surface S_R with the mean free surface.

Two dimensions

Similar to the three dimensional analysis, we apply Green's second identity and utilize the boundary conditions to obtain

$$\phi_j = \frac{1}{\alpha}\int_{S_B}(G\frac{\partial\phi_j}{\partial n} - \phi_j\frac{\partial G}{\partial n})\,dS + \frac{1}{\alpha}\int_{S_F}\tau_0 G(2i\frac{\partial\phi_j}{\partial x} - 2k_0\cos\beta\phi_j + 2iQ_j)\,dS$$
$$- \frac{1}{\alpha}\int_{S_R^+} 2\tau_0 ik_0(1-\cos\beta)G\phi_j\,dS + \frac{1}{\alpha}\int_{S_R^-} 2\tau_0 ik_0(1+\cos\beta)G\phi_j\,dS, \tag{4.31}$$

where α takes the value π if the field point is on a smooth boundary surface; S_R^+ and S_R^- are two vertical lines at $x\to\infty$ and $x\to-\infty$ respectively. Ordering according to τ_0 yields

$$\phi_{j0} = \frac{1}{\alpha}\int_{S_B}(G\frac{\partial\phi_{j0}}{\partial n} - \phi_{j0}\frac{\partial G}{\partial n})\,dS, \tag{4.32}$$

$$\phi_{j1} = \frac{1}{\alpha}\int_{S_B}(G\frac{\partial\phi_{j1}}{\partial n} - \phi_{j1}\frac{\partial G}{\partial n})\,dS + \frac{1}{\alpha}J, \tag{4.33}$$

where J is defined by

$$J = \int_{S_F} G(2i\frac{\partial\phi_{j0}}{\partial x} - 2k_0\cos\beta\phi_{j0} + 2iQ_j)\,dS$$
$$- \int_{S_R^+} 2ik_0(1-\cos\beta)G\phi_{j0}\,dS + \int_{S_R^-} 2ik_0(1+\cos\beta)G\phi_{j0}\,dS. \tag{4.34}$$

Again, the last two integrals can be integrated explicitly by using the asymptotic expressions (i.e. $(\phi_j, G)\sim e^{k_0 z}$)

$$J = 2i \int_{S_F} G\left(\frac{\partial \phi_{j0}}{\partial x} + k_0 \cos\beta \phi_{j0} + Q_j\right) dS$$

$$- i \left[(1-\cos\beta)(G\phi_{j0})_{+\infty} - (1+\cos\beta)(G\phi_{j0})_{-\infty}\right]. \tag{4.35}$$

The last two free terms are evaluated at $x \to +\infty$ and $x \to -\infty$ respectively. However, since neither G nor ϕ_{j0} tends to a definite value at infinity, the above expression must be interpreted in a limit sense.

Recall that β only takes the value 0 or π. For head seas ($\beta=\pi$, that is, the incident waves come towards the body in the opposite direction of the forward speed.), the free term at $x \to -\infty$ in the above expression vanishes and

$$J = 2i\left[\int_{S_F} G\left(\frac{\partial \phi_{j0}}{\partial x} - ik_0 \phi_{j0} + Q_j\right) dS - (G\phi_{j0})_{+\infty}\right]. \tag{4.36}$$

The expression for the following sea ($\beta=0$) is similar, but different in some signs.

4.1.2 Expansion at encounter frequency

Alternatively, we may carry out the small forward speed perturbation analysis at the encounter frequency for the diffraction problem. Accordingly, for forced oscillations in otherwise calm water, we may expand the total solution at the frequency of oscillation.

Using the other small parameter $\tau = U\omega/g$, we suppose that the

velocity potential can be expanded as the series

$$\phi_j = \phi_{j0} + \tau \phi_{j1} + \ldots, \qquad (j=1,2,\ldots,7)$$

with ϕ_{j0} the solution at zero forward speed and ϕ_{j1} the correction term proportional to the forward speed. For the diffraction problem we also need to expand the incident wave potential of frequency ω_0 into the incident potential of frequency ω plus a correction term

$$\phi_{00} = \frac{ig}{\omega} e^{kz-ik(x\cos\beta+y\sin\beta)}, \tag{4.37}$$

$$\phi_{01} = \cos\beta[2k(z-ix\cos\beta-iy\sin\beta)-1] \frac{ig}{\omega} e^{kz-ik(x\cos\beta+y\sin\beta)}. \tag{4.38}$$

The free surface condition (4.7) is expanded into

$$-k\phi_{j0} + \frac{\partial\phi_{j0}}{\partial z} = 0, \qquad \text{on } z=0, \tag{4.39}$$

$$-k\phi_{j1} + \frac{\partial\phi_{j1}}{\partial z} = 2i\frac{\partial\phi_{j0}}{\partial x} + 2iQ_j, \qquad \text{on } z=0, \tag{4.40}$$

where Q_j has the same definition as in the wave frequency expansion.

At infinity, Q_j tends to zero. The rate of decay of Q_j is much faster than that of the other term on the right hand side of equation (4.40) in three dimensions, whereas the other terms do not decay to zero in two dimensions.

The body surface condition is expanded into

$$\frac{\partial\phi_{70}}{\partial n} = -\frac{\partial\phi_{00}}{\partial n}, \qquad \frac{\partial\phi_{71}}{\partial n} = -\frac{\partial\phi_{01}}{\partial n}, \tag{4.41}$$

$$\frac{\partial\phi_{j0}}{\partial n} = n_j, \qquad \frac{\partial\phi_{j1}}{\partial n} = -\frac{i}{k} m_j, \qquad \text{on } S_B. \quad (j=1,2,\ldots,6) \tag{4.42}$$

At infinity the disturbance potentials satisfy

$$\frac{\partial \phi_{j0}}{\partial R} = -ik\phi_{j0}, \qquad \text{as } R\to\infty, \tag{4.43}$$

$$\frac{\partial \phi_{j1}}{\partial R} = -ik\phi_{j1} - 2ik\cos\theta\phi_{j0}, \qquad \text{as } R\to\infty, \tag{4.44}$$

for three dimensional problems, where $x=R\cos\theta$ $y=R\sin\theta$; or

$$\frac{\partial \phi_{j0}}{\partial x} = -ik\phi_{j0}, \qquad \frac{\partial \phi_{j1}}{\partial x} = -ik\phi_{j1} - 2ik\phi_{j0}, \qquad \text{as } x\to\infty, \tag{4.45}$$

$$\frac{\partial \phi_{j0}}{\partial x} = ik\phi_{j0}, \qquad \frac{\partial \phi_{j1}}{\partial x} = ik\phi_{j1} - 2ik\phi_{j0}, \qquad \text{as } x\to-\infty, \tag{4.46}$$

for two dimensional problems.

Following similar procedures to those used in the wave frequency expansion, i.e., applying Green's second identity, utilizing the boundary conditions, and then ordering according to τ, we obtain the zeroth order and the first order potentials as follows

$$\phi_{j0} = \frac{1}{\alpha}\int_{S_B} (G\frac{\partial \phi_{j0}}{\partial n} - \phi_{j0}\frac{\partial G}{\partial n})\, dS, \tag{4.47}$$

$$\phi_{j1} = \frac{1}{\alpha}\int_{S_B} (G\frac{\partial \phi_{j1}}{\partial n} - \phi_{j1}\frac{\partial G}{\partial n})\, dS + \frac{1}{\alpha} J. \tag{4.48}$$

For three dimensional problems, J is found to have the form

$$J = 2i\int_{S_F} G(\frac{\partial \phi_{j0}}{\partial x} + Q_j)\, dS - \oint_{C_R} i\cos\theta G\phi_{j0}\, dl, \tag{4.49}$$

where α takes the value 2π if the field point is on a smooth boundary surface; the surfaces S_B, S_R, S_F and the line C_R are defined as in Section 4.1.1; and the line integral is obtained from the itegration

over S_R with respect to the z-coordinate.

For two dimensional problems, J is found to have the form

$$J = 2i\int_{S_F} G(\frac{\partial \phi_{j0}}{\partial x} + Q_j)\, dS - i(G\phi_{j0})_{+\infty} + i(G\phi_{j0})_{-\infty}, \tag{4.50}$$

where α takes the value π, if the field point is on a smooth boundary surface; the last two terms are evaluated at $x \to +\infty$ and $x \to -\infty$ respectively; and the whole expression must be interpreted in a limit sense.

4.1.3 Discussion

The above perturbation formulations have been derived formally without discussing their convergence. In fact, some subtle considerations may be required to justify the perturbation procedure. For the moment, we shall ignore that point. Instead, let us focus our attention on the numerical implementation. The theoretical considerations concerning the convergence of the perturbation procedure will be discussed in the last section of the present chapter.

The boundary integral expression obtained may be solved by a standard boundary element technique. It can be expected that the computation will be dominated by the evaluation of the free surface integral J, because the integrand is an oscillatory function. In principle, once the boundary value problem is solved, ϕ_0, and hence the integrand, can be computed numerically from the boundary integral

expression. Clearly, this can not be expected to be satisfactory for evaluation of J. Therefore, it is desirable to find some analytical expressions for the velocity potential.

4.2 Multipole expansion solution at zero forward speed

4.2.1 Introduction

In finite depth water, eigenfunction expansions can be applied to construct an analytical expression for the velocity potential, valid in a domain exterior to the body. However, as the water depth increases, the eigenvalues tend to pack together, and the eigenfunctions become undistinguishable from one to another. Consequently, an unrealistic number of eigenfunctions is required in the series expression. In such circumstances, it is appropriate to find alternative expressions.

In infinite depth water, multipole expansions may be utilized to describe the velocity potential. For two dimensional motions, Ursell (1949) has constructed a set of multipoles placed on the mean free surface. These multipole potentials are simple elementary functions, and easy to evaluate. Two wave potentials are added to the set to satisfy the radiation condition. He has shown the existence of the expansion of the velocity potential in terms of these multipoles. Using these multipoles, Ursell solved the heaving motion of a semi-immersed circle. His method was extended to three dimensions by Havelock (1955) for the heaving motion of a semi-immersed sphere.

For completely submerged bodies, Ursell (1950) constructed another set of multipoles in two dimensions. These multipole potentials are more complicated, since they are in integral forms. The multipole potentials are derived from the derivatives of the pulsating-source potential with respect to appropriate parameters. All terms contribute to the velocity potential at infinity. That is, unlike the multipoles for the floating bodies, the wave terms and local disturbance terms are not separated. These multipoles are not easy to use, particularly in calculation of a free surface integral involving the velocity potential. Both two dimensional and three dimensional multipole expansions are reviewed by Thorne (1953), who has also given forms in finite depth water.

In the following a new multipole expansion is presented. Both submerged bodies and floating bodies are treated in the same manner. Local disturbances and far field expressions are noticeably separated in the multipole expansions. These new multipoles can be regarded as generalizations of Ursell's (1949) multipoles for floating bodies. In fact, Ursell's multipoles can be recovered from the present multipoles by allowing the multipoles being placed on the mean free surface.

4.2.2 Two dimensional multipoles

Let a Cartesian coordinate system be defined such that the z-axis is pointing upwards with the origin on the mean free surface and the x-axis is lying horizontally. We seek the velocity potential

outside a circle of radius a with the centre at (0,f) ($f \leq 0$) satisfying

$$\nabla^2\phi = 0 \qquad \text{in } \Omega, \tag{4.51}$$

$$\phi_z - k\phi = 0 \qquad \text{on } z=0, \tag{4.52}$$

$$\phi_n = v_n(\theta) \qquad \text{on } r=a, \quad (r=\sqrt{x^2+(z-f)^2}) \tag{4.53}$$

$$\phi_x \sim \pm ik\phi \qquad \text{as } x \to \mp\infty, \quad \text{respectively}, \tag{4.54}$$

where subscripts on ϕ denote derivatives; Ω denotes the fluid domain; $v_n(\theta)$ is the prescribed normal velocity with the direction of the normal defined out of the fluid; and k is the wavenumber, given by $k=\omega^2/g$. The last condition (radiation condition) is necessary to ensure that ϕ so defined represents the wave potential due to the motion of the body or due to the modification by the body of an incident wave train. (Note that we are here using ϕ to represent the zero-speed potentials ϕ_{j0})

First we shall find the velocity potentials of some singularities, placed at point (0,f), satisfying the Laplace equation and the free surface condition (4.52). These can be constructed from the simple singular solutions of the Laplace equation. By separation of variables in a polar coordinate system, the simplest singular solutions of the two dimensional Laplace equation are found to be

$$\ln\frac{1}{r}, \quad \frac{\cos m\theta}{r^m}, \quad \frac{\sin m\theta}{r^m}, \qquad (x=r\sin\theta,\ z-f=-r\cos\theta)$$

and their images above the mean free surface

$$\ln\frac{1}{r'},\quad \frac{\cos m\theta'}{r'^{m}},\quad \frac{\sin m\theta'}{r'^{m}},\qquad (x=r'\sin\theta',\ z+f=r'\cos\theta')$$

where the polar coordinates (r,θ) and (r',θ') are defined in Figure 4.1.

We note that the sum of a singular solution and its image satisfies the "rigid wall" condition $\partial\phi/\partial z=0$ on $z=0$, whereas the difference satisfies condition $\phi=0$ on $z=0$. This suggests that it is possible to construct a linear combination of such sums and differences to satisfy the free surface condition (4.52). For symmetrical flow the solution may be written in the form of

$$c_m = a^m\left[\frac{\cos m\theta}{r^m} + \frac{\cos m\theta'}{r'^{m}} + A\left(\frac{\cos(m-1)\theta}{r^{m-1}} - \frac{\cos(m-1)\theta'}{r'^{m-1}}\right)\right],$$

for $m>1$. Substitution of c_m into the free surface condition (4.52) yields the constant as $A=k/(m-1)$. A similar procedure can be followed for the anti-symmetrical flow. We find

$$c_1 = a\left[\frac{\cos\theta}{r} + \frac{\cos\theta'}{r} + k\ln\frac{r'}{r}\right], \tag{4.55}$$

$$c_m = a^m\left[\frac{\cos m\theta}{r^m} + \frac{\cos m\theta'}{r'^{m}} + \frac{k}{m-1}\left(\frac{\cos(m-1)\theta}{r^{m-1}} - \frac{\cos(m-1)\theta'}{r'^{m-1}}\right)\right], \tag{4.56}$$

$$s_m = a^m\left[\frac{\sin m\theta}{r^m} + \frac{\sin m\theta'}{r'^{m}} + \frac{k}{m-1}\left(\frac{\sin(m-1)\theta}{r^{m-1}} - \frac{\sin(m-1)\theta'}{r'^{m-1}}\right)\right], \tag{4.57}$$

for $m=2,3,\ldots$. These singular solutions are wave-free potentials. They decay to zero at large distances as $|x|\to\infty$. In other words they correspond to a local disturbance only.

A potential representing outgoing waves at infinity is required. For symmetrical motion, such a potential is found to be the

familiar pulsating source potential

$$c_0 = \ln\frac{r'}{r} + 2\oint_0^\infty \frac{e^{\lambda(z+f)}}{\lambda-k}\cos\lambda x\, d\lambda, \tag{4.58}$$

where $\oint$ denotes that the path of the contour integral is above the pole. For anti-symmetrical motion, the wave potential is found to be the dipole potential, derived from $-a\frac{\partial c_0}{\partial x}$,

$$s_1 = a\{\frac{\sin\theta}{r} + \frac{\sin\theta'}{r'} + 2k\oint_0^\infty \frac{e^{\lambda(z+f)}}{\lambda-k}\sin\lambda x\, d\lambda\ \}. \tag{4.59}$$

These two wave potentials (4.58) and (4.59) can be equivalently expressed in terms of the exponential integral $E_1(Z')$ as defined in Abramowitz and Stegun[1]

$$c_0 = \ln\frac{r'}{r} + 2\{\mathrm{Re}[e^{Z'}E_1(Z')] - \pi i e^{k(f+z)-ik|x|}\}, \tag{4.60}$$

$$s_1 = a\{\frac{\sin\theta}{r} + \frac{\sin\theta'}{r'} + 2k[\mathrm{Im}[e^{Z'}E_1(Z')] + \mathrm{sgn}(x)\pi e^{k(f+z)-ik|x|}]\}, \tag{4.61}$$

where $Z'=k(z+f+ix)=kr'e^{i\theta'}$; $\mathrm{sgn}(x)=1$ for $x>0$, and $\mathrm{sgn}(x)=-1$ for $x<0$. It can be verified that the radiation condition (4.54) is satisfied, since

$$e^{Z'}E_1(Z') \sim O(\frac{1}{|x|}),\ \ln\frac{r'}{r} \sim O(\frac{1}{|x|}),\quad \text{as } |x|\to\infty.$$

For bodies floating on the free surface, we simply let f be zero. The multipoles are simplified to

$$c_0 = 2\mathrm{Re}[e^{Z'}E_1(Z')] - \pi i e^{kz-ik|x|}, \tag{4.62}$$

$$c_{2m} = 2a^{2m}[\frac{\cos 2m\theta}{r^{2m}} + \frac{k}{2m-1}\frac{\cos(2m-1)\theta}{r^{2m-1}}], \qquad (m=1,2,\ldots) \tag{4.63}$$

$$s_1 = 2a\{\frac{\sin\theta}{r} + 2k[\mathrm{Im}[e^{Z'}E_1(Z')] + \mathrm{sgn}(x)\pi e^{kz-ik|x|}]\}, \tag{4.64}$$

$$s_{2m+1} = 2a^{2m+1}\left[\frac{\sin(2m+1)\theta}{r^{2m+1}} + \frac{k}{2m}\,\frac{\sin 2m\theta}{r^{2m}}\right]. \qquad (m=1,2,\ldots) \tag{4.65}$$

The other terms become zero. Now the multipoles degenerate to those obtained by Ursell (1949).

We may express the velocity potential in terms of a series of functions c_0, c_m and s_m $(m=1,2,\ldots)$

$$\phi = a_0 c_0 + \sum_{m=1}^{\infty} [a_m c_m + b_m s_m]. \tag{4.66}$$

The series satisfies the governing equation and all boundary conditions except the condition on the body surface. The unknown coefficients a_m and b_m are then determined from the body surface condition.

A general justification of the existence of expansion (4.66) is difficult to obtain. In principle, one needs to prove that for any given function $v_n(\theta)$ there exists a set of coefficients a_0, a_m and b_m such that the series is convergent and its radial derivative contains the component $v_n(\theta)$ on r=a. For the case f=0 (floating bodies), Ursell (1949) has shown that such an expansion is possible, at least for ka<1.5. For completely submerged bodies, Ursell (1950) has proven the existence of a different multipole expansion. For the present multipole expansion, we shall assume the velocity potential can be uniquely expressed by equation (4.66) without giving proof.

It is interesting to see the limit case at zero frequency. As

$ka \to 0$ and $|f| \to \infty$,

$$c_m \simeq 2\ln\frac{1}{r} + \ldots, \quad c_m \simeq 2a^m \frac{\cos 2m\theta}{r^{2m}}, \quad s_1 \simeq 2a\frac{\sin\theta}{r}, \quad s_{2m+1} \simeq 2a^{2m+1}\frac{\sin(2m+1)\theta}{r^{2m+1}}.$$

The series (4.66) becomes a Fourier series expansion over $(0,\pi/2)$, and the multipole expansion certainly exists.

4.2.3 Three dimensional multipoles

Three dimensional multipoles can be derived by following the same procedure.

As shown in Figure 4.2, a Cartesian coordinate system is defined with the Oxy plane at the mean free surface and the z-axis pointing upwards. The cylindrical polar coordinates (R,α,z) and spherical polar coordinates (r,α,θ) are defined by $x=R\cos\alpha$, $y=R\sin\alpha$; $\cos\theta=-(z-f)/r$, $\sin\theta=R/r$. Also defined are the polar coordinates (r',α,θ') by $\cos\theta'=(z+f)/r'$, $\sin\theta'=R/r'$. We seek the velocity potential $\Phi=\mathrm{Re}[\phi e^{i\omega t}]$ outside a sphere of radius a with the centre at $(0,0,f)$ $(f\leq 0)$ satisfying

$$\nabla^2\phi = 0 \qquad \text{in } \Omega, \tag{4.67}$$

$$\phi_z - k\phi = 0 \qquad \text{on } z=0, \tag{4.68}$$

$$\phi_n = v_n(\alpha,\theta) \qquad \text{on } r=a, \quad (r=\sqrt{R^2+(z-f)^2}) \tag{4.69}$$

$$\sqrt{kR}\left(\frac{\partial\phi}{\partial R} + ik\phi\right) \to 0 \qquad \text{as } R \to +\infty. \tag{4.70}$$

Here again we are dealing with the zero-speed potentials ϕ_{j0}, represented by ϕ for simplicity.

The simplest solutions of the Laplace equation obtained from separation of variables are

$$\frac{P_n^m(\mu)}{r^{n+1}}\cos m\alpha, \quad \frac{P_n^m(\mu)}{r^{n+1}}\sin m\alpha, \qquad (\mu=\cos\theta=-\frac{z-f}{r})$$

and their images above the mean free surface

$$\frac{P_n^m(\mu')}{r'^{n+1}}\cos m\alpha, \quad \frac{P_n^m(\mu')}{r'^{n+1}}\sin m\alpha, \qquad (\mu'=\cos\theta'=\frac{z+f}{r'})$$

where $n\geq m=0,1,2,\ldots$; $P_n^m(\mu)$ is the associated Legendre function as defined in Abramowitz and Stegun[1]: $P_n^m(\mu) = (-1)^m(1-\mu^2)^{m/2}\frac{d^m}{d\mu^m}P_n(\mu)$, with $P_n(\mu)$ the Legendre function.

From the facts that the sum of a singularity and its image satisfies $\partial\phi/\partial z = 0$ on $z=0$ and the difference satisfies $\phi=0$ on $z=0$, we find the following linear combinations of the sums and differences satisfy the free surface condition (4.70)

$$\phi_{nm} = a^{n+1}\{\frac{P_n^m(\mu)}{r^{n+1}} + \frac{P_n^m(\mu')}{r'^{n+1}} + \frac{k}{n-m}\left[\frac{P_{n-1}^m(\mu)}{r^n} - \frac{P_{n-1}^m(\mu')}{r'^n}\right]\} \tag{4.71}$$

for $n>m=0,1,2,\ldots$. These terms vanish at large distances: $\phi_{nm}\sim O(1/r^n)$ as $r\to\infty$. They are wave-free potentials. To find the wave terms, we make use of the solution obtained from separation of variables in cylindrical polar coordinates: $e^{\lambda(z+f)}J_m(\lambda R)\{\cos m\alpha, \sin m\alpha\}$, with $J_m(\lambda R)$ the first kind of Bessel function of mth order. Since in the wave-free terms n is required to be larger than m, the wave terms must be associated with terms at n=m. We seek the wave potential in the form of

$$\phi_{mm} = a^{m+1}\{\frac{P_m^m(\mu)}{r^{m+1}} + \int_0^\infty A(\lambda)e^{\lambda(z+f)}J_m(\lambda R)\, d\lambda\ \}.$$

From $(\frac{\partial}{\partial z} - k)\frac{P_n^m(\mu)}{r^{n+1}} = -(\frac{\partial}{\partial z} + k)\frac{P_n^m(\mu')}{r'^{n+1}}$ on $z=0$ and

$$\frac{P_n^m(-\mu')}{r'^{n+1}} = \frac{1}{(n-m)!}\int_0^\infty \lambda^n e^{\lambda(z+f)}J_m(\lambda R)\, d\lambda, \quad (\text{for } z+f<0) \tag{4.72}$$

(Gray et al. (1966) p.100) and also ${}_n^m P\ (-\mu') = (-1)_n^{n-m} P\ (\mu')$, we can deduce $A(\lambda)$ by substituting ϕ_{mm} into the free surface condition (4.68). We obtain

$$\phi_{mm} = a^{m+1}\{\frac{P_m^m(\mu)}{r^{m+1}} + (-1)^m \int_0^\infty \frac{(\lambda+k)\lambda^m}{\lambda-k} e^{\lambda(z+f)}J_m(\lambda R)\, d\lambda\ \},$$

$$= a^{m+1}\{\frac{P_m^m(\mu)}{r^{m+1}} + \frac{P_m^m(\mu')}{r'^{m+1}} + 2k(-1)^m \int_0^\infty \frac{\lambda^m}{\lambda-k} e^{\lambda(z+f)}J_m(\lambda R)\, d\lambda\ \}. \tag{4.73}$$

The path of the contour integral is defined above the pole. In particularly, from $P_0^0=1$, we find that ϕ_{00} is the familiar pulsating source potential

$$\phi_{00} = a\ \{\frac{1}{r} + \frac{1}{r'} + 2k\int_0^\infty \frac{1}{\lambda-k} e^{\lambda(z+f)}J_0(\lambda R)\, d\lambda\ \}. \tag{4.74}$$

At large distances

$$\phi_{mm} \sim \sqrt{\frac{2}{\pi kR}}\, e^{k(z+f)-ikR} + O(\frac{1}{R}), \qquad R\to\infty,$$

represents outgoing waves, and the radiation condition is satisfied.

For bodies floating on the free surface, we let f be made zero. Then $\mu'=-\mu$ and $r'=r$. The multipoles have simpler forms,

$$\phi_{nm} = 2a^{n+1}\{\frac{P_n^m(\mu)}{r^{n+1}} + \frac{k}{n-m}\frac{P_{n-1}^m(\mu)}{r^n}\}, \qquad \text{(for n-m even)} \tag{4.75}$$

$$\phi_{mm} = a^{m+1}\{(1+(-1)^m)\frac{P_m^m(\mu)}{r^{m+1}} + 2k(-1)^m \int_0^\infty \frac{\lambda^m}{\lambda-k} e^{\lambda z} J_m(\lambda R)\, d\lambda\}. \tag{4.76}$$

The other terms (i.e. n-m odd) become zero.

The zero-speed velocity potential ϕ may be expressed in a series in terms of these singular solutions

$$\phi = \sum_{n=0}^{\infty}\sum_{m=0}^{n}(a_{nm}\cos m\alpha + b_{nm}\sin m\alpha)\,\phi_{nm} \tag{4.77}$$

$$= \sum_{m=0}^{\infty}[(\sum_{n=m}^{\infty} a_{nm}\phi_{nm})\cos m\alpha + (\sum_{n=m}^{\infty} b_{nm}\phi_{nm})\sin m\alpha] \tag{4.78}$$

For given prescribed motion $V_n(\alpha,\theta)$, the unknown coefficients a_m and b_m can be determined from the body surface condition (4.69).

For the special case of the axisymmetrical motion about the z-axis (m=0), the three dimensional multipoles have been pointed out by Havelock (1955), also discussed by MacCamy (1954). The general expressions derived here agree with those in Wehausen and Laitone (1960) (equations (13.20) and (13.21)). In the present context, the multipoles are constructed in a manner which shows clearly the physical implication. The two dimensional multipoles derived here seem to be original.

4.3 Numerical implementation

Although the integral formulation obtained in Section 4.1 can be solved by standard numerical discretization on the body surface, it may not be appropriate to apply the multipole expansion directly on the body surface, if the body is not a sphere or a circular cylinder. Therefore, it was decided to use a coupled numerical technique.

The fundamental idea of a coupled numerical technique is to divide the fluid domain into two or more domains by some artificial control surfaces, and apply different numerical formulations on each domain. These formulations are matched over the joint surfaces.

In the present numerical implementation, two dimensional motions are considered. This problem may be related to a horizontal cylindrical offshore structure, or an elongated ship in beam waves together with a lateral forward speed (or current). The fluid domain is divided into an inner domain close to the body and an outer domain outside an artificial circle S_J, which encloses the body, as shown by Figure 4.3. For a deeply submerged body, S_J is taken as a full circle and completely submerged. For floating bodies, S_J is taken as a semicircle with the centre on the free surface. In the inner domain a closed boundary integral expression with the simple Rankine source is used, whereas in the outer domain the integral expressions derived in Section 3.1 may be used. For the zero-speed problem another possibility, which we have deliberately developed, is to apply the multipole expansion. The matching procedure for the zero-speed problem is discussed first.

4.3.1 The zero-speed potential

In the inner domain, a similar boundary integral expression to those obtained in Section 4.1 is applied, but with a simpler Rankine source Green function.

$$\phi(\vec{x}) = \frac{1}{\alpha}\oint_S \left(G\frac{\partial\phi}{\partial n} - \phi\frac{\partial G}{\partial n}\right) dS, \qquad \left(\alpha = \begin{cases} \pi, & \text{for } \vec{x} \text{ on smooth S,} \\ 2\pi, & \text{for } \vec{x} \text{ in S,} \\ 0, & \text{for } \vec{x} \text{ outside S.} \end{cases}\right) \tag{4.79}$$

where $\vec{x}$ denotes the field point (x,z); S consists of S_B, S_J and the portion of free surface between these two surfaces, if any; the direction of the normal is defined to be out of the fluid enclosed by S. Here, we are dealing with the zero-speed potentials ϕ_{j0}, but for simplicity these are represented by ϕ.

The Rankine source Green function is defined as

$$G(\vec{x},\vec{\xi}) = \ln\frac{1}{r}, \qquad r=\sqrt{(x-\xi)^2+(z-\zeta)^2}. \tag{4.80}$$

This function is in fact a sink potential, but we refer it as source in the sense that the strength is interpreted to be negative. By taking the field point (x,z) on the boundary S, the velocity potential on the boundary can be solved. The boundary surface is discretized into elements and over each element the variations of the velocity potential and of its derivatives are approximated by shape functions $N_L(\gamma)$

$$\phi = \sum_{L=1}^{m} N_L(\gamma)\phi_L, \tag{4.81}$$

$$\frac{\partial \phi}{\partial n} = \sum_{L=1}^{m} N_L(\gamma)\left(\frac{\partial \phi}{\partial n}\right)_L, \tag{4.82}$$

where ϕ_L and $\left(\frac{\partial \phi}{\partial n}\right)_L$ are values at the node L with L locally labelled. In the implementation developed here isoparametric quadratic elements were used. The three shape functions are therefore given by

$$N_1(\gamma) = \frac{1}{2}\gamma(\gamma-1), \quad N_2(\gamma) = 1-\gamma^2, \quad N_3(\gamma) = \frac{1}{2}\gamma(\gamma+1) \quad (-1\leq\gamma\leq 1). \tag{4.83}$$

The discretized form of the integral expression (4.79) can be written in matrix form as

$$[H]\underline{\phi} = [G]\left(\frac{\partial \phi}{\partial \underline{n}}\right), \tag{4.84}$$

where $\underline{\phi} = (\phi_1, \phi_2, \ldots)^T$, $\left(\frac{\partial \phi}{\partial \underline{n}}\right) = \left(\left(\frac{\partial \phi}{\partial n}\right)_1, \left(\frac{\partial \phi}{\partial n}\right)_2, \ldots\right)^T$ are column vectors of nodal values, with T denoting the transpose. The elements in the matrices [H] and [G] are given by

$$h_{ij} = \alpha\delta_{ij}\phi_i + \sum_k \int_{\Delta S_k} N_{L(j)}(\gamma)\,\frac{\partial G_i}{\partial n}\,dS, \tag{4.85}$$

$$g_{ij} = \sum_k \int_{\Delta S_k} N_{L(j)}(\gamma)\,G_i\,dS, \tag{4.86}$$

where δ is the Kroneker delta function, and ΔS_k is the "area" of an element. L(j) designates the transformation between the global nodal number j and the local nodal number L. G_i and $\frac{\partial G_i}{\partial n}$ stand for the values at $(\vec{x}_i, \vec{\xi})$, with $\vec{\xi}$ the variable of integration. The summation is over those elements that share the node j.

The value of the normal derivative on S_B is known and that on S_F can be eliminated from the boundary condition. To solve equation

(4.84) it is also necessary to eliminate the unknown normal derivative on the joint surface S_J. This can be achieved by matching the solution with the outer domain expression as shown below. Two possibilities exist and both are investigated.

4.3.1.1 BIE-BMP matching

First, the multipole expansion may be utilized to represent the velocity potential in the outer domain. Let the number of nodes on the joint surface be denoted by N_J. Then truncating the multipole expansion (4.66) after N_J terms yields

$$\phi \simeq \underline{W}\,\underline{A}, \tag{4.87}$$

$$\frac{\partial \phi}{\partial n} \simeq \underline{V}\,\underline{A}\ , \tag{4.88}$$

where

$$\underline{W} \equiv (s_1, c_1, s_2, c_2, s_3, c_3, \ldots, c_0), \qquad \underline{V} \equiv \frac{\partial \underline{W}}{\partial n}, \tag{4.89}$$

$$\underline{A} \equiv (b_1, a_1, b_2, a_2, b_3, a_3, \ldots, a_0)^T, \tag{4.90}$$

wher T denotes transpose. Here, we take the normal derivative as the radial derivative $\partial/\partial n = \partial/\partial r$, Applying this equation over the nodal points on the joint surface gives N_J equations for the potential and its derivative. In matrix form, these are

$$\underline{\phi} = [W]\underline{A}, \tag{4.91}$$

$$(\frac{\partial \phi}{\partial \underline{n}}) = [V]\underline{A}, \tag{4.92}$$

where [W] and [V] are N_J by N_J square matrices. Eliminating $\underline{A}$ from equations (4.91) and (4.92), we obtain

$$(\frac{\partial \phi}{\partial \underline{n}}) = [V][W]^{-1}\underline{\phi} \ . \tag{4.93}$$

Now we impose matching conditions over the joint surface S_J by requiring the continuity of the pressure (i.e. ϕ) and the normal velocity of the fluid,

$$\phi_{\text{inner domain}} = \phi_{\text{outer domain}} \qquad \text{on } S_J, \tag{4.94}$$

$$(\frac{\partial \phi}{\partial n})_{\text{inner domain}} = (\frac{\partial \phi}{\partial n})_{\text{outer domain}} \qquad \text{on } S_J. \tag{4.95}$$

From equations (4.93) (4.94) and (4.95), the normal derivative over S_J in equation (4.84) can be eliminated, and therefore the equation (4.84) can be solved. We refer to this coupling method as the BIE-BMP method. Up to this point the boundary value problem is solved in principle.

Having obtained ϕ on S_J, we can recover the coefficients in the multipole expansion from equation (4.91), if necessary.

4.3.1.2 BIE-BIE matching

Alternatively, we can apply the integral expression derived in Section 3.1 in the outer domain and match it with the inner domain integral expression (4.79). The only change for the outer domain expression is that the integral now is over the joint surface S_J, rather than over the body surface S_B which is the case in Section

3.1. That is,

$$\phi = -\frac{1}{\alpha}\int_{S_J} (G\frac{\partial \phi}{\partial n} - \phi\frac{\partial G}{\partial n})\, dS. \tag{4.96}$$

Here, the Green function is the pulsating source potential. The normal is taken as the positive normal concerning the inner domain flow, i.e. $\partial/\partial n = \partial/\partial r$. As a result, a negative sign appears in front of the integral. After a similar numerical discretization to that of the inner domain, the discretized form of equation (4.96) is written as

$$[H_1]\underline{\phi} = [G_1](\underline{\frac{\partial \phi}{\partial n}}). \tag{4.97}$$

Hence,

$$(\underline{\frac{\partial \phi}{\partial n}}) = [F]\underline{\phi}, \tag{4.98}$$

where

$$[F] = [G_1]^{-1}[H_1]. \tag{4.99}$$

The coefficients in the matrices are defined similarly to those in the inner domain, except that the Green function is changed and the integration surface is only on S_J. Quadratic isoparametric elements are used in the implementation.

The matching can be completed by eliminating the unknown normal derivative on S_J in the inner domain formulation from the above expression. We refer to this coupling method as the BIE-BIE method. The BIE-BIE method may not necessarily be very efficient

compared with the BIE-BMP method, but it provides us with an independent check for our multipole expansion solution.

The pulsating source Green function used in the numerical implementation can be expressed in terms of the exponential integral

$$G = \ln\frac{r'}{r} + 2\mathcal{P}\int_0^\infty \frac{e^{\lambda(z+\zeta)}}{\lambda-k}\cos\lambda(x-\xi)d\lambda,$$

$$= \ln\frac{r'}{r} + 2\mathrm{Re}[e^{Z_2}E_1(Z_2)] - 2\pi i e^{k(z+\zeta)-ik|x-\xi|}, \tag{4.100}$$

where $Z_2=k(z+\zeta)+ik(x-\xi)$, and the path of integration is taken above the pole. The Green function can be evaluated from a combination of ascending series, a continued fraction, etc. to achieve optimum efficiency, as described by Newman (1985).

4.3.2 The forward speed correction

4.3.2.1 BIE-BIE matching

The numerical discretization for the forward speed correction is identical to that for the zero-speed problem, but there is only one possible matching, i.e. BIE-BIE. Applying the formulation derived in Section 3.1 on the joint surface S_J, it follows that

$$\phi = -\frac{1}{\alpha}\int_{S_J}\left(G\frac{\partial\phi}{\partial n} - \phi\frac{\partial G}{\partial n}\right) dS + J, \tag{4.101}$$

where the free surface integral J is defined by equation (4.36) or (4.50) as appropriate, over the free surface bounded by S_J, and only

involves the zero-speed potentials and the steady potential. Following the same procedure in the zero-speed problems, the discretized form of the integral expression is expressed as

$$[H_1]\underline{\phi} = [G_1](\frac{\partial \phi}{\partial \underline{n}}) - \underline{J}. \tag{4.102}$$

where $\underline{J}$ is the column vector of values of the free surface integral; $[H_1]$ and $[G_1]$ are identical to these given in equation (4.97). Rearranging equation (4.102), it follows that

$$(\frac{\partial \phi}{\partial \underline{n}}) = [F]\underline{\phi} + [D], \tag{4.103}$$

where

$$[D] = [G_1]^{-1}\underline{J}, \tag{4.104}$$

and $[F]$ is given by equation (4.99). By eliminating the normal derivative form the above equation in the inner domain expression, the matching is thereby completed.

In the numerical calculation, when the forward speed correction was required, the BIE-BIE matching was always used for both the zero-speed solution and the forwad speed correction. One advantage is that all the matrices involved only need to be evaluated once for both zero-speed problem and forward speed correction problem because they are identical in the two problems. Once the zero-speed potential is solved, the multipole expansion expression is used and the coefficients are determined from the values of the zero-speed potential on the joint surface S_J. In this way the zero-speed potential in the outer domain was calculated analytically and the

free surface integral was computed efficiently.

It is noted that the steady potential is also required. This was first solved by the boundary integral method, using the Rakine source and its image above the free surface as the Green function; and then the steady potential in the outer domain was expressed analytically by the zero frequency asymptote of the multipole expansion derived in Section 4.2.

Evaluation of the free surface integral is the major difficulty in solving the forward speed correction potential. Another difficulty in the forward speed correction problem is the second derivatives associated with m_j for the radiation problem. Both difficulties are dealt with in the following two sections.

4.3.2.2 Avoiding the second derivatives

Three dimensions

In the boundary integral formulation the following integral needs to be calculated

$$\int_{S_B} m_i G \, dS \qquad (i=1,\ldots,6) \tag{4.105}$$

This integral contains second derivatives of the steady potential associated with m_j. Because it is the potential itself that is usually available in the first place, calculation of m_j is very difficult. Excessive errors can be introduced, if direct numerical

methods are applied. It is shown below that this difficult may be circumvented by using an integral relation obtained from Stokes theorem.

As derived in Appendix E, for a differentiable function f, there exists the following identity

$$\int_{S_B} [\, m_i f + n_i(\vec{W}.\vec{\nabla}f) \,]\, dS = \oint_{C_W} \frac{dl}{\sqrt{1-n_3^2}}\, n_i f(\vec{k}.\vec{W}) \qquad (i=1,\ldots,6). \tag{4.106}$$

By utilizing this integral identity, the necessity of evaluating m_j can be avoided. The integrand now only contains first derivatives, which can be evaluated from shape functions. This integral identity was first derived by Ogilvie and Tuck (1969). However, their expression has an error in the sign of the line integral. It seems that this error has not been recognized publicly.

Special attention is required in applying the integral identity to the boundary integral equation for the velocity potential, because of the singularity of the Green function. It is necessary to discuss the procedure in detail.

In fact, the integral (4.105) exists only in a Cauchy principal value sense. It is perhaps more appropriate to rewrite it explicitly as the Cauchy principal value integral, that is as the integral over the submerged body surface but excluding a small circle (3D) S_ϵ about the pole, as shown in Figure 4.4

$$\int_{S_B} m_i G \, dS = \lim_{\epsilon \to 0} \int_{S_B - S_\epsilon} m_i G \, dS. \tag{4.107}$$

If the pole happens to be on the free surface, S_ϵ may be defined as a semi-circle, shown in Figure 4.4. Over the surface $S_B - S_\epsilon$ the Green function is differentiable and therefore the integral identity can be applied for f=G. Because now the surface $S_B - S_\epsilon$ is not only bounded by C_W, but also by the boundary of S_ϵ, say C_ϵ, a more general integral identity may be employed. From Appendix E, it can be deduced that the following relation exists

$$\int_{S_B - S_\epsilon} m_i G \, dS = -\int_{S_B - S_\epsilon} n_i (\vec{W}.\vec{\nabla}G) \, dS + \oint_{C_W} n_i G(\vec{t}\times\vec{n}.\vec{W}) \, dl + \oint_{C_\epsilon} n_i G(\vec{t}\times\vec{n}.\vec{W}) \, dl, \tag{4.108}$$

where $\vec{t}$ is defined as the direction vector of the curve, satisfying the right hand screw rule with the normal on the surface. It can be shown that the integral over C_ϵ vanishes as $\epsilon \to 0$. In fact, (see Figure 4.4)

$$\begin{aligned} \oint_{C_\epsilon} n_i G(\vec{t}\times\vec{n}.\vec{W}) \, dl &= -\oint_{C_\epsilon} n_i G(\vec{e}_\epsilon.\vec{W}) \, dl \\ &\simeq -\int_0^{2\pi} n_i \frac{1}{\epsilon} |\vec{W}| \cos(\theta - \theta_0) \, \epsilon \, d\theta = 0 \qquad (\epsilon \to 0, \; G \simeq \frac{1}{\epsilon}), \end{aligned} \tag{4.109}$$

where θ_0 is the angle of the steady velocity measured in the local polar coordinate system, as shown in Figure 4.4. The second expression is derived by approximating the steady velocity and the component of the normal at the centre of the circle.

If the pole is on the free surface, the bounds of the above

integral will be $(\pi,2\pi)$. Similarly,

$$\oint_{C_\epsilon} n_i G(\vec{t}\times\vec{n}\cdot\vec{W})\, dl = -\, n_i|\vec{W}| \int_{\pi}^{2\pi} \cos(\theta-\theta_0)\, d\theta \simeq -2n_i|\vec{W}|\sin\theta_0$$

$$\simeq 2n_i(\vec{t}\times\vec{n}\cdot\vec{W})\Big|_Q \qquad (\epsilon \to 0,\ G \simeq \frac{1}{\epsilon}). \tag{4.110}$$

Here Q is used to denote the position of the pole. It should be noted that by assuming $G \simeq 1/\epsilon$ as $\epsilon \to 0$, it is implied that G is a Rankine source; if a wave source potential $G = 1/r+H$ is used, the coefficient should be doubled because $G \simeq 2/\epsilon$ at the pole on the free surface.

Substituting equations (4.109) and (4.110) into equations (4.108), it follows that

$$\int_{S_B} m_i G\, dS = -\int_{S_B} n_i(\vec{W}\cdot\vec{\nabla}G)\, dS + \begin{cases} \oint_{C_0} n_i G(\vec{t}\times\vec{n}\cdot\vec{W})\, dl, & (Q \text{ below } S_F) \\ PV \oint_{C_0} n_i G(\vec{t}\times\vec{n}\cdot\vec{W})\, dl + 2n_i(\vec{t}\times\vec{n}\cdot\vec{W})\Big|_Q, & (Q \text{ on } S_F) \end{cases} \tag{4.111}$$

On the mean free surface,

$$\vec{t}\times\vec{n}\cdot\vec{W} = -\frac{(n_3\vec{n}-\vec{k})\cdot\vec{W}}{\sqrt{1-n_3^2}} = \frac{\vec{k}\cdot\vec{W}}{\sqrt{1-n_3^2}}. \tag{4.112}$$

At small forward speed, the steady potential satisfies the "rigid wall" condition: $\vec{k}\cdot\vec{W} = 0$. The line integral vanishes, and a much simpler identity is obtained

$$\int_{S_B} m_i G \, dS = -\int_{S_B} n_i (\vec{W}.\vec{\nabla}G) \, dS. \tag{4.113}$$

Two dimensions

A similar procedure can be applied to two dimensions, but some particular features should be noted. In two dimensions, the counterpart to the line integral is now a pair of functions evaluated at isolated points. The analysis for three dimensions can be best followed by interpreting the two dimensional problem as a piece of "chip" of a three dimensional problem in which all variables are constant along one axis (see Figure 4.4).

If the pole is located below the free surface, the generalized integral identity is obtained in the form of

$$\int_{S_B-S_\epsilon} m_i G \, dS = -\int_{S_B-S_\epsilon} n_i (\vec{W}.\vec{\nabla}G) \, dS + n_i G(\vec{\tau}.\vec{W})\Big|_P - n_i G(\vec{\tau}.\vec{W})\Big|_Q + n_i G(\vec{\tau}.\vec{W})\Big|_E - n_i G(\vec{\tau}.\vec{W})\Big|_F \tag{4.114}$$

where P, Q are the upstream and downstream intersection points of the body within the free surface; E, F are the end points of the small segment S_ϵ whose middle point coincides with the pole, as shown in Figure 4.5. In the limit $\epsilon \to 0$, the terms at E and F cancel each other. Hence

$$\int_{S_B} m_i G \, dS = -\int_{S_B} n_i (\vec{W}.\vec{\nabla}G) \, dS + n_i G(\vec{\tau}.\vec{W})\Big|_P - n_i G(\vec{\tau}.\vec{W})\Big|_Q \tag{4.115}$$

If the pole is on the free surface, say on P, the small segment S_ϵ is defined by Figure 4.5. These terms corresponding to the line integrals in three dimensional problems become

$$n_i G(\vec{r}.\vec{W})\Big|_E - n_i G(\vec{r}.\vec{W})\Big|_Q. \tag{4.116}$$

It is observed that as $\epsilon \to 0$ the term at E may be singular, if the steady velocity does not approach zero rapidly. This may occur if the forward speed is not small. Although further consideration is necessary in general, this does not affect the present study, as explained below.

At small forward speed, due to the "rigid wall" condition, it is clear in equation (4.115) that there is no contribution from the "line integral", if the source point is below the free surface. The same is also true for the source point on the free surface, but needs to be justified because the Green function is singular in this case. Under the "rigid wall" free surface condition and the impermeable body surface condition, the steady flow resembles a corner flow around the upstream and downstream points P and Q. The complex velocity potential of a corner flow is familiar to us, given by (e.g. Newman 1977),

$$F(Z) = Z^n \qquad (Z=x+iy),$$

where x y are local coordinates, defined such that the Ox axis is parallel to one side of "wall", and the origin is at the corner; $n=\pi/\alpha$ with α the interior angle. The velocity is then obtained as

$$u - iv = \frac{dF}{dz} = nz^{n-1} = nr^{n-1}\, e^{i(n-1)\theta} \qquad (x=r\cos\theta,\ y=r\sin\theta)$$

Therefore, the steady velocity is proportional to r^{n-1}, i.e.

$$|\vec{W}| \sim A(\theta)r^{n-1} \qquad (r\to 0),$$

where $A(\theta)$ is a function of θ. Because for interior corner flow ($\alpha<\pi$), n-1>0, it follows that

$$|G(\vec{\tau}.\vec{W})n_i| \sim A(\theta)n_i r^{n-1}\ln\frac{1}{r} \to 0 \qquad (r\to 0).$$

The conclusion is justified. It finally follows that

$$\int_{S_B} m_i G\, dS = -\int_{S_B} n_i(\vec{W}.\vec{\nabla}G)\, dS. \tag{4.117}$$

4.3.2.3 Evaluating the free surface integral in the wave frequency expansion

The free surface integral to be calculated is as follows

$$J = 2i\int_{S_F} G(\phi_x - ik\phi + Q)\, dS - 2i(G\phi)_{+\infty}, \tag{4.118}$$

where ϕ denotes any of the zero-speed potentials ϕ_{j0} for j=1,2,...,7; Q denotes any of the Q_j's defined in equation (4.17); and k is the zero-speed wave number, i.e. $k=k_0=\omega_0^2/g$. Because, as in Section 4.2, all variables concerned are zero-speed variables in this sub-section, the subscript "0" is neglected completely for convenience.

For deeply submerged bodies, S_J is taken to be completely

submerged. The integration surface S_F is the whole free surface, and the integrand is always bounded. For surface piercing bodies, S_J is defined as a semi-circle. The integration surface S_F is an incomplete free surface bounded by S_J. For convenience in computation, the integration domain S_F is subdivided into two domains, as shown by Figure 4.3. The partition is made in such a way that if we draw two vertical lines across the outer bounds of S_{F1}, then the surface S_J will be located within the two lines. Following the subdivision, the free surface integral is rewritten in the form of

$$J = 2i\int_{S_{F1}} G(\phi_x - ik\phi + Q)\, dS + 2i[\int_{S_{F2}} G(\phi_x - ik\phi + Q)\, dS - (G\phi)_{+\infty}]. \tag{4.119}$$

In the inner surface S_{F1}, the integral is computed numerically, using the Gaussian quadrature formula. When the source point is located at the intersection of S_J with S_{F1}, the integrand is a logarithmic singularity (2D) and the integral is computed from a logarithmic-Gaussian quadrature formula. The procedure is similar to that used in formating the BIE matrices. On the outer surface S_{F2}, the integral is treated analytically in combination with numerical integration.

At positive infinity on the free surface, the integrand $G(\phi_x - ik\phi)$ in the second integral becomes an oscillatory function with a constant amplitude. Direct numerical integration is out of question. In fact, the terms in the square brackets are defined in a limit sense as pointed out in Section 4.1. In the implementation, the asymptote of the integrand is separated from the remaining terms of the integrand and integrated explicitly. After the extraction of the

asymptotic solution the integral becomes convergent, but contains a slowly decaying and oscillatory term in the integrand. This term is evaluated by means of some recurrence relations. The other terms of the integral are evaluated numerically. Details are shown below.

The behaviour of the integrand is examined first. From the multipole expansion in Section 4.2, the velocity potential on the free surface is written as follows

$$\phi = a_0 c_0(x) + \sum_{m=1}^{\infty}[a_m c_m(x)+b_m s_m(x)], \tag{4.120}$$

where a_m b_m are complex coefficients and $c_m(x)$ $s_m(x)$ are given in the form of

$$c_0(x) = 2\int_0^{\infty} \frac{e^{\lambda f}}{\lambda-k}\cos\lambda x d\lambda = 2\{\mathrm{Re}[e^{Z}E_1(Z)] - \pi i e^{kf-ik|x|}\}, \tag{4.121}$$

$$c_1(x) = 2a\frac{\cos\theta}{r} = 2\mathrm{Re}[\frac{a}{f-ix}], \tag{4.122}$$

$$c_m(x) = 2a^m \frac{\cos m\theta}{r^m} = 2\mathrm{Re}[(\frac{a}{f-ix})^m], \qquad (m=2,3,4\ldots) \tag{4.123}$$

$$\begin{aligned} s_1(x) &= 2a\frac{\sin\theta}{r} + 2ka\int_0^{\infty} \frac{e^{\lambda f}}{\lambda-k}\sin\lambda x dx \\ &= 2\{\mathrm{Im}(\frac{a}{f-ix}) - ka[\mathrm{Im}[e^{Z}E_1(Z)] - \mathrm{sgn}(x)\pi e^{kf-ik|x|}]\}, \end{aligned} \tag{4.124}$$

$$s_m(x) = 2a^m \frac{\sin m\theta}{r^m} = 2\mathrm{Im}[(\frac{a}{f-ix})^m], \qquad (m=2,3,4\ldots) \tag{4.125}$$

$$(f<0,\ Z=k(f-ix))$$

The derivative may be obtained by differentiating the series term by term. Derivatives of c_0 and s_1 can be obtained by interchanging the order of integration and differentiation. The derivatives of the

remaining terms can be obtained in a straightforward way. It follows that

$$\frac{\partial c_0}{\partial x} = -\frac{1}{a}s_1, \tag{4.126}$$

$$\frac{\partial c_m}{\partial x} = -\frac{m}{a}s_{m+1}, \qquad (m=1,2,3\ldots), \tag{4.127}$$

$$\frac{\partial s_1}{\partial x} = \frac{1}{a}[c_2 - kac_1 + (ka)^2 c_0], \tag{4.128}$$

$$\frac{\partial s_m}{\partial x} = \frac{m}{a}c_{m+1}, \qquad (m=2,3,4\ldots). \tag{4.129}$$

The derivative of the potential is then obtained as follows

$$\phi_x = \frac{1}{a}[\ -a_0 s_1 + b_1(-kac_1+(ka)^2 c_0) + \sum_{m=2}^{\infty}(m-1)(-a_{m-1}s_m + b_{m-1}c_m)\ ]. \tag{4.130}$$

For numerical purposes, it is necessary to separate "local" terms and the "far" field terms of the Green function and of the potential. Denoting the "local" terms by the subscript "L" and the "far" field terms by the subscript "W", we obtain that

$$G = G_L + G_W, \quad \phi = \phi_L + \phi_W, \quad \phi_x = \phi_{Lx} + \phi_{Wx}, \tag{4.131}$$

where

$$G_L = 2\mathrm{Re}[e^{Z_2}E_1(Z_2)], \tag{4.132}$$

$$G_2 = -2\pi i e^{k\zeta - ik|x-\xi|}, \qquad (Z_2 = k\zeta + ik(x-\xi)), \tag{4.133}$$

$$\phi_L = 2a_0\ \mathrm{Re}[e^{Z}E_1(Z)] - 2b_1 ka\ \mathrm{Im}[e^{Z}E_1(Z)]$$

$$+ 2\sum_{m=1}^{\infty} \{a_m \mathrm{Re}[(\frac{a}{f-ix})^m] + b_m \mathrm{Im}[(\frac{a}{f-ix})^m]\}, \tag{4.134}$$

$$\phi_W = -2[a_0 + b_1 ika\,\mathrm{sgn}(x)]\; i\pi e^{kf-ik|x|}, \tag{4.135}$$

$$\phi_{Lx} = -2a_0\{\mathrm{Im}(\frac{1}{f-ix}) - k\mathrm{Im}[e^Z E_1(Z)]\}$$

$$-2kab_1\{\mathrm{Re}(\frac{1}{f-ix}) - k\mathrm{Re}[e^Z E_1(Z)]\}$$

$$+2\sum_{m=2}^{\infty}(m-1)\{-a_{m-1}\mathrm{Im}[\frac{a^{m-1}}{(f-ix)^m}] + b_{m-1}\mathrm{Re}[\frac{a^{m-1}}{(f-ix)^m}]\}, \tag{4.136}$$

$$\phi_{Wx} = -2(a_0\,\mathrm{sgn}(x) + ikab_1)k\pi e^{kf-ik|x|}. \tag{4.137}$$

$$(Z = k(f-ix))$$

Let us define

$$A_1 = -2ka(b_1 + ia_1), \tag{4.138}$$

$$A_m = 2[(m-1)b_{m-1} - ika\, a_m], \qquad (m>1) \tag{4.139}$$

$$B_1 = -2(a_0 + ikab_1), \tag{4.140}$$

$$B_m = -2[(m-1)a_{m-1} + ika\, b_m]. \qquad (m>1) \tag{4.141}$$

and introduce the notations f_L, f_W to denote the local term and the far field term of $\phi_x - ik\phi$, such that

$$f_L + f_W \equiv \phi_x - ik\phi. \tag{4.142}$$

Then,

$$f_L = A_1\hat{c}_1(x) + B_1[\hat{s}_1(x) + ikae^Z E_1(Z)] + \sum_{m=2}^{\infty}[A_m\hat{c}_m(x) + B_m\hat{s}_m(x)], \tag{4.143}$$

$$f_W = \begin{cases} 0, & \text{for } x<0, \\ 2\pi kaB_1 e^{kf-ikx}, & \text{for } x>0, \end{cases} \tag{4.144}$$

where

$$\hat{c}_m(x) \equiv \mathrm{Re}\left[\frac{a^{m-1}}{(f-ix)^m}\right], \tag{4.145}$$

$$\hat{s}_m(x) \equiv \mathrm{Im}\left[\frac{a^{m-1}}{(f-ix)^m}\right]. \tag{4.146}$$

Introducing the notations J_0, J_1, ..., we may separate the oscillatory terms such that

$$J = 2i\int_{S_{F1}} G(\phi_x - ik\phi + Q)\, dS + 2i(J_0+J_1+J_2+J_3), \tag{4.147}$$

where

$$J_0 = \int_{S_{F2}} G\, Q \; dS, \tag{4.148}$$

$$J_1 = \int_{S_{F2}} G_L f_L \, dS, \tag{4.149}$$

$$J_2 = \int_{S_{F2}} G_W f_L \, dS, \tag{4.150}$$

$$J_3 = \int_{S^+_{F2}} G_L f_W \, dS + \int_{S^+_{F2}} G_W f_W \, dS - h_{+\infty}, \tag{4.151}$$

and where $h_{+\infty} = (G\phi)_{x=+\infty} \simeq (G_W\phi_W)_{x=+\infty}$; S^+_{F2} is the positive half of S^+_{F2}.

Next, each term is treated in turn in the order of J_3, J_2, J_1 and J_0. It is found that the oscillatory terms J_2 and J_3 can be integrated explicitly.

From the expressions for G_W and f_W (both proportional to e^{-ikx}) and the fact that the positive half plane of S_{F2} is defined by

$p' < x < \infty$, it immediately follows that (note: $f_W = -2ik\phi_2$ for $x>0$)

$$\int_{S_{F2}^+} G_W f_W \, dx - h_{+\infty} = -(G_W \phi_W)_{p'}. \tag{4.152}$$

To calculate the other integral in J_3, let us write the Green function G_L in its integral form

$$G_L = 2\mathrm{Re}[e^{Z_2} E_1(Z_2)] = \int_0^{+\infty} \left(\frac{e^{t(-|x-\xi|+i\zeta)}}{t+ik} + \frac{e^{t(-|x-\xi|-i\zeta)}}{t-ik} \right) dt. \tag{4.153}$$

Substitution of G_L into the first integral of J_3 and interchanging the order of integration yields

$$\begin{aligned} \int_{S_{F2}^+} G_L f_W \, dS &= \int_0^{+\infty} \left(\frac{e^{ti\zeta}}{t+ik} + \frac{e^{-ti\zeta}}{t-ik} \right) dt \int_{p'}^{+\infty} f_W \, e^{-t|x-\xi|} dx \\ &= \int_0^{+\infty} \left(\frac{e^{ti\zeta}}{t+ik} + \frac{e^{-ti\zeta}}{t-ik} \right) \left[-2ik\phi_W(p') \frac{e^{-t|p'-\xi|}}{t+ik} \right] dt \\ &= -\phi_W(p') \alpha(|p'-\xi|), \end{aligned} \tag{4.154}$$

where $\alpha(|p'-\xi|)$ is defined as

$$\alpha(|p'-\xi|) = 2ik \int_0^{+\infty} \left(\frac{e^{ti\zeta}}{t+ik} + \frac{e^{-ti\zeta}}{t-ik} \right) \frac{e^{-t|p'-\xi|}}{t+ik} \, dt \tag{4.155}$$

From contour integration (see Appendix F), $\alpha(|p'-\xi|)$ can be expressed in terms of the exponential integral functions

$$\alpha(|p'-\xi|) = 2 - 2Z_2 e^{Z_2} E_1(Z_2) + \left[e^{Z_2} E_1(Z_2) - e^{-Z_2} E_1(-Z_2) \right]^*. \tag{4.156}$$

where $Z_2 = k\zeta + ik|p'-\xi|$; and * denotes the complex conjugate. If $Z_2 \to 0$,

then $\alpha \simeq 2+\pi i$, since $E_1(Z_2) \simeq -E_i(0^+)-\pi i = -E_1(0^+)-\pi i$.

To summarize, the explicit form of the integral J_3 is obtained as follows

$$J_3 = -\phi_W(p')\ [\alpha(|p'-\xi|) + G_W(|p'-\xi|)]. \tag{4.157}$$

Substitution of the series form of f_L into J_2 and integration term by term yields the following series expression

$$J_2 = B_1 g_0 + \sum_{m=1}^{\infty}\{A_m Re_j[g_m] + B_m Im_j[g_m]\}, \tag{4.158}$$

where

$$g_0 = ik\int_{S_{F2}} G_W e^Z E_1(Z)dS, \qquad (Z=k(f-ix)), \tag{4.159}$$

$$g_m = \int_{S_{F2}} G_W \frac{a^{m-1}}{(f-jx)^m}dS, \qquad (m=1,2,3\ldots), \tag{4.160}$$

where j is a novel imaginary unit, which satisfies the same algebraic rules as the familiar imaginary unit i. The complex function G_W remains as a complex function associated with the conventional imaginary unit i. g_m is defined as a generalised complex function associated with the two independent imaginary units i and j. The operators Re_j and Im_j are defined as taking the real part or imaginary part of the following variable with respect to the imaginary unit j only. That is to say the imaginary unit i is ignored in performing these operators. For example, $Re_j[1+i-2ij] = 1+i$, $Im_j[1+i-2ij] = -2i$. Similar rules apply for Re_i and Im_i.

We further denote the integration of g_m on the negative half

surface as g_m^- and that on the positive half surface as g_m^+. Thus $g_m=g_m^-+g_m^+$. Recurrence relations can be derived for g_m^- and g_m^+ From

$$G_{Wx}=-iksgn(x-\xi)G_W \tag{4.161}$$

and integration by parts, it follows that

$$g_m^-=\int_{-\infty}^{q'} G_W \frac{a^{m-1}}{(f-jx)^m}dx$$

$$=-\frac{j}{m-1}\{(\frac{a}{f-jx})^{m-1}G_W\Big|_{-\infty}^{q'}-ika\int_{-\infty}^{q'} G_W \frac{a^{m-2}}{(f-jx)^{m-1}}dx\},$$

$$g_m^+=\int_{p'}^{+\infty} G_W \frac{a^{m-1}}{(f-jx)^m}dx$$

$$=-\frac{j}{m-1}\{(\frac{a}{f-jx})^{m-1}G_W\Big|_{p'}^{+\infty}+ika\int_{p'}^{+\infty} G_W \frac{a^{m-2}}{(f-jx)^{m-1}}dx\},$$

That is, two recurrence relations are obtained

$$g_m^-=-\frac{j}{m-1}[(\frac{a}{f-jq'})^{m-1}G_W(|q-\xi|)-ikag_{m-1}^-], \tag{4.162}$$

$$g_m^+=\frac{j}{m-1}[(\frac{a}{f-jq'})^{m-1}G_W(|q-\xi|)-ikag_{m-1}^+]. \tag{4.163}$$

To utilize the recurrence relations, it is necessary to evaluate the values of g_1^- and g_1^+, defined by

$$g_1^-=\int_{-\infty}^{q'}\frac{G_W}{f-jx}dx=-2\pi ie^{k(\zeta-i\xi)}\int_{-\infty}^{q'}\frac{e^{ikx}}{f-jx}dx, \tag{4.164}$$

$$g_1^+=\int_{p'}^{+\infty}\frac{G_W}{f-jx}dx=-2\pi ie^{k(\zeta+i\xi)}\int_{p'}^{+\infty}\frac{e^{-ikx}}{f-jx}dx. \tag{4.165}$$

To calculate these two integrals, the real and imaginary parts of $(f-jx)^{-1}$ are separated and each is expressed in terms of complex

fractions $(f-ix)^{-1}$ and $(f+ix)^{-1}$

$$\frac{1}{f-jx} = \frac{1}{2}\left[\frac{1}{f-ix} + \frac{1}{f-ix} + \frac{j}{i}\left(\frac{1}{f-ix} - \frac{1}{f+ix}\right)\right].$$

From Appendix F, we have

$$\int_{\infty}^{q'} \frac{e^{ikx}}{f-ix} dx = -ie^{kf} E_1(k(f-iq')), \tag{4.166}$$

$$\int_{\infty}^{q'} \frac{e^{ikx}}{f+ix} dx = ie^{-kf} E_1(-k(f+iq')), \tag{4.167}$$

$$\int_{p'}^{+\infty} \frac{e^{-ikx}}{f-ix} dx = ie^{-kf} E_1(-k(f-ip')), \tag{4.168}$$

$$\int_{p'}^{+\infty} \frac{e^{-ikx}}{f+ix} dx = -ie^{kf} E_1(k(f+ip')). \tag{4.169}$$

It follows that

$$g_1^- = \frac{1}{2}[i(A_1^-+B_1^-)-j(A_1^--B_1^-)]\, G_W(|q'-\xi|), \tag{4.170}$$

$$g_1^+ = \frac{1}{2}[i(A^++B^+)+j(A^+-B^+)]\, G_W(|p'-\xi|), \tag{4.171}$$

where
$$A_1^- = e^{-k(f+iq')} E_1(-k(f+iq')),$$

$$B_1^- = -e^{k(f-iq')} E_1(k(f-iq')),$$

$$A_1^+ = e^{-k(f-ip')} E_1(-k(f-ip')),$$

$$B_1^+ = -e^{k(f+ip')} E_1(k(f+ip')).$$

Particularly, if $p'=-q'$, then $A_1^-=A_1^+$, $B_1^-=B_1^+$. It is noted that an important feature in the coefficients is the linear dependence on G_W. It is found that the recurrence relations can be simplified into a

form which is source point (ξ,η) independent! Factorizing G_W, it follows that

$$\hat{g}_m^- = -\frac{j}{m-1}\left[\left(\frac{a}{f-jq'}\right)^{m-1} - ika\hat{g}_{m-1}^-\right], \tag{4.172}$$

$$\hat{g}_m^+ = \frac{j}{m-1}\left[\left(\frac{a}{f-jp'}\right)^{m-1} - ika\hat{g}_{m-1}^+\right], \tag{4.173}$$

for m>1, where

$$g_m^- = \hat{g}_m^- G_W(|q'-\xi|), \tag{4.174}$$

$$g_m^+ = \hat{g}_m^+ G_W(|p'-\xi|), \tag{4.175}$$

and

$$\hat{g}_1^- = \frac{1}{2}[i(A_1^- + B_1^-) - j(A_1^- - B_1^-)], \tag{4.176}$$

$$\hat{g}_1^+ = \frac{1}{2}[i(A_1^+ + B_1^+) + j(A_1^+ - B_1^+)]. \tag{4.177}$$

For numerical purposes, it is necessary to separate the real and imaginary part with respect to j. It follows that

$$\mathrm{Re}_j[\hat{g}_m^-] = \frac{1}{m-1}\{\mathrm{Im}_j[\left(\frac{a}{f-jq'}\right)^{m-1}] - ika\,\mathrm{Im}_j[\hat{g}_{m-1}^-]\}, \tag{4.178}$$

$$\mathrm{Im}_j[\hat{g}_m^-] = -\frac{1}{m-1}\{\mathrm{Re}_j[\left(\frac{a}{f-jq'}\right)^{m-1}] - ika\,\mathrm{Re}_j[\hat{g}_{m-1}^-]\}, \tag{4.179}$$

$$\mathrm{Re}_j[\hat{g}_m^+] = -\frac{1}{m-1}\{\mathrm{Im}_j[\left(\frac{a}{f-jp'}\right)^{m-1}] - ika\,\mathrm{Im}_j[\hat{g}_{m-1}^+]\}, \tag{4.180}$$

$$\mathrm{Im}_j[\hat{g}_m^+] = \frac{1}{m-1}\{\mathrm{Re}_j[\left(\frac{a}{f-jp'}\right)^{m-1}] - ika\,\mathrm{Re}_j[\hat{g}_{m-1}^+]\}. \tag{4.181}$$

The evaluation of g_m for m=1,2,3... is completed.

The remaining g_0 term can be evaluated by expressing the

exponential integral function in an integral form and changing the order of integration. From

$$e^{Z}E_1(Z) = \begin{cases} \int_0^{+\infty} \frac{e^{t(x+if)}}{t+ik}\,dt, & (x<0), \\ \int_0^{+\infty} \frac{e^{-t(x+if)}}{t-ik}\,dt, & (x>0), \end{cases} \tag{4.182}$$

it follows that

$$g_0^- = -ik\int_{\infty}^{q'} G_W e^{Z}E_1(Z)dx = 2\pi k\, e^{k\zeta}\int_0^{\infty}\frac{e^{tif}}{t+ik}dt\int_{\infty}^{q'} e^{tx}\, e^{ik(x-\xi)}dx$$

$$= -ikG_W(|q'-\xi|)\int_0^{\infty}\frac{e^{t(q'+if)}}{(f+ik)(f+ik)}dt$$

$$= G_W(|q'-\xi|)\,[1 - k(f-iq')\, e^{k(f-iq')}E_1(k(f-iq'))], \tag{4.183}$$

$$g_0^+ = -ik\int_{p'}^{+\infty} G_W e^{Z}E_1(Z)dx = 2\pi k\, e^{k\zeta}\int_0^{\infty}\frac{e^{-tif}}{t-ik}\,dt\int_{p'}^{+\infty} e^{-tx}.e^{-ik(x-\xi)}dx$$

$$= -ikG_W(|p'-\xi|)\int_0^{\infty}\frac{e^{-t(p'+if)}}{(f-ik)(f+ik)}dt$$

$$= \frac{1}{2}G_W(|p'-\xi|)\,[e^{k(f-ip')}E_1(k(f-ip')) - e^{-k(f-ip')}E_1(-k(f-ip'))]. \tag{4.184}$$

Here again, g_0^- and g_0^+ are proportional to G_W. Hence, we extend the definition (4.174) and (4.175) to m=0 too, i.e.

$$\hat{g}_0^- = 1-k(f-iq')e^{k(f-iq')}E_1(k(f-iq')), \tag{4.185}$$

$$\hat{g}_0^+ = \frac{1}{2}[e^{k(f-ip')}E_1(k(f-ip')) - e^{-k(f-ip')}E_1(-k(f-ip'))]. \tag{4.186}$$

To summarize, it has been shown that, apart from a localized domain, the oscillatory non-decaying term (J_3) and the oscillatory

slowly decaying (J_2) term of the free surface integral can be extracted out and integrated explicitly. The remaining term J_1 is quite smooth and is decaying fast. Numerical integration is satisfactory. The other term J_0 is oscillatory, but decaying very rapidly under the double-body approximation for the steady potential. Therefore, numerical integration is also found to be satisfactory, although some analytical integration is possible.

4.3.2.4 Evaluating the free surface integral in the encounter frequency expansion

The evaluation of the free surface integral in the expansion at encounter frequency follows closely that of the expansion at wave frequency. The integral to be calculated is

$$J = 2i\int_{S_F} G(\phi_x + Q)\, dS - i[(G\phi)_{+\infty} - (G\phi)_{-\infty}], \tag{4.187}$$

As before, we may split the integral into following components

$$J = 2i\int_{S_{F1}} G(\phi_x + Q)\, dS + 2i(J_0+J_1+J_2+J_3), \tag{4.188}$$

where

$$J_0 = \int_{S_{F2}} G\, Q\, dS, \tag{4.189}$$

$$J_1 = \int_{S_{F2}} G_L \phi_{Lx} dS, \tag{4.190}$$

$$J_2 = \int_{S_{F2}} G_W \phi_{Lx} dS, \tag{4.191}$$

$$J_3 = \int_{S_{F2}} G_L \phi_{Wx} dS + \int_{S_{F2}} G_W \phi_{Wx} dS - \frac{1}{2}(h_{+\infty} - h_{-\infty}), \tag{4.192}$$

and where $h_{+\infty} = (G\phi)_{x=+\infty} \simeq (G_W \phi_W)_{x=+\infty}$, $h_{-\infty} = (G\phi)_{x=-\infty} \simeq (G_W \phi_W)_{x=-\infty}$.

Following a similar analysis to the wave frequency expansion, we obtain

$$J_3 = \frac{1}{2}\{\phi_W(q')[\alpha(|q'-\xi|)+G_W(|q'-\xi|)] - \phi_W(p')[\alpha(|p'-\xi|)+G_W(|p'-\xi|)]\}. \tag{4.193}$$

where $\alpha(X)$ $(X>0)$ is defined as before; and

$$J_2 = A_1 Re_j[g_0] + B_1 Im_j[g_0] + \sum_{m=1}^{\infty}\{A_m Re_j[g_m] + B_m Im_j[g_m]\}, \tag{4.194}$$

where

$$A_1 = -2ka\, b_1, \qquad A_m = 2(m-1)\, b_{m-1}, \tag{4.195}$$

$$B_1 = -2\, a_0, \qquad B_m = -2(m-1) a_{m-1}; \tag{4.196}$$

and g_m are defined as before except g_0, which is now redefined as

$$g_0 = -k\int_{S_{F2}} G_W e^Z E_1(Z) dS, \qquad (Z=k(f-jx)). \tag{4.197}$$

In this sub-section k is defined as $k=\omega^2/g$, with ω the frequency of encounter or the frequency of forced oscillation. g_0 can be integrated in a similar way to the g_0 in the wave frequency

expansion. Utilizing the integral expression (4.182) and interchanging the order of integration, we obtain

$$g_0^- = -k\int_{\infty}^{q'} G_W e^Z E_1(Z)dx = 2\pi ike^{k\zeta}\int_0^{\infty}\frac{e^{tjf}}{t+jk}dt\int_{\infty}^{q'} e^{tx}\, e^{ik(x-\xi)}dx$$

$$= -kG_W(|q'-\xi|)\int_0^{\infty}\frac{e^{t(q'+jf)}}{(f+jk)(f+ik)}dt, \tag{4.198}$$

$$g_0^+ = -k\int_{p'}^{+\infty} G_W e^Z E_1(Z)dx = 2\pi ike^{k\zeta}\int_0^{\infty}\frac{e^{-tjf}}{t-jk}dt\int_{p'}^{+\infty} e^{-tx}.e^{-ik(x-\xi)}dx$$

$$= -kG_W(|p'-\xi|)\int_0^{\infty}\frac{e^{-t(p'+jf)}}{(f-jk)(f+ik)}dt, \tag{4.199}$$

Here again, g_0^- and g_0^+ are proportional to G_W. Hence, we apply the definition (4.174) and (4.175) here too. The remaining integrals are familiar. After separating the real and imaginary part with respect to j each term can be integrated explicitly

$$\hat{g}_0^- = \frac{1}{2}[i(A_0^-+B_0^-)-j(A_0^--B_0^-)], \tag{4.200}$$

$$\hat{g}_0^+ = \frac{1}{2}[i(A_0^++B_0^+)+j(A_0^+-B_0^+)], \tag{4.201}$$

where

$$A_0^- = \frac{1}{2}[e^{k(f+iq')}E_1(k(f+iq')) - e^{-k(f+iq')}E_1(-k(f+iq'))],$$

$$B_0^- = 1-k(f-iq')e^{k(f-iq')}E_1(k(f-iq')),$$

$$A_0^+ = \frac{1}{2}[e^{k(f-ip')}E_1(k(f-ip')) - e^{-k(f-ip')}E_1(-k(f-ip'))],$$

$$B_0^+ = 1-k(f+ip')e^{k(f+ip')}E_1(k(f+ip')).$$

If $p'=-q'$, then $A_0^-=A_0^+$, $B_0^-=B_0^+$. Again, the remaining terms J_0, J_1 can be integrated satisfactorily by numerical integration.

4.4 Discussion

The procedure presented in Section 4.1 is not very rigorous from a mathematical point of view. The expansion for the velocity potential into a zero-speed solution and a forward speed correction term is not appropriate at infinity, because the forward speed not only modifies the magnitude of the velocity potential, but also modifies the period in space. This can be clearly shown by considering the simple example of expanding $\sin(1+\epsilon)x$ at $\epsilon=0$. From a Taylor expansion,

$$\sin(1+\epsilon)x \simeq \sin x + \epsilon x \cos x + O(\epsilon^2).$$

The expansion is not uniformly convergent, because it is not valid at $x\to\infty$. The velocity potential for the forward speed problem is of the same nature as the above simple example. Therefore, strictly speaking, a matched expansion may be necessary in the small forward speed theory. However, it can be shown that although the intermediate procedures in Section 4.1 may not appear to be very rigorous, the final expressions for the velocity potential are precise, provided the formulation is not intended to apply in the far field.

Let us consider the two dimensional, encounter frequency expansion as an example. In this section, the notations of ϕ_j, ϕ_{j0} and ϕ_{j1} are used in the same meaning as in Section 4.1. From Green's

second identity and the boundary conditions, it follows that

$$\phi_j = \frac{1}{\alpha}\int_{S_B} (G\frac{\partial \phi_j}{\partial n} - \phi_j\frac{\partial G}{\partial n})\, dS + \frac{\tau}{\alpha}J(\phi_j) \tag{4.202}$$

where

$$J(\phi_j) = \int_{S_F} G(2i\frac{\partial \phi_j}{\partial x}+2iQ\ )\, dS \ - \int_{S_R^+} 2ik\ G\phi_j dS + \int_{S_R^-} 2ik\ G\phi_j dS. \tag{4.203}$$

G is the pulsating source potential. Q is defined similarly to equation (4.17), except ϕ_{j0} there being replaced by ϕ_j. In particular, for radiation potentials

$$Q = -\vec{\nabla}\phi.\vec{\nabla}\phi_j + \frac{1}{2}\phi_{zz}\phi_j. \tag{4.204}$$

The expressions (4.202) and (4.203) are valid in the entire fluid domain. Let us now carry out a perturbation analysis. In the fluid domain around the body, ϕ_j can be expanded into a series according the the small parameter τ, such that $\phi_j = \phi_{j0} + \tau\phi_{j1} + O(\tau^2)$. Because

$$\phi_{j0} = \frac{1}{\alpha}\int_{S_B} (G\frac{\partial \phi_{j0}}{\partial n} - \phi_{j0}\frac{\partial G}{\partial n})\, dS, \tag{4.205}$$

application of the expansion to equation (4.202) leads to

$$\phi_{j1} = \frac{1}{\alpha}\int_{S_B} (G\frac{\partial \phi_{j1}}{\partial n} - \phi_{j1}\frac{\partial G}{\partial n})\, dS + \frac{1}{\alpha}J(\phi_j). \tag{4.206}$$

The question now is whether the potential ϕ_j in the functional $J(\phi_j)$ can be replaced by ϕ_{j0}. It is shown below that the answer is

positive.

Let the local disturbance be denoted by the subscript "L" and the far field expression by the subscript "W", i.e.

$$\phi_j = \phi_{jL} + \phi_{jW}, \qquad G = G_L + G_W; \tag{4.207}$$

and define ϕ_{j0L}, ϕ_{j0W}, ϕ_{j1L} and ϕ_{j1W} in the similar way. According to this definition, G_L and G_W are given by equation (4.132) and (4.133); and ϕ_{j0L} and ϕ_{j0W} are identical to ϕ_L and ϕ_W which are defined by equations (4.134) and (4.135) in Section 4.3.2.3.

The exact forms of ϕ_{jL} and ϕ_{jW} are not known, but from the asymptotic analysis (see Appendix B), it is known that ϕ_{jW} behaves as follows

$$\begin{aligned} \phi_{jW} &= A^{+} e^{k_2(z-ix)}, && \text{as } x>0, \\ \phi_{jW} &= A^{-} e^{k_4(z+ix)}, && \text{as } x<0, \end{aligned} \tag{4.208}$$

where $k_2 = k(1+2\tau)$, $k_4 = k(1-2\tau)$; $A^{\pm}$ are the wave amplitudes at $x\to\pm\infty$, which can be regarded as the two dimensional Kochin functions. In the far field, because $\phi_j \simeq \phi_{jW}$, $G \simeq G_W$, the vertical integration over $S_R^{\pm}$ can be performed explicitly. It follows that

$$J = 2i \int_{S_F} G(\phi_{jx}+Q)\, dS - i(G_W\phi_{jW})_{+\infty} + i(G_W\phi_{jW})_{-\infty} + O(\tau). \tag{4.209}$$

For convenience, we subdivide the free surface into S_{F1} and S_{F2} in the same manner described in Section 4.3, and focus our

attention on the contribution from S_{F2}. S_{F1} is defined slightly different here from the S_{F1} defined in Section 4.3 in that the present inner side is bounded by S_B, whereas that in Section 4.3 is bounded by S_J; but S_{F2} may be regarded just the same here and in Section 4.3. Separating the local terms and far field terms, it follows that

$$J = 2i \underbrace{\int_{S_{F1}} G(\phi_{jx}+Q)\, dS}_{(I_0)} + 2i \underbrace{\int_{S_{F2}} G(\phi_{jLx}+Q)\, dS}_{(I_1)} + 2i \underbrace{\int_{S_{F2}} G_L \phi_{jWx}\, dS}_{(I_2)}$$
$$+ 2i[\underbrace{\int_{S_{F2}} G_W \phi_{jWx}\, dS}_{(I_3)} - (G_W \phi_{jW})_{+\infty} + (G_W \phi_{jW})_{-\infty}]. \tag{4.210}$$

We may group these terms and denote each group as I_0, I_1, I_2, I_3 respectively, as highlighted in the brackets above.

Because S_{F1} is localized to the body, the expansion is applicable and the ϕ_j in the I_0 term can be simply approximated by ϕ_{j0}. For the I_1 term, because the function $\phi_{jLx}+Q$ is a local disturbance function, the expansion is also applicable. Therefore, we may write the following equations

$$I_0 = 2i \int_{S_{F1}} G(\phi_{j0x}+Q_0)\, dS + O(\tau), \tag{4.211}$$

$$I_1 = 2i \int_{S_{F2}} G(\phi_{j0Lx}+Q_0)\, dS + O(\tau), \tag{4.212}$$

where Q_0 denotes $Q(\phi_{j0})$ which is identical to Q_j defined in equation (4.17).

The other two terms, i.e. I_2 and I_3 can be integrated explicitly. The term I_2 can be evaluated in a similar way to evaluating J_3 in Section 4.3.2.3. Utilizing the integral form of G_L in equation (4.153) and interchanging the order of integration in I_2, we obtain

$$\begin{aligned} I_2 &= 2i \int_0^{+\infty} \left(\frac{e^{ti\zeta}}{t+ik} + \frac{e^{-ti\zeta}}{t-ik}\right) dt \int_{S_{F2}} \phi_{jWx}\, e^{-t|x-\xi|} dx \\ &= 2i \int_0^{+\infty} \left(\frac{e^{ti\zeta}}{t+ik} + \frac{e^{-ti\zeta}}{t-ik}\right) \left[ik_4 \phi_{jW}(q') \frac{e^{-t|q'-\xi|}}{t+ik_4} - ik_2 \phi_{jW}(p') \frac{e^{-t|p'-\xi|}}{t+ik_2}\right] dt \\ &= i[\phi_{jW}(q')\alpha_4(|q'-\xi|) - \phi_{jW}(p')\alpha_2(|p'-\xi|)], \end{aligned} \tag{4.213}$$

where $\alpha_j(X)$ is defined by

$$\alpha_j(X) = 2ik_j \int_0^{+\infty} \left(\frac{e^{ti\zeta}}{t+ik} + \frac{e^{-ti\zeta}}{t-ik}\right) \frac{e^{-tX}}{t+ik_j} \qquad (X>0). \tag{4.214}$$

$\alpha_j(X)$ can be expressed in terms of exponential integrals as follows

$$\begin{aligned} \alpha_j(X) &= \frac{2k_j}{k_j-k} \int_0^{+\infty} \left(\frac{e^{-t(X-i\zeta)}}{t+ik} - \frac{e^{-t(X-i\xi)}}{t+ik_j}\right) dt \\ &\quad + \frac{2k_j}{k_j+k} \int_0^{+\infty} \left(\frac{e^{-t(X+i\zeta)}}{t-ik} - \frac{e^{-t(X+i\xi)}}{t+ik_j}\right) dt \\ &= 2\frac{1\pm 2\tau}{\pm 2\tau} \left[e^{k(\zeta+iX)} E_1(k(\zeta+iX)) - e^{k_j(\zeta+iX)} E_1(k_j(\zeta+iX)) \right] \\ &\quad + \frac{1\pm 2\tau}{1\pm\tau} \left[e^{k(\zeta-iX)} E_1(k(\zeta-iX)) - e^{-k_j(\zeta-iX)} E_1(-k_j(\zeta-iX)) \right], \end{aligned} \tag{4.215}$$

where the "+" sign is for j=2 and the "-" sign is for j=4. Since we are only intending to apply the expansion in the fluid domain around

the body, that is , ζ, X are finite values, the exponential integral of the k_j terms may be expanded into a Taylor series at k. From

$$\frac{d}{dZ}e^{Z}E_1(Z) = e^{Z}E_1(Z) - \frac{1}{Z}, \tag{4.216}$$

it immediately follows that with $Z_2 = k(\zeta+iX)$

$$\alpha_j(X) = 2 - 2Z_2e^{Z_2}E_1(Z_2) + [\, e^{Z_2}E_1(Z_2) - e^{-Z_2}E_1(-Z_2) \,]^* + O(\tau), \tag{4.217}$$

which is actually identical to the $\alpha(X)$ defined by equation (4.156). Furthermore, because p' and q' are finite values, there exist

$$\phi_{jW}(p') = \phi_{j0W}(p') + O(\tau), \qquad \phi_{jW}(q') = \phi_{j0W}(q') + O(\tau),$$

Hence,

$$I_2 = i[\phi_{j0W}(q')\alpha(|q'-\xi|) - \phi_{j0W}(p')\alpha(|p'-\xi|)] + O(\tau). \tag{4.218}$$

Following the procedures from equation (4.213) to equation (4.218) in the reverse order, we conclude that I_2 can be expressed as follows

$$I_2 = 2i \int_{S_{F2}} G_L\phi_{j0Wx}\, dS + O(\tau) \tag{4.219}$$

which is equivalent to the simple replacement of ϕ_{jW} by ϕ_{j0W} in equation (4.210).

The I_3 term can be integrated explicitly as well. From the expressions (4.132) and (4.208) for G_W and ϕ_{jW} respectively, it follows that

$$I_3 = 2i\left[\frac{ik_2}{ik_2+ik}(G_W\phi_{jW})\Big|_{p'}^{+\infty} + \frac{ik_4}{ik_4+ik}(G_W\phi_{jW})\Big|_{-\infty}^{q'}\right] - i(G_W\phi_{jW})_{+\infty} + i(G_W\phi_{jW})_{-\infty}$$

$$= i\tau\left[\frac{1}{1+\tau}(G_W\phi_{jW})_{+\infty} + \frac{1}{1-\tau}(G_W\phi_{jW})_{-\infty}\right] + i\left[\frac{1-2\tau}{1-\tau}(G_W\phi_{jW})_{q'} - \frac{1+2\tau}{1+\tau}(G_W\phi_{jW})_{p'}\right]$$

$$= i\left[(G_W\phi_{jW})_{q'} - (G_W\phi_{jW})_{p'}\right] + O(\tau) \tag{4.220}$$

Although the forward speed expansion is not applicable to the content in the first pair of square brackets in the second equation, it can, however, be simply omitted because it is of order $O(\tau)$. The final expression is, again, a local function and the forward speed expansion can be applied. It follows that

$$I_3 = i\left[(G_W\phi_{j0W})_{q'} - (G_W\phi_{j0W})_{p'}\right] + O(\tau). \tag{4.221}$$

By reversing the procedures for I_3, it follows that

$$I_3 = 2i\left[\int_{S_{F2}} G_W\phi_{j0Wx}\, dS - (G_W\phi_{j0W})_{+\infty} + (G_W\phi_{j0W})_{-\infty}\right], \tag{4.222}$$

which again is equivalent to replacing ϕ_{jW} by ϕ_{j0W} in equation (4.210).

Finally, from equations (4.210) to (4.212), (4.219) and (4.222), it can be concluded that

$$J = 2i\int_{S_F} G(\phi_{j0x}+Q_0)\, dS - i(G_W\phi_{j0W})_{+\infty} + i(G_W\phi_{j0W})_{-\infty} + O(\tau), \tag{4.223}$$

which justifies the small forward speed perturbation formulation in Section 4.1. The same procedures can be directly applied to the two

dimensional wave frequency expansion, and the same conclusion can be achieved. From the above analysis, it is seen that although the small forward speed perturbation analysis may not be appropriate in the far field, the integral expression can be perturbed as a whole. The final perturbation formulations presented in Section 4.1 are precise, although a simplified but less rigorous approach is taken for the intermediate procedures becuase the approach is straightforward. The same conclusion is also expected to hold for three dimensional motions.

Chapter 5

DYNAMICS OF RIGID BODIES

In this chapter, the formulations of forces of the zeroth order, first order and second order; and the equations of motions are examined at small forward speed.

5.1 Forces

For a body moving through waves at forward speed, there are several components of forces: the buoyancy force and hydro-restoring forces due to the hydro-static pressure; the steady resistance and lift force associated with a body moving steadily in otherwise calm water; and the hydrodynamic forces associated with waves incident upon the body and the oscillatory motion of the body. Other forces, such as the viscous force and the wind force, are not considered here.

The buoyancy and the hydro-restoring forces are the most elementary topics. They are fully understood and the formulations will be recovered in the process of deriving hydrodynamic forces. The resistance and the lift force are of great concern in classical ship hydrodynamics. For small forward speed motions where the "double-body" flow approximation is acceptable, there will be no resistance.

The hydrodynamic forces due to unsteady motions are the major concern here. For samll amplitude waves, the hydrodynamic forces can be expressed in terms of the first order forces, the second order

forces, and so on. The formulations of the first order forces are well established under either zero or non-zero forward speed conditions. The second order forces have been extensively studied at zero forward speed, but formulations are frequently different from one to another, as pointed out by Hung and Eatock Taylor (1988). The major source of errors is due to the complexity of the problem, particularly the multiple choice of the reference point for the moment. Second order forces at non-zero forward speed have benn far less extensively studied. It will not be surprising if more diversity appears in the future.

The present study is restricted to small forward speed. The presentation follows closely the procedures outlined by Ogilvie (1983) for zero forward speed problems.

5.1.1 General

To derive the force up to the second order, it is necessary first to find the coordinate transformation between Oxyz and O'x'y'z' up to the second order. Following the conventions of equation (3.20), we make some additional definitions to represent the components of the first order and second order responses:

$\vec{\xi}^{(1)} = (\xi_{11}, \xi_{21}, \xi_{31})^T$: the first order displacement;

$\vec{\xi}^{(2)} = (\xi_{12}, \xi_{22}, \xi_{32})^T$: the second order displacement;

$\vec{\Omega}^{(1)} = (\xi_{41}, \xi_{51}, \xi_{61})^T$: the first order displacement;

$\vec{\Omega}^{(2)} = (\xi_{42}, \xi_{52}, \xi_{62})^T$: the second order displacement;

where as before T denotes the transpose.

The two position vectors $\vec{x}$ and $\vec{x}'$ are related by a linear transformation

$$\vec{x}' = \underset{\sim}{D}(\vec{x}-\vec{\xi}), \tag{5.1}$$

$$\vec{x} = \vec{\xi} + \underset{\sim}{D}^{T}\vec{x}'. \tag{5.2}$$

where $\underset{\sim}{D}$ is a 3x3 coordinate transformation matrix and $\underset{\sim}{D}^{T}$ is its transpose. For such matrices, the transpose is identical to the inverse, i.e. $\underset{\sim}{D}^{T} = \underset{\sim}{D}^{-1}$. In principle, $\underset{\sim}{D}$ could be defined by a single rotation of a coordinate system about a certain axis. However, that axis is constantly changing in time so we must use a known reference frame. In most textbooks, Euler angles are usually used to define the orientation of a body; but in ship hydrodynamics it is conventional to use three angles with respect to the three Cartesian axes, i.e roll, pitch and yaw respectively.

There is insufficient data to determine the transformation matrix if only the magnitudes of the three rotations are given. In such circumstances, more than one answer is possible because of the lack of commutativity in rotations. For example, if A, B denote two rotational transformation matrices, then AB does not equal BA. Therefore, orders of rotations must be defined as well as magnitudes. Here, following Ogilvie (1983), we take roll, pitch and yaw in turn. Let A, B and C denote the coordinate transformation matrices of roll, pitch and yaw respectively, then

$$A = \begin{bmatrix} 1 & 0 & 0 \\ 0 & \cos\xi_4 & \sin\xi_4 \\ 0 & -\sin\xi_4 & \cos\xi_4 \end{bmatrix}, \tag{5.3}$$

$$B = \begin{bmatrix} \cos\xi_5 & 0 & -\sin\xi_5 \\ 0 & 1 & 0 \\ \sin\xi_5 & 0 & \cos\xi_5 \end{bmatrix}, \tag{5.4}$$

$$C = \begin{bmatrix} \cos\xi_6 & \sin\xi_6 & 0 \\ -\sin\xi_6 & \cos\xi_6 & 0 \\ 0 & 0 & 1 \end{bmatrix}, \tag{5.5}$$

The new position vector is obtained form $\vec{x}' = CBA\vec{x}$. Hence, $\underset{\sim}{D} = CBA$, or

$$\underset{\sim}{D} = \begin{bmatrix} \cos\xi_5\cos\xi_6 & \cos\xi_4\sin\xi_6 & \sin\xi_4\sin\xi_6 \\ & +\sin\xi_4\sin\xi_5\cos\xi_6 & -\cos\xi_4\sin\xi_5\cos\xi_6 \\ -\cos\xi_5\sin\xi_6 & \cos\xi_4\cos\xi_6 & \sin\xi_4\cos\xi_6 \\ & -\sin\xi_4\sin\xi_5\sin\xi_6 & +\cos\xi_4\sin\xi_5\sin\xi_6 \\ \sin\xi_5 & -\sin\xi_4\cos\xi_5 & \cos\xi_4\cos\xi_5 \end{bmatrix}. \tag{5.6}$$

For small rotations, this can be approximated by

$$\underset{\sim}{D} = \begin{bmatrix} 1 - \frac{1}{2}(\xi_5^2+\xi_6^2) & \xi_6 + \xi_4\xi_5 & -\xi_5 + \xi_4\xi_6 \\ -\xi_6 & 1 - \frac{1}{2}(\xi_4^2+\xi_6^2) & \xi_4 + \xi_5\xi_6 \\ \xi_5 & -\xi_4 & 1 - \frac{1}{2}(\xi_4^2+\xi_5^2) \end{bmatrix} + O(\epsilon^3). \tag{5.7}$$

Recall that ϵ is the small perturbation parameter defined in Section 3.1.3. From equations (5.2) and (5.7), it follows that

$$\vec{x} = \vec{x}' + \vec{\xi} + \vec{\Omega}x\vec{x}' + \epsilon^2\underset{\sim}{H}\vec{x}' + O(\epsilon^3), \tag{5.8}$$

where

$$\epsilon^2 \underset{\sim}{H} = \begin{bmatrix} -\frac{1}{2}(\xi_5^2+\xi_6^2) & 0 & 0 \\ \xi_4\xi_5 & -\frac{1}{2}(\xi_4^2+\xi_6^2) & 0 \\ \xi_4\xi_6 & \xi_5\xi_6 & -\frac{1}{2}(\xi_4^2+\xi_5^2) \end{bmatrix}. \tag{5.9}$$

The translational displacement $\vec{\xi}$ is irrelevant in the transformation of the normal vectors. Hence

$$\vec{n} = \vec{n}' + \vec{\Omega}x\vec{n}' + \epsilon^2 \underset{\sim}{H}\vec{n}' + O(\epsilon^3). \tag{5.10}$$

From equations (5.8) and (5.10), it can be shown that

$$\vec{x}x\vec{n} = \vec{x}'x\vec{n}' + \vec{\xi}x\vec{n}' + \vec{\Omega}x(\vec{x}x\vec{n}') + \vec{\xi}x(\vec{\Omega}x\vec{n}') + \epsilon^2 \underset{\sim}{H}(\vec{x}x\vec{n}') + O(\epsilon^3). \tag{5.11}$$

Details may be found in Appendix G.

Having found the relations for coordinate transformation, we are now ready to derive expressions of the force and moment. Up to order $O(F_n)$ the total fluid pressure is given by

$$P = -\rho(gz + \Phi_t + \vec{W}.\vec{\nabla}\Phi + \frac{1}{2}\vec{\nabla}\Phi.\vec{\nabla}\Phi) + O(F_n^2). \tag{5.12}$$

The fluid force $\vec{F}$ and the moment $\vec{M}$ upon the body can be found from integration of pressure over the instantaneous body surface S_0

$$\vec{F} = \int_{S_0} P\vec{n}\, dS, \tag{5.13}$$

$$\vec{M} = \int_{S_0} P(\vec{x}x\vec{n})\, dS. \tag{5.14}$$

To carry out computation it is desirable to transfer the integrals over S_0 to integrals over the mean wetted body surface at

equilibrium. To ensure there is no loss of consistence, approximation will be pursued to the same degree as those already made. The same assumptions will be utilized: the steady velocity of the fluid and its derivatives are of order O(1); and the unsteady oscillatory motions of the fluid and the body are small, i.e. of order $O(\epsilon)$.

If only the first order hydrodynamic force and moment are to be calculated, equations (5.13) and (5.14) can be evaluated directly over S_B, which is defined before as the mean body surface confined below $z=\bar{\eta}$. The difference arising from the transformation would be a higher order quantity.

The difference must be taken into account where the second order force and moment are concerned. The same is also necessary if the first order hydro-restoring force and moment are to be calculated. Two adjustments are required: (a) the area of the mean body surface S_B is amended to be equal to the area of the wetted S_0; (b) the pressure and the normal vector on S_0 are expressed by values on the mean body surface from a Taylor expansion. For convenience, a point on the instantaneous body surface S_0 at time t is called the mapping of the same point when the body is at its equilibrium position. Similarly, the mapping of a line is referred to accordingly. With reference to Figure 5.1, the following surfaces are defined:

S_0': the surface on the instantaneous body surface below the mapping of $z=\bar{\eta}$ at equilibrium,

ΔS_0: the surface on the instantaneous body surface between $z=\eta$ and the mapping of $z=\bar{\eta}$ at equilibrium, i.e. S_0-S_0',

ΔS_B: the surface on the body at equilibrium between $z=\bar{\eta}$ and the mapping of $z=\eta$ on the instantaneous body surface.

Relations between areas of these surfaces are $S_B=S_0'$, $\Delta S_B=\Delta S_0$.

Without approximation the force can be re-written in the form of

$$\vec{F} = \int_{S_0'+\Delta S_0} P\vec{n}\, dS. \tag{5.15}$$

The displacement of a point on S_0 from its mapping point on $S_B+\Delta S_B$ is given by (cf. Ogilvie 1983)

$$\vec{\alpha} = \vec{x}\big|_{S_0} - \vec{x}\big|_{S_B+\Delta S_B} = (\vec{\xi} + \vec{\Omega}x\vec{x} + \epsilon^2\underset{\sim}{H}\vec{x})\big|_{S_B+\Delta S_B} + O(\epsilon^3), \tag{5.16}$$

and the normal vector is expressed as

$$\vec{n}\big|_{S_0} = (\vec{n} + \vec{\Omega}x\vec{n} + \epsilon^2\underset{\sim}{H}\vec{n})\big|_{S_B+\Delta S_B} + O(\epsilon^3). \tag{5.17}$$

From a Taylor series, the pressure is expanded to

$$P\big|_{S_0} = P\big|_{S_B+\Delta S_B} + \vec{\alpha}.\vec{\nabla}P\big|_{S_B+\Delta S_B} + \ldots. \tag{5.18}$$

For small forward speed the leading order of the total pressure is the hydrostatic pressure. This term does not have any effect after the second term in the Taylor series. Thus the third term is of order $O(\epsilon^3)$ for small forward speed and is to be omitted. (If the forward speed is not small but the steady body potential is small, e.g. a slender ship in longitudinal motion, the same conclusion may

also hold.) In general, a third term $\frac{1}{2!}(\vec{\alpha}.\vec{\nabla})^2 P$ should be included. should be included.

The integral over $S_0'+\Delta S_0$ can be transferred to an integral over $S_B+\Delta S_B$,

$$\vec{F} = \int_{S_B+\Delta S_B} (P + \vec{\alpha}.\vec{\nabla}P)(\vec{n} + \vec{\Omega}x\vec{n} + \epsilon^2 \underset{\sim}{H}\vec{n}) \, dS + O(\epsilon^3)$$

$$= \vec{F}_a + \vec{\Omega}x\vec{F}_a + \epsilon^2 \underset{\sim}{H}\vec{F}_a + O(\epsilon^3), \tag{5.19}$$

with

$$\vec{F}_a = \int_{S_B+\Delta S_B} (P + \vec{\alpha}.\vec{\nabla}P)\vec{n} \, dS. \tag{5.20}$$

The second equation of (5.19) is obtained by taking constants out of the integrals.

The integral over ΔS_B can be simplified to a line integral. Over the supplementary surface the hydrostatic pressure degenerates to a first order quantity. Hence, for small forward speed the total pressure is of first order. By definition the lower bound of this supplementary surface is $z=\bar{\eta}$. The upper bound is the mapping of $z=\bar{\eta}\big|_{S_0}$ on S_B, which can be found from reverse rotations and translations. From

$$\vec{x}\big|_{S_0} = (\vec{x} + \vec{\xi} + \vec{\Omega}x\vec{x})\big|_{S_B+\Delta S_B} + O(\epsilon^2), \tag{5.21}$$

(cf. equation (5.8)) taking the z-axis component on the free surface yields

$$\eta(x,y,t)\Big|_{S_0} = z\Big|_{S_B+\Delta S_B} + \epsilon(\xi_{31} + \xi_{41}y - \xi_{51}x)\Big|_{S_B+\Delta S_B} + O(\epsilon^2) \tag{5.22}$$

Strictly speaking, the coordinates x and y appearing on the left hand side denote different values from those appearing on the right hand side, and the relations can be found from the x-axis and y-axis components of equation (5.21). However, since $\eta = \epsilon\eta_1 + \ldots$ is of order $O(\epsilon)$ the resulting difference on η is of higher order magnitude. The left hand side can be evaluated on $S_B+\Delta S_B$ just as well. The upper bound of ΔS_B is found as

$$z = \epsilon[\eta_1 - (\xi_{31} + \xi_{41}y - \xi_{51}x)] + O(\epsilon^2). \tag{5.23}$$

Over ΔS_B an elementary surface is $dS \simeq dl\,dz/\sqrt{1-n_3^2}$ with dl taken on $z=\bar{\eta}$. The denominator is used to account for the angle of the body as it penetrates the free surface. In Ogilvie's (1983) derivation the body is assumed perpendicular to the mean free surface. In that case, $n_3 = 0$ and the denominator becomes one.

From (5.23), the integration over the supplementary surface can be reduced to a line integral

$$\begin{aligned}
&\int_{\Delta S_B} (P + \vec{\alpha}.\vec{\nabla}P)\vec{n}\, dS \\
&= -\rho \oint_{C_W} \frac{\vec{n}\,dl}{\sqrt{1-n_3^2}} \int_{\bar{\eta}=0}^{\epsilon[\eta_1 - (\xi_{31} + \xi_{41}y - \xi_{51}x)]} \{gz + \epsilon[\Phi_{1t} + \vec{W}.\vec{\nabla}\Phi_1 + g(\xi_{31} + \xi_{41}y - \xi_{51}x)]\}\, dz \\
&= \epsilon^2 \frac{1}{2}\rho g \oint_{C_W} \eta_{R1}^2 \frac{\vec{n}}{\sqrt{1-n_3^2}}\, dl + O(\epsilon^3),
\end{aligned} \tag{5.24}$$

where C_W is the mean water line $z=\bar{\eta}=0$; η_{R1} is the first order relative surface elevation, given by

$$\eta_{R1} = \eta_1 - (\xi_{31} + \xi_{41} y - \xi_{51} x). \tag{5.25}$$

In the derivation of equation (5.24) the condition that the steady surface elevation in the steady flow field is negligible, i.e. $\bar{\eta}=0$, is utilized. In general if the body has a significant forward speed, the free surface elevation can not be neglected and equation (5.24) will appear in a far more complicated form. For example, the steady pressure $\frac{1}{2}(\vec{W}.\vec{W}-U^2)$ must be included and the second order terms in the upper bound of the integral must be found.

To evaluate the integrals over S_B a systematic approach is required. Following the convention of perturbation theory, we shall express all quantities in the form of $\vec{f} = \vec{f}^{(0)} + \epsilon \vec{f}^{(1)} + \epsilon^2 \vec{f}^{(2)} + \ldots$. Of course, for some quantities such as the unsteady response of the body, the zeroth order quantities are zero. After ordering, we have

$$\vec{F}_a^{(1)} = \vec{F}_{aD}^{(1)} + \vec{F}_{aS}^{(1)}, \qquad \vec{F}_a^{(2)} = \vec{F}_{aD}^{(2)} + \vec{F}_{aE}^{(2)} + \vec{F}_{aS}^{(2)} + \vec{F}_{aT}^{(2)}, \tag{5.26}$$

where the notations are defined by

$$\vec{F}_a^{(0)} = \int_{S_B} P^{(0)} \vec{n} \, dS; \tag{5.27}$$

$$\vec{F}_{aD}^{(1)} = \int_{S_B} P^{(1)} \vec{n} \, dS, \qquad \vec{F}_{aS}^{(1)} = \int_{S_B} (\vec{\xi}^{(1)} + \vec{\Omega}^{(1)} \times \vec{x}) . \vec{\nabla} P^{(0)} \vec{n} \, dS; \tag{5.28}$$

$$\vec{F}_{aD}^{(2)} = \int_{S_B} P^{(2)} \vec{n} \, dS, \qquad \vec{F}_{aS}^{(2)} = \int_{S_B} (\vec{\xi}^{(2)} + \vec{\Omega}^{(2)} \times \vec{x}) . \vec{\nabla} P^{(0)} \vec{n} \, dS, \tag{5.29}$$

$$\vec{F}^{(2)}_{aE} = \int_{S_B} (\vec{\xi}^{(1)} + \vec{\Omega}^{(1)}_{x\vec{x}}).\vec{\nabla}P^{(1)}\vec{n}\, dS + \frac{1}{2}\rho g \oint_{C_W} \eta^2_{R1} \frac{\vec{n}}{\sqrt{1-n_3^2}}\, dl, \tag{5.30}$$

$$\vec{F}^{(2)}_{aT} = \int_{S_B} (\underset{\sim}{H}\vec{x}).\vec{\nabla}P^{(0)}\vec{n}\, dS; \tag{5.31}$$

and where

$$P^{(0)} = -\rho g z, \tag{5.32}$$

$$P^{(1)} = -\rho(\Phi_{1t} + \vec{W}.\vec{\nabla}\Phi_{1t}), \tag{5.33}$$

$$P^{(2)} = -\rho(\Phi_{2t} + \vec{W}.\vec{\nabla}\Phi_{2t} + \frac{1}{2}\vec{\nabla}\Phi_1.\vec{\nabla}\Phi_1), \tag{5.34}$$

$$\vec{\alpha}^{(1)} = \vec{\xi}^{(1)} + \vec{\Omega}^{(1)}_{x\vec{x}} = \begin{bmatrix} \xi_{11} + \xi_{51}z - \xi_{61}y \\ \xi_{21} + \xi_{61}x - \xi_{41}z \\ \xi_{31} + \xi_{41}y - \xi_{51}x \end{bmatrix}, \tag{5.35}$$

$$\vec{\alpha}^{(2)} = \vec{\xi}^{(2)} + \vec{\Omega}^{(2)}_{x\vec{x}} + \underset{\sim}{H}\vec{x}$$

$$= \begin{bmatrix} \xi_{12} + \xi_{52}z - \xi_{62}y \\ \xi_{22} + \xi_{62}x - \xi_{42}z \\ \xi_{32} + \xi_{42}y - \xi_{52}x \end{bmatrix} + \begin{bmatrix} -\frac{1}{2}(\xi^2_{51}+\xi^2_{61})x \\ -\frac{1}{2}(\xi^2_{41}+\xi^2_{61})y + \xi_{51}\xi_{41}x \\ -\frac{1}{2}(\xi^2_{41}+\xi^2_{51})z + \xi_{61}\xi_{51}y + \xi_{61}\xi_{41}x \end{bmatrix}.$$

The hydrostatic pressure dependent terms can be integrated explicitly. For this purpose some hydrostatic identities are found useful:

$$\int_{S_B} \vec{n}\, ds = \vec{k}\, A_W\,, \qquad \int_{S_B} \vec{n}x_i dS = \vec{k}A_W x_{if} - \vec{e}_i V\,, \qquad (i=1,2,3) \tag{5.36}$$

with the CENTRE OF FLOTATION defined by

$$x_f = \frac{1}{A_W}\int_{S_W} x\, dxdy, \qquad y_f = \frac{1}{A_W}\int_{S_W} y\, dxdy, \qquad z_f = 0, \tag{5.37}$$

where S_W is the water plane of the body and A_W is the area of the water plane; V is the volume of the submerged portion of the body. These identities can be verified from certain Gaussian theorems.

Utilizing these identities, we obtain

$$\vec{F}_a^{(0)} = \rho g V \vec{k}, \tag{5.38}$$

$$\vec{F}_{aS}^{(r)} = -\rho g \int_{S_B} (\xi_{3r} + \xi_{4r} y - \xi_{5r} x)\vec{n}\, dS$$

$$= -\rho g A_W (\xi_{3r} + \xi_{4r} y_f - \xi_{5r} x_f)\vec{k} - \rho g V(\xi_{5r}\vec{i} - \xi_{4r}\vec{j}), \quad (r=1,2) \tag{5.39}$$

$$\vec{F}_{aT}^{(2)} = -\rho g \int_{S_B} (-\frac{\xi_{41}^2+\xi_{51}^2}{2} z + \xi_{61}\xi_{51} y + \xi_{61}\xi_{41} x)\vec{n}\, dS$$

$$= -\rho g[-\vec{i}\xi_{41}\xi_{61} V - \vec{j}\xi_{51}\xi_{61} V + \vec{k}(\frac{\xi_{41}^2+\xi_{51}^2}{2} V + \xi_{61}\xi_{51} A_W y_f + \xi_{61}\xi_{41} A_W x_f)]. \tag{5.40}$$

Ordering equation (5.19) yields

$$\vec{F}^{(0)} = \vec{F}_a^{(0)}, \tag{5.41}$$

$$\vec{F}^{(1)} = \vec{F}_a^{(1)} + \vec{\Omega}^{(1)} x \vec{F}_a^{(0)}, \tag{5.42}$$

$$\vec{F}^{(2)} = \vec{F}_a^{(2)} + \vec{\Omega}^{(2)} x \vec{F}_a^{(0)} + \vec{\Omega}^{(1)} x \vec{F}_a^{(1)} + \underset{\sim}{H}\vec{F}_a^{(0)}. \tag{5.43}$$

Substituting equations (5.38) to (5.40), we obtain

$$\vec{F}^{(0)} = \rho g V \vec{k}, \tag{5.44}$$

$$\vec{F}^{(1)} = -\rho \int_{S_B} (\Phi_{1t} + \vec{W}.\vec{\nabla}\Phi_1)\vec{n}\, dS + \vec{F}_S^{(1)}, \tag{5.45}$$

$$\begin{aligned}\vec{F}^{(2)} = {} & \frac{1}{2}\rho g \oint_{C_W} \eta_{R1}^2 \frac{\vec{n}}{\sqrt{1-n_3^2}}\, dl \\ & - \rho \int_{S_B} (\Phi_{2t} + \vec{W}.\vec{\nabla}\Phi_2 + \frac{1}{2}\vec{\nabla}\Phi_1.\vec{\nabla}\Phi_1)\vec{n}\, dS \\ & - \rho \int_{S_B} [(\vec{\xi}^{(1)} + \vec{\Omega}^{(1)} x \vec{x}).\vec{\nabla}(\Phi_{1t} + \vec{W}.\vec{\nabla}\Phi_1)]\vec{n}\, dS \\ & + \vec{\Omega}^{(1)} x (\vec{F}_D^{(1)} + \vec{F}_S^{(1)}) \\ & + \vec{F}_S^{(2)} - \rho g A_W \xi_{61}(\xi_{41} x_f + \xi_{51} y_f)\vec{k},\end{aligned} \tag{5.46}$$

where $\vec{F}_D^{(1)}$ is defined as the first order hydrodynamic force, given by the integral in equation (5.45); and η_{R1} is given by equation (5.25). The first order and the second order hydro-restoring forces are given by

$$\vec{F}_S^{(r)} = \vec{F}_{aS}^{(r)} + \vec{\Omega}^{(r)} x \vec{F}_{aS}^{(0)}, \tag{5.47}$$

or

$$\vec{F}_S^{(r)} = -\rho g A_W(\xi_{3r} + \xi_{4r} y_f - \xi_{5r} x_f)\vec{k}. \qquad (r=1,2) \tag{5.48}$$

Comparison with Hung's (1988) zero-speed formulation shows that the last two terms in (5.46) are missing in his formulation. One of these two terms is due to the second order response, which is assumed eliminated by some external force in Hung's analysis. The other term, i.e. the interaction among the first order rotations, comes from the

integration of $(\underset{\sim}{H}\vec{x}).\vec{\nabla}P^{(0)}$. The present fomula agrees with that of Ogilvie (1983). In comparison with Ogilvie's formula, it should be noted

that a cancellation between the term $\vec{\Omega}^{(1)}x\vec{F}_S^{(1)}$ and the part of the water line integral $\frac{1}{2}\rho g \oint_{C_W} (\xi_{31}+\xi_{41}y-\xi_{41}x)^2 \vec{n}\, dl$ is utilized in Ogilvie's formula, where the body is assumed "wall-sided" ($n_3=0$).

Let us now turn our attention to the moment. Similarly to the force, the moment (5.14) can be equivalently written as follows

$$\vec{M} = \int_{S_0'+\Delta S_0} P(\vec{x}x\vec{n})\, dS. \tag{5.49}$$

This is can be transferred into an integral over $S_B+\Delta S_B$ from the Taylor series (5.11) and (5.18) of the integrand,

$$\begin{aligned}\vec{M} &= \int_{S_B+\Delta S_B} (P + \vec{\alpha}.\vec{\nabla}P)[\vec{x}x\vec{n} + \vec{\Omega}x(\vec{x}x\vec{n}) + \vec{\xi}x(\vec{n}+\vec{\Omega}x\vec{n}) + \epsilon^2\underset{\sim}{H}(\vec{x}x\vec{n})]\, dS \\ &= \vec{M}_a + \vec{\Omega}x\vec{M}_a + \epsilon^2\underset{\sim}{H}\vec{M}_a + \vec{\xi}x\vec{F} + O(\epsilon^3),\end{aligned} \tag{5.50}$$

with

$$\vec{M}_a = \int_{S_B+\Delta S_B} (P + \vec{\alpha}.\vec{\nabla}P)(\vec{x}x\vec{n})\, dS. \tag{5.51}$$

The second equation of (5.50) is obtained by taking constants out of the integrals. The force $\vec{F}$ is given by equations (5.44) to (5.46) and it only needs to be evaluated up to first order because $\vec{\xi}$ is also small.

The integral for the moment now reduces to an integral of $\vec{M}_a$. Over the supplementary surface the hydrostatic pressure degenerates to a first order quantity, and so does the total pressure for small forward speed. Similarly to equation (5.24), we obtain

$$\int_{\Delta S_B} (P + \vec{\alpha}.\vec{\nabla}P)(\vec{x}\times\vec{n})\, dS = \epsilon^2 \frac{1}{2}\rho g \oint_{C_W} \eta_{R1}^2 \frac{\vec{x}\times\vec{n}}{\sqrt{1-n_3^2}}\, dl \quad + O(\epsilon^3). \tag{5.52}$$

Ordering the moment expression (5.50) yields

$$\vec{M}_a^{(1)} = \vec{M}_{aD}^{(1)} + \vec{M}_{aS}^{(1)}, \qquad \vec{M}_a^{(2)} = \vec{M}_{aD}^{(2)} + \vec{M}_{aE}^{(2)} + \vec{M}_{aS}^{(2)} + \vec{M}_{aT}^{(2)}, \tag{5.53}$$

with the notations defined by

$$\vec{M}_a^{(0)} = \int_{S_B} P^{(0)}(\vec{x}\times\vec{n})\, dS; \tag{5.54}$$

$$\vec{M}_{aD}^{(1)} = \int_{S_B} P^{(1)}(\vec{x}\times\vec{n})\, dS, \quad \vec{M}_{aS}^{(1)} = \int_{S_B} (\vec{\xi}^{(1)}+\vec{\Omega}^{(1)}\times\vec{x}).\vec{\nabla}P^{(0)}(\vec{x}\times\vec{n})\, dS; \tag{5.55}$$

$$\vec{M}_{aD}^{(2)} = \int_{S_B} P^{(2)}(\vec{x}\times\vec{n})\, dS, \quad \vec{M}_{aS}^{(2)} = \int_{S_B} (\vec{\xi}^{(2)}+\vec{\Omega}^{(2)}\times\vec{x}).\vec{\nabla}P^{(0)}(\vec{x}\times\vec{n})\, dS, \tag{5.56}$$

$$\vec{M}_{aE}^{(2)} = \int_{S_B} (\vec{\xi}^{(1)}+\vec{\Omega}^{(1)}\times\vec{x}).\vec{\nabla}P^{(1)}(\vec{x}\times\vec{n})\, dS + \frac{1}{2}\rho g \oint_{C_W} \eta_{R1}^2 \frac{\vec{x}\times\vec{n}}{\sqrt{1-n_3^2}}\, dl, \tag{5.57}$$

$$\vec{M}_{aT}^{(2)} = \int_{S_B} (\underset{\sim}{H}\vec{x}).\vec{\nabla}P^{(0)}(\vec{x}\times\vec{n})\, dS. \tag{5.58}$$

Again, hydrostatic pressure dependent terms can be integrated explicitly. We obtain

$$\vec{M}_a^{(0)} = \rho g V \begin{bmatrix} y_b \\ -x_b \\ o \end{bmatrix}, \tag{5.59}$$

$$\vec{M}_{aS}^{(r)} = -\rho g \int_{S_B} (\xi_{3r}+y\xi_{4r}-x\xi_{5r})(\vec{x}\times\vec{n})\, dS$$

$$= -\rho g \int_V \vec{\nabla}\times[\vec{x}(\xi_{3r}+y\xi_{4r}-x\xi_{5r})]dV + \rho g \int_{S_W} (\xi_{3r}+y\xi_{4r}-x\xi_{5r}) \begin{bmatrix} -y \\ x \\ 0 \end{bmatrix} dS$$

$$= -\rho g V \begin{bmatrix} \xi_{4r} z_b \\ \xi_{5r} z_b \\ -\xi_{4r} x_b - \xi_{5r} y_b \end{bmatrix} + \rho g \begin{bmatrix} -y_f \xi_{3r} A_W - \xi_{4r} S_{22} + \xi_{5r} S_{21} \\ x_f \xi_{3r} A_W + \xi_{4r} S_{21} - \xi_{5r} S_{11} \\ 0 \end{bmatrix}, \quad (r=1,2) \tag{5.60}$$

$$\vec{M}_{aT}^{(2)} = -\rho g \int_{S_m} [-\tfrac{1}{2}(\xi_{41}^2+\xi_{51}^2)z + \xi_{61}\xi_{51}y + \xi_{61}\xi_{41}x](\vec{x}\times\vec{n})\, dS$$

$$= -\rho g \int_V \vec{\nabla}\times\{\vec{x}[-\tfrac{1}{2}(\xi_{41}^2+\xi_{51}^2)z + \xi_{61}\xi_{51}y + \xi_{61}\xi_{41}x]\}\, dV$$

$$+ \rho g \int_{S_W} (\xi_{61}\xi_{51}y + \xi_{61}\xi_{41}x)(\vec{x}\times\vec{n})\, dS$$

$$= -\rho g V \begin{bmatrix} \xi_{61}\xi_{51}z_b + \frac{1}{2}y_b(\xi_{41}^2+\xi_{51}^2) \\ -\frac{1}{2}x_b(\xi_{41}^2+\xi_{51}^2) - z_b\xi_{61}\xi_{41} \\ y_b\xi_{61}\xi_{41} - x_b\xi_{61}\xi_{51} \end{bmatrix} + \rho g \xi_{61} \begin{bmatrix} -\xi_{51}S_{22} - \xi_{41}S_{12} \\ \xi_{51}S_{21} + \xi_{41}S_{11} \\ 0 \end{bmatrix}, \tag{5.61}$$

where (x_b, y_b, z_b) is the CENTRE OF BUOYANCY, defined by

$$x_b = \frac{1}{V}\int_V x\, dV, \quad y_b = \frac{1}{V}\int_V y\, dV, \quad z_b = \frac{1}{V}\int_V z\, dV, \tag{5.62}$$

and s_{ij} are the SECOND MOMENT of the water plane area, defined by

$$S_{ij} = \int_{S_W} x_i x_j \, dS. \qquad (i,j=1,2) \tag{5.63}$$

These are conventional definitions as frequently used in naval architecture. In deriving equation (5.61), some Gaussian theorems have been used to transform integrals over the surface S_B into volume integrals plus integrals over the water plane area.

Ordering equation (5.50) leads

$$\vec{M}^{(0)} = \vec{M}_a^{(0)}, \tag{5.64}$$

$$\vec{M}^{(1)} = \vec{M}_a^{(1)} + \vec{\Omega}^{(1)} x \vec{M}_a^{(0)} + \vec{\xi}^{(1)} x \vec{F}_a^{(0)}, \tag{5.65}$$

$$\vec{M}^{(2)} = \vec{M}_a^{(2)} + \vec{\Omega}^{(2)} x \vec{M}_a^{(0)} + \vec{\xi}^{(2)} x \vec{F}_a^{(0)} + \vec{\Omega}^{(1)} x \vec{M}_a^{(1)} + \vec{\xi}^{(1)} x \vec{F}_a^{(1)} + \underset{\sim}{H} \vec{M}_a^{(0)}. \tag{5.66}$$

Substitution of equations (5.59), (5.60) and (5.61) yields

$$\vec{M}^{(0)} = \rho g V \begin{bmatrix} y_b \\ -x_b \\ 0 \end{bmatrix}, \tag{5.67}$$

$$\vec{M}^{(1)} = -\rho \int_{S_B} (\Phi_{1t} + \vec{W}.\vec{\nabla}\Phi_1)(\vec{x} x \vec{n}) \, dS + \vec{M}_S^{(1)}, \tag{5.68}$$

$$\vec{M}^{(2)} = \frac{1}{2} \rho g \oint_{C_W} \eta_{R1}^2 \frac{\vec{x} x \vec{n}}{\sqrt{1-n_3^2}} \, dl$$

$$- \rho \int_{S_B} (\Phi_{2t} + \vec{W}.\vec{\nabla}\Phi_2 + \frac{1}{2}\vec{\nabla}\Phi_1.\vec{\nabla}\Phi_1)(\vec{x}x\vec{n})\ dS$$

$$- \rho \int_{S_B} (\vec{\xi}^{(1)}+\vec{\Omega}^{(1)}x\vec{x}).\vec{\nabla}(\Phi_{1t}+\vec{W}.\vec{\nabla}\Phi_1)(\vec{x}x\vec{n})\ dS$$

$$+ \vec{\Omega}^{(1)}x\vec{M}_D^{(1)} + \vec{\xi}^{(1)}x\vec{F}_D^{(1)}$$

$$+ \vec{M}_S^{(2)}$$

$$+ \rho g V \begin{bmatrix} -\frac{1}{2}(\xi_{41}^2+\xi_{61}^2)y_b - \xi_{51}\xi_{41}x_b \\ -\frac{1}{2}(\xi_{51}^2+\xi_{61}^2)x_b \\ 0 \end{bmatrix}$$

$$+ \rho g A_W \begin{bmatrix} -\xi_{61}\xi_{31}x_f - \xi_{21}(\xi_{31}+\xi_{41}y_f - \xi_{51}x_f) \\ -\xi_{61}\xi_{31}y_f - \xi_{11}(\xi_{31}+\xi_{41}y_f - \xi_{51}x_f) \\ \xi_{31}(\xi_{41}x_f+\xi_{51}y_f) \end{bmatrix}$$

$$+ \rho g \begin{bmatrix} \xi_{61}(\xi_{51}S_{11} - 2\xi_{41}S_{12} - \xi_{51}S_{22}) \\ \xi_{61}(\xi_{41}S_{11} - 2\xi_{51}S_{21} - \xi_{41}S_{22}) \\ \xi_{41}\xi_{51}(S_{22}-S_{11}) + (\xi_{41}^2 - \xi_{51}^2) \end{bmatrix}, \tag{5.69}$$

where $\vec{M}_D^{(1)}$ is defined as the first order hydrodynamic moment, given by the integral in equation (5.68); the first order and the second order hydro-restoring moments are given by

$$\vec{M}_S^{(r)} = \vec{M}_{aS}^{(r)} + \vec{\Omega}^{(r)}x\vec{M}_a^{(0)} + \vec{\xi}^{(r)}x\vec{F}_a^{(0)}, \qquad (r=1,2) \tag{5.70}$$

or

$$\vec{M}_S^{(r)} = \rho g V \begin{bmatrix} \xi_{2r} + x_b\xi_{6r} - z_b\xi_{4r} \\ -\xi_{1r} + y_b\xi_{6r} - z_b\xi_{5r} \\ 0 \end{bmatrix} + \rho g \begin{bmatrix} -y_f\xi_{3r}A_W - \xi_{4r}S_{22} + \xi_{5r}S_{21} \\ x_f\xi_{3r}A_W + \xi_{4r}S_{21} - \xi_{5r}S_{11} \\ 0 \end{bmatrix}. \tag{5.71}$$

The terms proportional to ρgV are due to buoyancy. For freely floating bodies, these terms cancel with the body weight moment, except the terms associated with z_b. The last four terms in equation (5.69) are not given in Ogilvie (1983). Otherwise, the present formula is identical to that of Ogilvie (1983), under the condition U=0.

5.1.2 Added mass and radiation damping

For simple harmonic motion, the time dependence of the first order hydrodynamic force (5.45) and the first order hydrodynamic moment (5.68) can be factorised. The components of the force that are associated with the radiation potentials can be more conveniently described in terms of added mass and radiation damping, defined by (Newman 1978)

$$\tau_{ij} = \omega^2 a_{ij} - i\omega b_{ij}$$

$$= \rho\omega^2 \int_{S_B} (\phi_j - \frac{i}{\omega}\vec{W}.\vec{\nabla}\phi_j) n_i \, dS, \tag{5.72}$$

for i,j=1,2,...,6. The added mass coefficients a_{ij} and the radiation damping coefficients b_{ij} correspond to the force components in phase with the acceleration and with the velocity respectively. These coefficients are real numbers, and are frequency dependent. If we let ξ_j be defined as the complex amplitude of the first order motion of the body: $\xi_{j1}=\mathrm{Re}[\xi_j e^{i\omega t}]$, together with equation (5.72), the six components of the first order hydrodynamic force in radiation

problems then take the form

$$F_i^{(1)}(t) = \mathrm{Re}\Big[\sum_{i=1}^{6} \xi_j \tau_{ij}\, e^{i\omega t}\Big]. \tag{5.73}$$

In accordance with the small forward speed perturbation analysis, the hydrodynamic transfer function τ_{ij} is further expressed as

$$\frac{\tau_{ij}}{\rho\omega^2 V} = \frac{a_{ij}}{\rho V} - i\frac{b_{ij}}{\rho\omega V}$$

$$- \frac{1}{V}\int_{S_B} \phi_{j0} n_i \, dS + \frac{\tau_0}{V}\int_{S_B} [\phi_{j1} - \frac{i}{k_0}\vec{\nabla}(\bar{\phi}-x).\vec{\nabla}\phi_{j0}]n_i \, dS \tag{5.74}$$

This expression is appropriate for both the wave frequency expansion and the encounter frequency expansion. For the latter, τ_0 and k_0 should be interpreted as τ and k.

5.1.3 Exciting forces

The first order exciting forces are due to the components of the first order hydrodynamic force (5.45) and the first order hydrodynamic moment (5.68) that are associated with the diffraction potential. The complex amplitude of the exciting force or moment is defined by (Newman 1978)

$$f_i = -\rho A \int_{S_B} (i\omega + \vec{W}.\vec{\nabla})(\phi_0 + \phi_7) n_i \, dS. \tag{5.75}$$

The six components of the exciting force are then written as

$$F_i^{(1)}(t) = \mathrm{Re}[f_i e^{i\omega t}] \tag{5.76}$$

None of the boundary conditions governing the first order incident potential or the diffraction potential is affected by the body motion. Therefore, the first order exciting force is independent of the body motion, just as the added mass and the radiation damping are independent of the amplitude of the incident waves.

In accordance with the wave frequency expansion in the small forward speed perturbation analysis, the exciting force can be further expressed in the form of

$$\frac{f_i}{\rho g A S} = -\frac{i\omega_0}{gS}\{\int_{S_B}(\phi_{00}+\phi_{70})n_i dS + \tau_0\int_{S_B}[-\cos\beta(\phi_{00}+\phi_{70}) + \phi_{71} - \frac{i}{k_0}\vec{\nabla}(\phi-x).\vec{\nabla}(\phi_{00}+\phi_{70})]n_i dS\}. \tag{5.77}$$

Note that for the wave frequency expansion $\phi_{01}=0$. S has the dimension of area, used for non-dimensionalization. For floating bodies, S is usually taken as the water plane area A_W, whereas for submerged bodies, the vertically projected area of the body is taken. At zero forward speed, the magnitude of the non-dimensionalized heave exciting force tends to one in the long wave limit for surface-piercing bodies, i.e. $|f_3|/\rho g A A_W \to 1$, as $\omega \to 0$. This is because when the wavelength is long compared with the body dimensions, the modification of the body to the flow is negligible. The Froude-Krylov force is the leading order term, and furthermore the incident potential can be taken out of the integral in equation (5.77) and evaluated at a suitable point on or inside the body. The remaining

surface integral of the normal component would be zero, except the components of the vertical force and the horizontal moment. Similarly, for submerged bodies, all components of the exciting force and moment are zero in the long wave limit. It is noted that the denominator $\rho g A A_W$ is, in fact, the hydrostatic force, which implies that in the long wave limit, the leading order of the exciting force is the variation of the buoyancy, associated with rise and fall of the free surface elevation; the inertial force is negligible in the long wave limit.

5.1.4 Mean drift forces

In regular waves, the first order force or moment is sinusoidal in time, oscillating at the frequency of the incident waves. The second order force or moment, however, contains a double frequency oscillatory component and a time independent component due to the quadratic cross-product terms in the pressure integration. Taking the time average of equations (5.46) yields

$$\bar{\vec{F}}^{(2)} = \frac{1}{2}\rho g \oint_{C_W} \overline{\eta_{R1}^2} \frac{\vec{n}}{\sqrt{1-n_3^2}}\, dl \qquad (\bar{F}_I)$$

$$- \rho \int_{S_B} \overline{\frac{1}{2}\vec{\nabla}\Phi_1 . \vec{\nabla}\Phi_1}\ \vec{n}\, dS \qquad (\bar{F}_{II})$$

$$- \rho \int_{S_B} \overline{(\vec{\xi}^{(1)} + \vec{\Omega}^{(1)}{}_{\vec{x}\vec{x}}) . \vec{\nabla}(\Phi_{1t} + \vec{W} . \vec{\nabla}\Phi_1)}\vec{n}\, dS \qquad (\bar{F}_{III})$$

$$+ \overline{\vec{\Omega}^{(1)} \times \vec{F}_D^{(1)}} - \rho g A_W \begin{bmatrix} \xi_{51}(\xi_{31}+\xi_{41}y_f-\xi_{51}x_f) \\ -\xi_{41}(\xi_{31}+\xi_{41}y_f-\xi_{51}x_f) \\ \xi_{61}(\xi_{41}x_f+\xi_{51}y_f) \end{bmatrix}. \qquad (\bar{F}_{IV})$$

(5.78)

For convenience, the formula is divided into four groups: $\bar{F}_I$, $\bar{F}_{II}$, $\bar{F}_{III}$ and $\bar{F}_{IV}$ as shown above. Components in each direction will be denoted by $\bar{F}_i$. From

$$\mathrm{Re}[Ae^{i\omega t}]\mathrm{Re}[Be^{i\omega t}] = \tfrac{1}{2}\mathrm{Re}[AB^*] = \tfrac{1}{2}\mathrm{Re}[A^*B], \tag{5.79}$$

it follows that

$$\bar{F}_i = \frac{1}{4}\rho g \oint_{C_W} \mathrm{Re}[\eta_R^* \eta_R] \frac{n_i}{\sqrt{1-n_3^2}}\, dl \qquad (\bar{F}_I)$$

$$- \frac{\rho}{4} \int_{S_B} \mathrm{Re}[\vec{\nabla}\phi^* . \vec{\nabla}\phi] n_i \, dS \qquad (\bar{F}_{II})$$

$$- \frac{\rho}{2} \int_{S_B} \mathrm{Re}[\alpha_j^* \frac{\partial}{\partial x_j}(i\omega\phi + \vec{W}.\vec{\nabla}\phi)] n_i \, dS \qquad (\bar{F}_{III})$$

$$+ \begin{cases} \frac{1}{2}\mathrm{Re}[\, \xi_5^* f_{D3} - \xi_6^* f_{D2} \,] - \frac{1}{2}\rho g A_W \mathrm{Re}[\, \xi_5^*(\xi_3+\xi_4 y_f - \xi_5 x_f) \,], & \text{for } i=1 \\ \frac{1}{2}\mathrm{Re}[\, \xi_6^* f_{D1} - \xi_4^* f_{D3} \,] - \frac{1}{2}\rho g A_W \mathrm{Re}[-\xi_4^*(\xi_3+\xi_4 y_f - \xi_5 x_f) \,], & \text{for } i=2 \\ \frac{1}{2}\mathrm{Re}[\, \xi_4^* f_{D2} - \xi_5^* f_{D1} \,] - \frac{1}{2}\rho g A_W \mathrm{Re}[\, \xi_6^*(\xi_4 x_f + \xi_5 y_f) \,], & \text{for } i=3 \end{cases} \qquad (\bar{F}_{IV})$$

(5.80)

where the velocity potential ϕ, and the displacements of the body ξ_j are understood as first order complex amplitudes; and α_i, f_{Di} are the first order complex amplitudes of the total displacement and hydrodynamic forces respectively, defined by

$$\begin{bmatrix} \alpha_1 \\ \alpha_2 \\ \alpha_3 \end{bmatrix} = \begin{bmatrix} \xi_1+\xi_5 z-\xi_6 y \\ \xi_2+\xi_6 x-\xi_4 z \\ \xi_3+\xi_4 y-\xi_5 x \end{bmatrix}, \tag{5.81}$$

$$f_{Di} = f_i + \sum_{j=1}^{6} \xi_j r_{ij} \, . \tag{5.82}$$

An expression for the moment may be obtained similarly.

5.2 Equations of motion

Having obtained the force and moment, we are now in a position to derive the equation of motion of the body. The motion of a freely floating or restrained offshore structure is analogous to a mechanical oscillator. The first order equations of motion have been described in detail in many basic text books. The forward speed does not influence the principles used in deriving the equations, although it may influence certain features of the final equations. The second order motion is less widely described. Ogilvie (1983) has derived the second order equations of motion for zero-forard speed motion. Since the equation for the rotational motion can be written with respect to the origin, the centre of gravity, or any other point, even the first order equations can appear to be very different. For this reason, it is necessary to derive the equations of motion in this section to avoid misquoting other authors. The rotational motion below is described with respect to the origin. For the sake of completeness the second order equations of motion are also given.

5.2.1 The first order equations of motion

The equations of motion of a rigid body can be derived from the conservation of momentum. Generally, the motion is in six degrees of freedom.

Apart from the wave forces, the environmental loading upon the body also contains restraining forces (from the mooring lines, for example), gravity, etc. Let F_m, T denote the restraining force and moment; ρ_B denote the density of the body mass; $\vec{x}_G$ the centre of the body mass. From the conservation of linear and angular momentum, the equations of motion are expressed in the form of

$$\frac{d}{dt}\int_V \rho_B \dot{\vec{x}}\, dV = \vec{F} - Mg\vec{k} + \vec{F}_m , \tag{5.83}$$

$$\frac{d}{dt}\int_V \rho_B \vec{x}\times\dot{\vec{x}}\, dV = \vec{M} + \vec{x}_G \times (-Mg\vec{k}) + \vec{T}. \tag{5.84}$$

Here $\vec{F}$, $\vec{M}$ are given by equations (5.13) and (5.14); $\vec{x}$ is the position vector to the origin; and an overdot denotes the differentiation with respect to time, i.e. d/dt. Similarly, double overdots will be used to denote the second derivative in time.

The angular momentum equation can take different forms, since the value of the angular momentum and the moment depend on the reference point. In equation (5.84), the angular momentum and the moment are taken with respect to the origin. It is sometimes more

convenient to form the equation with respect to other points, for example, to the hinged point of an articulated column or to the centre of rotation of a moored or freely floating body. Suppose the centre of rotation is at position $\vec{x}_R$. Then, the equation with respect to the centre of rotation can be derived in a similar form to equation (5.84), from the basic relation for moments

$$\vec{M}_R = \vec{M} - \vec{x}_R \times \vec{F}$$

and with $\vec{x}\times\dot{\vec{x}}$ replaced by $(\vec{x}-\vec{x}_R)\times\dot{\vec{x}}$, where $\vec{M}_R$ is the moment to the centre of rotation. The relation also applies to the gravity and restraining moments. More information about first order equations of motion with respect to the centre of rotation may be found in the book of Mei (1982).

The left hand side terms of equations (5.83) and (5.84) can be regarded as body inertial force and moment. For small amplitude motion these two terms can be simplified to

$$\frac{d}{dt}\int_V \rho_B \dot{\vec{x}}\, dV = \int_V \rho_B \ddot{\vec{x}}\, dV = M(\ddot{\vec{\xi}} + \ddot{\vec{\Omega}} \times \vec{x}'_G), \tag{5.85}$$

$$\frac{d}{dt}\int_V \rho_B \vec{x}\times\dot{\vec{x}}\, dV = \int_V \rho_B \vec{x}\times\ddot{\vec{x}}\, dV = M\vec{x}'_G \times \ddot{\vec{\xi}} + I.\ddot{\vec{\Omega}}\ , \tag{5.86}$$

up to the order $O(\epsilon)$. The tensor I is defined by

$$I = \begin{bmatrix} I_{11} & I_{12} & I_{13} \\ I_{21} & I_{22} & I_{23} \\ I_{31} & I_{32} & I_{33} \end{bmatrix}; \tag{5.87}$$

with

$$I_{ii} = \int_V \rho_B(\vec{x}'.\vec{x}' - x_i' x_i')\, dV; \qquad I_{ij} = -\int_V \rho_B x_i' x_j'\, dV. \tag{5.88}$$

From the zeroth order quantities of equations (5.83) and (5.84), we obtain the static equilibrium equations

$$\rho g V - Mg + F_{m3}^{(0)} = 0, \tag{5.89}$$

$$\rho g V y_b - M g y_G' + T_1^{(0)} = 0\ , \tag{5.90}$$

$$-\rho g V x_b + M g x_G' + T_2^{(0)} = 0. \tag{5.91}$$

Other components are zero, i.e., $F_{m1}^{(0)} = F_{m2}^{(0)} = T_3^{(0)} = 0$. For freely floating bodies, the vertical component of the restraining force and the horizontal components of the restraining moment all become zero. Hence, $Mg = \rho g V$. That is to say, the buoyancy force is equal to the gravity but in the opposite direction, in accordance with Archimedes' principle. For freely floating bodies, one also obtains $x_b = x_G'$, $y_b = y_G'$. This suggests that the centre of the buoyancy is on the same vertical line as the centre of gravity. The vertical position of the centre of buoyancy is associated with the stability of the body.

From equations (5.83) and (5.84), the first order equations of motion are obtained as

$$M(\dot{\vec{\xi}}^{(1)} + \dot{\vec{\Omega}}^{(1)} x \vec{x_G'}) = \vec{F}^{(1)} + \vec{F}_m^{(1)}, \tag{5.92}$$

$$M\vec{x_G'} x \dot{\vec{\xi}}^{(1)} + I.\dot{\vec{\Omega}}^{(1)} = \vec{M}^{(1)} + \vec{T}^{(1)} + (\vec{\xi}^{(1)} + \vec{\Omega}^{(1)} x \vec{x_G'}) x (-Mg\vec{k}). \tag{5.93}$$

These contain six simultaneous linear equations. By substituting

equations (5.48) and (5.71) and moving the hydro-restoring force and moment on to the right hand side, the equations of motion can be re-written in the form of

$$m_{ij}\ddot{\xi}_{j1} + c_{ij}\xi_{j1} = F_i^{(1)} + F_{mi}^{(1)}. \tag{5.94}$$

Here $F_i^{(1)}$ is the component of the first order generalized hydrodynamic force and $F_{mi}^{(1)}$ is the component of the generalized restraining force. The mass matrix $[m_{ij}]$ is given by

$$\begin{bmatrix} M & 0 & 0 & 0 & Mz'_G & -My'_G \\ 0 & M & 0 & -Mz'_G & 0 & Mx'_G \\ 0 & 0 & M & My'_G & -Mx'_G & 0 \\ 0 & -Mz'_G & My'_G & I_{11} & I_{12} & I_{13} \\ Mz'_G & 0 & -Mx'_G & I_{21} & I_{22} & I_{23} \\ -My'_G & Mx'_G & 0 & I_{31} & I_{32} & I_{33} \end{bmatrix} \tag{5.95}$$

The hydro-restoring coefficients matrix $[c_{ij}]$ is given by

$$\begin{bmatrix} 0 & 0 & 0 & 0 & 0 & 0 \\ 0 & 0 & 0 & 0 & 0 & 0 \\ 0 & 0 & \rho g A_W & \rho g A_W y_f & \rho g A_W x_f & 0 \\ 0 & -(\rho g V - Mg) & \rho g A_W y_f & \rho g S_{22} + \rho g V z_b - Mg z_G & -\rho g S_{21} & -(\rho g V x_b - Mg x_G) \\ \rho g V - Mg & 0 & -\rho g A_W x_f & -\rho g S_{12} & \rho g S_{11} + \rho g V z_b - Mg z_G & -(\rho g V y_b - Mg y_G) \\ 0 & 0 & 0 & 0 & 0 & 0 \end{bmatrix} \tag{5.96}$$

The coordinates hear are coordinates at the equilibrium position, independent of time. For convenience, the prime is omitted. The mass

matrix is symmetrical, but not the hydro-restoring coefficients matrix. The asymmetry of the hydro-restoring coefficients matrix is caused by the effect of the restraints. For unrestrained bodies, i.e. freely floating bodies, some terms in the matrix (5.96) vanish due to the requirements of the hydro-static equilibrium. The hydro-restoring coefficients matrix also becomes symmetrical.

For simple harmonic motion (in regular waves), following the decomposition of the first order hydrodynamic force in the previous sections, we can write the equations of motion in the form of

$$[-\omega^2(m_{ij}+a_{ij}) + i\omega b_{ij} + c_{ij}]\ \xi_j = f_i + f_{mi}. \qquad (i,j=1,2,\ldots,6) \tag{5.97}$$

These are six simultaneous linear equations. ξ_j is the complex amplitude of the six components of the motion. The ratio of ξ_j/A is known as the transfer function of the response to the incident waves.

5.2.2 The second order equations of motion

For the sake of completeness of formulation, the second order equations of motion are given in this section.

The principle used for the first order analysis can be extended. For this purpose, it is necessary to retain the second order terms in the procedure. From the coordinate transformation

$$\vec{x} = \vec{x}' + \vec{\xi} + \vec{\Omega}x\vec{x}' + \epsilon^2\underset{\sim}{H}\vec{x}' + O(\epsilon^3)$$

where $\vec{x}'$ denotes the mean position vector which is independent of time, we obtain

$$\dot{\vec{x}} = \dot{\vec{\xi}} + \dot{\vec{\Omega}}x\vec{x}' + \epsilon^2\dot{\underset{\sim}{H}}\vec{x}' + O(\epsilon^3). \tag{5.98}$$

Similarly, for the rotation motion,

$$\vec{x}x\dot{\vec{x}} = \vec{x}'x\dot{\vec{\xi}} + \dot{\vec{\Omega}}(\vec{x}'.\vec{x}') - \vec{x}'(\vec{x}'.\dot{\vec{\Omega}}) + \vec{x}'x(\epsilon^2\dot{\underset{\sim}{H}}\vec{x}') + \vec{\xi}x(\dot{\vec{\xi}} + \dot{\vec{\Omega}}x\vec{x}')$$
$$+(\vec{\Omega}x\vec{x}')x\dot{\vec{\xi}} - \vec{x}'(\vec{x}'.\dot{\vec{\Omega}}x\vec{\Omega}). \tag{5.99}$$

Substituting equations (5.98) and (5.99) into equations (5.83) and (5.84) and taking the second order terms lead to

$$M(\dot{\vec{\xi}}^{(2)} + \dot{\vec{\Omega}}^{(2)}x\vec{x}'_G) = \vec{F}^{(2)} + \vec{F}_m^{(2)}, \tag{5.100}$$

$$M\vec{x}'_Gx\dot{\vec{\xi}}^{(2)} + I.\dot{\vec{\Omega}}^{(2)} = \vec{M}^{(2)} + \vec{T}^{(2)} + (\vec{\xi}^{(2)} + \vec{\Omega}^{(2)}x\vec{x}'_G + \underset{\sim}{H}\vec{x}'_G)x(-Mg\vec{k})$$
$$- \vec{E} - \vec{\xi}^{(1)}x(\vec{F}^{(1)}+\vec{F}_m^{(1)}) - M(\vec{\Omega}^{(1)}x\vec{x}'_G)x\dot{\vec{\xi}}^{(1)} - I^a.(\dot{\vec{\Omega}}^{(1)}x\vec{\Omega}^{(1)}) \tag{5.101}$$

where the tensor I^a is defined in a similar way to the tensor I, with

$$I^a_{ij} = -\int_V \rho_B x'_i x'_j \, dV; \tag{5.102}$$

and the vector $\vec{E}$ is defined by

$$\vec{E} = \int_V \rho_B \vec{x}'x\dot{\underset{\sim}{H}}\vec{x}' \, dV = \begin{bmatrix} I^a_{3j}\dot{h}_{2j} - I^a_{2j}\dot{h}_{3j} \\ I^a_{1j}\dot{h}_{3j} - I^a_{3j}\dot{h}_{1j} \\ I^a_{2j}\dot{h}_{1j} - I^a_{1j}\dot{h}_{2j} \end{bmatrix}, \tag{5.103}$$

where $\dot{h}_{ij}$ is the second time derivative of the elements of the matrix $\underset{\sim}{H}$. For freely floating bodies many terms in the second order moment

of the body weight cancel buoyancy terms, i.e. terms proportional to V, in the second order fluid pressure moment, except those associated with z_b, z_G. There are also certain cancellations among terms associated with the interactions between the first order response and the first order force or moment.

5.3 Numerical considerations

Once the boundary value problem is solved, the computation for the linearized forces and motions of the body is straightforward, but care should be taken concerning the second order mean drift forces at forward speed. As can be seen from equation (5.78), the mean drift force contains second derivatives of the velocity potentials, which are very demanding for numerical accuracy. In particular, the normal component of the second derivative is more difficult to compute than the tangential component.

As in the technique used for solving the boundary value problem, calculation of the normal component of the second derivative can be circumvented by applying the integral theorem derived in Appendix E. We rewrite the terms to be evaluated as

$$\vec{\alpha}.\vec{\nabla}(\vec{W}.\vec{\nabla}\Phi) = \vec{\alpha}.[\vec{\nabla}\vec{W}.\vec{\nabla}\Phi + \vec{\nabla}\vec{\nabla}\Phi.\vec{W}]$$

$$= \vec{\alpha}.[\vec{\nabla}\Phi.\vec{\nabla}\vec{W} + \vec{W}.\vec{\nabla}\vec{\nabla}\Phi]$$

because $\vec{\nabla}x\vec{W}=0$, $\vec{\nabla}x\vec{\nabla}\Phi=0$. Hence,

$$\vec{\alpha}.\vec{\nabla}(\vec{W}.\vec{\nabla}\Phi) = \Phi_{1_j}\frac{\partial\vec{W}}{\partial l_j}.\vec{\alpha} + \vec{\alpha}.\ W_{1_j}\frac{\partial\nabla\Phi}{\partial l_j} + \Phi_n\frac{\partial\vec{W}}{\partial n}.\vec{\alpha} \qquad (W_n=0)$$

$$= \Phi_{1_j}\frac{\partial W_i}{\partial l_j}\alpha_i + W_{1_j}\frac{\partial}{\partial l_j}(\Phi_{x_i})\alpha_i - \Phi_n\alpha_i m_i.$$

$$(j=1,2,\ i=1,2,3) \qquad (5.104)$$

where $\partial/\partial l_1$, $\partial/\partial l_2$ denote derivatives in the two tangential directions. In the first two terms, the derivatives can be computed from the shape functions, while W_i, $\Phi_x i$ can be computed from the normal and tangential components of $\vec{W}$ and $\vec{\nabla}\Phi$. The normal component of $\vec{W}$ known from the boundary condition and its tangential components can be computed from shape functions. While the tangential components of $\vec{\nabla}\Phi$ can also be computed from the shape functions, the normal components may be computed from the indirect boundary integral formulation. The last term in equation (5.104) may be circumvented by applying the integral theorem derived in Appendix E:

$$-\int_{S_B}\Phi_n\alpha_i\vec{n}m_i\ dS = \int_{S_B}\vec{W}.\vec{\nabla}(\Phi_n\alpha_i\vec{n})n_i\ dS = \int_{S_B}W_{1_j}\frac{\partial}{\partial l_j}(\Phi_n\alpha_i\vec{n})n_i\ dS. \qquad (5.105)$$

The line integral is neglected for small forward speed.

Chapter 6

RESULTS AND DISCUSSION

Results obtained from the theory described in Chapter 4 and Chapter 5 are presented for two dimensional cylinders floating on the free surface or completely submerged. The results include added mass, radiation damping, exciting forces, dynamic responses of rigid bodies, second order mean drift forces and wave drift damping. The three modes of motion are referred to as sway, heave and roll, and are denoted by the subscripts "2", "3" and "4".

6.1 Semi-analytical solutions for a circular cylinder

The sway and heave radiation problems for a circular cylinder at zero-speed are firstly solved by the multipole expansion method presented in Section 4.2. Accounting the symmetry of the flow, the symmetrical multipoles are dropped in expression (4.66) for sway, and the anti-symmetrical multipoles are dropped for heave. The series (4.66) are then truncated after N terms, and the unkown coefficients are obtained from the body surface condition. For the complex radiation potential defined corresponding to unit amplitude of the velocity of forced oscillation, i.e. $\Phi_j = \mathrm{Re}[i\omega\phi_j \xi_j e^{i\omega t}]$, the body surface condition (4.53) becomes

$$\sum_{m=1}^{N} b_m \frac{\partial s_m}{\partial r} \simeq \sin\theta, \qquad \text{on } r=a, \tag{6.1}$$

for sway, or

$$a_0 \frac{\partial c_0}{\partial r} + \sum_{m=1}^{N-1} a_m \frac{\partial c_m}{\partial r} \simeq \cos\theta, \qquad \text{on } r=a, \tag{6.2}$$

for heave. The point collocation method is used to determine the coefficients with equally spaced points over half of the circular profile. Results are presented for submerged cylinders as well as for floating cylinders, with the depths of submergence ranging from h/a=0.25 to 3.0, where a is the radius and h is the distance of the axis to the mean free surface (as shown in Figure 6.1). In all the results, multipoles are placed on the axis of the cylinder (f=-h).

6.1.1 Convergence

The multipole expansion expression (4.66) converges very rapidly. The convergence is firstly shown in detail for a submergence h/a=2.0 in Tables 6.1 to 6.4; then illustrated briefly for other depths of submergence in Figure 6.2.

Tables 6.1 and 6.2 give the complex coefficients (in brackets) in the series expression of the velocity potential. Each column represents one set of coefficients with the mth row denoting b_m/a in Table 6.1 and a_{m-1}/a in Table 6.2. It is seen that for each set of coefficients, only the first two or three terms have significant values, and the results have little change for different N. That implies that the series converges rapidly and the solution is very stable. It may be interesting to notice that in Table 6.2 $a_0=-kaa_1$. That is a plain consequence of the fact that the net mass flux across the body surface is zero.

Tables 6.3 and 6.4 represent the nondimensionalized added mass and damping, which further corroborate the rapid convergence. For example, over the whole frequency range presented an absolute accuracy of $4x10^{-3}$ can be achieved by using 3 terms only! If more terms are used, the accuracy is improved dramatically. In particular, the solution of N=10 is identical to that of N=20 up to the fifth decimal place, which implies an error less than $5x10^{-6}$.

For other depths of submergence, the solution also converges fairly rapidly, provided that the cylinder is not too close to the free surface. It is observed numerically that for submerged cylinders, more terms are required if the cylinder is closer to the free surface. For example, if an accuracy of $4x10^{-3}$ is to be achieved, it requires that N=2 for h/a=3.0 or larger, N=3 for h/a=2.0, and N=7 for h/a=1.25. For floating cylinders, more terms of multipoles are necessary. The most demanding case is when the cylinder is just below or piercing the surface. This is not surprising, because in that case the body intersects the free surface at an angle of zero degree, which makes the linearized boundary value problem mathematically unstable and physically meaningless. A group of N~h/a curves is plotted in Figure 6.2, which estimates the approximate number of terms required to achieve a given accuracy for the added mass and damping.

What is surprising is that for a floating cylinder although the solution of the added mass and damping based on the multipoles (4.55) to (4.99) converges to definite values, the coefficients in the multipole expansion are not unique. The number of multipoles

required to achieve convergent results for a given accuarcy may be found in Figure 6.2. The phenomenon of non-unique multipole expansion coefficients is not fully understood yet. A possible explanation is that in that case the multipoles become linearly dependent on each other. Besides that, the fact that the body does not intersect the free surface at a right angle is also a source of suspicion.

6.1.2 Validation

To validate these results, comparisons are shown in Figure 6.3 for a submerged cylinder at several submergencies. Excellent agreement is found with values measured from the curves of Ogilvie's (1963) analytical solutions. Two sets of results for depths of submergence of h/a=2.0, and 0.5 are also presented in Tables 6.5 and 6.6 respectively, alongside solutions obtained by the numerical methods. Again, solutions from different methods are coherent.

An interesting alternative for computing the radiation damping is to use a relation derived from consideration of the energy flux and the work done by the damping force (Newman 1977, Chapter 6). This provides a means of self-checking. From this consideration, it can be shown that the diagonal damping coefficient is related to the far field wave amplitude by

$$\frac{b}{\rho\pi a^2\omega} = \frac{1}{\pi(ka)^2}\,|k\phi_W(z=0)|^2, \tag{6.3}$$

where $k\phi_W$ represents the complex amplitude of the surface elevation

at infinity, corresponding to unit amplitude of forced oscillation; and the far field expression of the velocity potential ϕ_W is given by

$$\phi_W = 2\pi b_1 ka \ \mathrm{sgn}(x) e^{k(f+z)-ik|x|}, \tag{6.4}$$

for sway, or

$$\phi_W = -i2\pi a_0 e^{k(f+z)-ik|x|}, \tag{6.5}$$

for heave. Computation from this wave amplitude relation is found to give precisely the same answer as that from pressure integration. For example, from the coefficient b_1/a obtained at N=10 given in Table 6.1 (the first row in each block) at ka=0.1 and 1.0, together with equations (6.3) to (6.5), the damping coefficients 0.10721 and 0.15771 for ka=0.1 and 1.0 respectively are recovered.

6.1.3 Some physical effects

From the results presented in Tables 6.5 to 6.8 and in Figure 6.3 to 6.5, some physical behaviour associated with the forced oscillation can be summarized. First, for the submerged cylinder, the diagonal added mass and damping in sway motion are identical to those in heave motion. These are achieved to a very high accuracy. Secondly, while the damping is always non-negative, the added masss can be negative. This occurs for a submerged cylinder, when it is very close to the free surface; about $h/a<1.125$. Negative added mass is also found for surface-piercing cylinders in sway motion, but not for heave motion. This happens when the cylinder is more than three quarters immersed, i.e. $h/a>0.5$. Thirdly, at certain frequencies, the heave damping for a surface-piercing cylinder is zero, which implies

that at these frequencies the forced heave oscillation does not transfer energy to the fluid and hence does not generate waves. The same does not appear to have happened for the sway over the computed frequency range. Lastly, as the cylinder emerges from below the free surface, the heave added mass and damping have a dramatic change, whereas those for sway change rather smoothly. In particular, the low frequency heave damping changes from zero to finite values, and the added mass jumps from finite to infinitive values.

6.1.4 Surface elevation

The free surface elevation has also been computed and results for a submerged cylinder at h/a=2.0 in forced sway oscillation are plotted in Figure 6.6a-h for ka=0.5, 1.0, 2.0 and 4.0 respectively. The real part and the imaginary part of $k\phi_L$, $k\phi_W$ and $k\phi$ are plotted for sway motion of a cylinder submerged at h/a=2.0, where ϕ denotes the sway radiation potential (i.e. ϕ_2 with the subscript "2" dropped for simplicity), ϕ_W is the far field expression defined by equation (6.4) and ϕ_L is the remaining local disturbance defined such that $\phi = \phi_W+\phi_L$. From the expression for the free surface elevation

$$\eta = -\frac{1}{g}\Phi_t = \mathrm{Re}[k\phi\xi_2 e^{i\omega t}], \tag{6.6}$$

it is known that $k\phi$ represents the complex amplitude due to unit forced oscillation. The real part of $k\phi$ can be regarded as the free surface elevation at the moment when the cylinder is at its positive maximum position, whereas the imaginary part as that when the cylinder returns to its centre of oscillation from the positive displacement.

From Figure 6.6a-h, it is seen that the local disturbance decays to zero rapidly and steadily. Usually after 4~5 times the radius away from the origin, $k\phi$ and $k\phi_W$ become undistinguishable in the curves, which suggests that the local disturbance is then negligible.

6.2 Zero-speed solutions

Motions of cylinders are solved by both the BIE-BMP and BIE-BIE methods for several cross-sections, including a circle, an ellipse, a triangle and a rectangle.

6.2.1 Comparison of theories

In Tables 6.5 to 6.8, numerical results of added mass and damping are presented for a submerged circular cylinder of a submergence h/a=2.0, and a floating circular cylinder of a submergence h/a=0.5 respectively. The agreement among the BIE-BMP, the BIE-BIE and the analytical solutions is up to four digital places. The same meshes are used for the BIE-BMP and BIE-BIE methods. For the submerged cylinder, 32 elements are used with 16 on S_B and 16 on S_J. For the floating cylinder, 20 elements are used with 8 on S_B, 8 on S_J and 4 on S_F. For practical application, coarser meshes may be used. For example, using 16 elements (with 8 on S_B and 8 on S_J) gives an accuracy of no fewer than three significant digital places for the cylinder submerged at h/a=2.0, which is usually sufficient in

application. In Tables 6.7 and 6.8 for the floating cylinder, the multipoles in the BIE-BMP method are placed on the mean free surface, whereas the analytical solutions are obtained by placing the multipoles at the axis of the cylinder.

In Figures 6.7 and 6.8, two meshes are presented for a submerged circle and a submerged rectangle. The rectangle has a beam B equal to the draft D. The added mass and damping for these cross-sections are plotted in Figures 6.9 to 6.12. Excellent agreement is achieved among results from the BIE-BIE method, the BIE-BMP method and results of other authors, such as the analytical solution of Ogilvie (1963) for the circle, and the boundary element solution of Maeda (1974) for the rectangle. It is seen that although the hydrodynamic coefficients in sway equal those in heave for a submerged circle, this is not the case for other geometries. For the rectangle, the sway damping is consistently larger than the heave damping, but the added mass follows no such pattern. As the submergence increases, the sway coefficients become closer to the heave coefficients.

In Figures 6.13 to 6.16, fine meshes are presented for a floating semicircle, an ellipse, a rectangle and a triangle. The major axis of the ellipse lies horizontally on the mean free surface and the ratio of the minor axis b to the major axis a is 0.5. The rectangle has a beam B of twice the draft D/2 (i.e. B=D). The added mass and damping obtained from these meshes are presented in Figures 6.17 to 6.20. The agreement between the BIE-BMP method and the BIE-BIE method is consistently good. Good agreement is also found compared with results of Nestegard and Sclavounos (1984), and Vugts

(1968). All coefficients are nondimensionalized based on the submerged volumes (areas) of the cylinders. It may be noted that the curves of nondimensional hydrodynamic coefficients for different cylinders are alike, but the sway coefficients for the triangle and the heave coefficients for the ellipse have pronounced large values.

More extensive results concerning the first order exciting forces, responses and second order mean drift forces are presented in Figures 6.23 to 6.56. These will be discussed latter in Section 6.3, together with the forward speed solutions.

6.2.2 Factors affecting accuracy

Extensive numerical studies showed that both the BIE-BMP method and the BIE-BIE method gave very accurate results, but the BIE-BMP method is far efficient if only the zero-speed solution is required. Because the numerical discretization in the inner domain is the same for both methods, the accuarcy of the two methods is largely affected by some common factors.

The number of elements is the foremost factor that affects the accuracy for both the BIE-BIE and BIE-BMP methods. The more elements are used, the more accurate are the results, but at the same time the more computing time is required. Therefore, for a given number of elements, the arrangement of meshes affects the accuracy to a certain extent. It is observed numerically that using more or less equally spaced elements is close to the optimum. This frequently suggests that the number of elements on S_J is about one and half times those

on the body surface S_B. Some local adjustment, such as using concentrated elements near sharp corners, may be helpful in improving the accuracy, but it is unecessary for the present computation.

The distance from the matching boundary S_J to the body is another factor that affects the accuracy (or efficiency). It is found that the accuracy is not sensitive to the radius of the matching surface S_J, if S_J is not too close to the body; but there is a range of R_J over which optimum efficiency may be achieved. This is because on the one hand keeping S_J closer to the body reduces the size of the matching boundary, and on the other hand finer meshes are required because the flow varies more strongly near the body. If we let R_C denote the radius of the circle circumscribing the body, it is observed that $R_J=1.5R_C$ is about the optimum value. This corresponds to $R_J=1.5a$ for the circle, $R_J=2.2(B/2)$ for the rectangle (B-beam, D-draft and B/D=1), and $R_J=2.5(B/2)$ for the triangle (B-beam, $\theta=60^o$). It may be expected that this 1.5 times rule also holds for other simple geometries.

Apart from the similarities in which the the accuracy of the two methods are affected, the accuracy of the BIE-BIE method is also affected by the irregular frequency. Irregular frequencies are the frequencies which coinside with the eigenvalues of an associated interior Dirichlet problem subjecting to a similar homogeneous free surface condition. These exist for floating bodies only. At irregular frequencies, the solution is not unique. The occurence of the irregular frequencies is a common drawback in most boundary integral formulations and the origin is purely due to mathematical treatment, not the physical performance. In the present BIE-BMP method, no

irregular frequencies are encountered over the whole frequency range and for any geometry computed; but in the present BIE-BIE method the irregular frequencies are observed, as shown in Figure 6.21. The irregular frequencies are usually not easy to predict, but in the present BIE-BIE method the prediction is a simple matter. This is because the outer boundary is constrained to be a semicircle for floating bodies. In fact, the first three irregular frequencies are known approximately (Sayer and Ursell 1977)

$$k_1 R_J \simeq 1.822, \quad k_2 R_J \simeq 3.289, \quad k_3 R_J \simeq 4.891.$$

In Figure 6.21, these correspond to ka at 1.21, 2.19 and 3.26 because R_J=1.5a is used in generating the figure. Higher irregular frequencies are not usually of practical interest.

Although it is possible to develop some sophysticated methods to remove the irregular frequencies, this is not necessary in the present method. This is because the irregular frequencies are known, and their pollution is narrow restricted to narrow bands, as can be seen in Figure 6.21. In computation, these frequencies can be simply skipped. Should the values at these frequencies be required, they may be interpolated from the values at neighbouring frequencies. Because of the existence of the irregular frequencies, it is advisable not to take large values of R_J in the BIE-BIE method.

6.3 Forward speed solutions

Results at forward speed are presented in Figures 6.22 to 6.58. All results, except some presented in Figure 6.22, are obtained from the wave frequency expansion. In all the results presented, a " free cylinder" is defined as a freely floating cylinder, but restrained from roll motion; and a "restrained cylinder" is a cylinder retrained from all modes of motions. In all the results presented, the Froude number is defined as $Fn=U/\sqrt{gL}$, where L is the half breadth of the cross-section. For the circular and the elliptic cylinders L=a, and for the rectangular cylinder L=B/2.

6.3.1 Comparison of the two expansions

In the present study two ways of perturbation have been developed, i.e. the wave frequency expansion and the encounter frequency expansion. Both have been implemented, and it is found that they agree very well.

To illustrate the agreement, the results of the cross coupling added mass and damping are compared in Figure 6.22. Those are nondimensionalized by $\rho\pi a^2\tau$ for added mass and $\rho\pi a^2\omega\tau$ for damping. They are plotted against ka ($k=\omega^2/g$). For the wave frequency expansion, τ may be interpreted as being τ_0. In general, the forward speed correction results from the two expansions are not comparable without specifying the value of the forward speed, because the results from the wave frequency expansion include the correction due to apparent appearance of the forward speed in the boundary

conditions as well as the effect due to the shift in frequency. The latter is affacted by the forward speed and the wavelength. However, for the particular case of the cross coupling coefficients, the effect due to frequency shift is zero. This is because $\tau_{ij}=0$ (for i not equal j) at zero speed for symmetrical bodies. Thus $\partial\tau_{ij}/\partial\omega=0$. Therefore, the cross coupling results are comparable in the form given in Figure 6.22.

It is seen that the agreement between the two methods is excellent. Results are also compared with those obtained by Wu using a formulation described in Wu and Eatock Taylor (1987). The results of Wu are obtained at Fn=0.032 (then divided by τ). The agreement is good.

6.3.2 Validation

The comparison in Figure 6.22 has already indicated some evidence to support the present small forward speed theory. To further validate the theory, more comparisons are made for the floating circular cylinder and the submerged circular cylinder.

In Figures 6.25 and 6.26, results of exciting forces and sway and heave responses for a floating circular cylinder with the axis on the mean free surface are compared with these of Zhao and Faltinsen (1988). Their formulation is also a small forward speed theory (or small current velocity as they referred to), but the method they used is quite different from the present method. In the present study the problem is solved by perturbating the solution in terms of the

zero-speed solution and the forward speed correction term, whereas in the paper of Zhao and Faltinsen (1988) the problem is solved directly. In their method, the fluid domain is also divided into an inner domain and an outer domain, and the problem is solved by coupling an integral formulation in the inner domain with a multipole expansion expression in the outer domain. The multipoles they used are derived from the translating pulsating source potential, which implies that the steady flow disturbance on the free surface in the outer domain is neglected. Therefore, the inner domain in their method must be taken sufficiently large, whereas the present partition of the inner and outer domain is free from this restriction.

From Figures 6.25 and 6.26, it is seen that the agreement is good. Further comparisons of the mean drift force and wave drift damping with those of Zhao and Faltinse (1988) have also made. These are shown in Figure 6.46 and 6.57. The agreement is again very good.

In Tables 6.9 to 6.11, results of added mass, radiation damping and exciting forces for a circular cylinder submerged at h=2a are compared with those of Wu, whose results are obtained from a fully linearized theory described in Wu and Eatock Taylor (1987). Their formulation does not require the forward speed being small, but the theory is based on the free surface condition (3.13) for the steady potential and (3.24) for the unsteady potential. Neither author's results in Tables 6.9 to 6.11 included the steady flow disturbance on the free surface. From these results, it is seen that for small forward speed such as Fn=0.032, the present small forward speed theory agrees well with their more conventional theory. For

higher forward speed, the two theories are less close, but the agreement is still satisfactory for Fn up to 0.128, which corresponds to a practical forward speed (or current velocity) $U \sim 1.28 MS^{-1}$ for a cylinder of radius 10m. In Table 6.11, very good agreement is found for the exciting forces for Fn up to 0.128.

To conclude, the good agreement indicates that the present small forward speed theory is successful.

6.3.3 First order motions

Having confirmed the validity of the present theory, we now turn our attention to the dynamic behaviour at forward speed. Four cylinders have been studied.

Firstly, a circular cylinder floating on the surface with its axis on the mean free surface has been studied. In Figures 6.23 and 6.24, results of added mass and damping are presented at Fn=-0.064, 0.0 and 0.064. An interesting discovery is that a small forward speed virtually has no influence on the diagonal added mass and damping coefficients. That is, the diagonal hydrodynamic coefficients at forward speed approximately equal these at zero speed. On the cross-coupling hydrodynamic coefficients, the forward speed has certain influences. Due to symmetry of the body the cross-coupling coefficients are identically zero at zero speed, but at forward speed, the cross-coupling coefficients are no longer zero, which implies that the sway and heave motions are coupled at forward speed.

It is interesting to examine the results in more detail. Figure 6.23 and 6.24 show that, for the cylinder moving against the incident waves (U>0), apart from a low frequency range the forced heave motion will cause an increase in sway added mass (a_{23}) and a decrease in sway radiation damping; whereas the forced sway motion will cause a decrease in heave added mass and an increase in heave radiation damping. If the cylinder moves with the waves (U<0), all conclusions reverse.

A significant relation revealed in these figures is that the $\tau_{23}(U)=\tau_{32}(-U)$, which satisfies the well known Timman-Newman (1962) relation for symmetrical body. The general Timman-Newman relation states that ffor i not equal j, $\tau_{ij}(U)=\tau_{ji}(-U)$ except $\tau_{15}=\tau_{51}$ and $\tau_{24}=\tau_{42}$.

Figure 6.25 represents the exciting forces on the floating cylinder. It is seen that the forward speed has an appreciable influence. For example, at a Froude number of 0.064, the magnitude of the sway exciting force increases by about 10~15% over a broad frequency range; the increase in heave force is about half of that in sway force and only occurs at higher frequencies. The magnitude of the sway exciting force always increases for the cylinder moving against incoming waves, and always decreases for the cylinder moving with incoming waves. The magnitude of the heave exciting force does not show this definite tendency. For positive forward speed, it first decreases in the low frequency range, then increases in the higher frequency range.

In Figure 6.26, it is shown that the forward speed also has an

appreciable influence on the responses: for Fn=±0.064, the responses can well be increased or decreased about 10%. Strikingly, the variation of the responses with respect to the forward speed does not follow the same tendency as the exciting forces. As shown in Figure 6.26, the heave response shows a definite tendency with respect to the forward speed, i.e. always increases for positive forward speed and always decreases for negative forward speed. The sway response shows an indefinite tendency similar to that of the heave exciting force. The difference tendencies in the variation of the forces and responses are due to the coupling effect. This can be clearly seen from Figure 6.27, where the variation of the responses in the single degree of freedom system follows exactly that of the exciting force. Due to the coupling effect the sway response becomes more close to its zero speed value than it otherwise would be in the single degree of freedom motion; the heave response becomes further apart from its zero speed value. An important situation is that the peak value of the heave resonance is considerable increased, when the cylinder is moving against the incident waves.

Secondly, a floating rectangular cylinder has been studied. From a mathematical point of view, the linearized formulation is not exactly appropriate for bodies with sharp corners such as the rectangular cylinder. This is because the Taylor series expansion performed in deriving the body surface condition (3.34) is not valid at sharp coners. However, extensive numerical studies performed here have shown that convergent results are possible in practice. This may suggest that the inappropriate treatment in deriving the body surface condition may only has a local effect. As a whole, the linearized

theory is still acceptable.

In Figures 6.28 and 6.29, results of the exciting forces and the responses are presented. It can be seen that the variations are similar to the circular cylinder. Notably is that the heave resonance of the floating rectangular cylinder is far more significant than that of the floating circular cylinder. The added mass and radiation damping coefficients are calculated but not presented because they are qualitatively very similar to those of the floating circular cylinder.

Thirdly, a submerged circular cylinder has been studied at two depths of submergencies, namely h/a=2.0 and h/a=1.5. The first order results are presented in Figures 6.30 to 6.34 for the cylinder neutrally submerged at h=2a. Most discoveries found in the results for the floating cylinders are confirmed: the forward speed has no influence on the diagonal hydrodynamic coefficients; the sway and heave motions at forward speed are coupled.

It is noted that all the damping coefficients are consistently smaller than those for floating bodies. The variation of the exciting forces due to the forward speed effect is of about the same order of magnitude as for the floating circular cylinder, but the variation of the dynamic responses is smaller than for the floating cylinder. Neither the forces nor the responses show a consistent increase or decrease for a give direction of advance; but at higher frequency, like the case for floating cylinders, the forces or responses always increase for the cylinder moving against incoming waves and decrease for the cylinder moving with the waves.

The influence of the forward speed on the sway motion is very similar to the influence on the heave motion. The same is also true for the exciting forces. It is known that at zero speed, the magnitude of the sway exciting force or the response is equal to that of the heave exciting force or the response. From the present results it is found that at small forward the two responses are nearly the same; but the forward speed has a slightly stronger influence on the peak values of the heave exciting force, which may not be clear from the figures because of the scaling. This finding is consistent with the finding of Grue (1986) for large forward speed. Unlike the floating cylinder case, the coupling effect for the submerged cylinder is not significant. In fact, in Figure 6.33 the coupling is rarely visible except in the very low frequency range.

As one of the advantages of the present small forward speed theory, the effect of the steady flow in the free surface condition for the unsteady flow can be examined. In Figure 6.34, the complete results are represented by lines, and the results from neglecting the steady potential disturbance (Q_j terms) on the free surface are shown by markers. The figure shows that indeed the steady potential disturbance is negligible at h/a=2.0.

In Figures 6.35 to 6.39, a complete set of the first order results for the circular cylinder submerged at h/a=1.5 is shown. In these results, the solution obtained from the simplified method which neglects the steady flow disturbance on the free surface (Q_j terms) is compared with the complete solution. Throughout these results, it is clear that apart from diagonal added mass and radiation damping

coefficients, the steady flow disturbance on the free surface has an appreciable influence. The steady flow disturbance in fact increases the variation of the all the other quantities with respect to the forward speed. Therefore, it is important to take into account the steady flow disturbance in the free surface condition for the unsteady potential, when the depth of submergency is smaller than 2.0.

Finally, a submerged elliptic cylinder has been studied. The cross section of cylinder has a minor axis b equal to half of the major axis a, and the major axis is lying horizontally. The cylinder is submerged at h/a=2.0.

The reason for studying the elliptic cylinder is due to the fact the solution for a submerged circular cylinder may not be typical. This is because a submerged circular cylinder has some unique characteristics, which other geometries do not have. For example, at zero speed, a restrained or neutrally buoyant circular cylinder free to respond does not reflect an incoming wave train (Ogilvie 1963). At forward speed, a submerged circular cylinder in waves only generates two new waves in the subcritical flow, instead of typically four new waves (Grue and Palm 1985).

In Figures 6.40 to 6.44, a complete set of the first results are presented for the cylinder submerged at h/a=2.0. Results show very similar behaviour to that of the submerged circular cylinder. Added mass, radiation damping and the exciting forces in sway are considerably smaller than those in heave, whereas, strikingly, the magnitudes of the sway response and the heave response are quite

close. The steady flow disturbance again appears insignificant at this depth of submegence, as shown in Figure 6.44.

6.3.4 Second order mean drift forces

Figure 6.45 shows the horizontal mean drift forces for a floating circular cylinder restrained from time periodic motions, and Figure 6.46 showed that for the cylinder free to respond in sway and heave. For k_0a <0.5, the force on the free cylinder is virtually zero, whereas the force on the restrained cylinder has an appreciable value in the same frequency range. At higher frequency, the forces on the two cylinders are not much different because the responses are small. In both cases, the force consistently increases for the cylinder moving against incoming waves and consistently decreases for the cylinder moving with incoming waves. As expected the influence of the forward speed is stronger than that on the first order quantities. For example, a 15~20% increase (or decrease) may be observed at Fn=0.032 (-0.032). It may be observed that the influence of the forward speed does not appear to be exactly linear, which implies that nonlinear effects of using equation (5.80) becomes gradually significant at higher frequencies. The comparison with that of Zhao and Faltinsen (1988) shows excellent agreement.

Figure 6.47 and 6.48 represents the vertical mean drift force for the same restrained and free cylinder. While the force on the restrained cylinder is always downwards, the force on the free cylinder is firstly upwards at small frequencies and then changes back to downwards at higher frequencies. A positive forward speed

reduces the upwards force and increases the downwards force.

Figure 6.49 and 6.50 shows the horizontal and vertical forces for a floating rectangular cylinder of the same dimensions studied before. These results are seen similar to those of the floating circular cylinder.

Figure 6.51 shows the horizontal force for a submerged circular at h=2a. At zero speed the force is known to be identically zero for both restrained cylinder and free cylinder (Ogilvie 1963). At forward speed, the figure shows that the force is practically zero as well. The tiny curves presented in the figure may be regarded as numerical errors rather than any meaningful results, since it is seen that the positive and negative forward speed give more or less the same numbers, which must be due to the quadratic quantities in the forward speed. According to the restrictions of the present theory, these quadratic terms are considered as errors.

Figure 6.52 shows the vertical mean drift force for the submerged circular cylinder. For the free cylinder, the force is considerably smaller than the force for the restrained cylinder. A positive forward speed slightly increases the force on the free cylinder, whereas the forward speed has no practical influence on the force on the restrained cylinder.

Since the submerged circular cylinder may not represent a typical geometry, the mean drift forces on the elliptic cylinder studied before are presented in Figure 6.53 and 6.54. While the vertical mean drift force leads to the same conclusions as for the

circular cylinder, the horizontal mean drift force is not the same. The horizontal force for the free cylinder is identically zero, but this may not be the case for the restrained cylinder. The curves in Figure 6.53 may have a certain physical meaning, although similar to those for the circular cylinder their magnitudes are also quite small (about 1% of the vertical mean drift force). For $k_0 a<0.6$, the horizontal mean drift force increases for increasing forward speed.

To summarize the results for the mean drift forces, it is concluded that for submerged cylinders, the horizontal mean drift force is either zero or very small, and the vertical mean drift force is not much influenced by the forward speed; for the floating cylinder, the forward speed has a strong influence on both vertical and horizontal mean drift forces. Therefore, it may be worthwhile to study the horizontal mean drift force for the floating cylinders in more detail.

In Figure 6.55, different components contributing to the horizontal force are presented for the restrained floating circular cylinder at Fn=0.0 and Fn=0.032. These contributions are defined in equation (5.80). It is seen that the water line integral ($\bar{F}_I$) and the quadratic pressure integral ($\bar{F}_{II}$) are the two major dominating components. The water line component is in the direction of the total horizontal mean drift force and the quadratic pressure component is in the opposite direction. A stiking feature is that the water line component is just about twice the total horizontal mean drift force while the quadratic pressure component is about the same as the total horizontal mean drift force but in the opposite direction. This indicates that the sectional force close to the free surface is more

predominant, which partially explains the insignificance of the horizontal mean drift force on submerged cylinders.

Figure 6.56 is similar to Figure 6.55, but the cylinder is free to response in sway and heave. In this case, the water line component is slightly more than twice the total horizontal mean drift force; the quadratic pressure component is larger than the magnitude of the total mean drift force; and the total mean drift force is considerably smaller than that for the restrained cylinder in the low frequency range and slightly smaller in the higher frequency range.

Finally, from the result for the horizontal mean drift force, we may estimate the wave drift damping from the principle of gradient of added resistance.

Figure 6.57 represents the predicted wave drift damping for the floating circular cylinder. The solid line represents the result for free cylinder and the chain line represent the result for restrained cylinder. It may be seen that for $k_0a>1.5$ the predicted wave drift damping is almost linearly proportional to k_0a. The present prediction shows good agreement with that of Zhao and Faltinsen (1988).

Figure 6.58 represents the predicted wave drift damping for the floating rectangular cylinder. It shows a sharper peak near the resonance frequency than for the circular cylinder.

Chapter 7

CONCLUSIONS

A theoretical analysis has been carried out for the first order hydrodynamic forces and motions, as well as second order mean drift forces for large bodies at forward speed. A small forward speed perturbation theory has been presented. Succeful numerical implementations for two dimensional cylinders corroborate the correctness and effectiveness of the theory. Through the extensive numerical studies for several floating and submerged cyliners, some major conclusions may be listed below.

1. At forward speed, the time periodic motions of a rigid body in waves are coupled. At small forward speed, the coupling effect is usually small for submerged bodies, but significant for floating bodies.

2. The forward speed does not affect the diagonal added mass and radiation damping coefficients. For symmetrical bodies, the cross-coupling added mass and radiation damping coefficients are no longer zero at forward speed, but the magnitude is much smaller than the diagonal coefficients.

3. The forward speed has an appreciable influence on the exciting forces on both floating bodies and submerged bodies. The forces in the high frequency range usually increase for bodies moving against the waves, and decrease for bodies moving with the waves, but the conclusion can not be generalized in the low frequency range.

4. The forward speed has a significant influence on the time periodic responses of floating bodies, but has a small influence for deeply submerged bodies. The responses are usully increased in the high frequency range for bodies moving against waves.

5. For floating bodies, the mean drift forces are strongly affected by the forward speed. The horizontal mean drift force for a circular cylinder increases for the cylinder moving against waves and decreases for the cylinder moving with waves. For submerged bodies, the forward speed has little influence on the mean drift forces up to the first order in forward speed. In particular, the horizontal mean drift force usually remains zero or very small.

6. For floating bodies, the principle of gradient of added resistance may be applied to predict the wave drift damping. Because it is found that the horizontal mean drift force has an appreciable component linearly proportional to the forward speed. For submerged bodies, however, further consideration appears to be necessary, because the horizontal mean drift force usually does not have, or has only very small component linearly proportional to the forward speed.

ACKNOWLEDGEMENTS

I am grateful to the Chinese Educational Committee and the British Council for their joint financial support provided in the course of the PhD research.

I would like to express my sincere gratitude to my supervisor, Professor Eatock Taylor, for his invaluable guidance and constant inspiration over years.

I further thank Dr G.X. Wu for providing some numerical results for comparison. I also wish to extend my gratitude to all my colleagues. Particularly, I would like express my thanks to Dr Se-Ming Hung and F.P. Chau for many friendly discussion about second order hydrodynamics; to Justin Knoop for generously spending a lot of his valuable time in helping me to transfer files among Euclid, HP and VAX computer systems; to Paul Sincock for frequent help in sorting out difficulties with the BBC computer.

Finally, I would like to thank my parents and my family for their constant encouragement and support; to thank my wife Xiaoling for her cheerful company in the computer laboratory in many weekends.

REFERENCES

Abramowitz, M. and Stegun, I.A. Handbook of Mathematical Functions, Dover Publ., New York, 1965.

Agnon, Y. and Mei, C.C. Slow-drift motion of a two-dimensional block in beam seas, J. Fluid Mech., Vol.151, pp.279-294, 1985.

Baba, E. and Hara, M. Numerical evaluation of a wave-resistance theory for slow ships, Proc. 2nd Int. Conf. Num. Ship Hydrodyn., pp.17-29, University of California, Berkeley, 1977.

Bai, K.J. A localized finite element method for steady two-dimensional free-surface flow problems, Proc. 1st Int. Conf. Num. Ship Hydrodyn., pp.209-230, Bethesda, Maryland, 1975.

Bai, K.J. A localized finite element method for steady three-dimensional free-surface flow problems, Proc. 2nd Int. Conf. Num. Ship Hydrodyn., pp.78-87, University of California, Berkeley, 1977.

Bai, K.J. A localized finite element method for three-dimensional ship motion problems, Proc. 3rd Int. Conf. Num. Ship Hydrodyn., pp.449-462, Paris, 1981.

Bougis, J. and Vallier, P. Forces and moments in the rigid connections between a barge and its tug with forward speed in waves, Proc. 3rd Int. Conf. Num. Ship Hydrodyn., pp.517-530, Paris, 1981.

Brard, R. The representation of a given ship form by singularity distribution when the boundary condition on the free surface is linearized, J. Ship Res., Vol.16, pp.79-92, 1972.

Brown, D.T. Eatock Taylor, R. and Patel, M.H. Barge motions in random seas-a comparison of theory and experiment, J. Fluid Mech., Vol.129, pp.385-409, 1983.

Chang, M.S. and Pien, P.C. Hydrodynamic force on a body moving beneath a free surface, Proc. 1st Int. Conf. Num. Ship Hydrodyn., pp.539-559, Bethesda, Maryland, 1975.

Chang, M.S. Computation of three-dimensional ship-motions with forward speed, Proc. 2nd Int. Conf. Num. Ship Hudrodyn., pp.124-135, University of Califonia, Berkeley, 1977.

Chapman, R.B. Numerical solution for hydrodynamics forces on a surface-piercing plate oscillating in yaw and sway, Proc. 1st Int. Conf. Num. Ship Hydrodyn., pp.333-350, Nethesda, Maryland, 1975.

Chau, F.P. and Eatock Taylor, R. Second order velocity potential for arbitrary bodies in waves, Proc. 3rd Int. Workshop on Water waves and Floating bodies, Wood Hole, U.S.A., 1988.

Chen, C.Y. and Noblesse, F. Comparison between theoretical predictions of wave resistance and experimetal data for the Wigley hull, J. Ship Res., Vol.27, pp.215-226, 1983.

Cummins, W.E. The wave resistance of a floating slender body, Ph.D. Thesis, American University, Washington, D.C., 1965.

Eatock Taylor, R. and Zietsman, J. A comparison of localised finite element formulations for two-dimensional wave diffraction and radiation problems, Int. J. Num. Methods in Engineering, Vol.17, pp.1355-1384, 1981.

Eatock Taylor, R. and Zietsman, J. Hydrodynamic loading on multicomponent bodies, Proc. 3rd Int. Conf. on Behaviour of Offshore Structures, p424, 1982.

Eatock Taylor, R. and Wu, G.X. Wave resistance and lift on cylinders by a coupled element technique, Int. Shipbuilding Progress, Vol.33, pp.2-9, 1986.

Eatock Taylor,R. and Hung, S.M. Second order diffraction forces on a vertical cylinder in regular waves, Applied Ocean Res., Vol.9, pp.19-30, 1987.

Eatock Taylor,R., Hung, S.M. and Mitchell, K.L. Advances in the prediction of low frequency drift behaviour. Proc. 5th BOSS Conference, pp.651-666, Trondheim, 1988.

Eatock Taylor, R., Hu, C.S. and Nielsen, F.G. Mean drift forces on a slowly advancing vertical cylinder in long waves, to be published in Applied Ocean Research, 1990.

Faltinsen, O.M. and Michelsen, F.C. Motions of large structures in waves at zero Froude number, Proc. Int. Symp. on the Dynamics of Marine Vehicles and Structures in Waves, pp.91-106, University College London, 1974.

Faltinsen, O.M. Bow flow and added resistance of slender ships at high Froude numbers and low wave lengths, J. Ship Res., Vol.27, pp.160-171, 1983.

Faltinsen, O.M. Slow drift damping and response of a moored ship in irregular waves, Proc. 5th Int. Offshore Mechanics and Arctic Engineering Symposium, pp.297-303, 1986.

Frank, W. Oscillation of cylinders in or below the free surface of deep fluids, Report No.2375, Naval Ship Research and Development Center, Bethesda, Md., 1967.

Froude, W. On the rolling motion of ships, Trans. Inst. Nav. Archit., Vol.2, pp.180-229, 1861.

Gadd, G.E. A method of computing the flow and surface wave pattern around full forms, Trans. Roy. Inst. Nav. Archit., Vol.118, pp.207-219, 1976.

Garrison, C.J. Hydrodynamics loading of large offshore structures: three-dimensional source distribution methods, Chapter 3, Numerical Methods in Offshore Engineering, Ed. O.C. Zienkiewicz, R. Lewis, and K.E. Stagg, Wiley, Chichester, 1978.

Gerritsma, J. A note on the application of ship motion theory, Schiffstechnik, Vol.23, pp.181-185, 1976.

Gerritsma, J. and Beukelman, W. Analysis of the modified strip thoery for the calculation of ship motions and wave bending moments, Int. Shipbuilding Progress, Vol.14, pp.319-337, 1967.

Giesing, J.P. and Smith, A.M.O. Potential flow about two-dimensional hydrofoils, J. Fluid Mech., Vol.28, pp.113-129, 1967.

Gray, A., Mathews, G.B. and Macrobert, T.M. A Treatise on Bessel Functions and Their Applications to Physics, 2nd ed. Dover Publ, Inc. 1966.

Grekas, A. and Delhommeau, G. Diffraction-radiation en presence d'un courant, Proc. of the Association Technique Maritime et Aeronautique (ATMA), Paris, 1983.

Grim, O. A method for a more precise computation of heaving and pitching motions both in calm water and in waves, Proc. Symp. Nav. Hydrodyn., 3rd ACR-65, pp.483-524, Off. Nav. Res., Washington, D.C., 1960.

Grue, J. and Palm, E. Wave radiation and wave diffraction from a submerged body in a uniform current, J. Fluid Mech., Vol.151, pp.257-278, 1985.

Grue, J. Time-periodic wave loading on a submerged circular

cylinder in a current, J. Ship Res., Vol.30, p.153-161, 1986.

Grue, J. Wave drift damping and low frequency oscillations of an elliptic cylinder in irregular waves. Applied Ocean Research, Vol.10, pp.10-19, 1988.

Guevel, P. and Bougis, J. Ship-motions with forward speed in infinite depth, Int. Shipbuilding Progress, Vol.29, pp.103-117, 1982.

Guilloton, R. L'etude theorique du bateau en fluide parfait, Proc. of the Association Technique Maritime et Aeronautique (ATMA), pp.538-561, Paris, 1964.

Hanaoka, T. On the reverse flow theorem concerning wave-making theory. Proc. 9th Japan Nat'l Congr. Appl. Mech., pp.223-226, 1959.

Haskind, M.D. Two papers on the hydrodynamic theory of heaving and pitching of a ship: The hydrodynamics theory of the oscillation of a ship in waves; Oscillation of a ship on a calm sea, Prikl. Mat. Mekh. Vol.10, pp.33-66, 1946 (Engl. transl., Technical and Research Bulletin No.1-12, SNAME, April 1953.)

Haskind, M.D. (in Russian) On wave motion of a heave fluid, Prikl. Mat. Mekh. Vol.18, pp.15-26, 1954.

Haskind, M.D. (in Russian) The exciting forces and wetting of ships in waves. Izv. Akad. Nauk SSSR Otd. Tekh. nauk, Vol.7,

pp.65-79, 1957. English version available as David taylor Model Basin Translation No. 307.

Havelock, T.H. Some aspects of the theory of ship waves and wave resistance, Trans. North-East Coast Inst. Engrs and Shipbuilders, Vol.42, pp.71-83, 1926.

Havelock, T.H. The pressure of water waves upon a fixed obstacle, Proc. Roy. Soc., London, Series. A, Vol.963, pp.175-190, 1940.

Havelock, T.H. Waves due to a floating sphere making periodic heaving oscillations. Proc. Roy. Soc. London. Series A, Vol.231, pp.1-7, 1955.

Hearn, G.E., Tong, K.C. and Lau, S.M. Sensitivity of wave drift damping coefficients to the hydrodynamic models used in the added resistance gradient method. Proc. 6th Offshore Mechanics and Arctic Engineering Symposium, pp.213-225, Houston, 1987.

Hearn, G.E. and Tong, K.C. Wave drift damping coefficients predictions and their influence on the motions of moored semi-submersibles. Proc. Offshore Technology Conference, Houston, OTC 5455, 1987.

Hsu, F.M and Blenkarn, K.A. Analysis of peak mooring forces caused by slow vessel drift oscillation in random seas, Proc. of the Offshore Technology Conference. Paper 1159, 1970.

Hu, C.S. and Eatock Taylor, R. A small forward speed perturbation method for wave-body problems, Proc. 4th Int. Workshop on Water Waves and Floating Bodies, pp.97-100, Oystese, Norway, May 1989.

Huijsmans, R.H.M. and Hermans, A.J. A fast algorithm for computation of 3-D ship motions at moderate forward speed. Proc. 4th Int. Conf. Num. Ship Hydrodyn., pp.24-33, Washington, 1985.

Huijsmans, R.H.M. Wave drift forces in current, Proc. 16th Symp. Nav. Hydrodyn., Berkeley, 1986.

Hung, S.M. Second Order Wave Forces on Bodies in Regular and Bichromatic Seas, Ph.D Thesis, Faculty of Engineering, University of London, 1988.

Hung, S.M. and Eatock Taylor, R. The formulation of mean drift forces and moments for floating bodies, Proc. 3rd Int. Workshop on Water waves and Floating bodies, Wood Hole, U.S.A. 1988

Inglis, R.B. and Price, W.G. A three dimensional ship motion theory-comparison between theoretical predictions and experimental data of the hydrodynamics coefficients with forward speed, Trans. Roy. Inst. Nav. Archit., Vol.124, pp.141-157, 1982.

John, F. On the motion of floating bodies, Part I, Comm. Pure Appl. Math., Vol.2, pp.13-57, 1949.

John, F. On the motion of floating bodies, Part II, Comm. Pure Appl. Math., Vol.3, pp.45-101, 1950.

Keller, J.B. and Ahluwalia, D.S. Wave resistance and wave patterns of thin ships, J. Ship Res., Vol.20, pp.1-6, 1976.

Keller, J.B. The ray theory of ship waves and the class of streamlined ships, J. Fluid Mech., Vol.91, pp.465-488, 1979.

Kim, M.H. and Yue, D.K.P. The compelete second-order diffraction waves aroud an axisymmetric body, Part I, monochromatic waves, J. Fluid Mech., Vol.200, pp.235-246, 1989.

Korvin-Kroukovsky, B.V. and Jacobs, W.R. Pitching and heaving motions of a ship in regular waves, Trans. Soc. Nav. Archit., Vol.65, pp.590-632, 1957.

Krylov, A. A new theory of the pitching motion of ships on waves, and of the stresses produced by this motion, Trans. Inst. Nav. Archit., Vol.37, pp.326-368, 1896.

Lighthill, J. Waves and dynamic loading, Proc. 2nd Int. Conf. Behaviour of Off-shore Structures, Vol.1, pp.1-40, 1979.

MacCamy, R.C. The motion of a floating sphere in surface waves. Wave Resistance Laboratory, University of California, Berkeley, Report, Series 61, Issue 4, 1954.

Maeda, H. Hydrodynamical forces on a cross-section of a

stationary structure, Proc. Int Symp. on the Dynamics of Marine Vehicles and Structures in Waves, pp.80-90, University College London, 1974.

Marthinsen, T. Calculation of slowly varying drift forces, Applied Ocean Res., Vol.5, pp.141-144, 1983.

Maruo, H. The drift of a body floating on waves, J. Ship Res., Vol.4, pp.1-10, 1960.

Matsui, T. Analysis of slowly varying wave drift forces on compliant structures, Proc. 5th Int. Offshore Mechanics and Arctic Engineering Symp., Vol.1, pp.289-296, Tokyo, 1986.

Mei, C.C. Numerical methods in water-wave diffraction and radiation, Ann. Review Fluid Mech., Vol.10, pp.393-416, 1978.

Mei, C.C. The Applied Dynamics of Ocean Surface Waves, A wiley-Interscience Publication, 1982.

Mei, C.C. and Chen, H.S. A hybrid method for steady linearized free surface flow, Int. J. Num. Meth. in Eng., Vol.10, pp.1153-1175, 1976.

Michell, J.H. The wave resistance of a ship, Phil. Mag., Vol.45, pp.196-123, 1898.

Mo, A. and Palm, E. On radiated and scattered waves from a submerged elliptic cylinder in a uniform current, J. Ship Res.,

Vol.31, pp.23-32, 1987.

Molin, B. Second order diffraction loads upon three-dimensional bodies, Applied Ocean Research, Vol.1, pp.197-202, 1979.

Morison, J.R., O'Brien, M.P., Johnson, J.W. and Schaaf, S.A. The forces exterted by surface waves on piles, Petroleum Trans., AIME, Vol.189, p.149, 1950.

Musker, A.J. A panel method for predicting ship wave resistance, Proc. 17th Symp. Nav. Hydrodyn., pp.1-7, The Hague, 1988.

Nakamura, S., Saito, K. and Takagi, M. On the increased damping of a moored body during low-frequency motions in waves, Proc. 5th Int. Offshore Mechanics and Arctic Engineering Symposium, pp.281-287, Tokyo, 1986.

Nayfeh, A.H. Perturbation Methods, Wiley, New York, 1973.

Nestegard, A. and Sclavounos, P.D. A numerical solution of two-dimensional deep water wave-body problems, J. Ship Res., Vol.28, No.1, pp.48-54, 1984.

Newman, J.N. The damping and wave resistance of a pitching and heaving ship, J. Ship Res., Vol.3, pp.1-19, 1959.

Newman, J.N. A linearized theory for the motion of a thin ship in regular waves, J. Ship Res., Vol.3, pp.1-19, 1961.

Newman, J.N. and Tuck, E.O. Current progress in the slender-body theory of ship motions, Proc. 5th Symp. Nav. Hydrodyn., 1964.

Newman, J.N. The exciting forces on a moving body in waves, J. Ship Res., Vol.9, pp.190-199, 1965.

Newman, J.N. The drift force and moment on ships in waves, J. Ship Res., Vol.11, pp.51-60, 1967.

Newman, J.N. Second-order slowly-varying forces on vessels in irregular waves, Proc. Int. Symp. on Dynamics of Marine Vehicles and Structures in Waves, University College London, pp.182-186, 1974.

Newman, J.N. Marine Hydrodynamics. M.I.T. Press, Mass. 1977.

Newman,J.N. The theory of ship motions, Adv. Appl. Mech., pp.221-283, 1978.

Newman, J.N. and Sclavounos, P.D. The unified theory of ship motions, Proc. 13th Symp. Nav. Hydrodyn., 1980.

Newman, J.N. The evaluation of free-surface Green functions, Proc. 4th Int. Conf. on Num. Ship Hydrodyn., pp.4-23, Washington, D.C., 1985.

Noblesse, F. A slender-ship theory of wave resistance, J. Ship

Res., Vol.27, pp.13-33, 1983.

Ogilvie, T.F. First- and second-order forces on a cylinder submerged under a free surface, J. Fluid Mech. Vol.16, pp.451-472, 1963.

Ogilvie, T.F. and Tuck, E.O. A rational strip theory for ship motions, Part I, Report No.013, Dept. Nav. Archit. Mar. Eng., University of Michigan, Ann Aabor, 1969.

Ogilvie, T.F. Singular-perturbation problems in ship hydrodynamics, Adv. Appl. Mech., Vol.17, pp.91-188, 1977.

Ogilvie, T.F. Second order hydrodynamic effects on ocean platforms, Proc. Int. Workshop On Ship and Platform Motions, University of California, Berkeley, pp.205-265, 1983.

Peters, A.S. and Stoker, J.J. The motion of a ship, as a floating rigid body, in a seaway, Commun. Pure Appl. Math., Vol.10, pp399-490, 1957.

Pinkster, J.A. Low frequency second order wave exciting forces on floating structures, The Netherlands Ship Model Basin, Report 650, 1980.

Qi, X.-Y., Feng, Y. and Zhang, J.-L. Low-frequency surge motion of TLP in survival sea state, Proc. 5th Int. Offshore Mechanics and Arctic Engineering Symposium, pp.120-125, 1986.

Salvesen, N., Tuck, E.O. and Faltinsen, O.M. Ship motions and sea loads, Trans. Soc. Nav. Archit. Mar. Eng., Vol.78, pp.259-287, 1970.

Sarpkaya, T. and Isaacson, M. Mechanics of Wave Forces on Offshore Structures, Van Nostrand Reinhold, New York, 1981.

Sayer, P. and Ursell, F. Integral equation methods for calculating the virtual mass in water of finite depth, Proc. 2nd Int. Conf. Num. Ship Hydrodyn., University of California, Berkeley, pp.176-184, 1977.

Sclavounos, P.D. The interaction of an incident wave field with a floating slender-body at zero speed, Proc. 3rd Int. Conf. Num. Ship Hydrodyn., Paris, 1981.

Sclavounos, P.D. The diffraction of free-surface waves by a slender ship, J. Ship Res., Vol.28, pp.29-47, 1984.

Simon, M.J. and Ursell, F. Uniqueness in the linearized 2-D water wave problems, J. Fluid Mech., Vol.148, pp.137-154, 1984.

Takagi, M. An examination of the ship motion theory as compared with experiments, Proc. Int. Symp. on the Dynamics of Marine Vehicles and Structures in Waves, University College London, pp.151-159, 1974.

Thorne, R.C. Multipole expansions in the theory of surface waves. Proc. Camb. Phil. Soc. 49, pp.707-716, 1953.

Timman, R., and Newman, J.N. The coupled damping coefficients of symmetric ships, J. Ship Res., Vol.5, pp.34-55, 1962.

Triantafyllou, M.S. A consistent hydrodynamics theory for moored and positioned vessels, J. Ship Res., Vol.26, pp.97-105, 1982.

Ursell F. On the heaving motion of a circular cylinder on the surface of a fluid, Quart. J. Mech. Appl Math. 2, pp.218-231, 1949.

Ursell, F. Surface waves on deep water in the presence of a submerged cylinder I, II, Proc. Camb. Phil. Soc. Vol.46, pp.141-52, pp.153-158, 1950.

Ursell, F. Slender oscillating ships at zero forward speed, J. Fluid Mech. Vol.19, pp496-516, 1962.

Ursell, F. The expansion of water wave potentials at great distances, Proc. Camb. Phil. Soc., Vol.64, pp.811-826, 1968.

Ursell, F. Irregular frequencies and the motion of floating bodies, J. Fluid Mech., Vol.105, pp.143-156, 1981.

Verhagen, J.H.G. and van Sluijs, M.F. The low-frequency drift force on a floating body in waves, Int. Shipbuilding Progress, Vol.17, pp.136-145, 1970.

Vugts, J.H. The hydrodynamic coefficients for swaying, heaving and rolling cylinders in a free surface, Int. Shipbuilding Progress, Vol.15, pp.251-276, 1968.

Wehausen, J.V. and Laitone, E.V. Surface waves. Handbuch der Physik, Vol.IX, Berlin, Springer-Verlag, 1960.

Wehausen, J.V. The wave resistance of ships, Adv. Appl. Mech., Vol.13, pp.93-245, 1973.

Wichers, J.E.W. and van Sluijs, M.F. The influence of waves on the low frequency hydrodynamic coefficients of moored vessels, Proc. Offshore Technology Conference, Houston, OTC 3625, 1979.

Wichers, J.E.W. On the low-frequency surge motions of vessels moored in high seas, Proc. Offshore Technology Conference, Houston, OTC 4437, 1982.

Wichers, J.E.W. and Huijismans, R.H.M. On the low frequency hydrodynamic damping forces acting on offshore moored vessels. Proc. Offshore Technology Conference, Houston, OTC 4831, 1984.

Wichers, J.E.W. Progress in computer simulation of SPM moored vessels, Proc. Offshore Technology Conference, Paper 5175, Houston, 1986.

Wu, G.X. Hydrodynamics forces on oscillating submerged bodies at forward speed, Ph.D. Thesis, Faculty of Engineering, University of London, 1986.

Wu, G.X. and Eatock Taylor, R. Hydrodynamic forces on submerged oscillating cylinders at forward speed, Proc. Roy. Soc. London, A, Vol.414, pp.149-170, 1987.

Wu, G.X. and Eatock Taylor, R. Radiation and diffraction of water waves by a submerged sphere at forward speed, Proc. Roy. Soc. London, Series A, Vol.417, pp.433-461, 1988.

Yamamoto, Y. et al. Nonlinear effects for ship motion in heave seas, Int. Shipbuilding Progress, Vol.29, No.333, 1982.

Yeung, R.W. and Bouger, Y.C. Hybrid integral equation method for the steady ship-wave problem, Proc. 2nd Int. Conf. on Num. Ship Hydrodyn., pp.160-175, University of California, Berkeley, 1977.

Zhao, R. and Faltinsen, O.M. Interaction between waves and current on a two-dimensional body in the free surface, Appl. Ocean Res., Vol.10, pp.87-99, 1988.

Zhao, R., Faltinsen, O.M., Krokstad, J.R. and Anaesland, V. Wave current interaction effects on large volume structures, Proc. 5th Int. Conf. on Behaviour of Offshore Structures, pp.623-638, 1988.

Zhou, C. and Lui, P. L.-F. Second order low frequency wave forces on a vertical circular cylinder, J. Fluid Mech., Vol.175, pp.143-155, 1987.

Appendix A SOME VECTOR IDENTITIES

$$\vec{A}.(\vec{B}x\vec{C}) = (\vec{A}x\vec{B}).\vec{C} = \vec{B}.(\vec{C}x\vec{A}) \tag{A.1}$$

$$\vec{A}X(\vec{B}X\vec{C}) = \vec{B}(\vec{A}.\vec{C}) - \vec{C}(\vec{A}.\vec{B}) \tag{A.2}$$

$$\vec{B}x(\vec{\nabla}x\vec{A}) = \vec{\nabla}\vec{A}.\vec{B} - \vec{B}.\vec{\nabla}\vec{A} \tag{A.3}$$

$$\vec{\nabla}X\vec{\nabla}a = 0 \tag{A.4}$$

$$\vec{\nabla}x(\vec{B}x\vec{C}) = (\vec{\nabla}.\vec{C})\vec{B} - (\vec{\nabla}.\vec{B})\vec{C} + \vec{C}.\vec{\nabla}\vec{B} - \vec{B}.\vec{\nabla}\vec{C} \tag{A.5}$$

$$\vec{A}.\vec{\nabla}(\vec{x}x\vec{B}) = \vec{A}x\vec{B} + \vec{x}x(\vec{A}.\vec{\nabla}\vec{B}) \qquad (\vec{x} = x\vec{i} + y\vec{j} + z\vec{k}) \tag{A.6}$$

Stokes theorem:

For a differentiable vector function $\vec{A}$ defined over a smooth surface S which is bounded by the curve C, if the unit normal vector $\vec{n}$ of the surface and the direction of the the curve C are defined to satisfy the right hand screw law, then

$$\int_S \vec{n}.(\vec{\nabla}x\vec{A})\ dS = \oint_C \vec{A}.d\vec{l}.$$

Gauss theorems:

For a differentiable vector function $\vec{A}$ or scalar function A defined over a volume domain V which is enclosed by a smooth surface S, let $\vec{n}$ denote the unit normal vector directed out of the volume; then

$$\int_V \vec{\nabla}A\ dV = \oint_S \vec{n}A\ dS \tag{A.7}$$

$$\int_V \vec{\nabla}\vec{A}\ dV = \oint_S \vec{n}\vec{A}\ dS \tag{A.8}$$

$$\int_V \vec{\nabla}.\vec{A}\ dV = \oint_S \vec{n}.\vec{A}\ dS \tag{A.9}$$

$$\int_V \vec{\nabla}x\vec{A}\ dV = \oint_S \vec{n}x\vec{A}\ dS \tag{A.10}$$

Generally, let $\hat{}$ denote a generalized operater (e.g. $\vec{a}\hat{}\vec{b} = \vec{a}x\vec{b}$, $a\hat{}b = ab$) and $\tilde{A}$ denote a generalized function (e.g a scalar function $\tilde{A} = a$, a tensor $\tilde{A} = \vec{a}\vec{b}$), then

$$\int_V \vec{\nabla}\hat{}\tilde{A}\ dV = \oint_S \vec{n}\hat{}\tilde{A}\ dS. \tag{A.11}$$

Appendix B GREEN FUNCTIONS AND ASYMPTOTIC EXPRESSIONS

For unsteady motions at forward speed, the Green function is defined as the velocity potential of a pulsating translating source, which satisfies the Laplace equation in the whole fluid domain, except at the source point (ξ,η,ζ). Let the Green function be expressed as $Ge^{i\omega t}$, then G satisfies the following free surface condition

$$-\omega^2 G - 2i\omega U G_x + g G_z + U^2 G_{xx} = 0, \qquad \text{on } z=0. \tag{B.1}$$

It also satisfies an appropriate radiation condition.

Three dimensions

Haskind (1946) derived the Green function as follows

$$G = \frac{1}{r} - \frac{1}{r'} - \frac{k}{\pi}\int_{-\pi}^{+\pi}\int_{0}^{\infty} \frac{\lambda e^{\lambda[z+\zeta+i(x-\xi)\cos\beta+i(y-\eta)\sin\beta]}}{(\tau\lambda\cos\beta - k\,(1-i\mu))^2 - k\,\lambda}\, d\beta d\lambda, \tag{B.2}$$

where $r = [(x-\xi)^2+(y-\eta)^2+(z-\zeta)^2]^{1/2}$, $r' = [(x-\xi)^2+(y-\eta)^2+(z+\zeta)^2]^{1/2}$; μ is the Rayleigh viscosity; and $k=\omega^2/g$, $\tau=\omega U/g$. The same function is aslo derived by several other authors as described by Wehausen and Laitone (1960). Taking $\mu\to 0$, the Green function can be alternatively expressed in the form of (Wehausen and Laitone 1960)

$$G = \frac{1}{r} - \frac{1}{r'} + \frac{2}{\pi}\int_0^{\gamma} d\theta \int_0^{\infty} F(\theta,\lambda)\, d\lambda + \frac{2}{\pi}\int_{\gamma}^{\frac{\pi}{2}} d\theta \int_{L_1} F(\theta,\lambda)\, d\lambda$$
$$+ \frac{2}{\pi}\int_{\frac{\pi}{2}}^{\pi} d\theta \int_{L_2} F(\theta,\lambda)\, d\lambda, \tag{B.3}$$

where

$$F(\theta,\lambda) = \frac{\lambda e^{\lambda[z+\zeta-i(x-\xi)\cos\theta]}\cos[\lambda(y-\eta)\sin\theta]}{\lambda - \frac{1}{g}(\omega+\lambda U\cos\theta)^2}, \tag{B.4}$$

$$\gamma = \begin{cases} 0, & \text{for } \tau = \frac{U\omega}{g} < \frac{1}{4}; \\ \cos^{-1}(\frac{1}{4\tau}), & \text{for } \tau = \frac{U\omega}{g} \geq \frac{1}{4}. \end{cases} \tag{B.5}$$

The contours are defined by

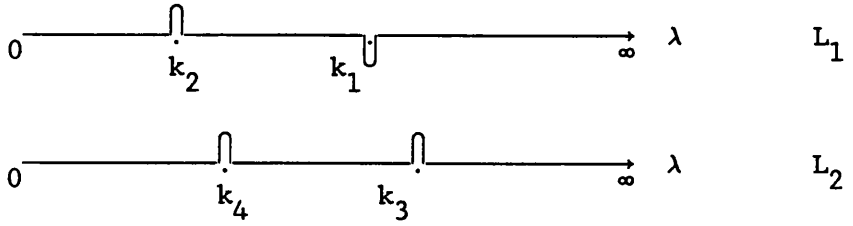

and the four wavenumbers are given by

$$k_{1,2} = \frac{1-2\tau\cos\theta \pm \sqrt{1-4\tau\cos\theta}}{2\tau^2\cos^2\theta}\, k, \qquad \text{for } \theta \in (0,\tfrac{\pi}{2}), \tag{B.6}$$

$$k_{3,4} = \frac{1-2\tau\cos\theta \pm \sqrt{1-4\tau\cos\theta}}{2\tau^2\cos^2\theta}\, k, \qquad \text{for } \theta \in (\tfrac{\pi}{2},\pi). \tag{B.7}$$

The four wavenumbers are roots of the equation $g\lambda-(\omega+U\lambda\cos\theta)^2=0$; among which k_1, k_2 are the two roots over the range of $\theta\in(0,\pi/2)$, whereas k_3, k_4 are the two roots over $\theta\in(\pi/2,\pi)$. In the range of

$(0,\gamma)$, there is no real root. Therefore, the first integral over λ is simply written as an integral over $(0,\infty)$.

The asymptotic behaviour of the Green function has been studied by many authors. It is found that $\tau=1/4$ is a critical value for the wave patterns in the far field. For the supercritical motion ($\tau>1/4$), there are two waves (k_3, k_4 waves) and both are located downstream. For the subcritical motion ($\tau<1/4$), there are four waves. One of them is located upstream (k_2 wave). The other three (k_1, k_3 and k_4 waves) are located downstream. For finite values of τ, the asymptotic expression is very complicated and the contributions from the wave numbers have to be determined numerically by solving a stationary phase equation. However, for $\tau\to 0$ with a given frequency, two wavenumbers become infintely large, that is, $k_1=k_3\simeq g/U^2>>1$. Because of the exponential decay, the two short crest waves are negligible. Only two waves survive and the behaviour in the far field is simpler. It can be shown that for very small τ, the asymptotic expression of the Green function can be expressed as follows

$$G = 2(1+2\tau\cos\alpha)\sqrt{2\pi k}/R \exp\{k(1+2\tau\cos\alpha)[z+\zeta-i(R-\xi\cos\theta-\eta\sin\theta)]-i\tfrac{\pi}{4}\} + O(\tfrac{1}{R}) \qquad (B.8)$$

where the polar coordinates are defined as follows

$$x-\xi = R_1\cos\alpha, \qquad y-\eta = R_1\sin\alpha;$$
$$x = R\cos\theta, \qquad y = R\sin\theta.$$

The expression was first given by Haskind (1946), but the paper contained an error. In his expression α is incorrectly taken as θ. Although this is valid for the first α in equation (B.8), it is not

correct for the term $R\cos\alpha$. In fact, from

$$R_1 = \sqrt{R^2 - 2R(\xi\cos\theta+\eta\sin\theta) + (\xi^2+\eta^2)} \simeq R - (\xi\cos\theta+\eta\sin\theta) + O(\frac{1}{R}),$$

it follows that

$$\begin{aligned} R\cos\alpha = \frac{R}{R_1}(x-\xi) &= (R\cos\theta-\xi)(1 + \frac{\xi\cos\theta+\eta\sin\theta}{R} + O(\frac{1}{R^2})) \\ &= R\cos\theta - \xi\sin^2\theta + \eta\sin\theta\cos\theta + O(\frac{1}{R}). \end{aligned} \tag{B.9}$$

It is possible to derive the expression (B.8) from the original Green function, but it is more convenient to start from the asymptotic expression for finite value of τ given by Newman (1959). As shown by Newman, the asymptotic expression for the Green function can be expressed in the form of

$$G = \sqrt{\frac{8\pi}{R}} \sum_{i=1}^{2} \sum_{n} (\pm)\{ \frac{\lambda_i(u_n)\sin^2\theta}{\sin^2 u_n |\frac{d\theta}{du_n}\cos(u_n-\theta)|} \}^{\frac{1}{2}}$$

$$\exp\{ \lambda_i(u_n)[z+\zeta+iR\cos(u_n-\theta)-\xi\cos u_n - i\eta\sin u_n] + i\frac{\pi}{2} \pm i\frac{\pi}{4} \} + O(\frac{1}{R}). \tag{B.10}$$

where $(\pm)$ signs after the summation correspond to the signs in equation (62) in Newman (1959). The sign of $i\pi/4$ is the same as the second derivative of g_i at u_n, and g_i is defined as

$$g_i \equiv \lambda_i(u)\cos(u-\theta). \tag{B.11}$$

u_n are the roots of $\frac{\partial g_i}{\partial u} = 0$. The second summation in equation (B.10) is over all u_n. The two wave numbers are defined as

$$\lambda_{1,2} = \frac{1+2\tau\cos u \pm \sqrt{1+4\tau\cos u}}{2\tau^2\cos^2 u}\, k. \tag{B.12}$$

For $\tau \to 0$,

$$\lambda_1 \simeq \frac{k}{\tau^2\cos^2 u} \to \infty,$$

$$\lambda_2 \simeq k(1-2\cos u).$$

Because $\lambda_1 \to \infty$, the λ_1 terms in equation (B.10) can be neglected. Hence,

$$G = \sqrt{\frac{8\pi}{R}} \sum_n (\pm)\left\{ \frac{\lambda_2(u_n)\,\sin^2\theta}{\sin^2 u_n \left|\frac{d\theta}{du_n}\cos(u_n-\theta)\right|} \right\}^{\frac{1}{2}}$$

$$\exp\left\{ \lambda_2(u_n)[z+\zeta+iR\cos(u_n-\theta)-\xi\cos u_n - i\eta\sin u_n] + i\frac{\pi}{2} \pm i\frac{\pi}{4} \right\} + O\left(\frac{1}{R}\right). \tag{B.13}$$

From equations (B.11) and (B.12), it follows that u_n is determined from the following equation

$$\operatorname{ctg}\theta = -\operatorname{tg} u + \frac{(1+4\tau\cos u)^{\frac{1}{2}}}{\sin u \cos u}. \tag{B.14}$$

For $\tau \to 0$, it follows that

$$\sin(u-\theta) = 2\tau\sin\theta. \tag{B.15}$$

From equation (62) in Newman (1959), it is known that u_n is defined in the domain

$$\frac{\pi}{2} < u_n - \theta < \frac{3\pi}{2}.$$

Therefore, only single root is found, given by

$$u_1 = \theta + \pi - 2\tau\sin\theta. \tag{B.16}$$

We have

$$\lambda_2 = k(1+2\tau\cos\theta),$$

$$\left\{ \frac{\lambda_2(u_1)\,\sin^2\theta}{\sin^2 u_1 \left|\frac{d\theta}{du_1}\cos(u_1-\theta)\right|} \right\}^{\frac{1}{2}} = \sqrt{k}\,(1+2\tau\cos\theta).$$

Finally,

$$G = -\sqrt{\frac{8\pi}{R}}\,\sqrt{k}(1+2\tau\cos\theta)\,\exp\{\,\lambda_2(z+\zeta-iR+\xi\cos\theta+i\eta\sin\theta) + i\frac{\pi}{2} + i\frac{\pi}{4}\,\}$$
$$\exp\{2\tau i(\xi\sin^2\theta-\eta\sin\theta\cos\theta)\} \quad + O(\frac{1}{R}) \tag{B.17}$$

From equation (B.9), it immediately follows that equation (B.17) is identical to equation (B.8). The proof is completed.

Two dimensions

For two dimensional motions, a translating pulsating source potential can be written as follows (Haskind 1954)

$$G = \ln\frac{r'}{r} + \frac{1}{\sqrt{1-4\tau}}\left[\int_{\infty}^{Z}\frac{e^{-ik_1(Z-u)}}{u-\bar{Z}_0}\,du - \int_{-\infty}^{Z}\frac{e^{-ik_2(Z-u)}}{u-\bar{Z}_0}\,du\right]$$
$$+ \frac{1}{\sqrt{1+4\tau}}\left[\int_{\infty}^{\bar{Z}}\frac{e^{ik_3(\bar{Z}-\bar{u})}}{\bar{u}-Z_0}\,du - \int_{\infty}^{\bar{Z}}\frac{e^{ik_4(\bar{Z}-\bar{u})}}{\bar{u}-Z_0}\,du\right]. \tag{B.18}$$

where $Z=x+iz$, $Z_0=\xi+i\zeta$; $r = [(x-\xi)^2+(z-\zeta)^2]^{1/2}$, $r'= [(x-\xi)^2+(z+\zeta)^2]^{1/2}$; an overbar denotes complex conjugate; and the four wavenumbers are defined by

$$k_{1,2} = \frac{1-2\tau\pm\sqrt{1-4\tau}}{2\tau^2}\, k, \qquad k_{3,4} = \frac{1+2\tau\pm\sqrt{1+4\tau}}{2\tau^2}\, k, \tag{B.19}$$

with $k=\frac{\omega^2}{g}$ and $\tau=\frac{U\omega}{g}$. The four wavenumbers are roots of the following two equations (i) $\omega=U\lambda\pm\sqrt{g\lambda}$ ($\lambda=k_3,k_4$) and (ii) $\omega=\sqrt{g\lambda}\pm U\lambda$ ($\lambda=k_1,k_2$), where ω is positive and known.

The wave patterns in the far field is very similar to the three dimensional motions. That is, for the supercritical motion ($\tau>1/4$), there are two waves (k_3, k_4 waves) and both are located downstream. For the subcritical motion ($\tau<1/4$), there are four waves. One of them is located upstream (k_2 wave). The other three (k_1, k_3 and k_4 waves) are located downstream. However, unlike its three dimensional counterpart, the asymptotic expression for the two dimensional Green function can be expressed in a very simple for arbitrary value of τ. Particularly, for $\tau<1/4$, Haskind (1954) has shown that the asymptotic expression is

$$G = -\frac{2\pi i}{\sqrt{1-4\tau}}\, e^{k_2\bar{\chi}}, \qquad x\to+\infty,$$

$$G = -\frac{2\pi i}{\sqrt{1-4\tau}}\, e^{k_1\bar{\chi}} + \frac{2\pi i}{\sqrt{1+4\tau}}\,(e^{k_3\chi} - e^{k_4\chi}), \qquad x\to-\infty, \tag{B.20}$$

where $\chi\equiv z+\zeta+i(x-\xi)$. It may be noted that k_1 wave has a positive celerity. That is, it travells towards the source. Its group velocity ($c_g=d\omega/dk_1$) is, however, negative. Therefore, the k_1 wave is located downstream.

For $\tau \to 0$,

$$k_2 \simeq k(1+2\tau), \quad k_4 \simeq k(1-2\tau), \quad k_1 \simeq k_3 \simeq \frac{k}{\tau^2} \to \infty. \tag{B.21}$$

Because of the exponential decaying, k_1, k_3 waves can be neglected, and only two waves survive. The asymptotic expression is simplified into

$$G = -\frac{2\pi i}{\sqrt{1-4\tau}} e^{k_2 \bar{\chi}}, \qquad x \to +\infty,$$

$$G = -\frac{2\pi i}{\sqrt{1+4\tau}} e^{k_4 \chi}, \qquad x \to -\infty. \tag{B.22}$$

Appendix C RATE OF CHANGE OF MOMENTUM

Consider an incompressible fluid in a volume Ω enclosed by a surface S. Let $\vec{V}$ denote the fluid velocity. Then the linear momentum is given by

$$\vec{I} = \rho \int_{\Omega} \vec{V} \, dS, \tag{C.1}$$

and the angular momentum with respect to the origin is given by

$$\vec{L} = \rho \int_{\Omega} \vec{x} \times \vec{V} \, dS. \tag{C.2}$$

The rate of change of the linear momentum is

$$\frac{d\vec{I}}{dt} = \rho \int_{\Omega} \frac{\partial \vec{V}}{\partial t} \, dS + \rho \oint_{S} \vec{V} U_n \, dS, \tag{C.3}$$

where U_n is the normal component of the velocity of the surface S and the direction of the normal is defined out of Ω. The volume integral can be transformed in another form by using the differential momentum equation

$$\frac{\partial \vec{V}}{\partial t} + \vec{V} \cdot \vec{\nabla}\vec{V} = -\vec{\nabla}\left(\frac{P}{\rho} + gz\right). \tag{C.4}$$

Since $\vec{V} \cdot \vec{\nabla}\vec{V} = \nabla \cdot (\vec{V}\vec{V})$ (This can be proved conveniently in a Cartesian coordinate system: $\vec{V} \cdot \vec{\nabla}\vec{V} = V_i \frac{\partial \vec{V}}{\partial x_i} = \frac{\partial}{\partial x_i}(V_i \vec{V}) - (\frac{\partial}{\partial x_i} V_i)\vec{V} = \nabla \cdot (\vec{V}\vec{V}) - (\vec{\nabla} \cdot \vec{V})\vec{V}$ and $\vec{\nabla} \cdot \vec{V} = 0$ for incompressible fluids.), it follows that

$$\frac{\partial \vec{V}}{\partial t} = -\vec{\nabla} \cdot (\vec{V}\vec{V}) - \vec{V}\left(\frac{P}{\rho} + gz\right). \tag{C.5}$$

Thus

$$\frac{d\vec{I}}{dt} = -\rho \int_{\Omega} \vec{\nabla}.(\vec{\nabla}\vec{\nabla})\ d\Omega - \rho \int_{\Omega} \vec{\nabla}(\frac{P}{\rho} + gz)\ d\Omega + \rho \oint_{S} \vec{\nabla} U_n\ dS. \tag{C.6}$$

From the Gauss theorem, it follows that

$$\int_{\Omega} \vec{\nabla}.(\vec{\nabla}\vec{\nabla})\ d\Omega = \oint_{S} \vec{n}.\vec{\nabla}\vec{\nabla}\ dS = \oint_{S} V_n \vec{\nabla}\ dS, \tag{C.7}$$

$$\int_{\Omega} \vec{\nabla}(\frac{P}{\rho} + gz)\ d\Omega = \oint_{S} \vec{n}(\frac{P}{\rho} + gz)\ dS. \tag{C.8}$$

Hence

$$\frac{d\vec{I}}{dt} = -\rho \oint_{S} [\vec{\nabla}(V_n - U_n) + (\frac{P}{\rho} + gz)\vec{n}]\ dS. \tag{C.9}$$

The rate of change of the angular momentum is

$$\frac{d\vec{L}}{dt} = \rho \int_{\Omega} \frac{\partial}{\partial t}(\vec{x}x\vec{\nabla})\ dS + \rho \oint_{S} (\vec{x}x\vec{\nabla})U_n\ dS. \tag{C.10}$$

Substitution of the differential momentum equation yields

$$\frac{d\vec{L}}{dt} = \rho \int_{\Omega} \frac{\partial\vec{x}}{\partial t}x\vec{\nabla}\ dS - \rho \int_{\Omega} [\vec{x}x(\vec{\nabla}.\vec{\nabla}\vec{\nabla}) + \vec{x}x\vec{\nabla}(\frac{P}{\rho} + gz)]\ dS + \rho \oint_{S} (\vec{x}x\vec{\nabla})U_n\ dS. \tag{C.11}$$

However, since

$$\vec{x}x\vec{\nabla}(\frac{P}{\rho} + gz) = -\vec{\nabla}x[(\frac{P}{\rho} + gz)\vec{x}], \tag{C.12}$$

and

$$\vec{x}x\vec{\nabla}(\vec{\nabla}.\vec{\nabla}\vec{\nabla}) = -\vec{\nabla}.[\vec{\nabla}(\vec{x}x\vec{\nabla})], \qquad (\frac{\partial\vec{x}}{\partial x_i} = \vec{e}_i \text{ used}) \tag{C.13}$$

the volume integrals can be reduced to surface integrals from the Gauss theorem

$$\frac{d\vec{L}}{dt} = \rho \int_{\Omega} \frac{\partial \vec{x}}{\partial t} x \vec{V} \, dS - \rho \oint_{S} [(\vec{x} x \vec{V})(V_n - U_n) + (\vec{x} x \vec{n})(\frac{P}{\rho} + gz)] \, dS. \tag{C.14}$$

If the coordinate system is moving at a translation velocity $\vec{U}$,

$$\frac{\partial \vec{x}}{\partial t} = -\vec{U}. \tag{C.15}$$

Hence

$$\frac{d\vec{L}}{dt} = -\rho \vec{U} x \int_{\Omega} \vec{V} \, dS - \rho \oint_{S} [(\vec{x} x \vec{V})(V_n - U_n) + (\vec{x} x \vec{n})(\frac{P}{\rho} + gz)] \, dS. \tag{C.16}$$

Appendix D SERIES EXPANSION OF THE THREE DIMENSIONAL GREEN FUNCTION

The zero-speed Green function G_0 and the forward speed correction Green function G_1 defined in equations (3.95) and (3.96) can be expressed in ascending series. For small kR_1, from Abramowitz and Stegun (1965)

$$J_0(\lambda R_1) = \sum_{n=0}^{\infty} \frac{(-1)^n (\lambda R_1)^{2n}}{2^{2n}(n!)^2},$$

$$J_1(\lambda R_1) = \sum_{n=0}^{\infty} \frac{(-1)^n (\lambda R_1)^{2n+1}}{2^{2n+1} n!(n+1)!},$$

equations (3.95) and (3.96) can be written as follows

$$G_0 = \frac{1}{r} + \frac{1}{r'} + 2k\left[\sum_{n=0}^{\infty} \frac{(-1)^n R_1^{2n}}{2^{2n}(n!)^2} I_{2n} - \pi i e^{-Y} J_0(kR_1)\right], \tag{D.1}$$

$$G_1 = -4i\cos\alpha \sum_{n=0}^{\infty} \frac{(-1)^n R_1^{2n+1}}{2^{2n+1} n!(n+1)!} k_{2n+2} \tag{D.2}$$

where $Y = k|z+\zeta|$, and

$$I_{2n} = \int_0^{\infty} \frac{e^{\lambda(z+\zeta)}}{\lambda - k} \lambda^{2n} \, d\lambda, \tag{D.3}$$

$$k_{2n+2} = \int_0^{\infty} \frac{e^{\lambda(z+\zeta)}}{(\lambda - k(1-i\mu))^2} \lambda^{2n+3} \, d\lambda, \qquad (\mu \to 0) \tag{D.4}$$

where a bar indicates that the principal value is taken. Integration of I_{2n} yields

$$I_{2n} = \int_0^\infty \lambda^{2n-1} e^{\lambda(z+\zeta)}\, d\lambda + k \int_0^\infty \frac{e^{\lambda(z+\zeta)}}{\lambda-k}\, \lambda^{2n-1}\, d\lambda$$

$$= k^{2n}\Big[\sum_{m=1}^{2n} \frac{(m-1)!}{Y^m} + I_0\Big], \tag{D.5}$$

with

$$I_0 = \int_0^\infty \frac{e^{\lambda(z+\zeta)}}{\lambda-k}\, d\lambda = -e^{-Y} E_i(Y), \tag{D.6}$$

where $E_i(Y)$ is the exponential integral function.

Integration by part for k_{2n+1} yields

$$k_{2n+2} = k^{2n+2} \int_0^\infty \frac{e^{-tY}\, t^{2n+3}}{(t-(1-i\mu))^2}\, dt$$

$$= k^{2n+2}\Big[\int_0^\infty \frac{e^{-tY}}{(t-(1-i\mu))^2}\, dt + \int_0^\infty \frac{(t^{2n+3}-1)e^{-tY}}{(t-(1-i\mu))^2}\, dt\Big]$$

$$= k^{2n+2}\Big[-1-Y\int_0^\infty \frac{e^{-tY}}{t-(1-i\mu)}\, dt + \sum_{m=0}^{2n+2} \int_0^\infty \frac{t^m\, e^{-tY}}{t-(1-i\mu)}\, dt\Big].$$

From

$$\int_0^\infty \frac{t^m\, e^{-tY}}{t-(1-i\mu)}\, dt = \int_0^\infty t^{m-1}\, e^{-tY}\, dt + \int_0^\infty \frac{t^{m-1}\, e^{-tY}}{t-(1-i\mu)}\, dt$$

it follows that

$$k_{2n+2} = k^{2n+2}\Big[-1 + (2n+3-Y)\int_0^\infty \frac{e^{-tY}}{t-(1-i\mu)}\, dt + \sum_{m=0}^{2n+1} (2n+2-m)\int_0^\infty t^m e^{-tY} dt\Big]$$

$$= k^{2n+2}\Big[-1 + (2n+3-Y)e^{-Y}E_1(-Y) + \sum_{m=0}^{2n+1} (2n+2-m)\frac{m!}{Y^{m+1}}\Big], \tag{D.7}$$

where $E_1(Z)$ is the exponential integral function defined in Abramowitz and stegun (1965) and $E_1(-Y)=E(-Y+i0)=-(E_i(Y)+i\pi)$.

Finally, the following ascending series are obtained,

$$G_0= \frac{1}{r} + \frac{1}{r'} - 2\pi ike^{-Y}J_0(kR_1)+ 2k \sum_{n=0}^{\infty}\frac{(kR_1)^{2n}}{(-4)^n(n!)^2}\left[\sum_{m=1}^{2n}\frac{(m-1)!}{Y^m} - e^{-Y}E_i(Y)\right], \tag{D.8}$$

$$G_1=-2\pi i\cos\alpha k\sum_{n=0}^{\infty}\frac{(kR_1)^{2n+1}}{(-4)^n n!(n+1)!}\left[-1+(2n+3-Y)e^{-Y}E_1(-Y)+\sum_{m=1}^{2n+2}(2n+3-m)\frac{(m-1)!}{Y^m}\right]. \tag{D.9}$$

Appendix E DERIVATION OF AN INTEGRAL THEOREM

For a differentiable function f, there exists the following identity

$$\int_{S_B} [\, m_i f + n_i(\vec{W}.\vec{\nabla}f) \,]\, dS = \oint_{C_W} \frac{dl}{\sqrt{1-n_3^2}}\, n_i f(\vec{k}.\vec{W}) \qquad (i=1,\ldots,6), \tag{E.1}$$

where

$$(m_1,\ m_2,\ m_3) = -\vec{n}.\vec{\nabla}\vec{W},$$

$$(m_4,\ m_5,\ m_6) = -\vec{n}.\vec{\nabla}(\vec{x}\times\vec{W}).$$

Proof:

Let us first prove this for i=1,2,3. From Stokes' theorem

$$\int_{S_B} \vec{n}.(\vec{\nabla}\times\vec{q})\, dS = \oint_{C_W} \vec{q}.d\vec{l}, \tag{E.2}$$

where the normal and the direction of the curve satisfy the right hand screw rule. Let $\vec{q}=\vec{e}_i\times\vec{W}$ f. Then

$$\begin{aligned}
\vec{n}.(\vec{\nabla}\times\vec{q}) &= \vec{n}.[\vec{e}_j\times\frac{\partial}{\partial x_j}(\vec{e}_i\times f\vec{W})] \\
&= \vec{n}.[\vec{e}_j\times(\vec{e}_i\times\frac{\partial f}{\partial x_j}\vec{W}) + \vec{e}_j\times(\vec{e}_i\times f\frac{\partial\vec{W}}{\partial x_j})] \\
&= \vec{n}.[\vec{e}_i(\vec{\nabla}f.\vec{W}) - \frac{\partial f}{\partial x_i}\vec{W} + \vec{e}_i f(\vec{\nabla}.\vec{W}) - f\frac{\partial\vec{W}}{\partial x_i}] \\
&= n_i\vec{W}.\vec{\nabla}f - f\vec{e}_i.(\vec{\nabla}\vec{W}.\vec{n}). \qquad (\text{Note } \vec{n}.\vec{W}=0,\ \vec{\nabla}.\vec{W}=0)
\end{aligned} \tag{E.3}$$

Since

$$\vec{\nabla}x\vec{W}=0$$

and

$$\vec{n}x(\vec{\nabla}x\vec{W})=\vec{\nabla W}.\vec{n}-\vec{n}.\vec{\nabla W},$$

then

$$\vec{\nabla W}.\vec{n}=\vec{n}.\vec{\nabla W}.$$

Hence

$$\vec{n}.(\vec{\nabla}x\vec{q}) = n_i\vec{W}.\vec{\nabla}f + fm_i. \tag{E.4}$$

In the line integral $d\vec{l} = \frac{\vec{n}x\vec{k}}{\sqrt{1-n_3^2}}dl$,

$$\vec{q}.d\vec{l} = \vec{e}_i x f\vec{W}.d\vec{l} = \frac{fdl}{\sqrt{1-n_3^2}}\vec{e}_i.[\vec{n}(\vec{W}.\vec{k}) - \vec{k}(\vec{W}.\vec{n})] = \frac{dl}{\sqrt{1-n_3^2}}n_i f(\vec{W}.\vec{k}). \tag{E.5}$$

(If the Stokes' theorem is applied to an arbitrary surface instead of the body surface bounded by the water line on the free surface, then $d\vec{l} = (\vec{n}x\vec{t})x\vec{n}\ dl$ and $\vec{q}.d\vec{l} = n_i[\vec{W}.(\vec{t}x\vec{n})]\ dl$, where $\vec{t}$ denotes the direction of the curve.) From equations (E.2)-(E.5), the identity (E.1) is proved.

Next, for i=4,5,6, let

$$\vec{q}=(\vec{e}_{i-3}x\vec{x})x\vec{W}.$$

Then

$$\vec{n}.(\vec{\nabla}x\vec{q}) = \vec{n}.\frac{\partial}{\partial x_j}\{\vec{e}_j x[(\vec{e}_{i-3}\ x\vec{x})xf\vec{W}]\}.$$

After similar procedures for that of i=1,2,3, it follows that

$$\vec{n}.(\vec{\nabla}x\vec{q}) = n_i\vec{W}.\vec{\nabla}f + fm_i. \tag{E.6}$$

Also similarly, in the line integral

$$\vec{q}.d\vec{l} = \vec{e}_{i-3}xf\vec{W}.d\vec{l} = \frac{fdl}{\sqrt{1-n_3^2}}(\vec{e}_{i-3}x\vec{x}).[\vec{n}(\vec{W}.\vec{k}) - \vec{k}(\vec{W}.\vec{n})]$$

$$= \frac{fdl}{\sqrt{1-n_3^2}}\vec{e}_{i-3}.(\vec{x}x\vec{n})(\vec{W}.\vec{k}) = \frac{dl}{\sqrt{1-n_3^2}}n_i f(\vec{W}.\vec{k}) \tag{E.7}$$

From equations (E.2), (E.6) and (E.7), the identity (E.1) is proved.

Appendix F SOME INTEGRAL IDENTITIES

Let $E_1(Z)$ denote the exponential integral function defined in Abramowitz and Stegun (1965), i.e.

$$E_1(Z) \equiv \int_0^\infty \frac{e^{-Zt}}{t}\, dt, \tag{F.1}$$

where Z is a complex number and the path of the integral does not cross the negative real axis. Then there exist the following identities.

$$\int_0^\infty \frac{e^{\lambda(f-ix)}}{\lambda-k}\, d\lambda = e^{k(f-ix)}E_1(k(f-ix)), \qquad (x<0) \tag{F.2}$$

$$\int_0^\infty \frac{e^{\lambda(f-ix)}}{\lambda-k}\, d\lambda = e^{k(f-ix)}E_1(k(f-ix)) - 2\pi i e^{k(f-ix)}, \qquad (x>0) \tag{F.3}$$

$(f<0,\ k>0)$

For $k>0$, $\eta<0$, b being complex, there are

$$\int_0^\infty \frac{e^{i\eta t}}{t+ik}\, dt = e^{k\eta}E_1(k\eta+i0), \tag{F.4}$$

$$\int_0^\infty \frac{e^{-i\eta t}}{t+ik}\, dt = e^{-k\eta}E_1(-k\eta), \tag{F.5}$$

$$\int_0^\infty \frac{e^{-i\eta t}}{t-ik}\, dt = e^{k\eta}E_1(k\eta-i0), \tag{F.6}$$

$$\int_0^\infty \frac{e^{i\eta t}}{t-ik}\,dt = e^{-k\eta}E_1(-k\eta), \tag{F.7}$$

$$\int_0^\infty \frac{e^{-Zt}}{t+b}\,dt = e^{bZ}E_1(bZ), \qquad (\mathrm{Re}Z\geq 0) \tag{F.8}$$

$$\int_0^\infty \frac{e^{-Zt}}{(t+b)^2}\,dt = \frac{1}{b} - Z\int_0^\infty \frac{e^{-Zt}}{t+b}\,dt, \qquad (\mathrm{Re}Z\geq 0) \tag{F.9}$$

$$\int_0^\infty \frac{e^{-Zt}}{t^2+b^2}\,dt = \frac{1}{2ik}\int_0^\infty \left(\frac{1}{t-ik} - \frac{1}{t+ik}\right)e^{-Zt}dt. \tag{F.10}$$

These identities can be proved from contour integration. For example, let us prove the identity (F.4). Proof:

$$\int_0^\infty \frac{e^{i\eta t}}{t+ik}\,dt = \int_0^\infty \frac{e^{ik\eta m}}{m+i}\,dm \qquad (t=km)$$

$$= e^{k\eta}\int_i^{\infty+i} \frac{e^{ik\eta v}}{v}\,dv = e^{k\eta}\int_i^\infty \frac{e^{ik\eta v}}{v}\,dv \qquad (m+i=v)$$

$$= e^{k\eta}\int_{k\eta}^{i\infty} \frac{e^{-u}}{u}\,du = e^{k\eta}\int_{k\eta}^\infty \frac{e^{-u}}{u}\,du \qquad (ik\eta v=-u)$$

$$= e^{k\eta}E_1(k\eta+i0),$$

and the proof is completed. Other identities can be proved similarly.

Appendix G THE COORDINATE TRANSFORMATION

As shown in Chapter 5, up to second order, there are the following relations for coordinate transfomation

$$\vec{x} = \vec{x}' + \vec{\xi} + \vec{\Omega}x\vec{x}' + \epsilon^2\underset{\sim}{H}\vec{x}' + O(\epsilon^3), \tag{G.1}$$

$$\vec{n} = \vec{n}' + \vec{\Omega}x\vec{n}' + \epsilon^2\underset{\sim}{H}\vec{n}' + O(\epsilon^3). \tag{G.2}$$

From these two relations, the transformation for the generalized normal vector can be derived:

$$\begin{aligned}\vec{x}x\vec{n} &= (\vec{x}' + \vec{\xi} + \vec{\Omega}x\vec{x}' + \epsilon^2\underset{\sim}{H}\vec{x})x(\vec{n}' + \vec{\Omega}x\vec{n}' + \epsilon^2\underset{\sim}{H}\vec{n}') + O(\epsilon^3)\\ &= \vec{x}'x\vec{n}' + \vec{\xi}x\vec{n}' + [\vec{\xi}x(\vec{\Omega}x\vec{n}') + (\vec{\Omega}x\vec{x}')x\vec{n}'] + \vec{\xi}x(\vec{\Omega}x\vec{n}')\\ &\quad + [(\vec{\Omega}x\vec{x}')x(\vec{\Omega}x\vec{n}') + \epsilon^2\vec{x}'x\underset{\sim}{H}\vec{n}' + \epsilon^2(\underset{\sim}{H}\vec{x}')x\vec{n}'] + O(\epsilon^3).\end{aligned}$$

This can be further simplified. From equation (A.2), it follows that

$$\vec{\xi}x(\vec{\Omega}x\vec{n}') + (\vec{\Omega}x\vec{x}')x\vec{n}' = \vec{\Omega}x(\vec{x}x\vec{n}'),$$

$$(\vec{\Omega}x\vec{x}')x(\vec{\Omega}x\vec{n}') = \vec{\Omega}(\vec{\Omega}.\vec{x}'x\vec{n}').$$

Hence,

$$\begin{aligned}\vec{x}x\vec{n} &= \vec{x}'x\vec{n}' + \vec{\xi}x\vec{n}' + \vec{\Omega}x(\vec{x}'x\vec{n}') + \vec{\xi}x(\vec{\Omega}x\vec{n}')\\ &\quad + [\vec{\Omega}(\vec{\Omega}.\vec{x}'x\vec{n}') + \epsilon^2\vec{x}'x\underset{\sim}{H}\vec{n}' + \epsilon^2(\underset{\sim}{H}\vec{x}')x\vec{n}'] + O(\epsilon^3).\end{aligned}$$

The terms in the square brackets can be written in a more compact form. Let $\underset{\sim}{H}$ be denoted by $[h_{ij}]$. Then

$$\vec{\Omega}(\vec{\Omega}.\vec{x}'x\vec{n}') = \vec{\Omega}(\Omega_i n_{i+3}) = \epsilon^2\begin{bmatrix}(h_{11}-h_{22}-h_{33})n_4+h_{21}n_5+h_{31}n_6\\ h_{21}n_4+(h_{22}-h_{11}-h_{33})n_5+h_{32}n_6\\ h_{31}n_4+h_{32}n_5+(h_{33}-h_{11}-h_{22})n_6\end{bmatrix},$$

$$\vec{x}'x\underset{\sim}{H}\vec{n}' + (\underset{\sim}{H}\vec{x}')x\vec{n}'$$

$$= x'x\begin{bmatrix} h_{1j}n_j \\ h_{2j}n_j \\ h_{3j}n_j \end{bmatrix} + \begin{bmatrix} h_{1j}x'_j \\ h_{1j}x'_j \\ h_{3j}x'_j \end{bmatrix} xn' = \begin{bmatrix} (h_{22}+h_{33})n_4 - h_{21}n_5 - h_{31}n_6 \\ -h_{12}n_4 + (h_{11}+h_{33})n_5 - h_{32}n_6 \\ -h_{13}n_4 - h_{23}n_5 + (h_{11}+h_{22})n_6 \end{bmatrix}.$$

Note that $h_{12}=h_{13}=h_{23}=0$. Therefore,

$$\vec{\Omega}(\vec{\Omega}.\vec{x}'x\vec{n}') + \epsilon^2\vec{x}'x\underset{\sim}{H}\vec{n}' + \epsilon^2(\underset{\sim}{H}\vec{x}')x\vec{n}' = \begin{bmatrix} h_{11}n_4 \\ h_{21}n_4+h_{22}n_5 \\ h_{31}n_4+h_{32}n_5+h_{33}n_6 \end{bmatrix}$$

$$- \epsilon^2\underset{\sim}{H}(\vec{x}'x\vec{n}') \qquad \text{(G.3)}$$

Finally,

$$\vec{x}x\vec{n} = \vec{x}'x\vec{n}' + \vec{\xi}x\vec{n}' + \vec{\Omega}x(\vec{x}'x\vec{n}') + \vec{\xi}x(\vec{\Omega}x\vec{n}') + \epsilon^2\underset{\sim}{H}(\vec{x}'x\vec{n}') + O(\epsilon^3). \qquad \text{(G.4)}$$

Table 3.1 The ratio of B_{WD}/B_v ($k_0d=2, \omega_0/\omega_n=10, x_a/a=4$)

k_0A	k_0a			
	0.1	0.2	0.3	0.4
0.1	.005	.020	.044	.079
0.2	.020	.079	.177	.316
0.3	.044	.177	.399	.710
0.4	.079	.316	.710	1.262
τ	.04	.08	.12	.16

Table 6.1 Multipole expansion coefficients b_m/a in sway: h/a=2.0

ka=0.1		
N=3	N=5	N=10
(1.12902, -.05419)	(1.12687, -.05398)	(1.12685, -.05398)
(-.03087, .00391)	(-.02802, .00376)	(-.02799, .00376)
(.00605, -.00038)	(.00614, -.00038)	(.00608, -.00038)
	(-.00153, .00008)	(-.00141, .00007)
	(.00034, -.00002)	(.00034, -.00002)
		(-.00008, .00000)
		(.00002, .00000)
		(-.00001, .00000)
		(.00000, .00000)
		(.00000, .00000)

ka=1.0		
N=3	N=5	N=10
(.81792, -.14335)	(.81729, -.13229)	(.81717, -.13216)
(.03602, .06104)	(.03604, .05341)	(.03616, .05330)
(-.00417, -.01604)	(-.00353, -.01766)	(-.00370, -.01750)
	(-.00096, .00477)	(-.00073, .00452)
	(.00047, -.00093)	(.00051, -.00096)
		(-.00017, .00018)
		(.00004, -.00003)
		(-.00001, .00001)
		(.00000, .00000)
		(.00000, .00000)

Table 6.2 Multipole expansion coefficients a_{m-1}/a in heave: h/a=2.0

ka=0.1		
N=3	N=5	N=10
(-.11192, -.00532)	(-.11268, .00540)	(-.11269, .00540)
(1.12412, -.05347)	(1.12683, -.05398)	(1.12685, -.05398)
(-.02472, .00356)	(-.02796, .00376)	(-.02799, .00376)
	(.00603, -.00038)	(.00608, -.00038)
	(-.00128, .00007)	(-.00141, .00007)
		(.00034, -.00002)
		(-.00008, .00000)
		(.00002, -.00000)
		(-.00001, .00000)
		(.00000, -.00000)

ka=1.0		
N=3	N=5	N=10
(-.81798, -.11106)	(-.81703, .13198)	(-.81717, .13216)
(.81896, -.11203)	(.81703, .13198)	(-.81717, .13216)
(.03446, .03623)	(.03631, .05315)	(.03616, .05330)
	(-.00392, -.01726)	(-.00370, -.01750)
	(-.00036, .00402)	(-.00073, .00452)
		(.00051, -.00096)
		(-.00017, .00018)
		(.00004, -.00003)
		(-.00001, .00001)
		(.00000, .00000)

Table 6.3 Convergence of sway hydrodynamic coefficients for a submerged circular cylinder: h/a=2.0

(a) added mass				
ka	N=3	N=5	N=10	N=20
.10	1.25032	1.24812	1.24810	1.24810
.50	.86361	.86247	.86246	.86246
1.00	.70586	.70665	.70667	.70667
2.00	.79025	.79243	.79243	.79243
4.00	.84855	.85024	.85026	.85026
8.00	.86741	.86852	.86853	.86853
16.00	.87531	.87624	.87625	.87625
(b) radiation damping				
ka	N=3	N=5	N=10	N=20
.10	.10753	.10721	.10721	.10721
.50	.39999	.39658	.39656	.39656
1.00	.16016	.15774	.15771	.15771
2.00	.01305	.01074	.01075	.01075
4.00	.00005	.00002	.00001	.00001
8.00	.00000	.00000	.00000	.00000
16.00	.00000	.00000	.00000	.00000
δ_{abs}	4×10^{-3}	2×10^{-5}	-	-

Table 6.4 Convergence of heave hydrodynamic coefficients for a submerged circular cylinder: h/a=2.0

(a) added mass				
ka	N=3	N=5	N=10	N=20
.10	1.24511	1.24808	1.24810	1.24810
.50	.86220	.86245	.86246	.86246
1.00	.70962	.70669	.70667	.70667
2.00	.79349	.79243	.79243	.79243
4.00	.85178	.85027	.85026	.85026
8.00	.86953	.86853	.86853	.86853
16.00	.87710	.87625	.87625	.87625
(b) radiation damping				
ka	N=3	N=5	N=10	N=20
.10	.10623	.10720	.10721	.10721
.50	.39155	.39653	.39656	.39656
1.00	.15624	.15767	.15771	.15771
2.00	.00927	.01077	.01075	.01075
4.00	-.00007	.00000	.00001	.00001
8.00	.00000	.00000	.00000	.00000
16.00	.00000	.00000	.00000	.00000
δ_{abs}	4×10^{-3}	2×10^{-5}	-	-

Table 6.5 Added mass for a submerged circular cylinder: h/a=2.0

ka	$a_{22}/\rho\pi a^2$			$a_{33}/\rho\pi a^2$		
	BIE-BIE	BIE-BMP	analyt.	BIE-BIE	BIE-BMP	analyt.
.000	1.13465	1.13444	1.13458	1.13466	1.13444	1.13458
.100	1.24820	1.24795	1.24810	1.24818	1.24795	1.24810
.200	1.22577	1.22553	1.22569	1.22572	1.22553	1.22569
.300	1.10242	1.10223	1.10236	1.10239	1.10223	1.10236
.400	.96804	.96790	.96800	.96805	.96790	.96800
.500	.86250	.86239	.86246	.86252	.86239	.86246
.600	.79044	.79035	.79039	.79047	.79035	.79039
.700	.74556	.74547	.74550	.74558	.74547	.74550
.800	.72043	.72035	.72037	.72045	.72035	.72037
.900	.70898	.70891	.70893	.70901	.70891	.70893
1.000	.70672	.70664	.70667	.70674	.70664	.70667
1.200	.71769	.71761	.71766	.71771	.71761	.71766
1.400	.73735	.73726	.73732	.73736	.73726	.73732
1.600	.75811	.75801	.75809	.75812	.75801	.75809
1.800	.77679	.77669	.77678	.77680	.77669	.77678
2.000	.79243	.79232	.79243	.79244	.79232	.79243
4.000	.85028	.85015	.85026	.85029	.85015	.85026
8.000	.86856	.86843	.86853	.86856	.86843	.86853
16.000	.87628	.87615	.87625	.87629	.87615	.87625

Table 6.6 Radiation damping for a submerged circular cylinder: h/a=2.0

ka	$b_{22}/\rho\pi a^2\omega$			$b_{33}/\rho\pi a^2\omega$		
	BIE-BIE	BIE-BMP	analyt.	BIE-BIE	BIE-BMP	analyt.
.000	.00000	.00000	.00000	.00000	.00000	.00000
.100	.10723	.10719	.10721	.10726	.10719	.10721
.200	.28843	.28832	.28838	.28842	.28832	.28838
.300	.39934	.39920	.39929	.39929	.39920	.39929
.400	.42363	.42350	.42359	.42358	.42350	.42359
.500	.39659	.39648	.39656	.39655	.39648	.39656
.600	.34802	.34792	.34799	.34799	.34792	.34799
.700	.29423	.29415	.29420	.29421	.29415	.29420
.800	.24286	.24279	.24282	.24285	.24279	.24282
.900	.19705	.19700	.19701	.19704	.19700	.19701
1.000	.15776	.15772	.15771	.15775	.15772	.15771
1.200	.09795	.09792	.09790	.09794	.09792	.09790
1.400	.05873	.05871	.05868	.05872	.05871	.05868
1.600	.03419	.03419	.03415	.03419	.03419	.03415
1.800	.01941	.01941	.01937	.01941	.01941	.01937
2.000	.01077	.01077	.01075	.01077	.01077	.01075
4.000	.00001	.00001	.00001	.00001	.00001	.00001
8.000	.00000	.00000	.00000	.00000	.00000	.00000
16.000	.00000	.00000	.00000	.00000	.00000	.00000

Table 6.7 Added mass for a floating circular cylinder: h/a=0.5

ka	$a_{22}/\rho V_{wet}$			$a_{33}/\rho V_{wet}$		
	BIE-BIE	BIE-BMP	analyt.	BIE-BIE	BIE-BMP	analyt.
.000	1.48618	1.48593	1.48602	18.22529	18.16097	18.14833
.100	1.88486	1.88108	1.88449	.67707	.67528	.67720
.200	2.15650	2.15846	2.15591	.50414	.50400	.50435
.300	1.85093	1.85069	1.85059	.45646	.45646	.45672
.400	1.17205	1.17284	1.17233	.45536	.45534	.45565
.500	.61949	.61934	.62022	.47474	.47474	.47504
.600	.29203	.29195	.29296	.50241	.50239	.50271
.700	.11503	.11136	.11598	.53196	.53192	.53223
.800	.02251	.02199	.02339	.56003	.56000	.56029
.900	-.02327	-.02230	-.02251	.58500	.58501	.58528
1.000	-.04250	-.04124	-.04188	.60645	.60643	.60666
1.200	-.04067	-.03876	-.04013	.63873	.63865	.63888
1.400	-.01534	-.01279	-.01423	.65945	.65934	.65956
1.600	.00864	.02010	.02015	.67200	.67188	.67208
1.800	.05779	.05523	.05650	.67916	.67901	.67925
2.000	.09171	.09037	.09190	.68293	.68279	.68305

Table 6.8 Radiation damping for a floating circular cylinder: h/a=0.5

ka	$b_{22}/\rho V_{wet}\omega$			$b_{33}/\rho V_{wet}\omega$		
	BIE-BIE	BIE-BMP	analyt.	BIE-BIE	BIE-BMP	analyt.
.000	.00000	.00000	.00000	1.19672	1.18857	1.18698
.100	.18275	.18001	.18269	.71693	.71856	.71636
.200	.80269	.80555	.80226	.48260	.48244	.48219
.300	1.55575	1.55523	1.55475	.32559	.32548	.32526
.400	1.85762	1.85721	1.85647	.21515	.21503	.21488
.500	1.75238	1.75185	1.75149	.13745	.13739	.13725
.600	1.52056	1.51995	1.52000	.08385	.08379	.08371
.700	1.29098	1.30077	1.29073	.04803	.04793	.04794
.800	1.09497	1.09422	1.09495	.02508	.02508	.02505
.900	.93348	.93217	.93361	.01096	.01131	.01128
1.000	.80091	.80016	.80109	.00387	.00384	.00382
1.200	.60011	.59899	.60021	.00006	.00006	.00006
1.400	.45815	.46654	.45821	.00331	.00331	.00331
1.600	.34886	.35780	.35485	.00856	.00853	.00855
1.800	.28055	.28075	.27796	.01365	.01357	.01362
2.000	.22182	.22210	.21982	.01769	.01770	.01771

Table 6.9 Added mass for a submerged circular cylinder at forward speed: h=2a

	ka	$a_{22}/\rho\pi a^2$		$a_{33}/\rho\pi a^2$	
		present	Wu	present	Wu
F_n= .0	.3000	1.1024	-	1.1024	-
	.5000	.8625	-	.8625	-
	1.0000	.7067	-	.7067	-
	1.5000	.7479	-	.7479	-
F_n= .032	.3105	1.0877	1.0917	1.0877	1.0916
	.5226	.8426	.8434	.8426	.8432
	1.0640	.7075	.7090	.7075	.7094
	1.6180	.7601	.7632	.7602	.7615
F_n= .064	.3210	1.0730	1.0958	1.0729	1.0960
	.5453	.8226	.8312	.8226	.8307
	1.1280	.7082	.7190	.7082	.7191
	1.7350	.7724	.7803	.7724	.7784
F_n= .128	.3421	1.0435	1.1291	1.0435	1.1300
	.5905	.7827	.8170	.7827	.8153
	1.2560	.7097	.7588	.7097	.7579
	1.9700	.7970	.8186	.7970	.8152

Table 6.10 Radiation damping for a submerged circular cylinder at forward speed: h=2a

	ka	$b_{22}/\rho\pi a^2$		$b_{33}/\rho\pi a^2$	
		present	Wu	present	Wu
F_n= .0	.3000	.3993	-	.3993	-
	.5000	.3966	-	.3966	-
	1.0000	.1578	-	.1578	-
	1.5000	.0450	-	.0450	-
F_n= .032	.3105	.4060	.4071	.4059	.4073
	.5226	.3872	.3878	.3872	.3865
	1.0640	.1347	.1343	.1347	.1341
	1.6180	.0307	.0320	.0307	.0319
F_n= .064	.3210	.4126	.4209	.4125	.3908
	.5453	.3778	.3775	.3778	.3778
	1.1280	.1117	.1108	.1117	.1105
	1.7350	.0163	.0223	.0163	.0221
F_n= .128	.3421	.4258	.4619	.4258	.4664
	.5905	.3590	.3536	.3590	.3549
	1.2560	.0655	.0669	.0655	.0660
	1.9700	-.0123	.0130	-.0123	.0127

Table 6.11 Exciting forces for a submerged circular cylinder at forward speed: h=2a

	ka	$\|f_2\|$ /ρgA2a		$\|f_3\|$ /ρgA2a	
		present	Wu	present	Wu
F_n= .0	.3000	.5600	-	.5600	-
	.5000	.5581	-	.5581	-
	1.0000	.3520	-	.3520	-
	1.5000	.1879	-	.1879	-
F_n= .032	.3105	.5559	.5551	.5533	.5528
	.5226	.5560	.5552	.5539	.5532
	1.0640	.3527	.3522	.3515	.3513
	1.6180	.1883	.1883	.1877	.1877
F_n= .064	.3210	.5518	.5514	.5467	.5468
	.5453	.5539	.5532	.5497	.5493
	1.1280	.3945	.3527	.3919	.3507
	1.7350	.1888	.1886	.1875	.1873
F_n= .128	.3421	.5437	.5452	.5336	.5359
	.5905	.5501	.5497	.5416	.5419
	1.2560	.3957	.3536	.3906	.3489
	1.9700	.1897	.1889	.1872	.1862

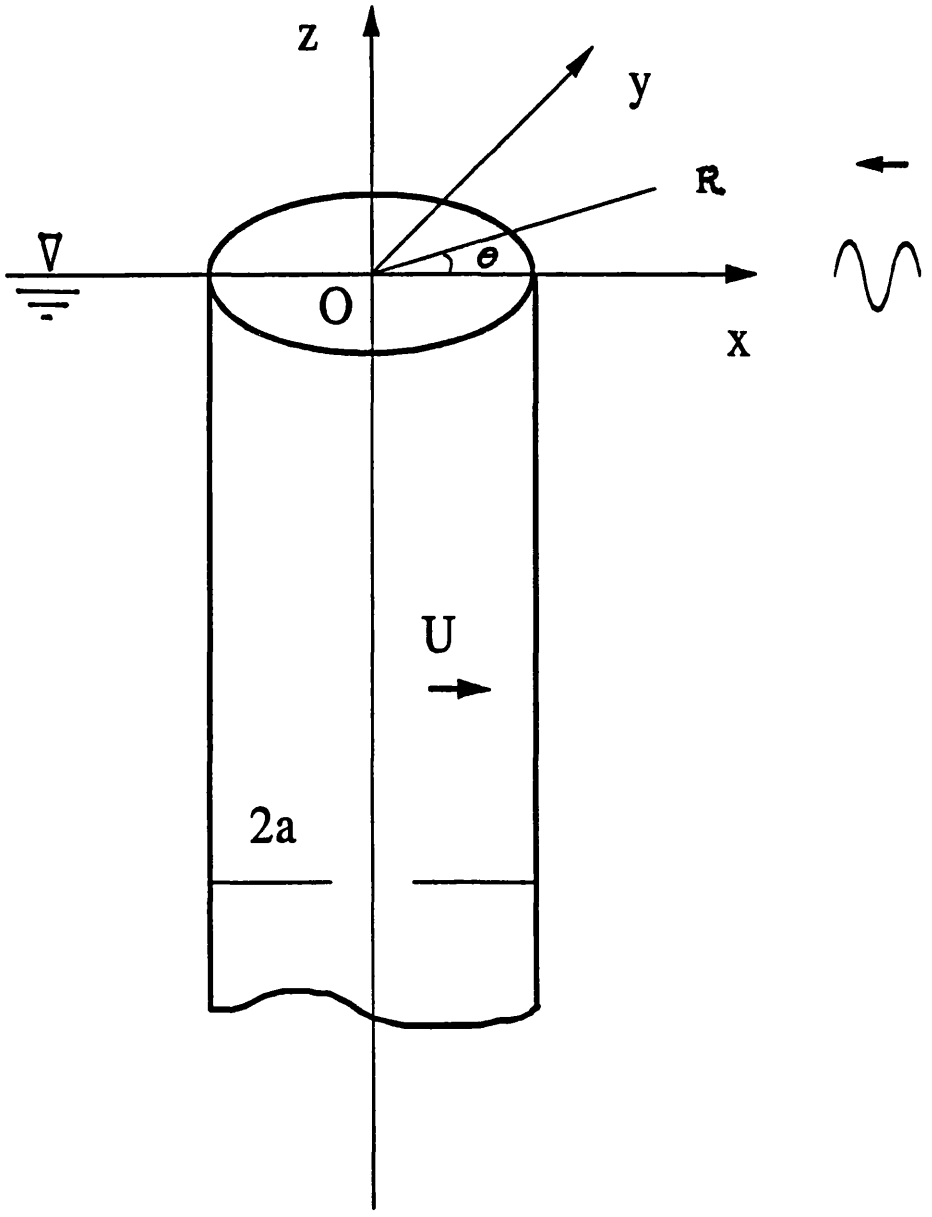

Figure 3.1 Definition of coordinate systems for a vertical cylinder

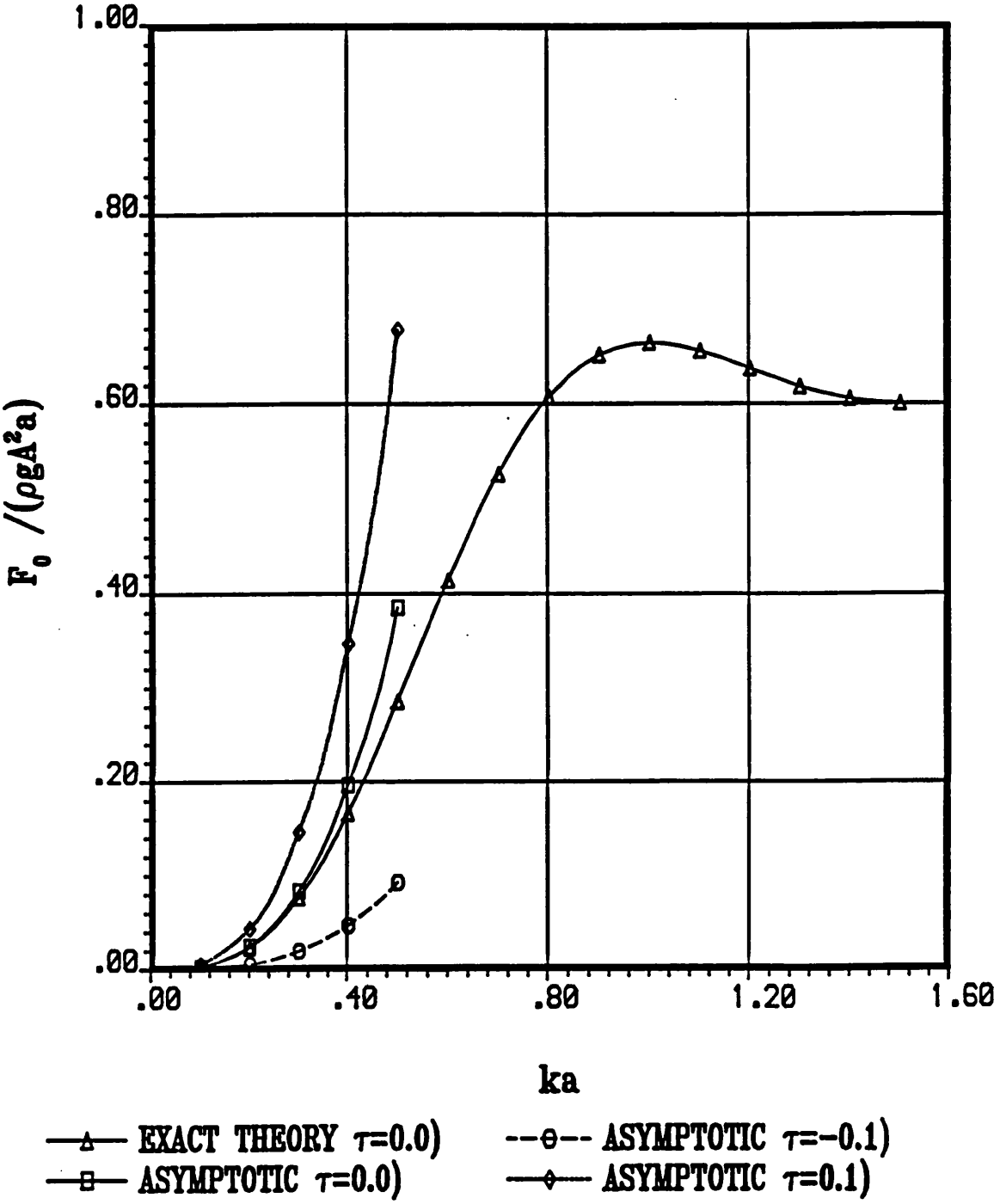

Figure 3.2 Mean drift force on the cylinder

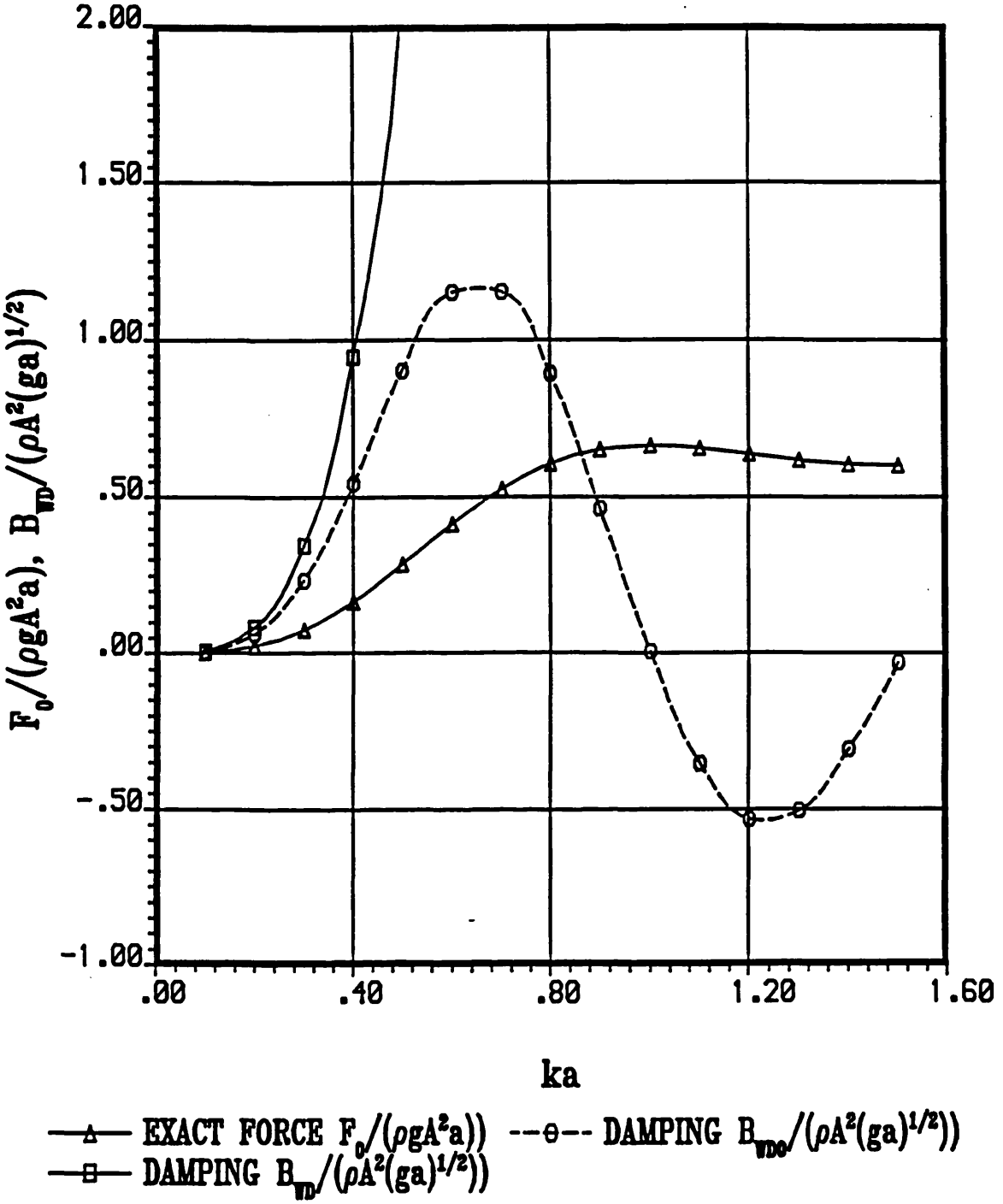

Figure 3.3 Mean drift force and wave drift damping on the cylinder

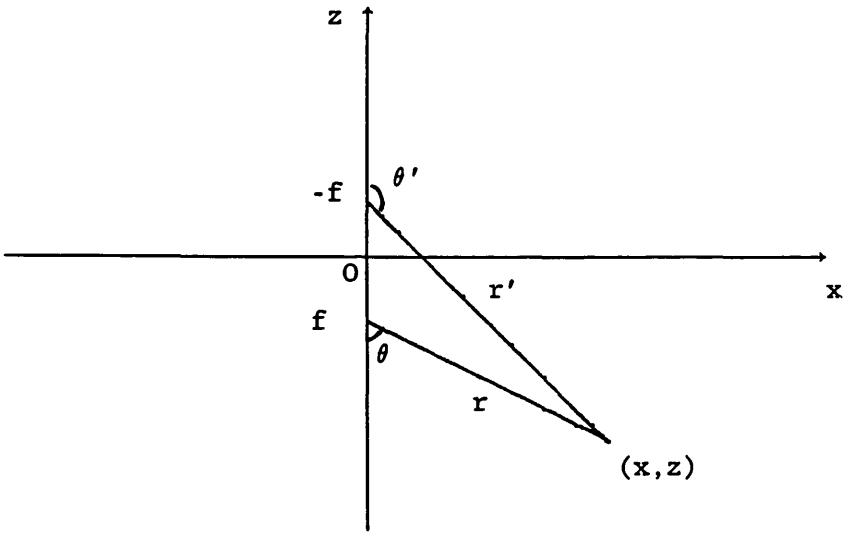

Figure 4.1 Definition of coordinate systems in 2D

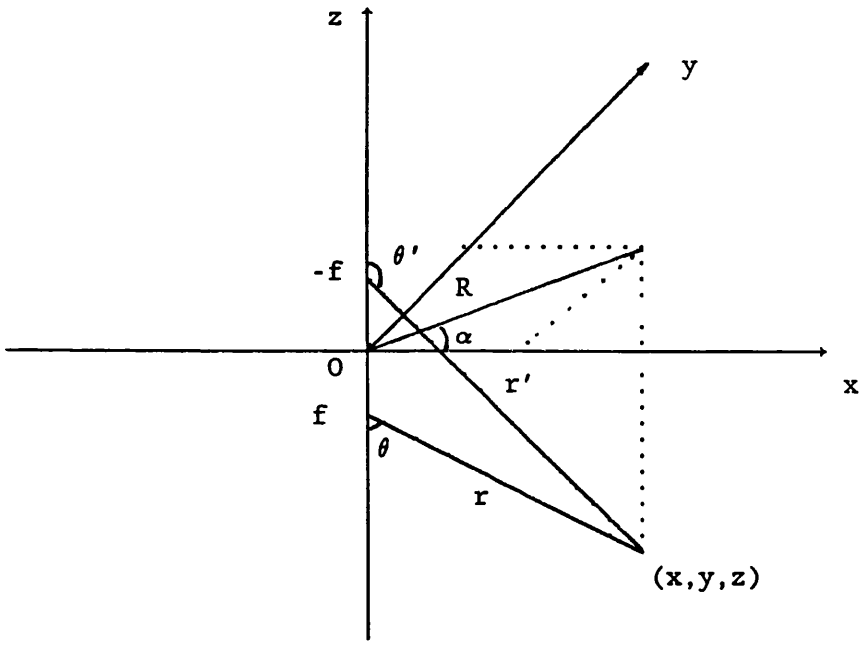

Figure 4.2 Definition of coordinate systems in 3D

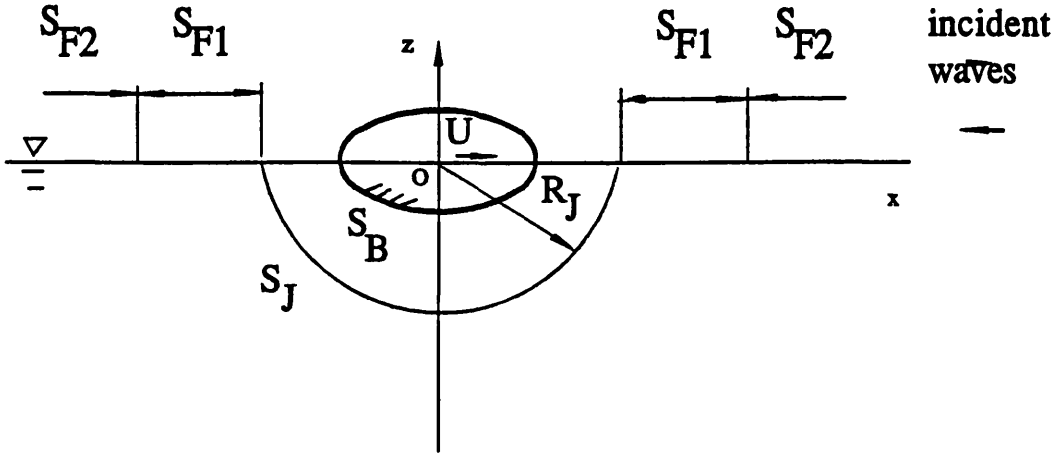

(a) floating body

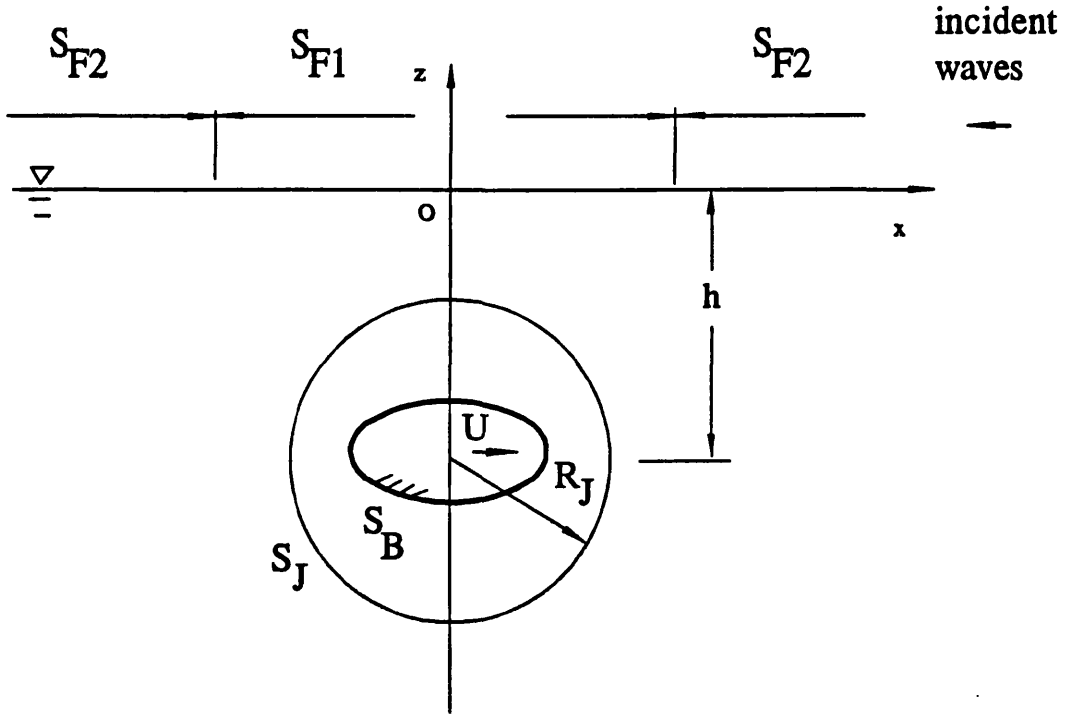

(b) submerged body

Figure 4.3 Geometry and fluid domains

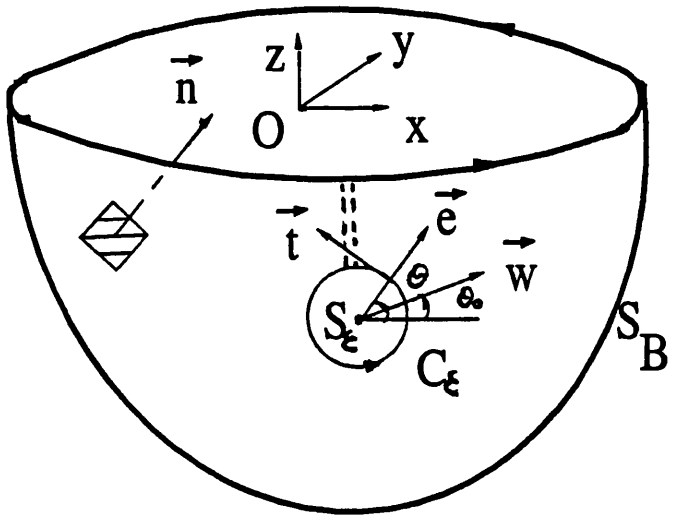

(a) pole below the free surface

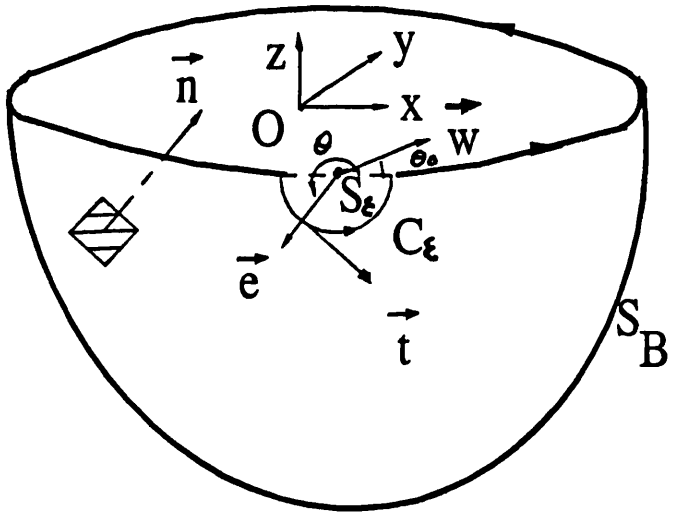

(b) pole on the free surface

Figure 4.4 Definition of S_ε and C_ε; 3D

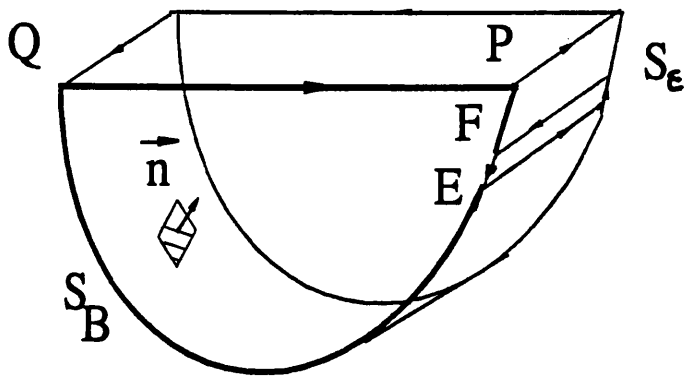

(a) pole below the free surface

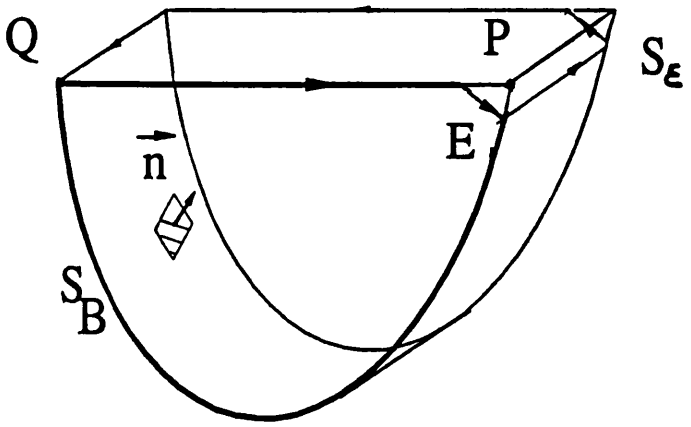

(b) pole on the free surface

Figure 4.5 Definition of S_ϵ; 2D

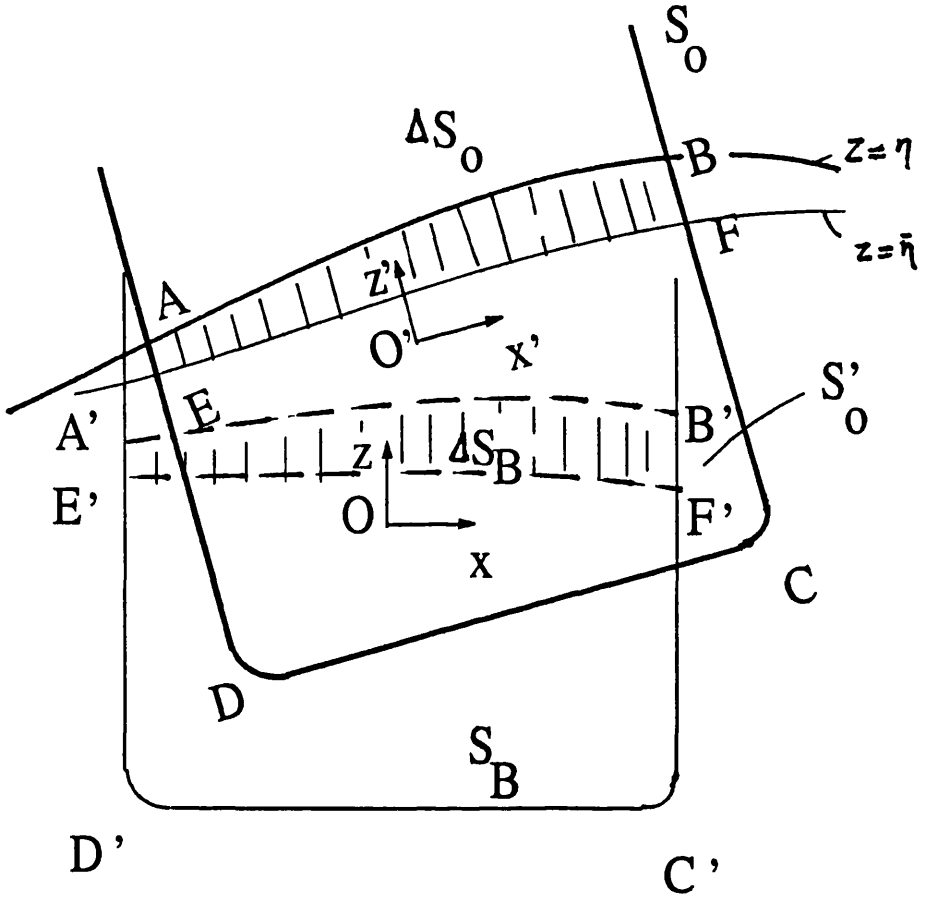

Figure 5.1 The fixed and moving body surfaces

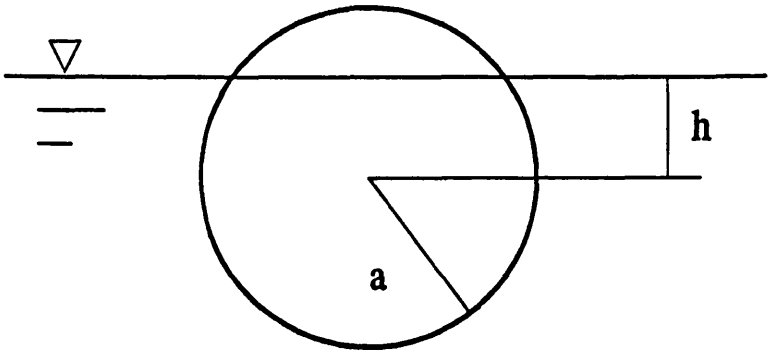

Figure 6.1 Sketch of a circular cylinder

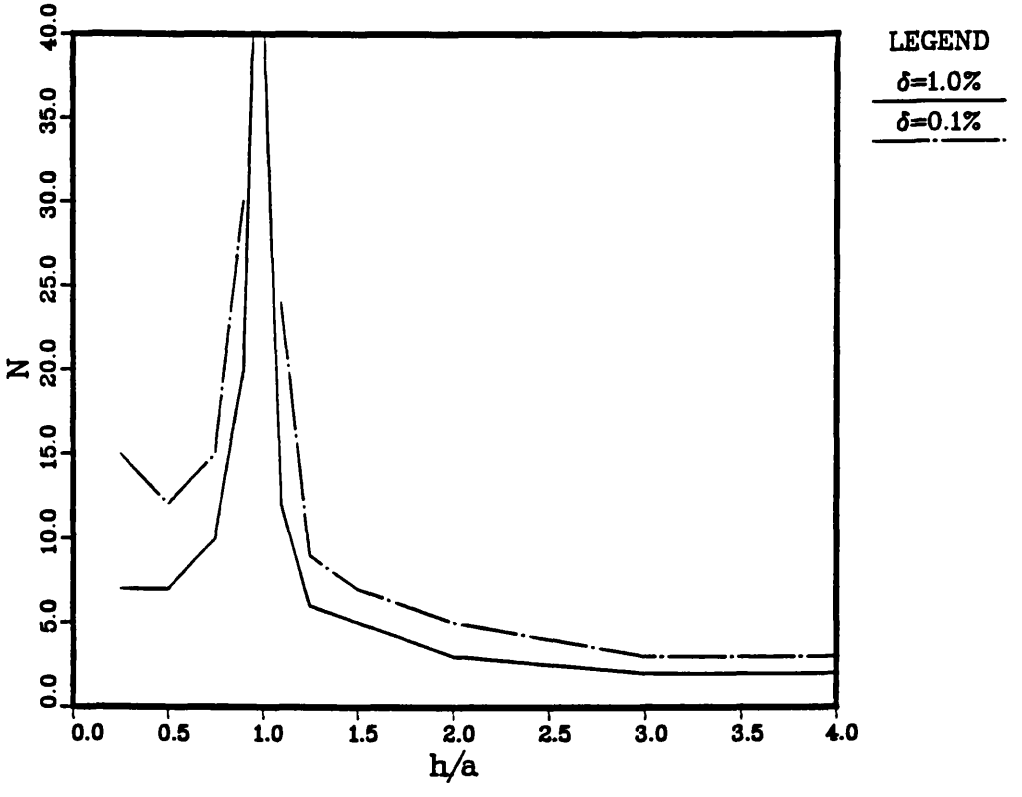

Figure 6.2 N-h/a curve for a circular cylinder

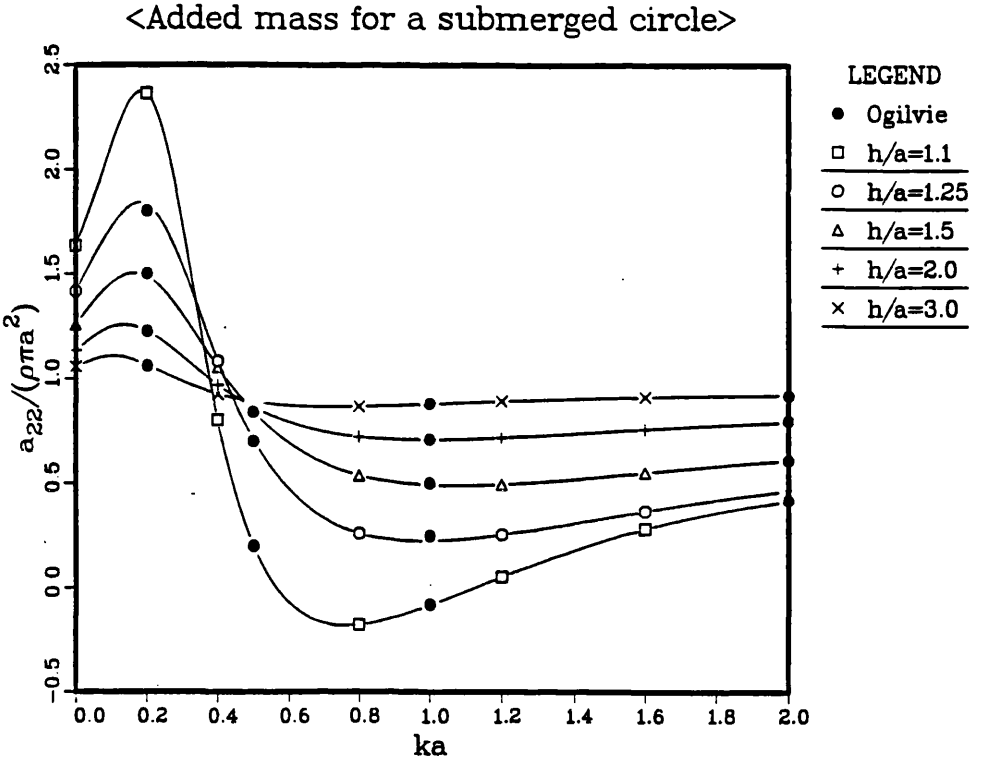

Figure 6.3a A submerged circular cylinder: sway/heave added mass

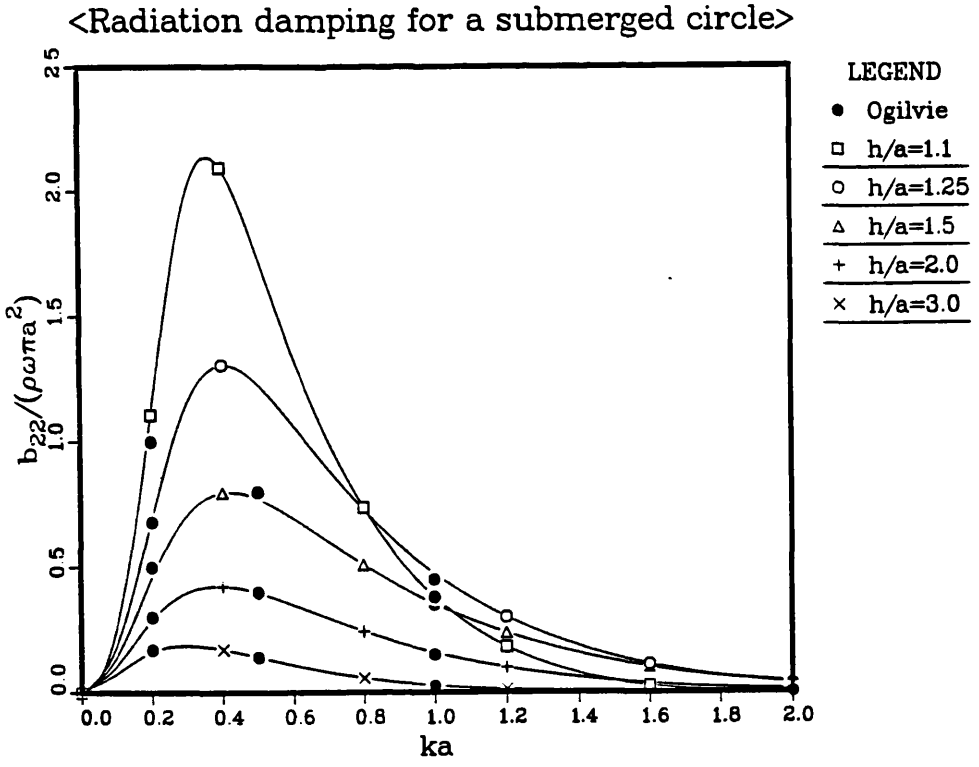

Figure 6.3b A submerged circular cylinder: sway/heave radiation damping

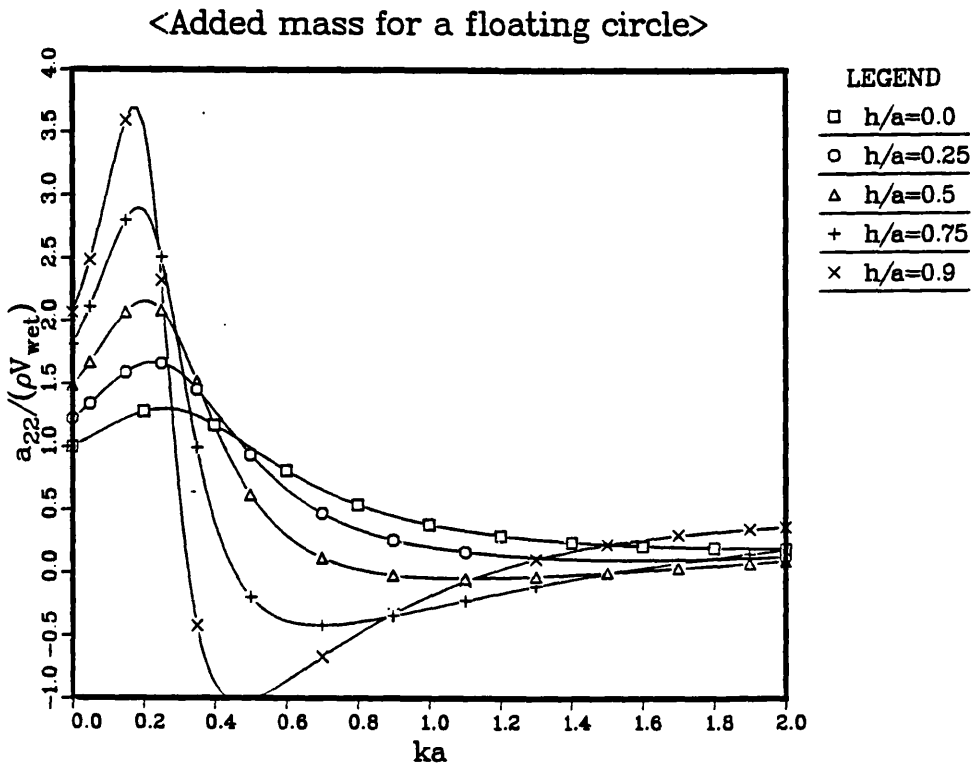

Figure 6.4a A surface-piercing circular cylinder: sway added mass

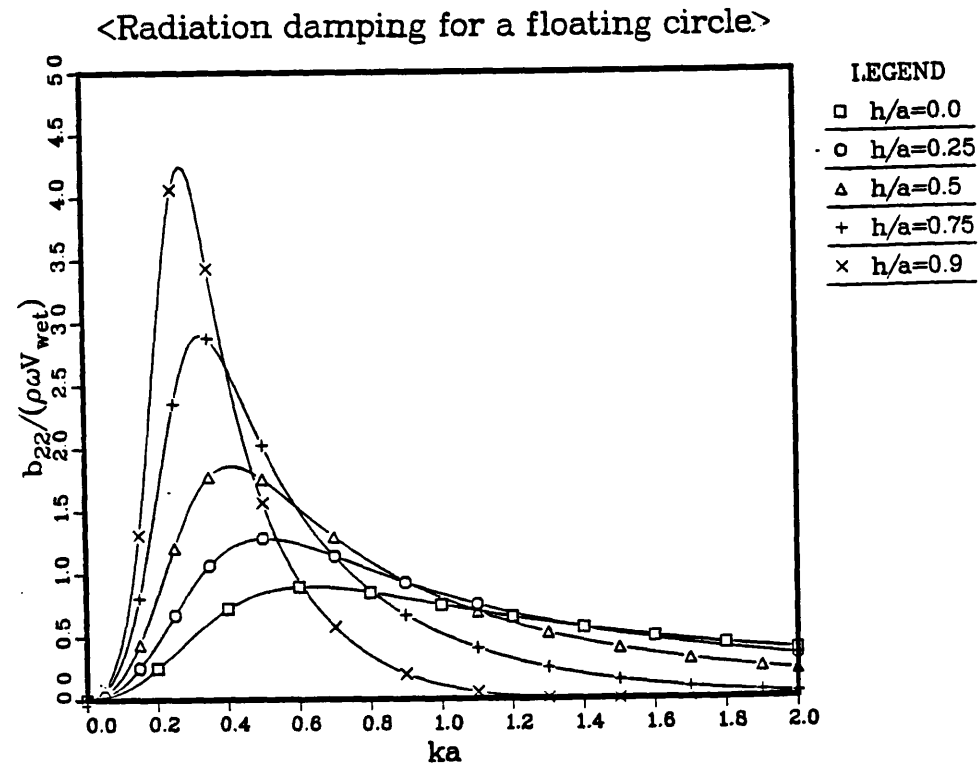

Figure 6.4b A surface-piercing circular cylinder: sway radiation damping

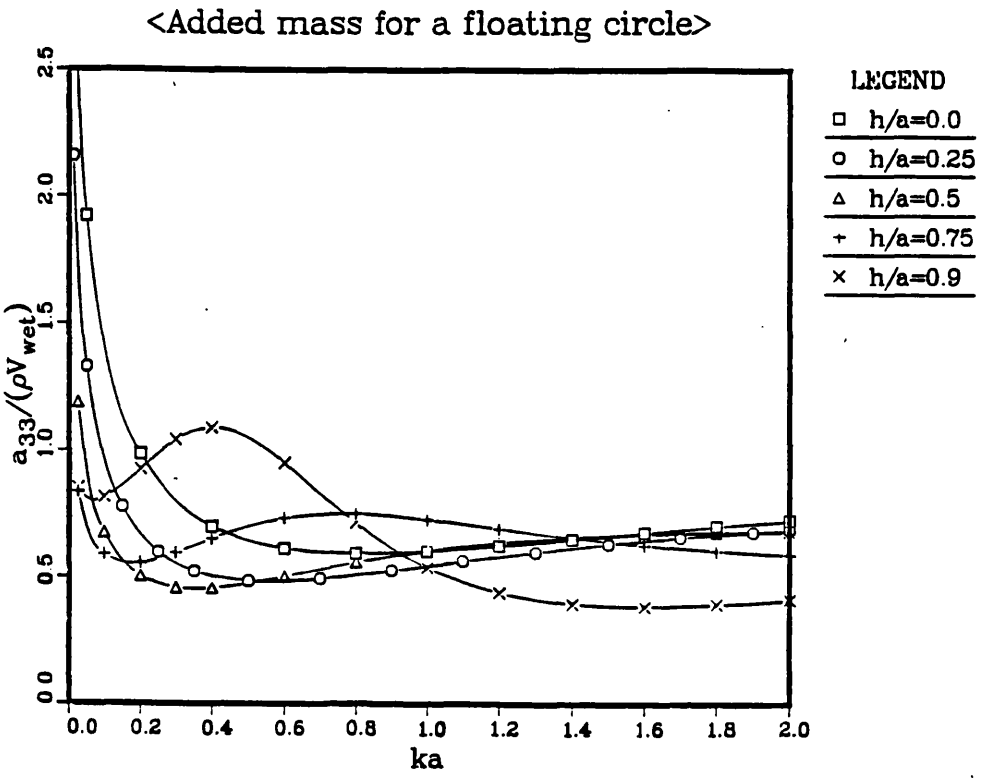

Figure 6.5a A surface-piercing circular cylinder: heave added mass

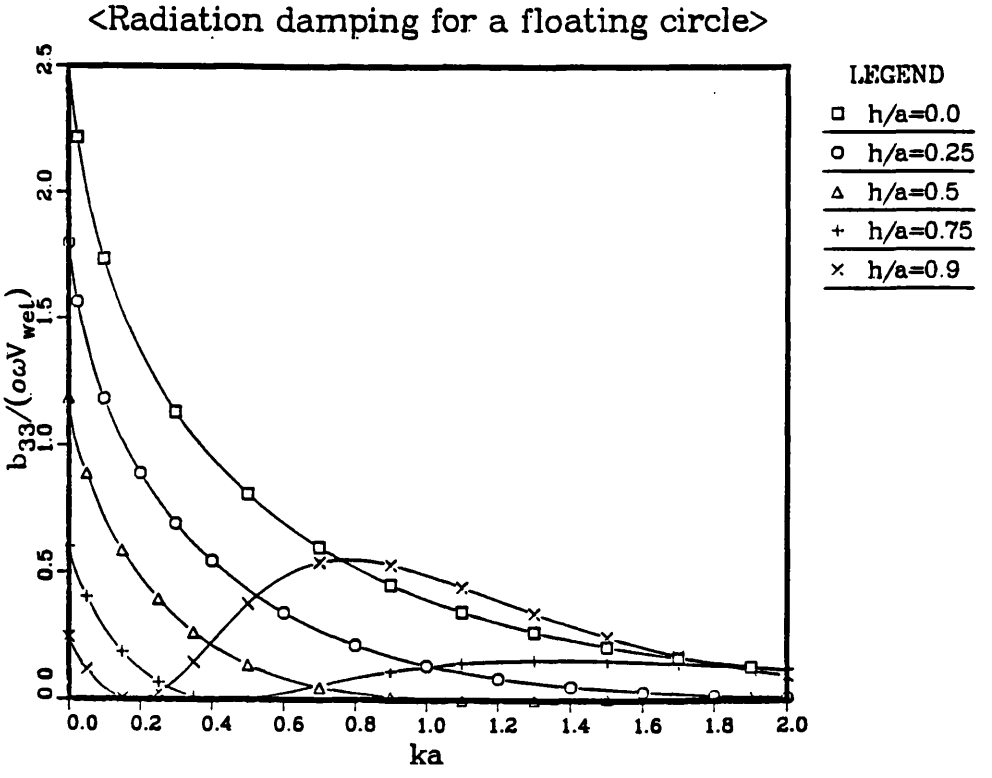

Figure 6.5b A surface-piercing circular cylinder: heave radiation damping

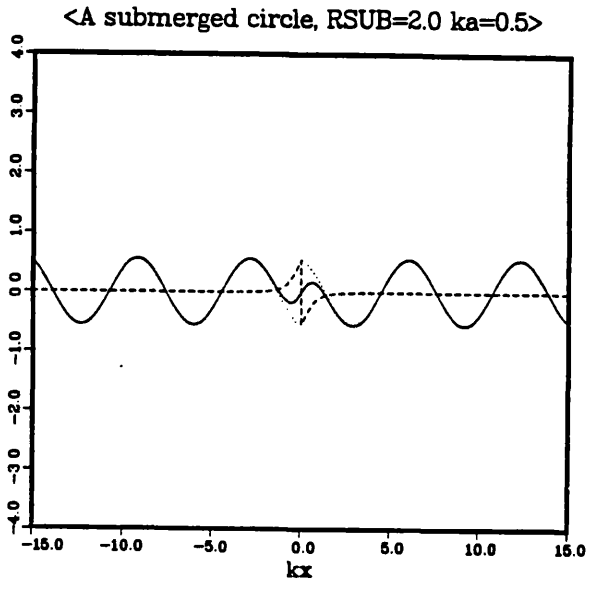

(a) ka=0.5; real part

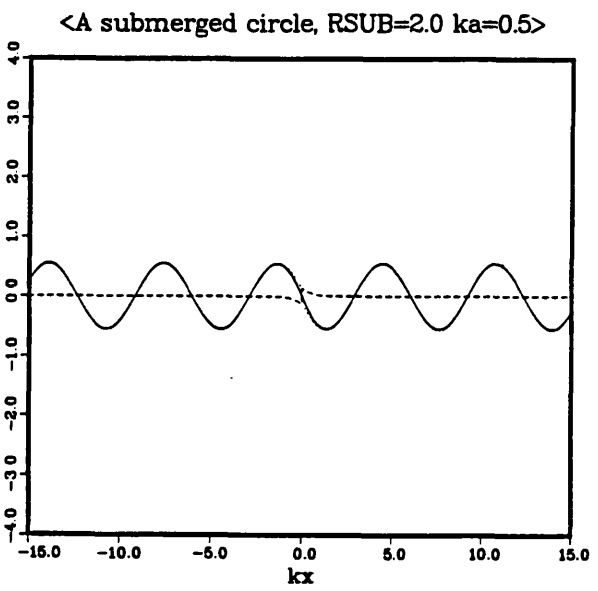

(b) ka=0.5; imaginary part

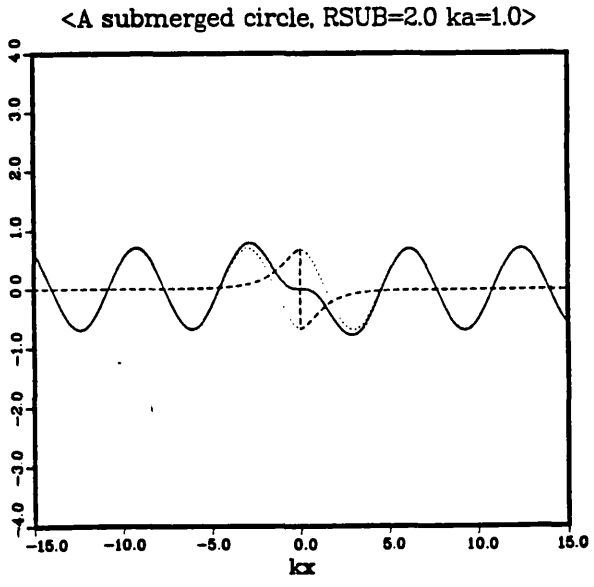

(c) ka=1.0; real part

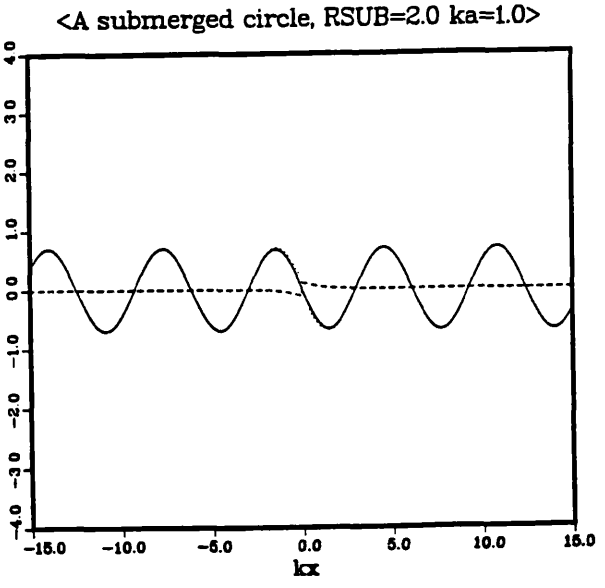

(d) ka=1.0; imaginary part

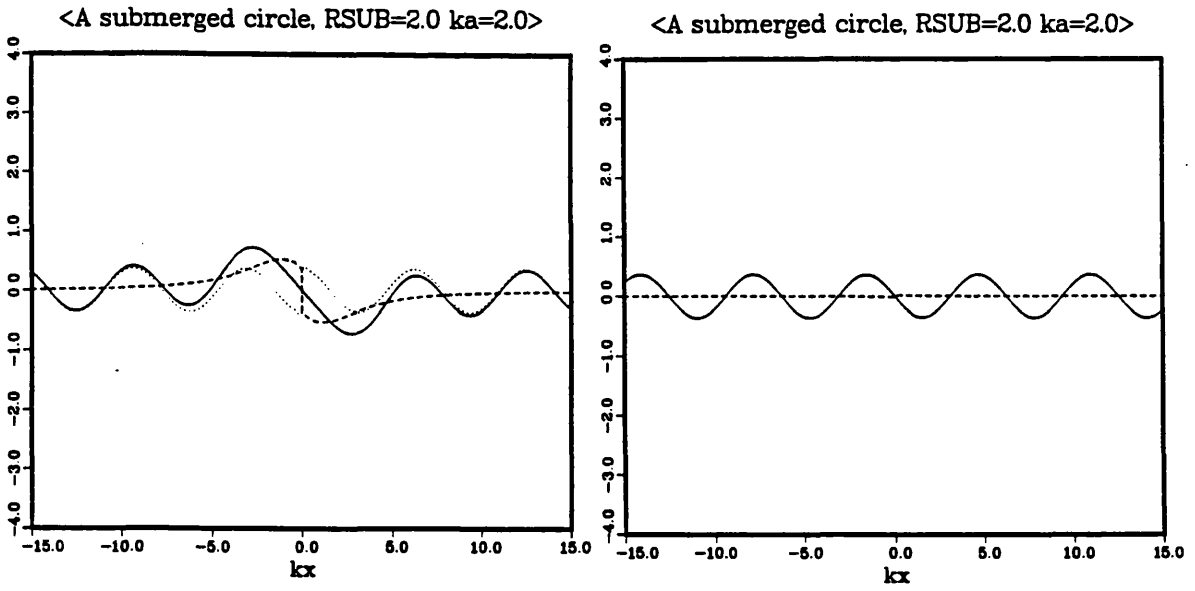

(e) ka=2.0; real part

(f) ka=2.0; imaginary part

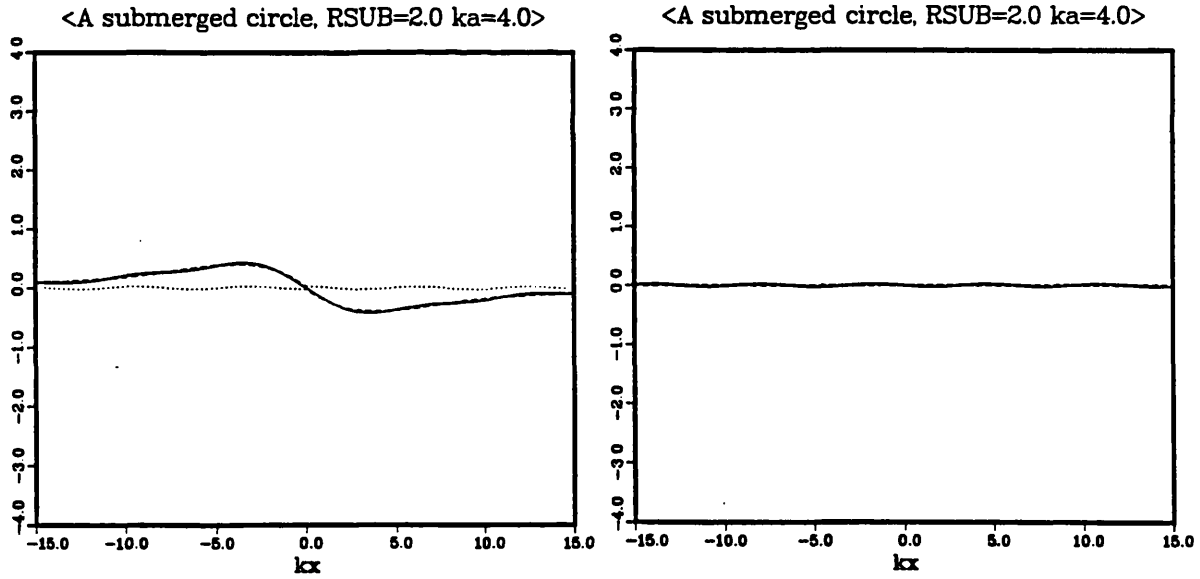

(g) ka=4.0; real part

(h) ka=4.0; imaginary part

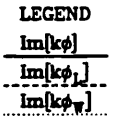

Figure 6.6 Free surface elevation due to sway of a submerged circular cylinder: h/a=2.0

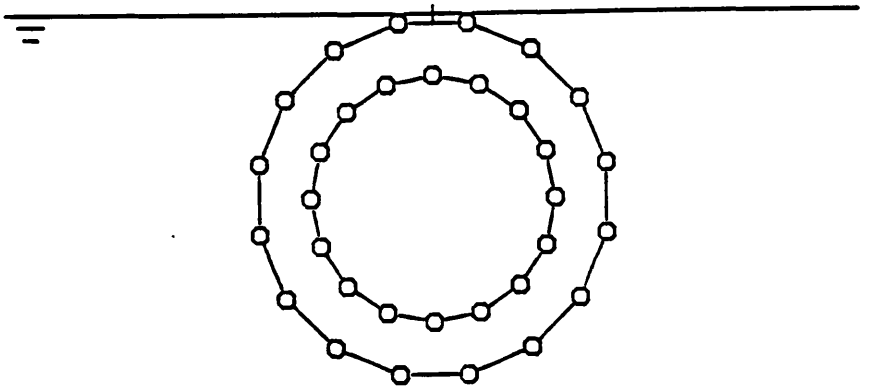

Figure 6.7 Mesh of a submerged circular cylinder

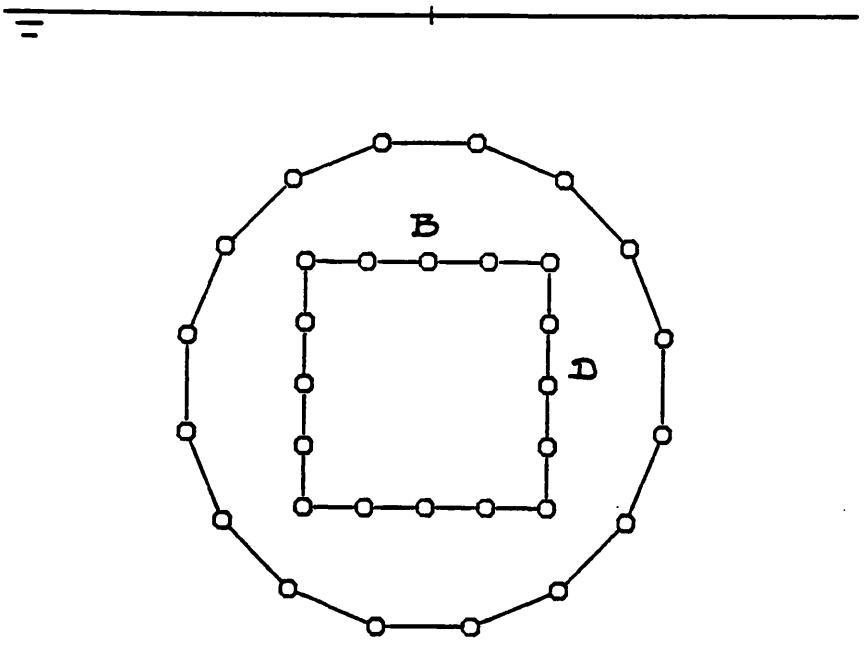

Figure 6.8 Mesh of a submerged rectangular cylinder

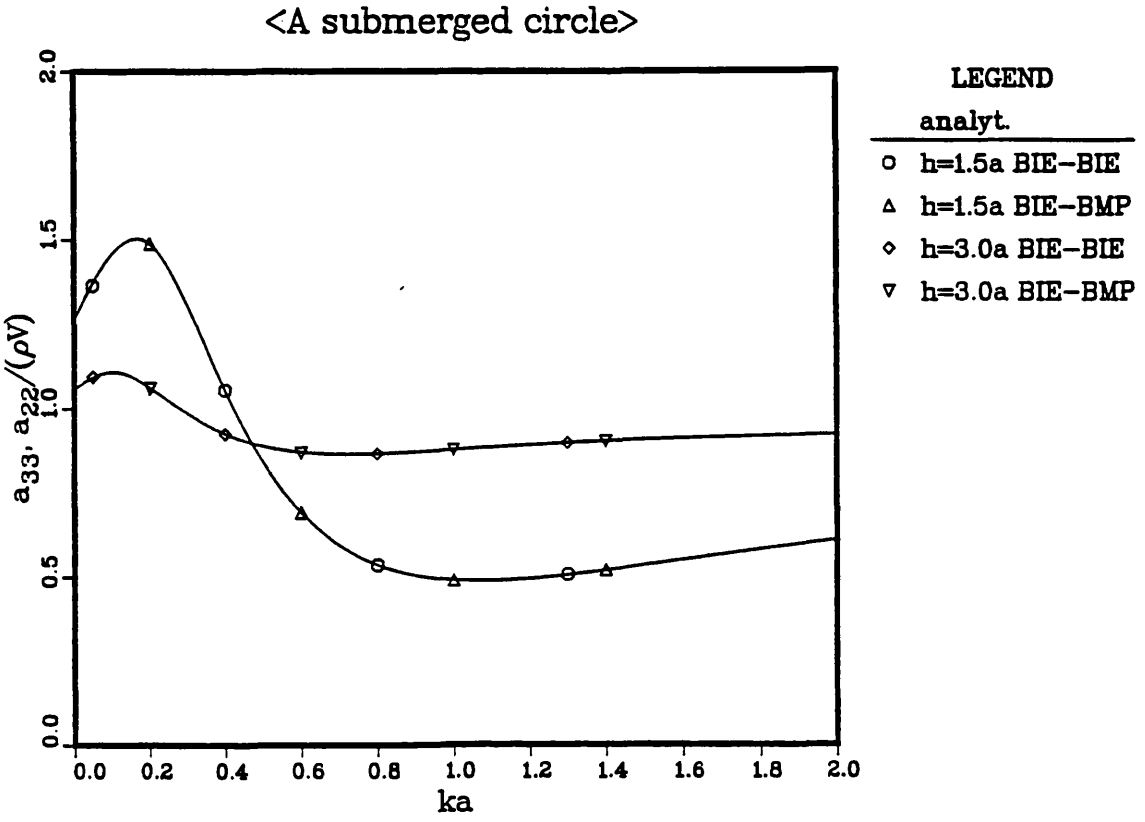

Figure 6.9 Added mass for a submerged circular cylinder

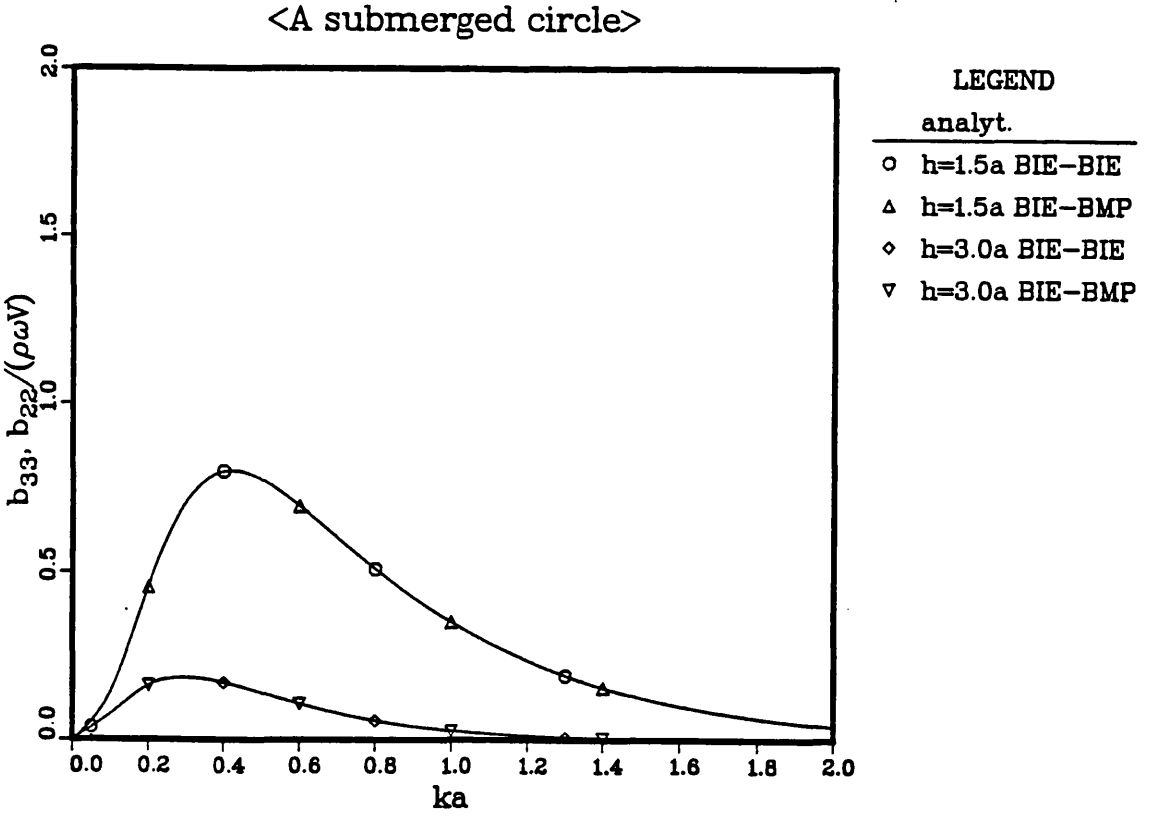

Figure 6.10 Radiation damping for a submerged circular cylinder

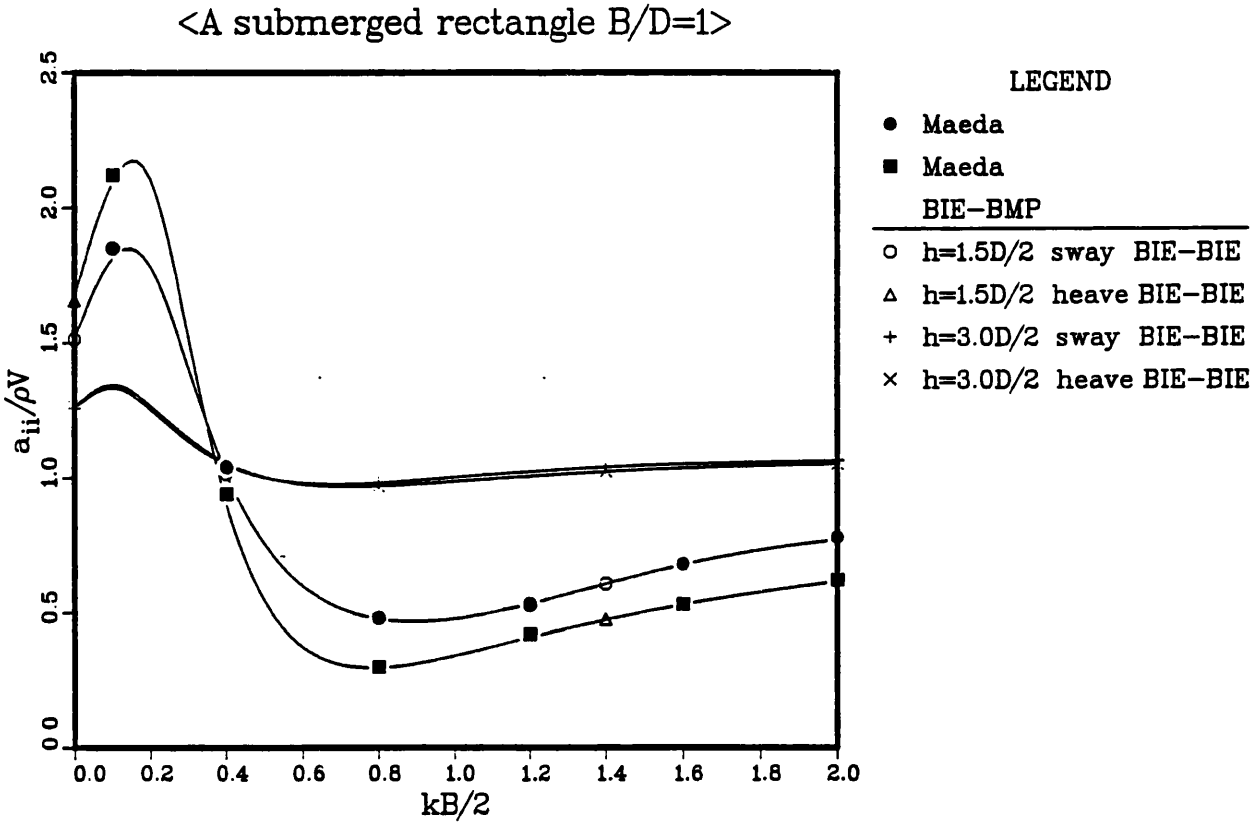

Figure 6.11 Added mass for a submerged rectangular cylinder

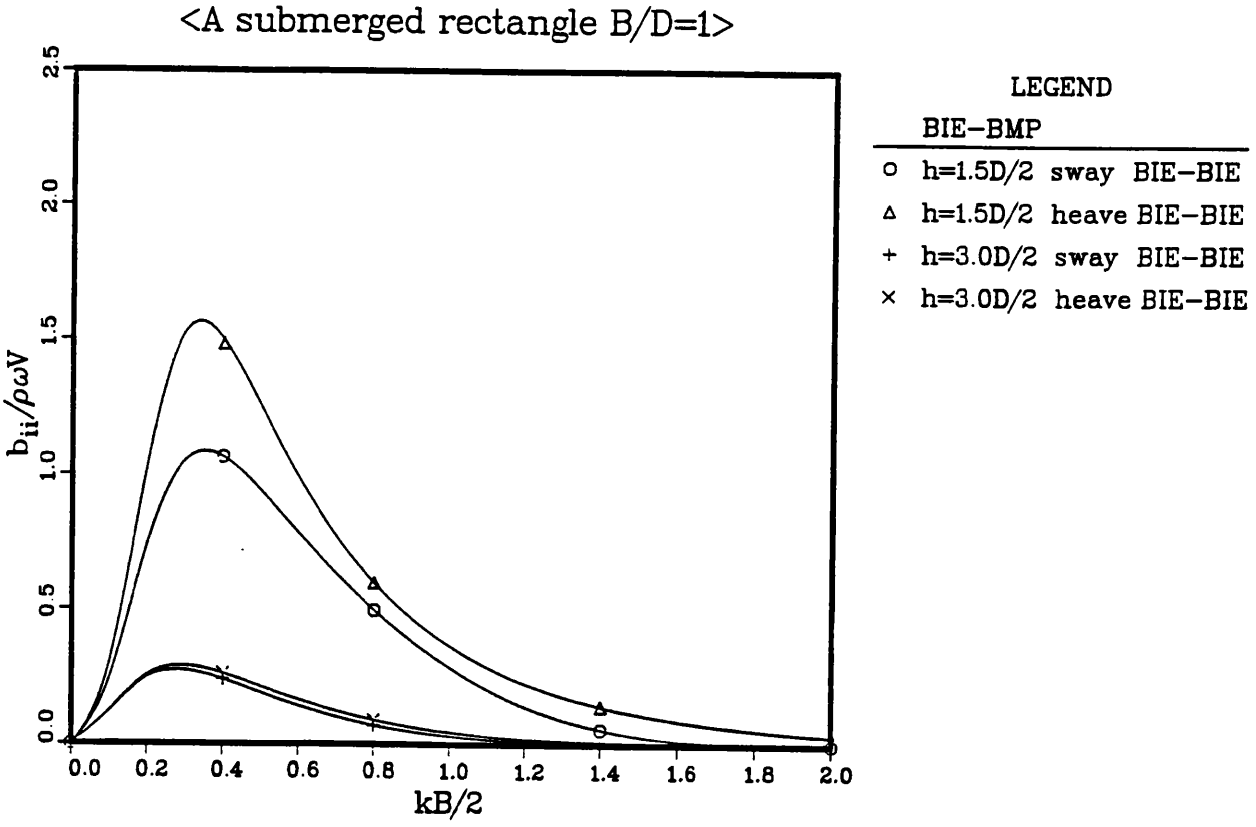

Figure 6.12 Radiation damping for a submerged rectangular cylinder

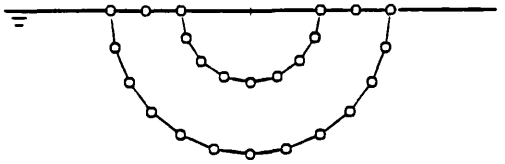

Figure 6.13 Mesh of a floating circular cylinder

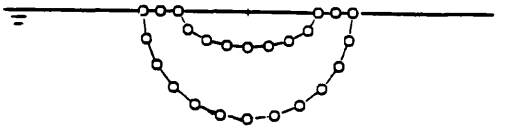

Figure 6.14 Mesh of a floating elliptic cylinder

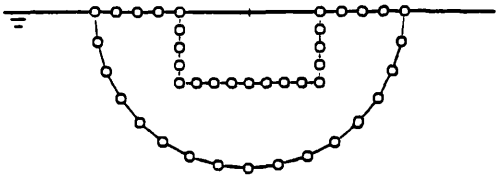

Figure 6.15 Mesh of a floating rectangular cylinder

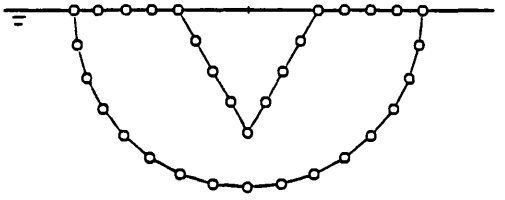

Figure 6.16 Mesh of a floating triangular cylinder

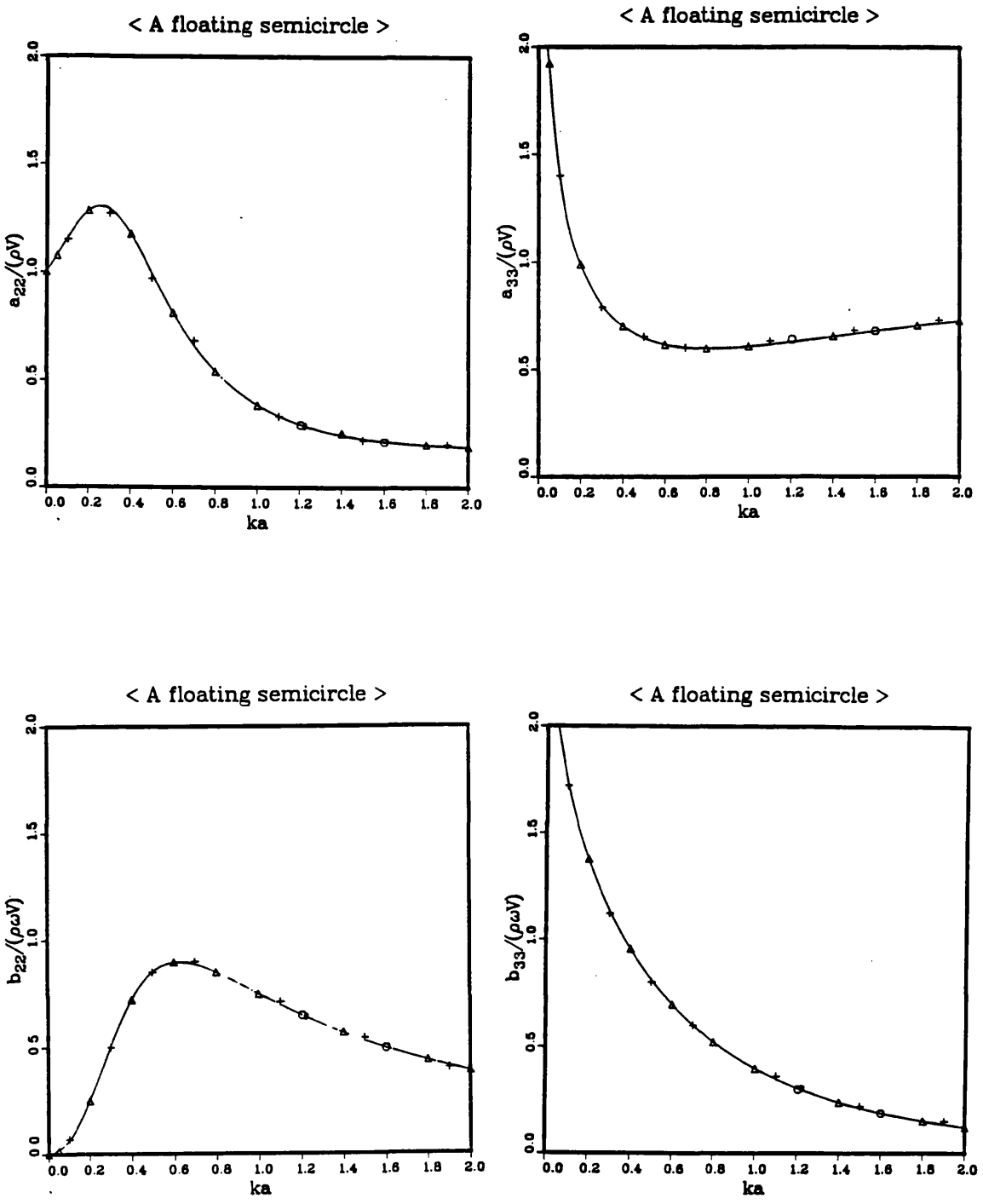

Figure 6.17 Added mass and radiation damping for a floating circular cylinder

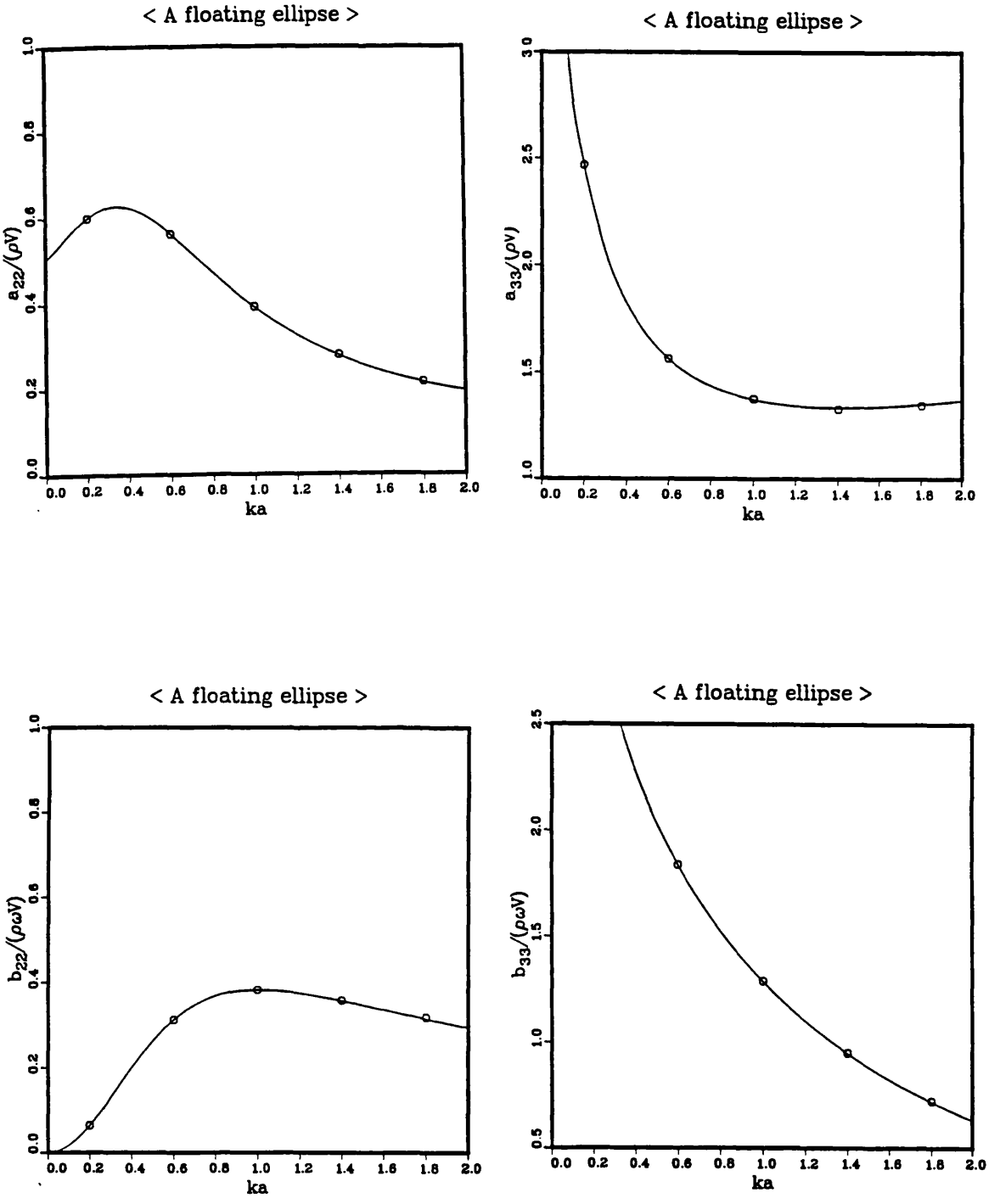

Figure 6.18 Added mass and radiation damping for a floating elliptic cylinder: b/a=0.5

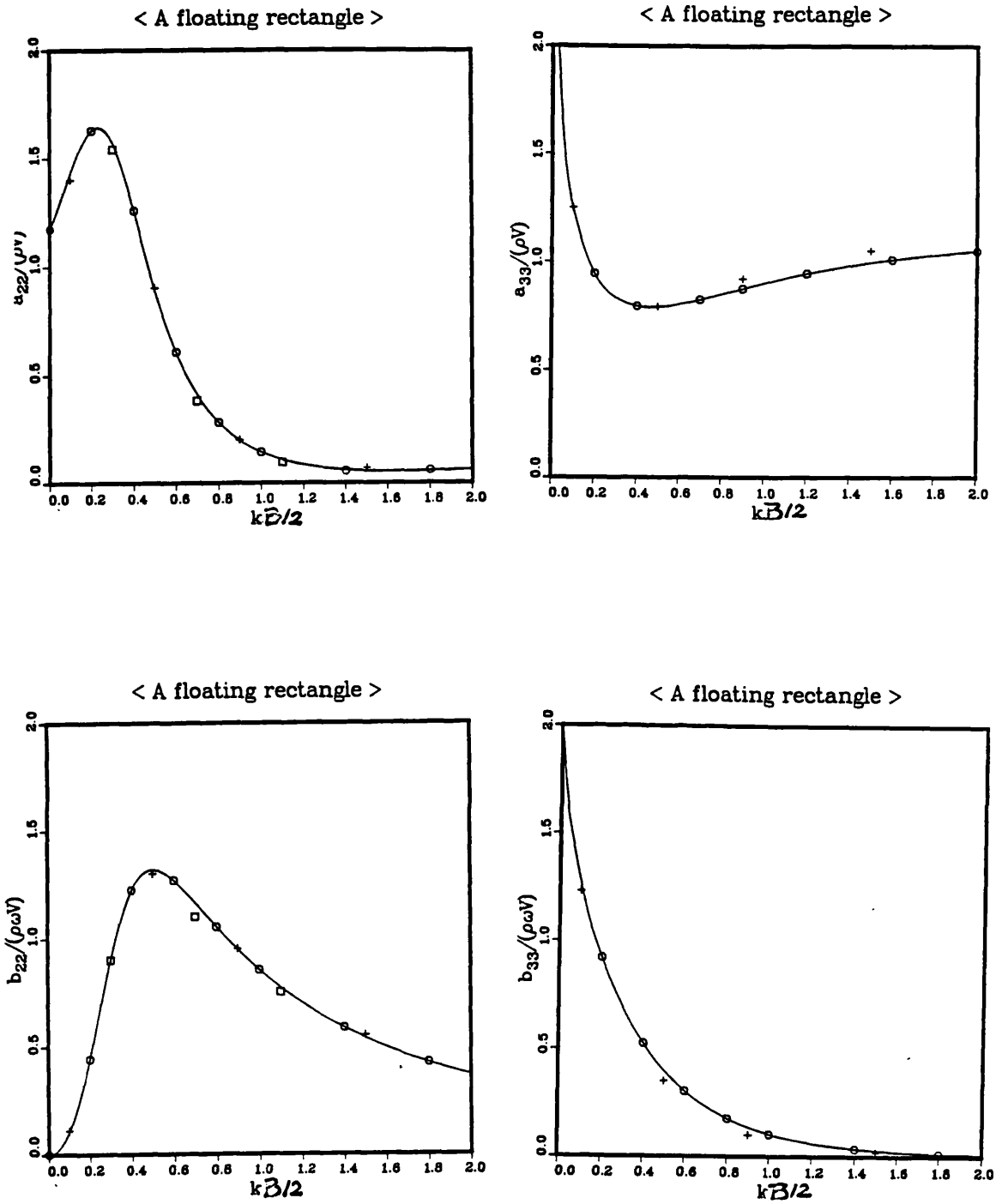

Figure 6.19 Added mass and radiation damping for a floating rectangular cylinder

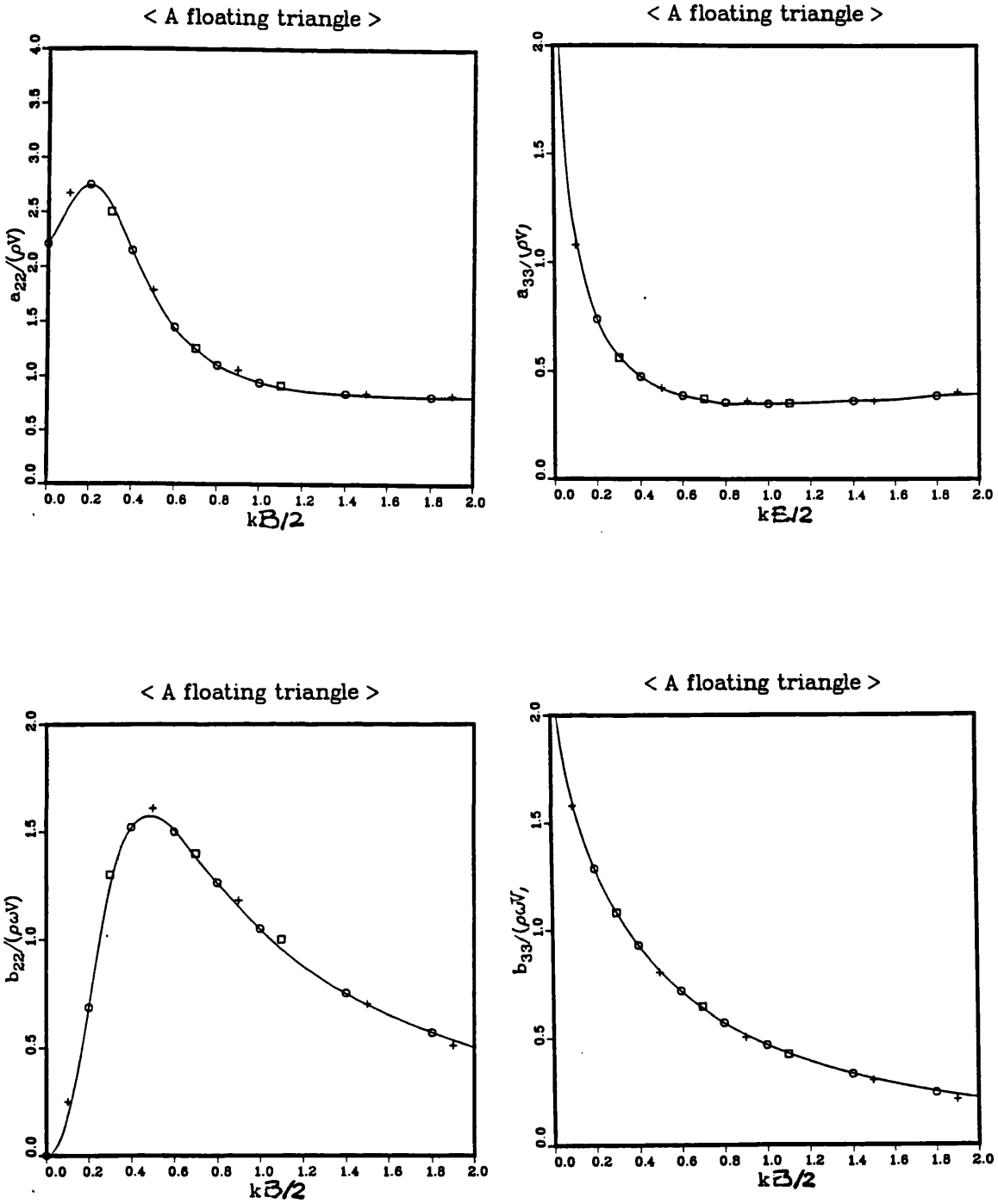

Figure 6.20 Added mass and radiation damping for a floating triangular cylinder

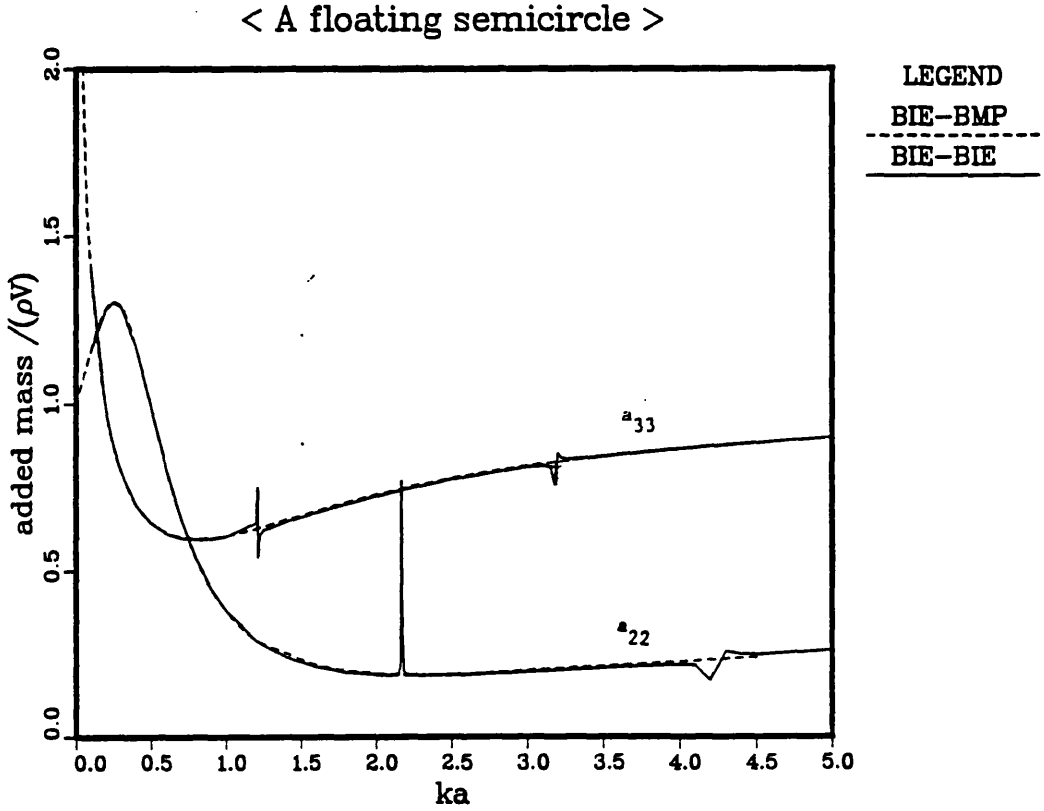

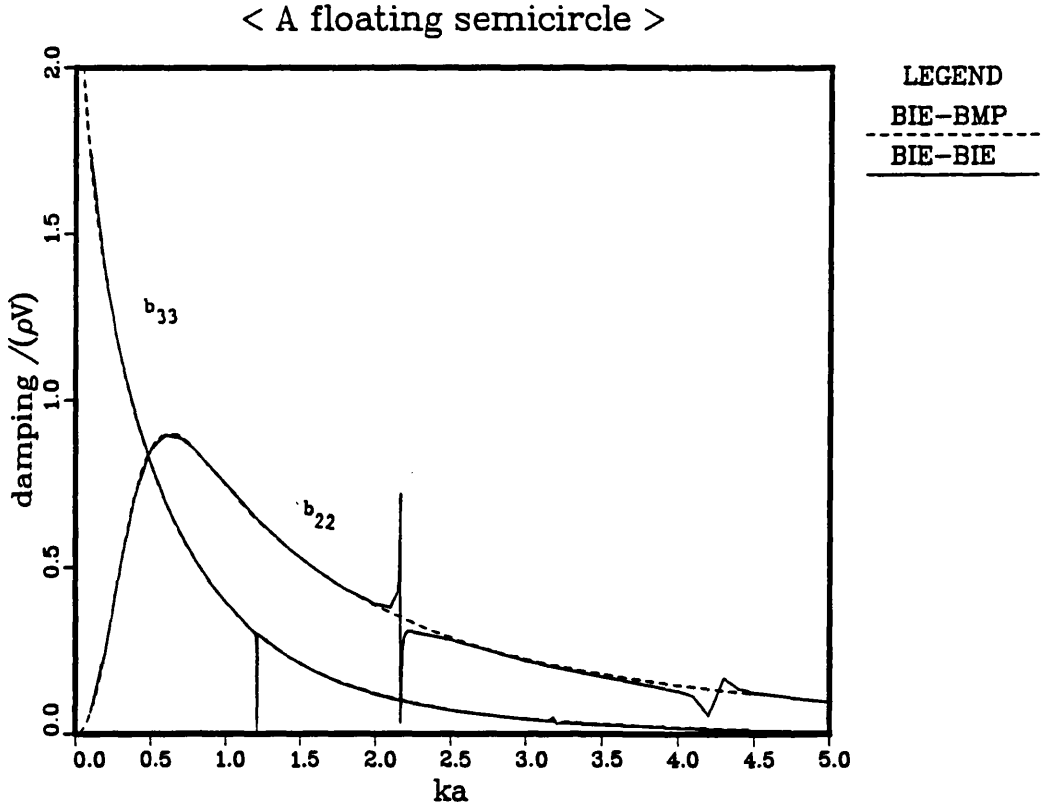

Figure 6.21 Irregular frequencies: k_1R_J=1.822, k_2R_J=3.289, k_3R_J=4.891 ... (R_J=1.5a)

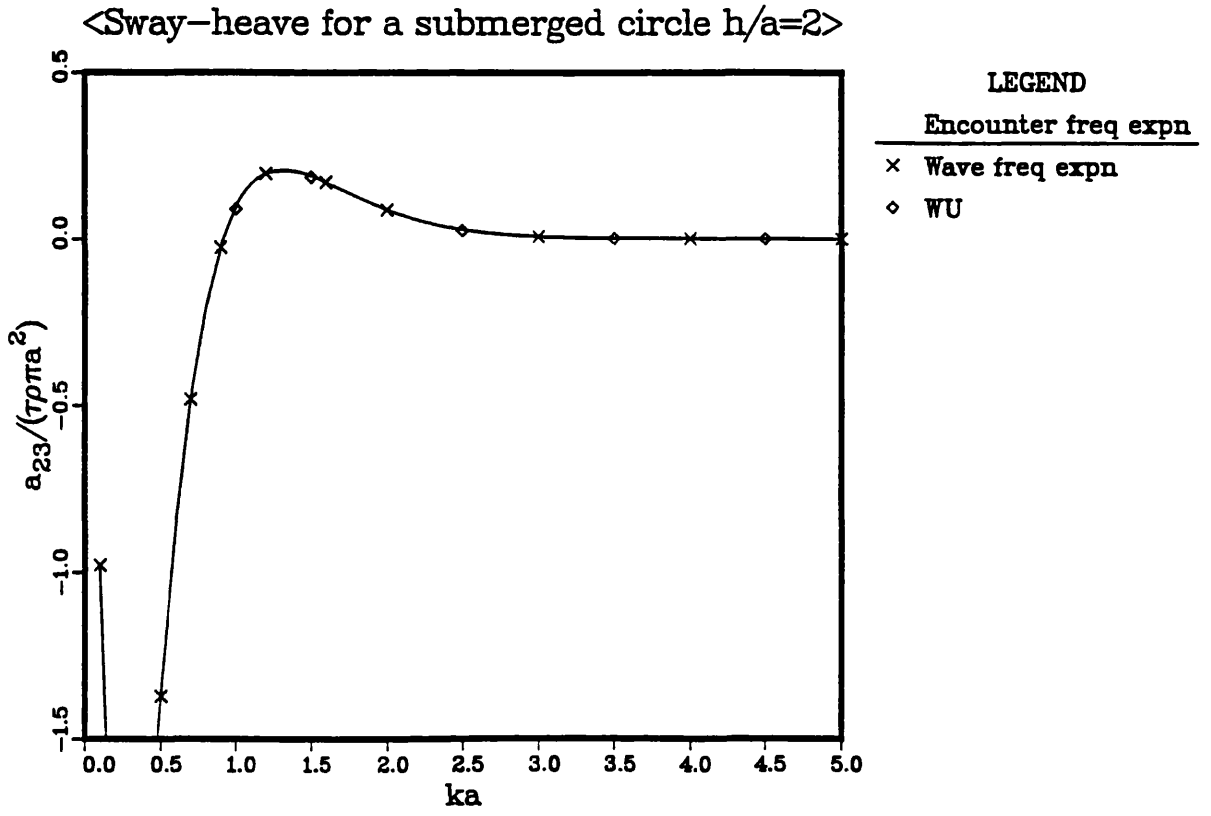

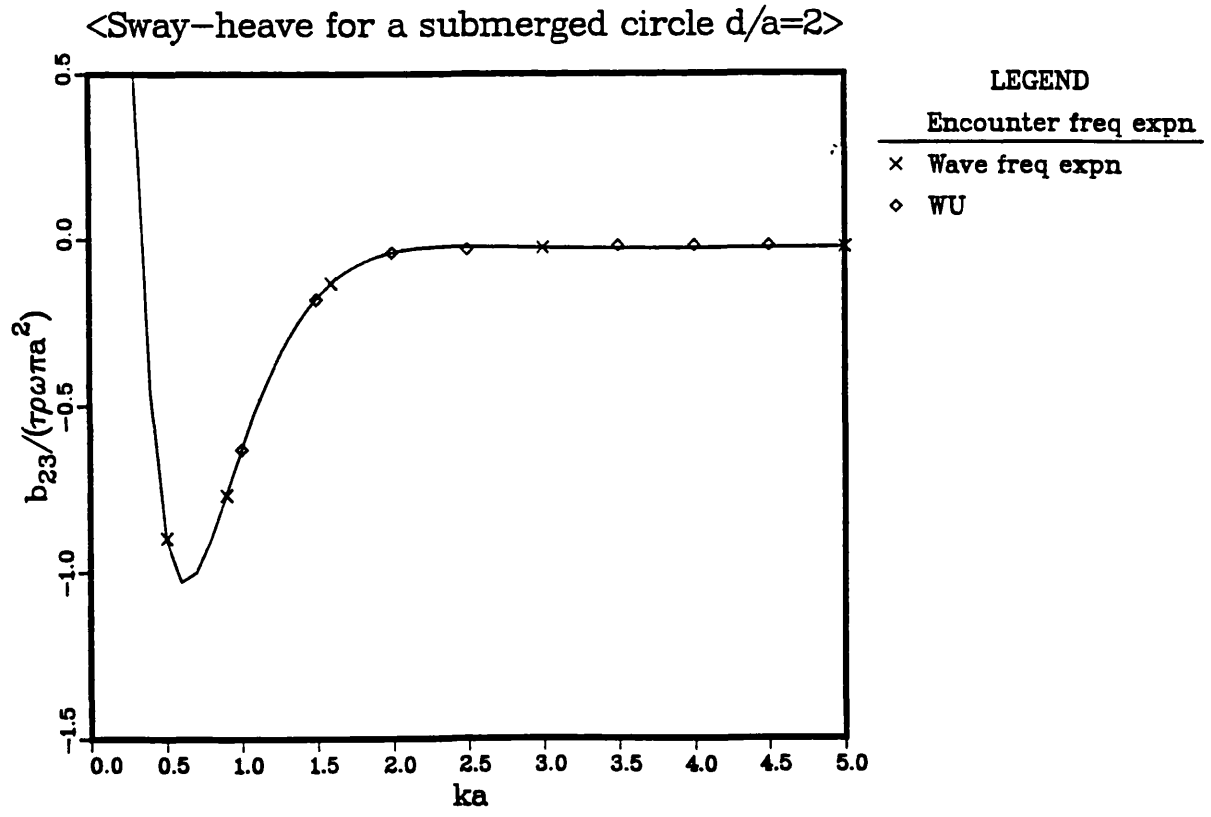

Figure 6.22 Comparison of the wave frequency expansion with the encounter frequency expansion for a submerged circular cylinder: h/a=2.0

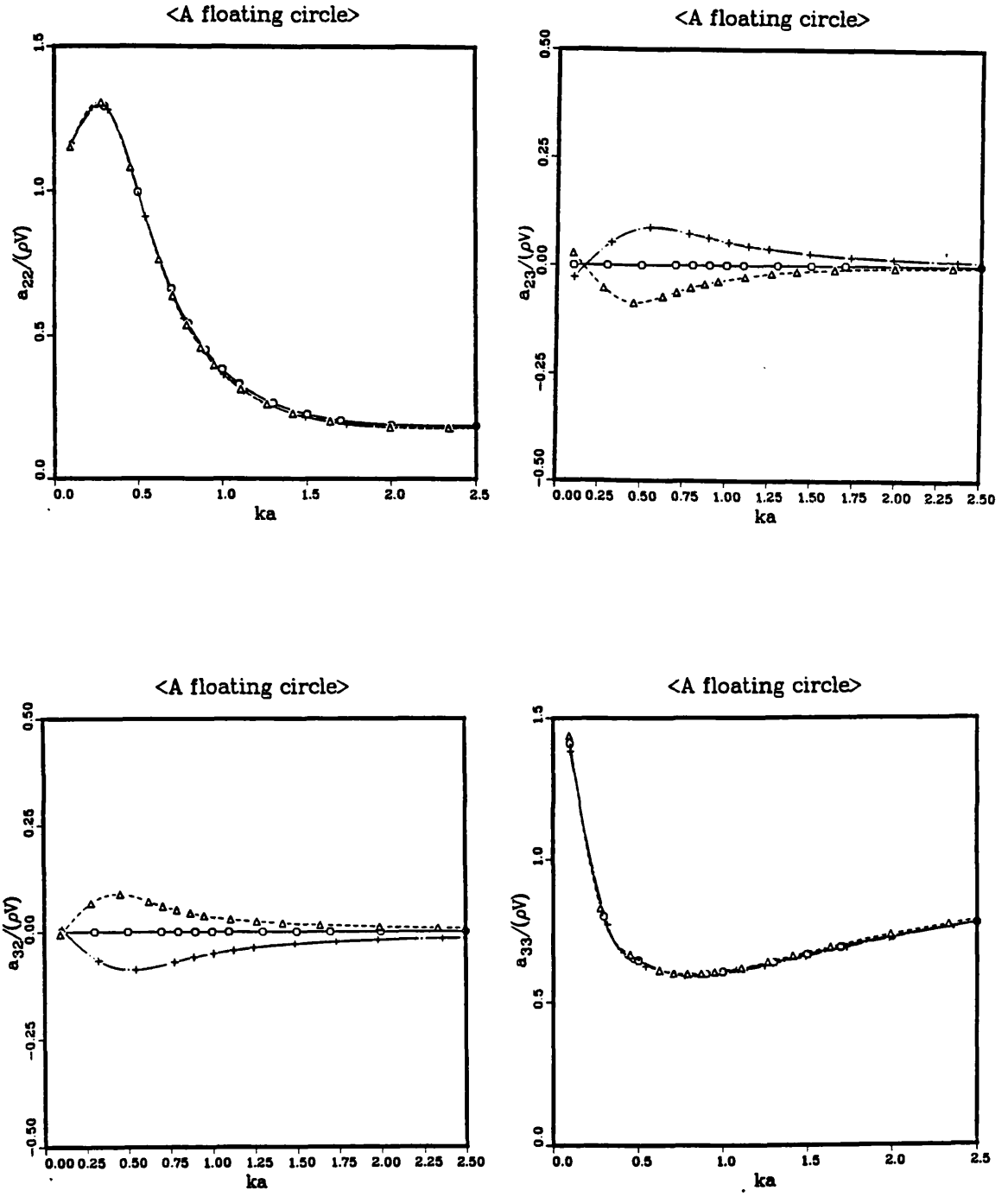

Figure 6.23 Added mass for a floating circular cylinder at forward speed

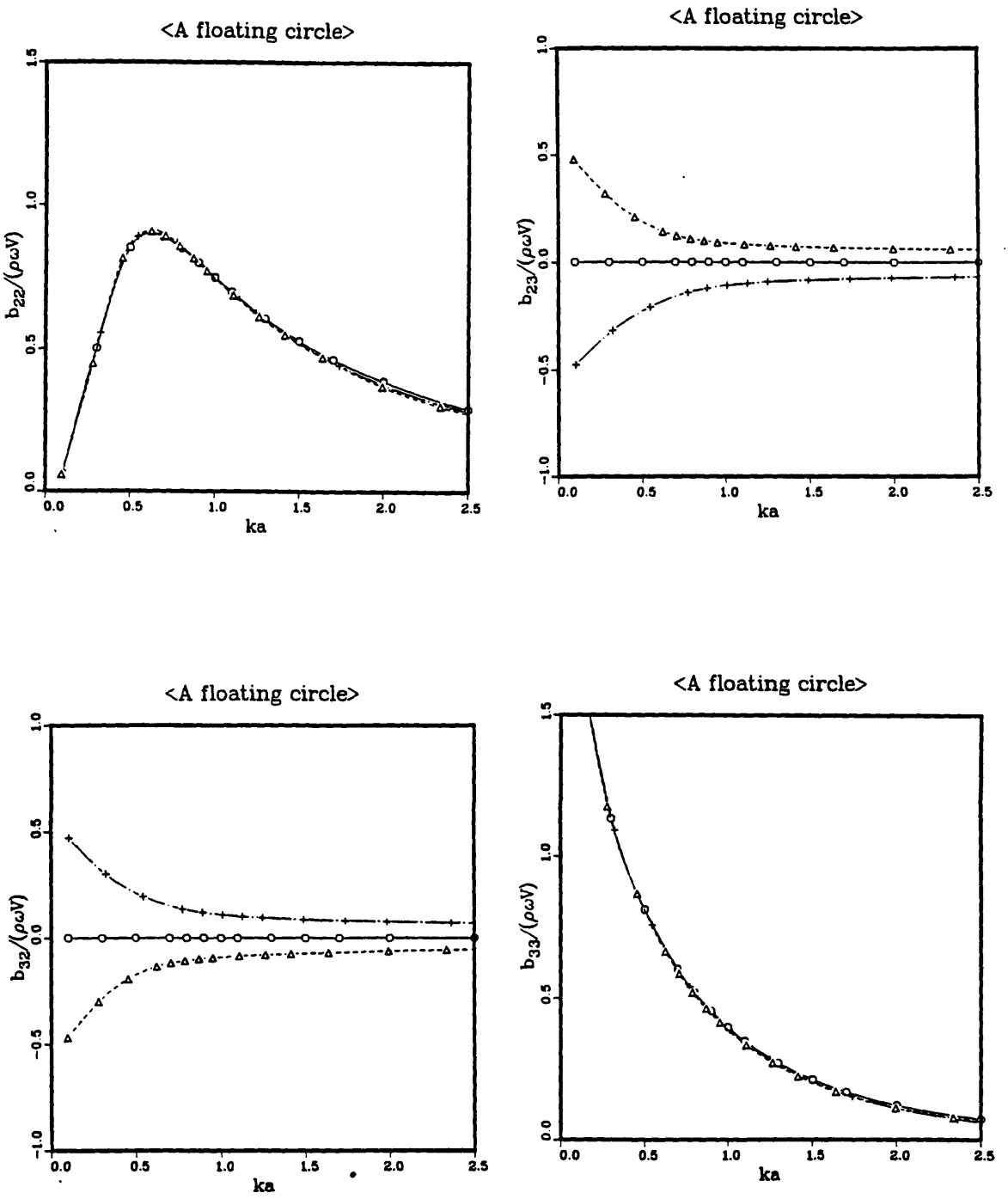

Figure 6.24 Radiation damping for a floating circular cylinder at forward speed

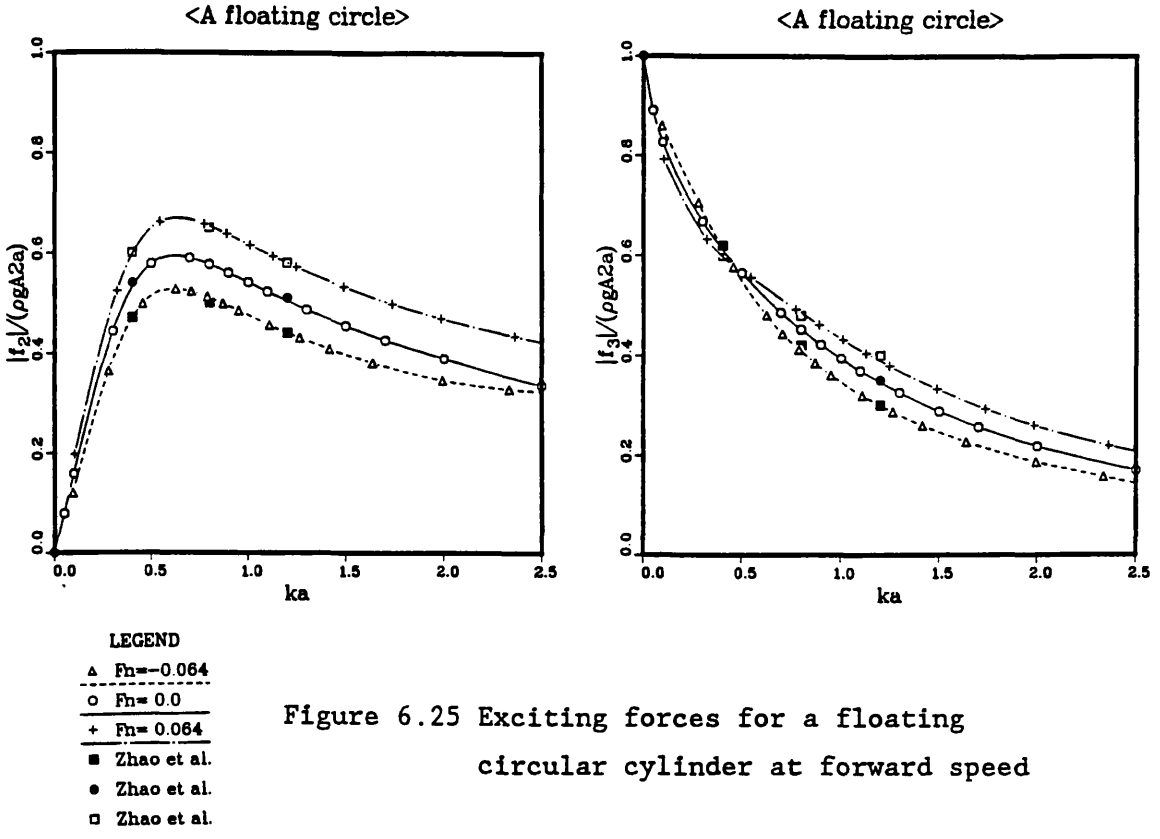

Figure 6.25 Exciting forces for a floating circular cylinder at forward speed

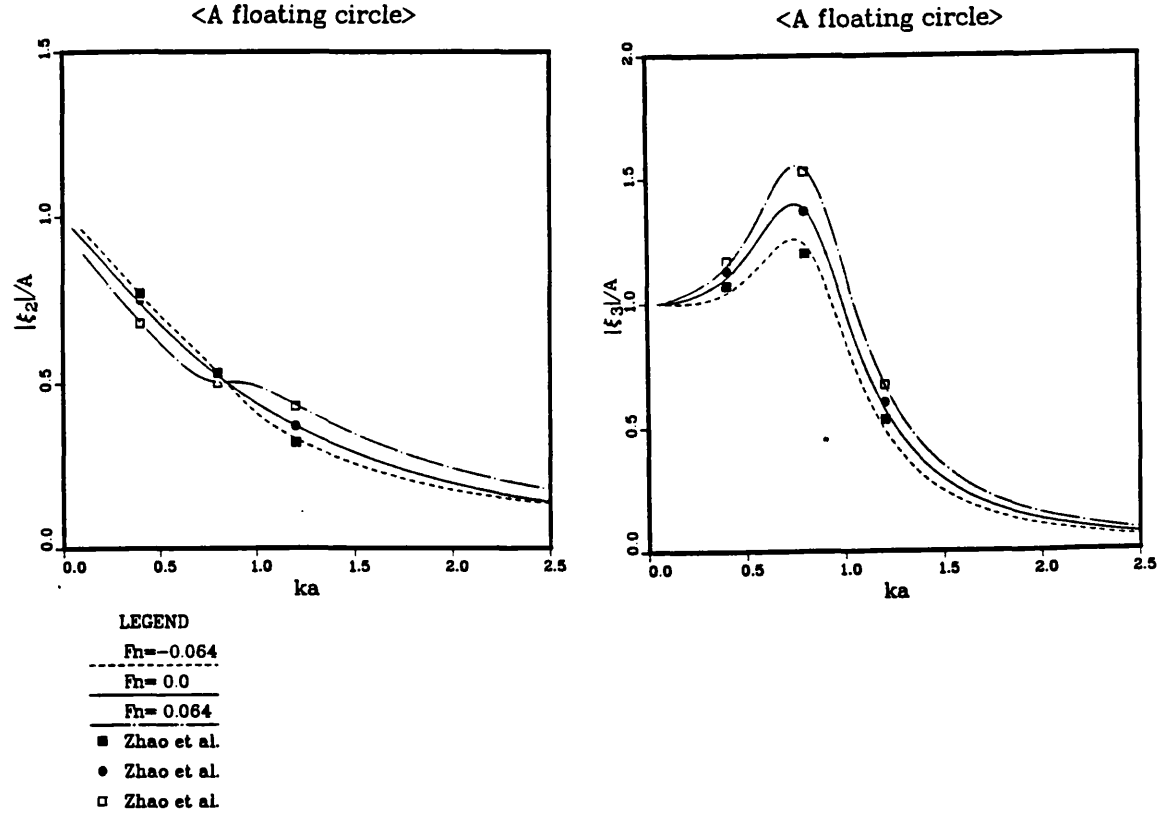

Figure 6.26 Dynamic responses of a floating circular cylinder at forward speed

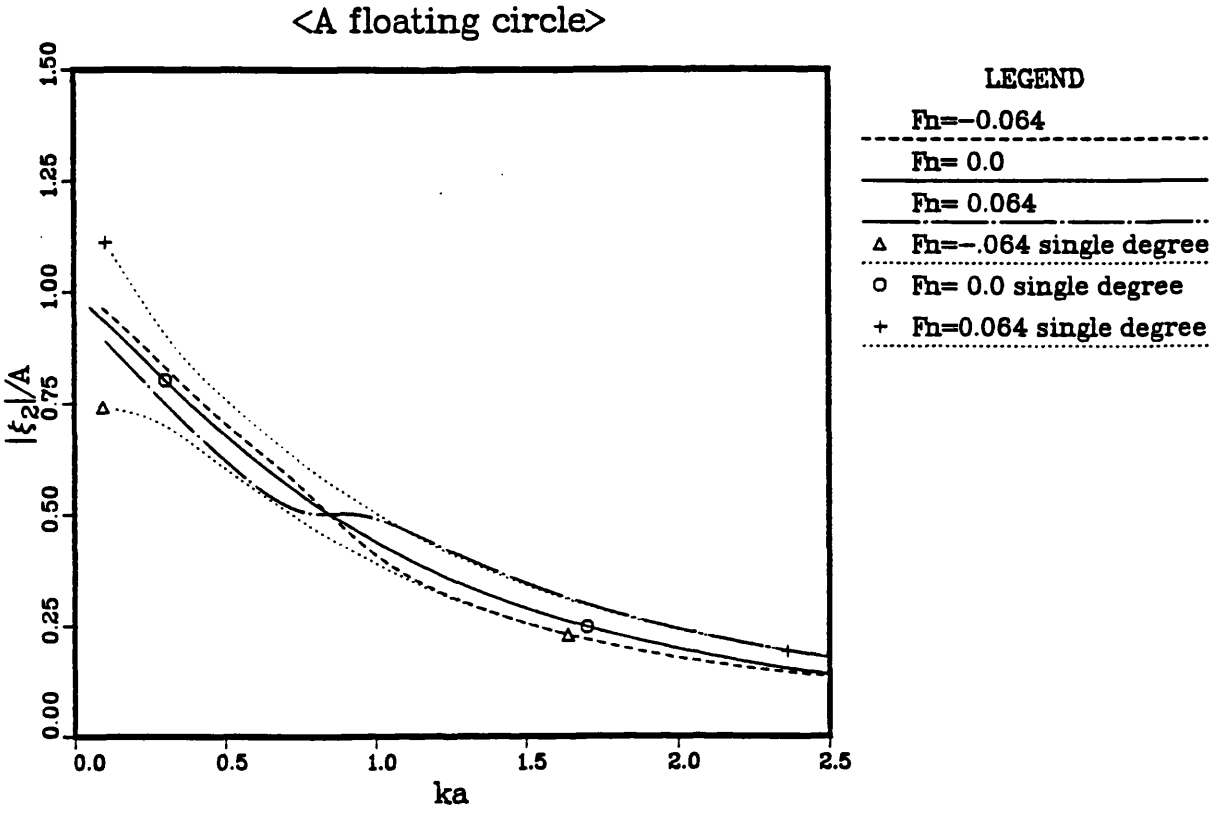

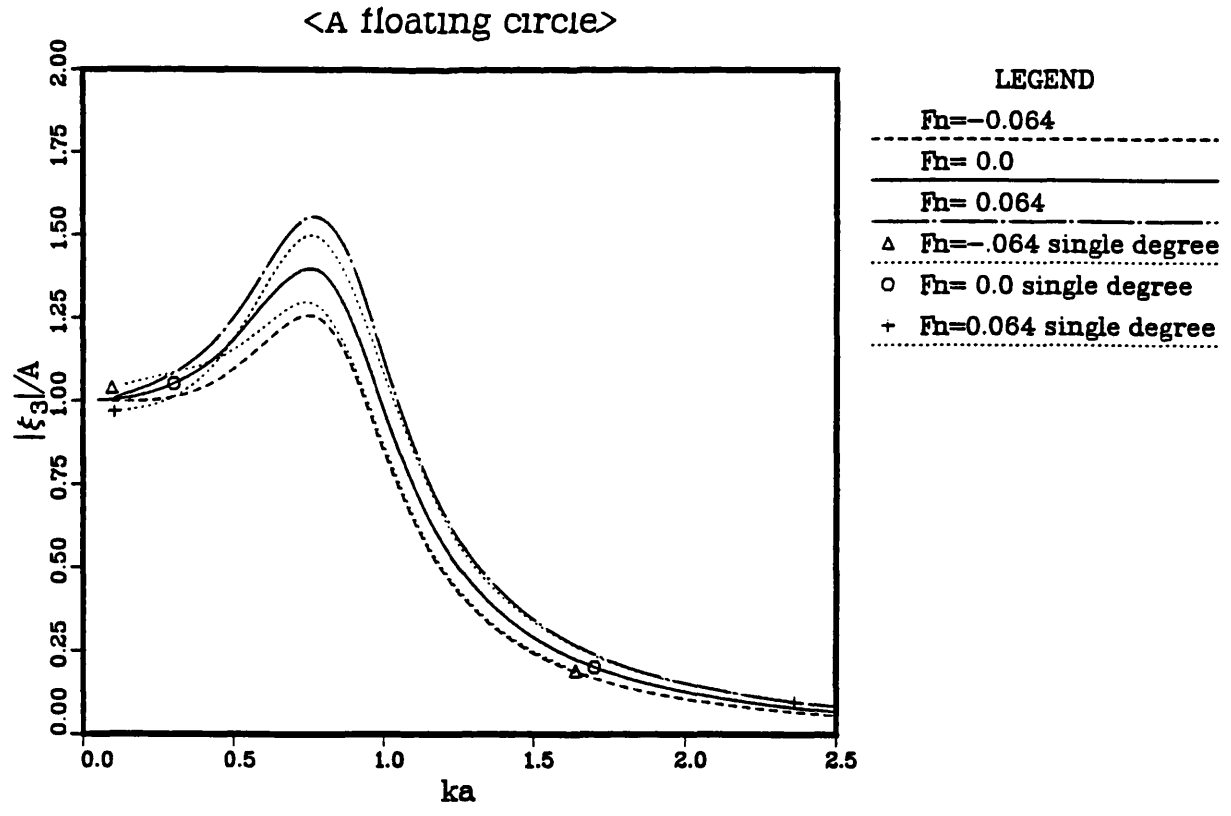

Figure 6.27 Coupling effects of responses of a floating circular cylinder at forward speed

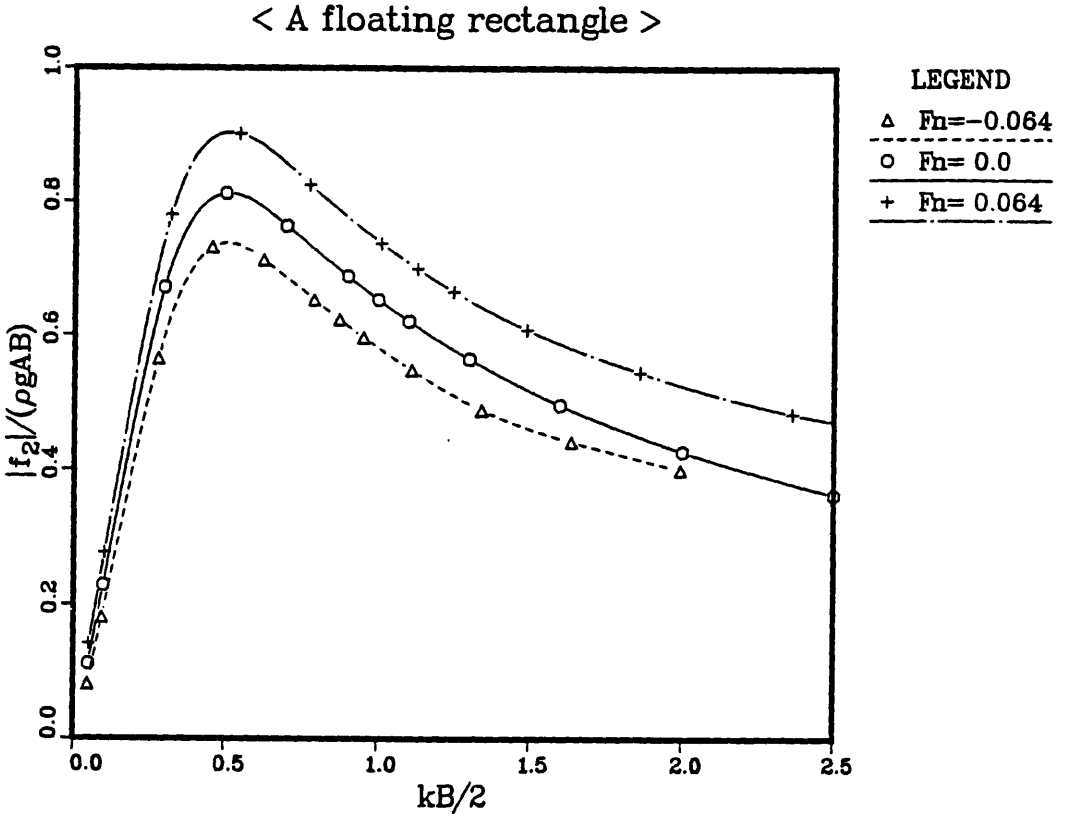

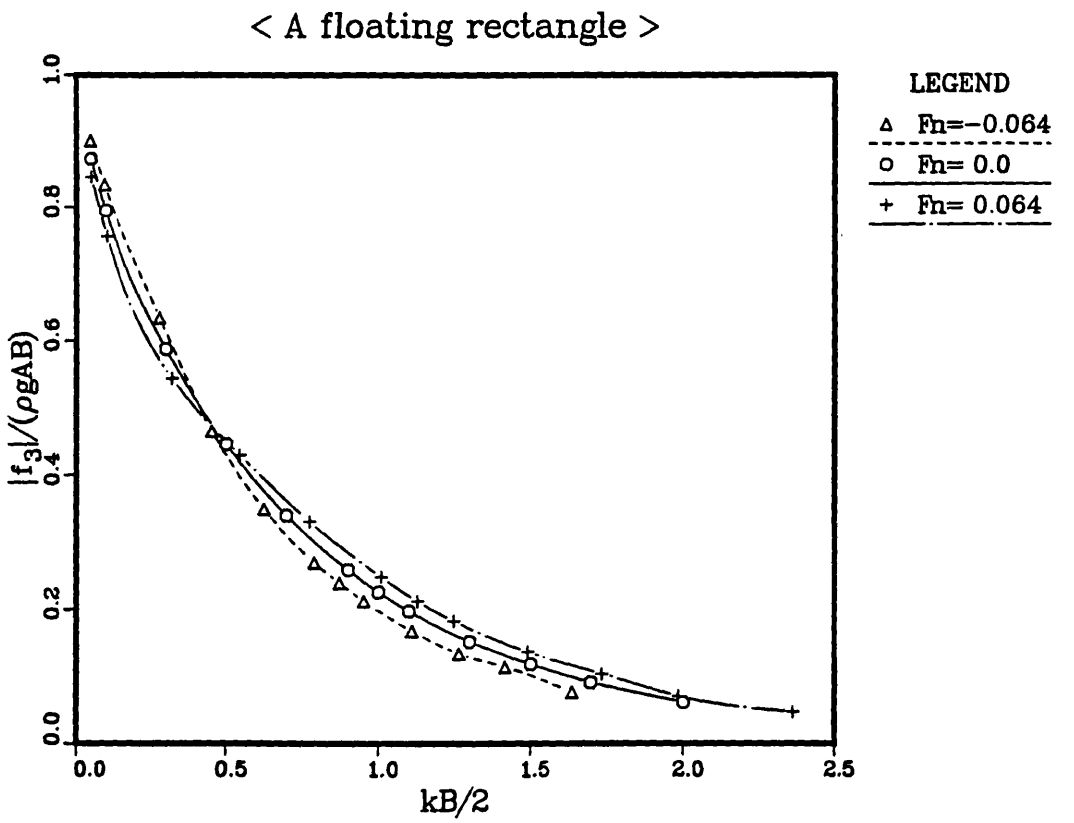

Figure 6.28 Exciting forces for a floating rectangular cylinder at forward speed

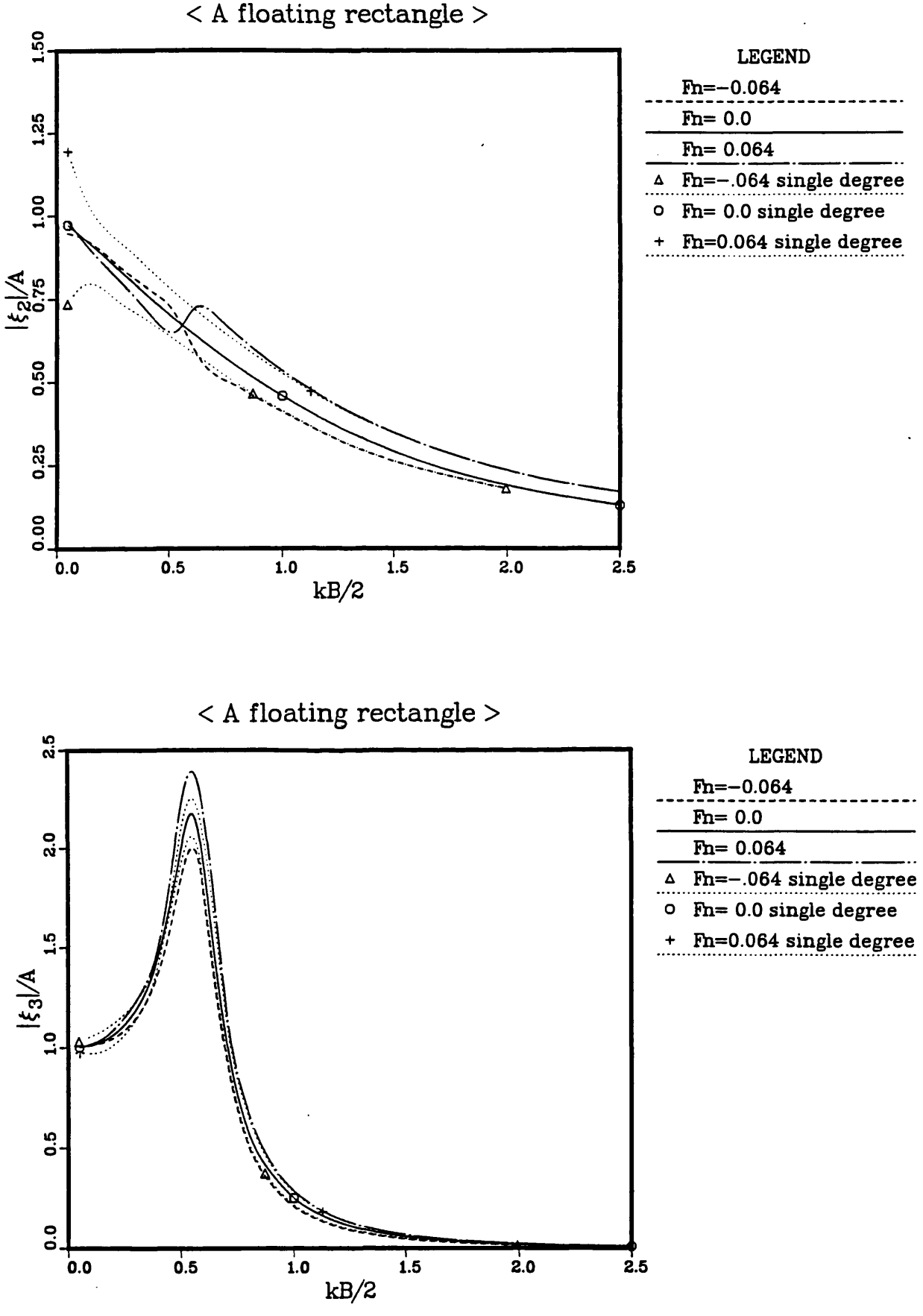

Figure 6.29 Dynamic responses of a floating rectangular cylinder at forward speed

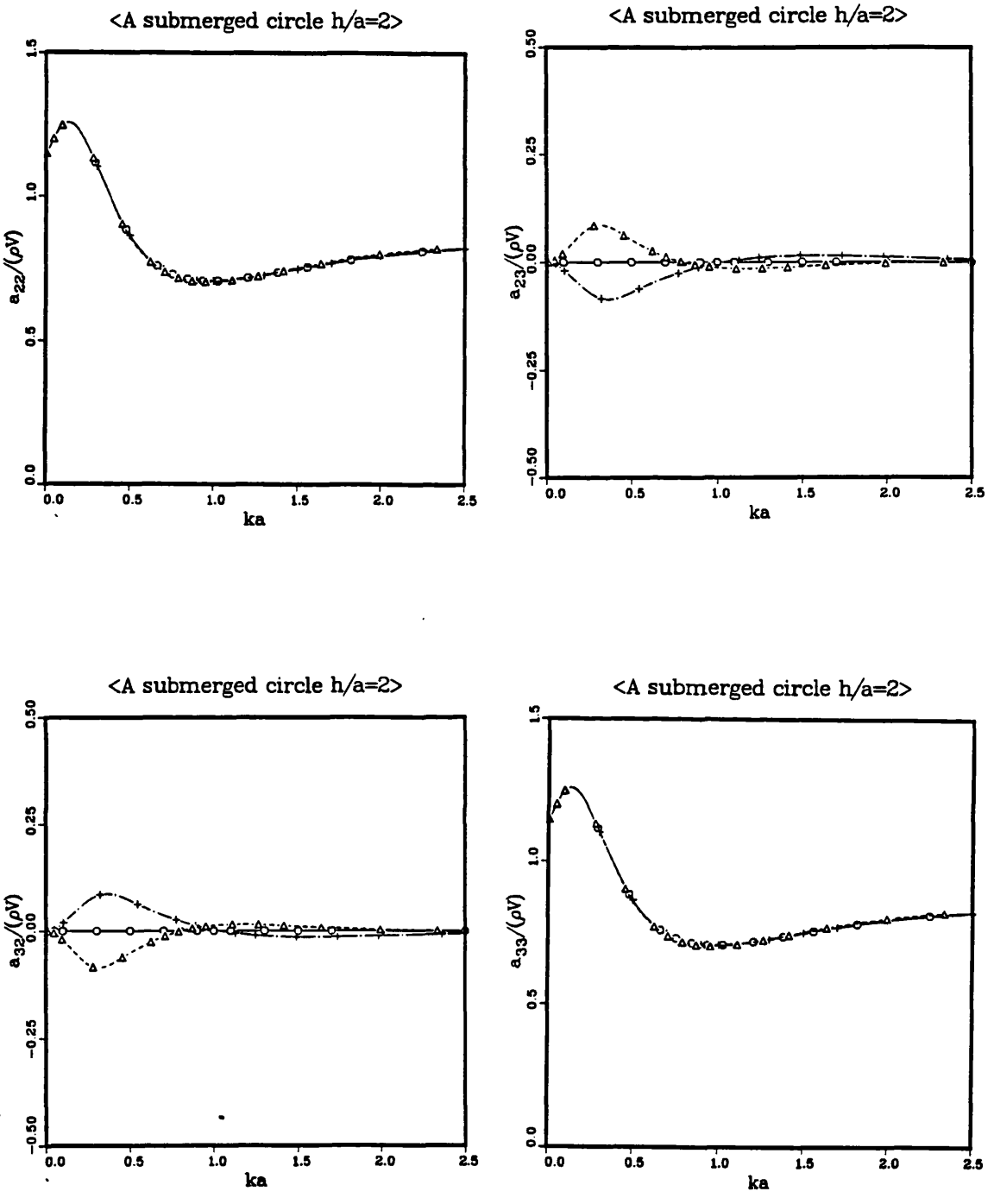

Figure 6.30 Added mass for a submerged circular cylinder at forward speed: h/a=2.0

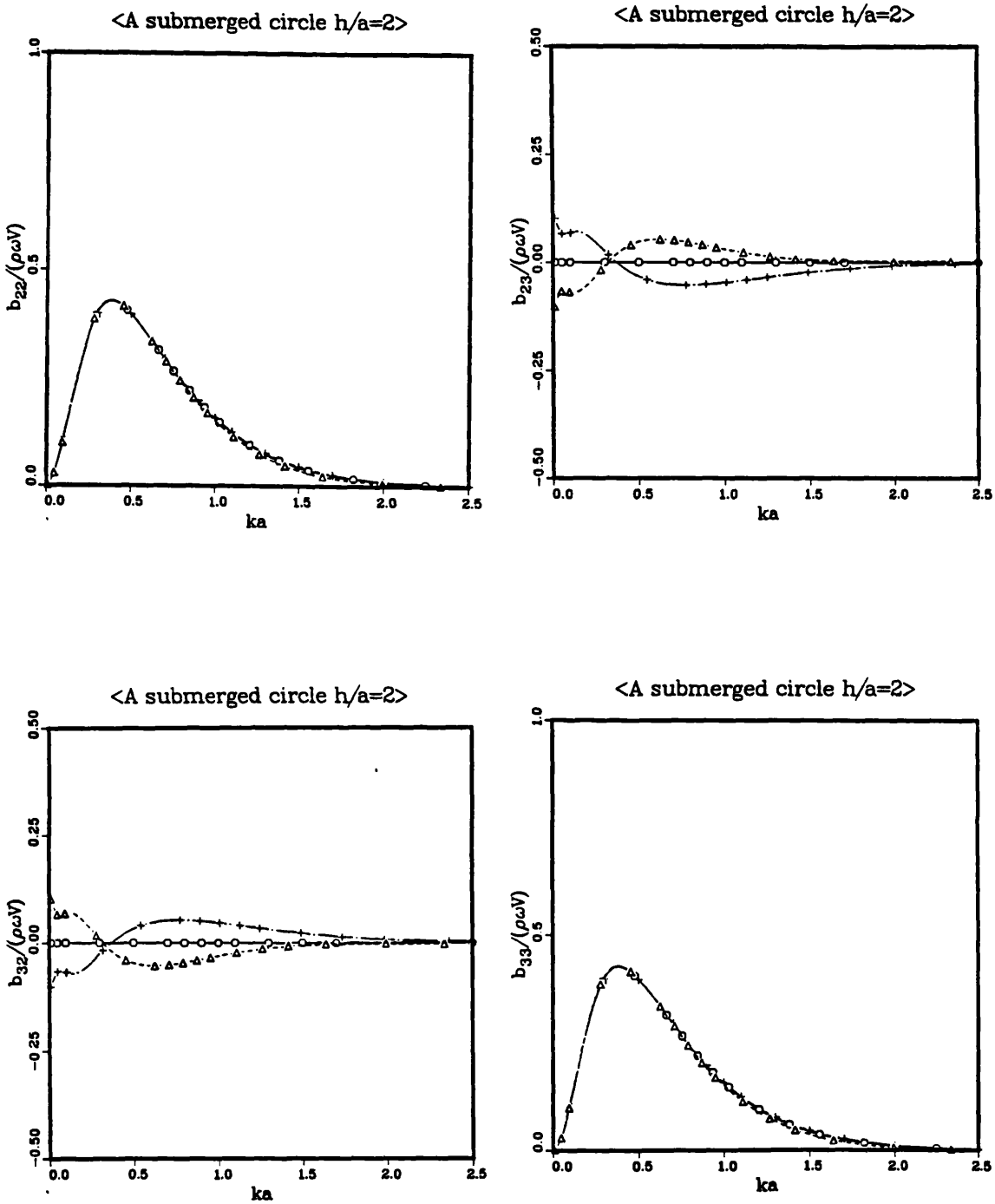

Figure 6.31 Radiation damping for a submerged circular cylinder at forward speed: h/a=2.0

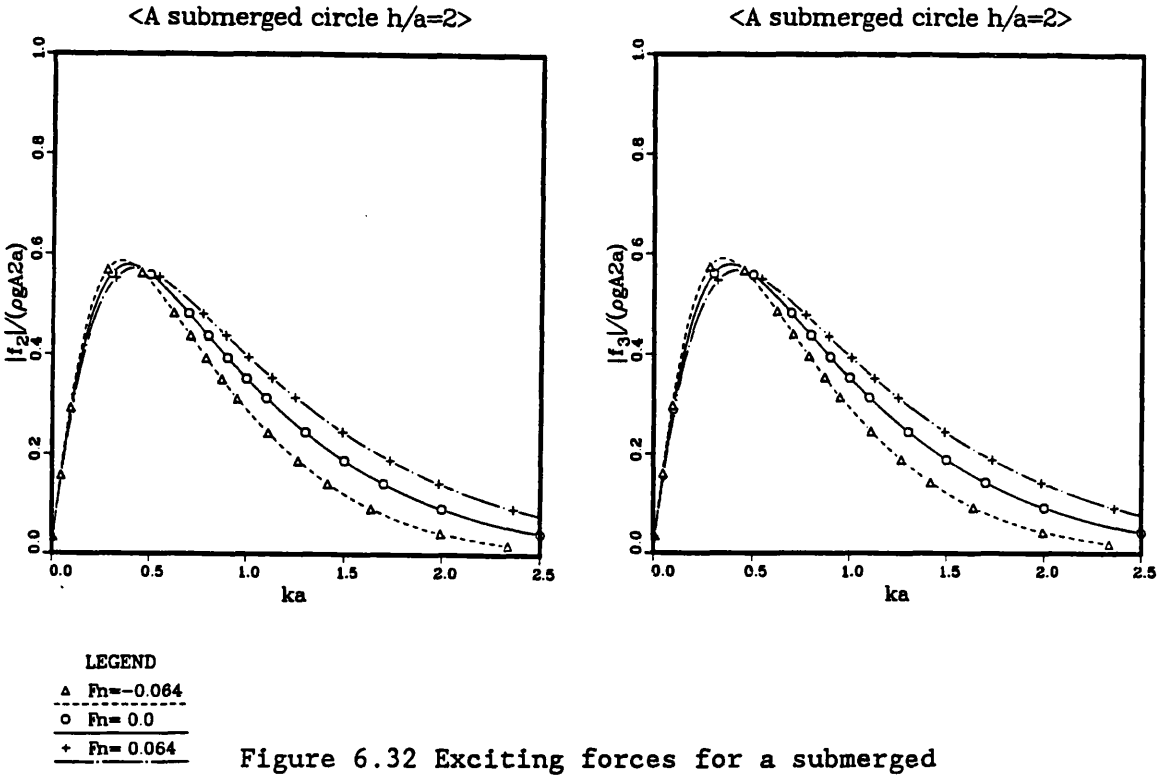

Figure 6.32 Exciting forces for a submerged circular cylinder at forward speed: h/a=2.0

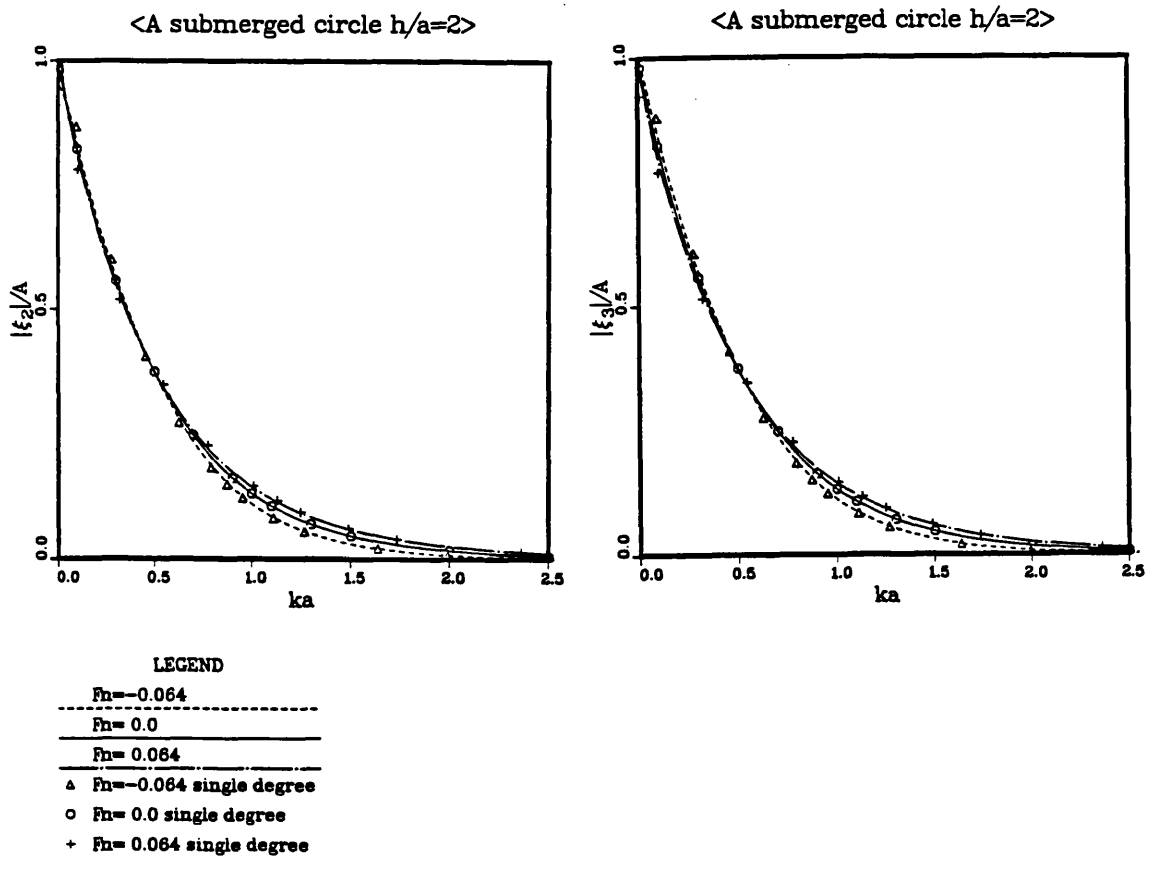

Figure 6.33 Dynamic responses of a submerged circular cylinder at forward speed: h/a=2.0

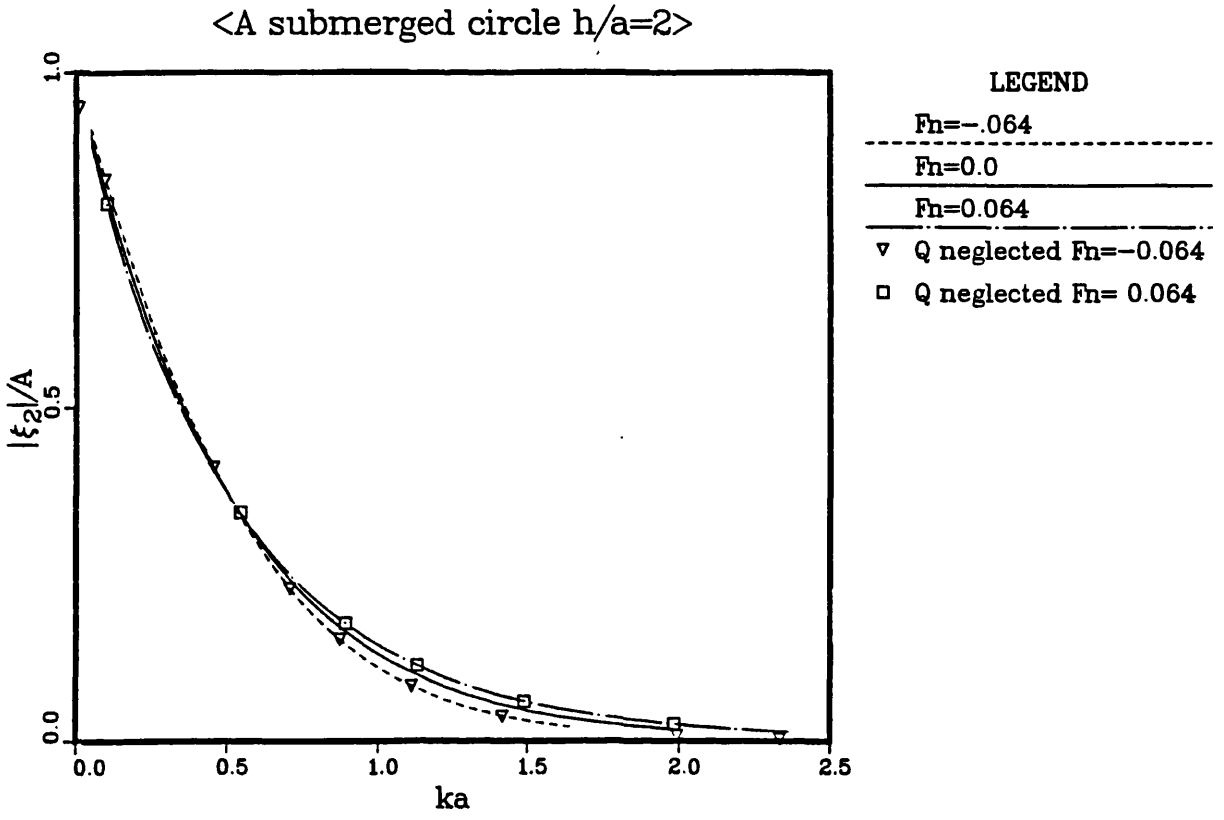

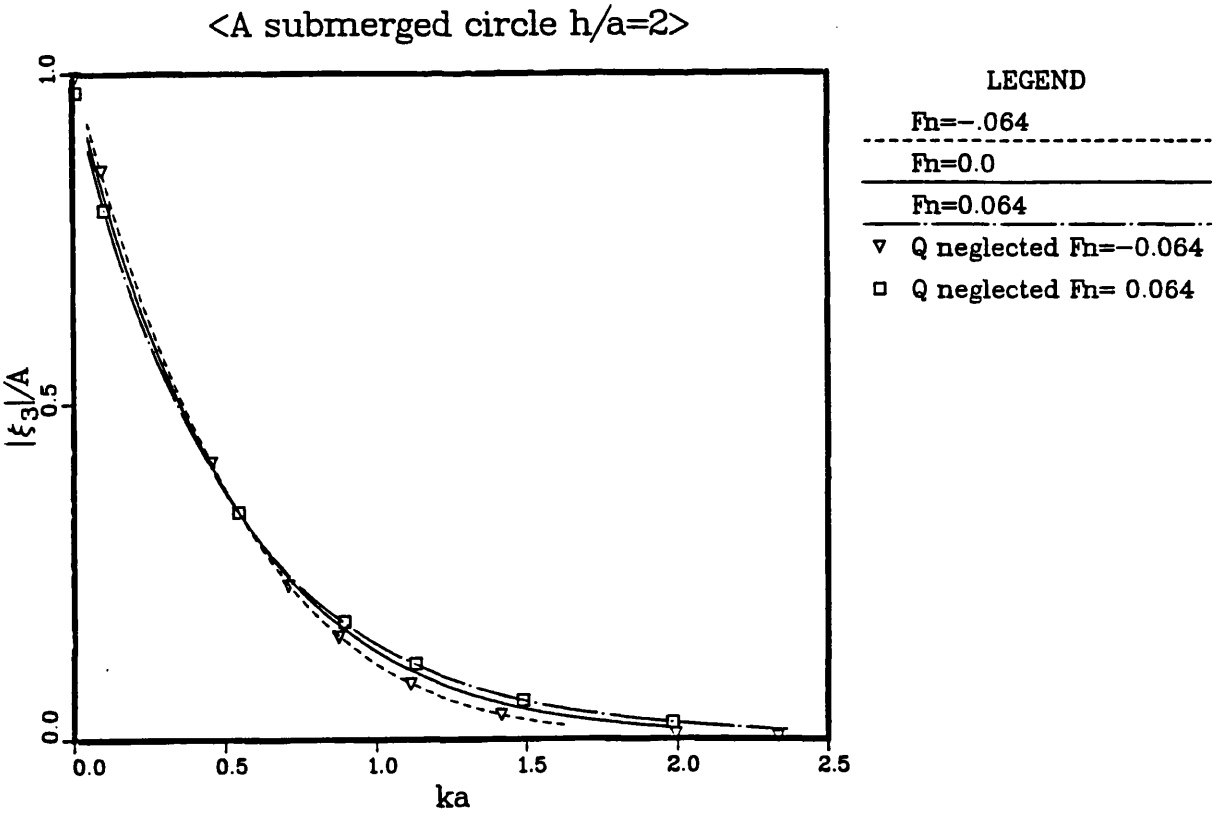

Figure 6.34 Influence of Q term on the responses of a submerged circular cylinder at forward speed: h/a=2

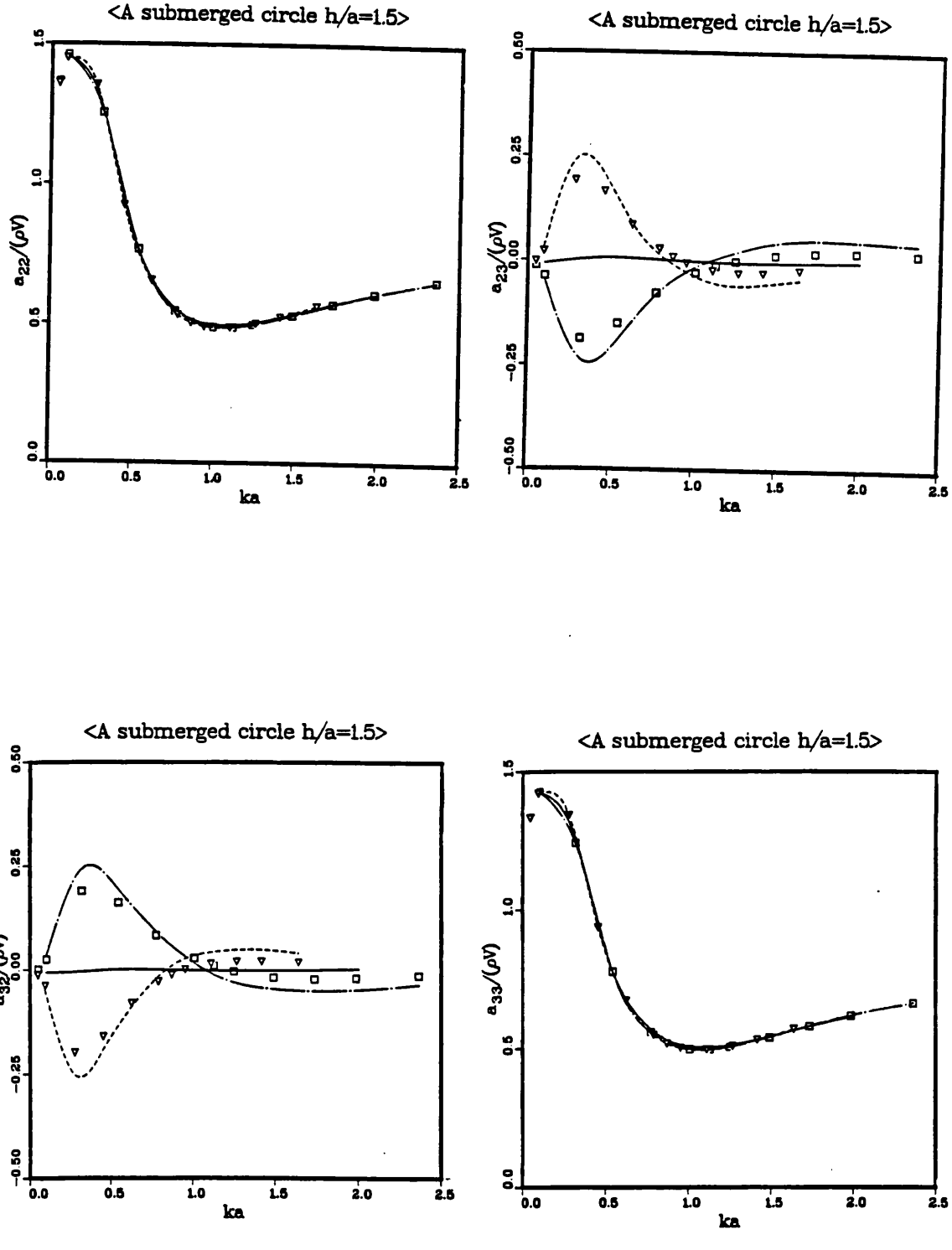

Figure 6.35 Added mass for a submerged circular cylinder at forward speed: h/a=1.5

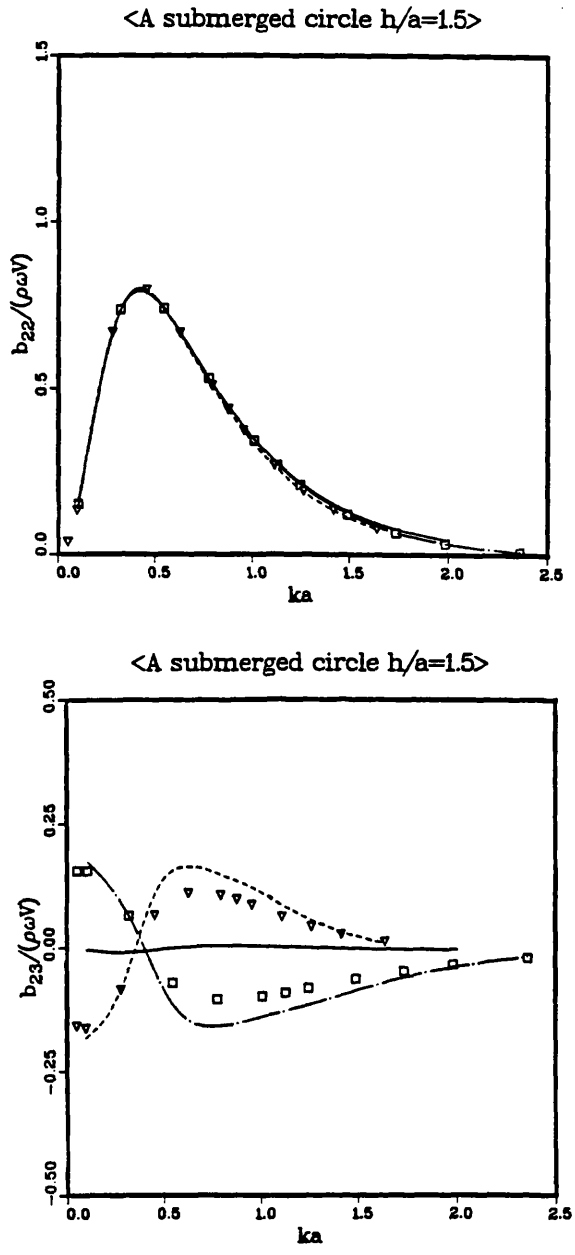

Figure 6.36 Radiation damping for a submerged circular cylinder at forward speed: h/a=1.5

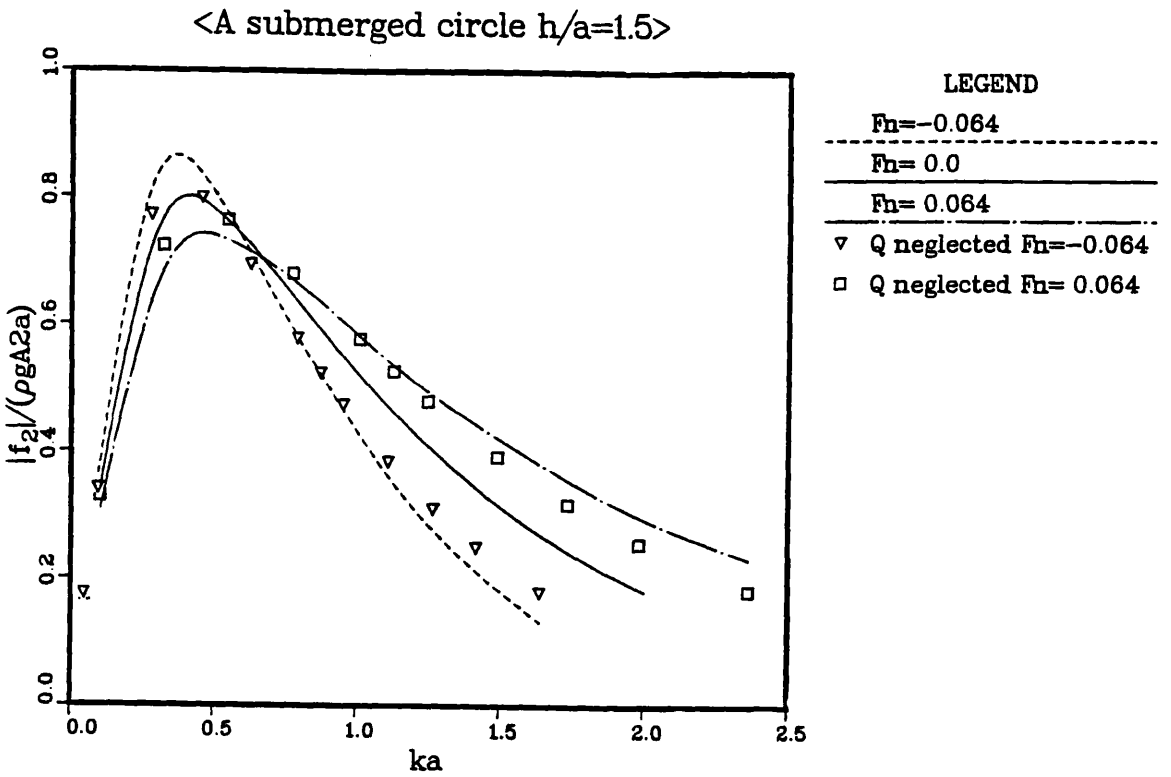

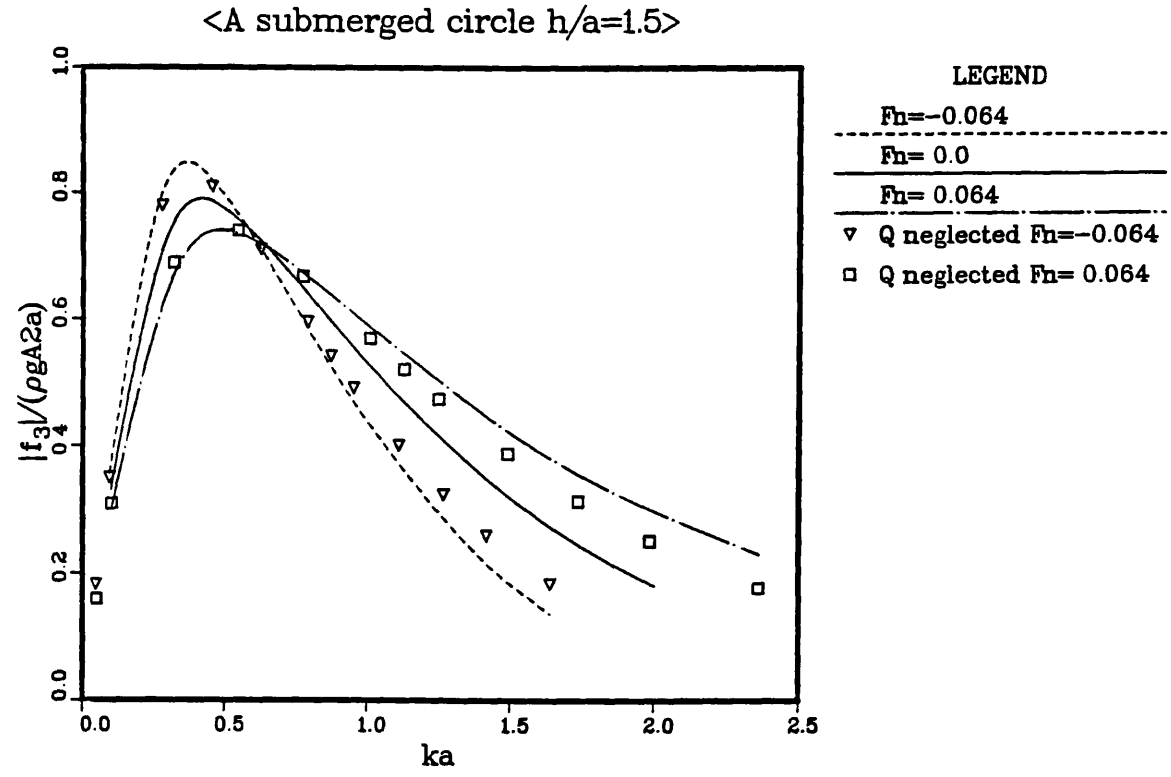

Figure 6.37 Exciting forces for a submerged circular cylinder at forward speed: h/a=1.5

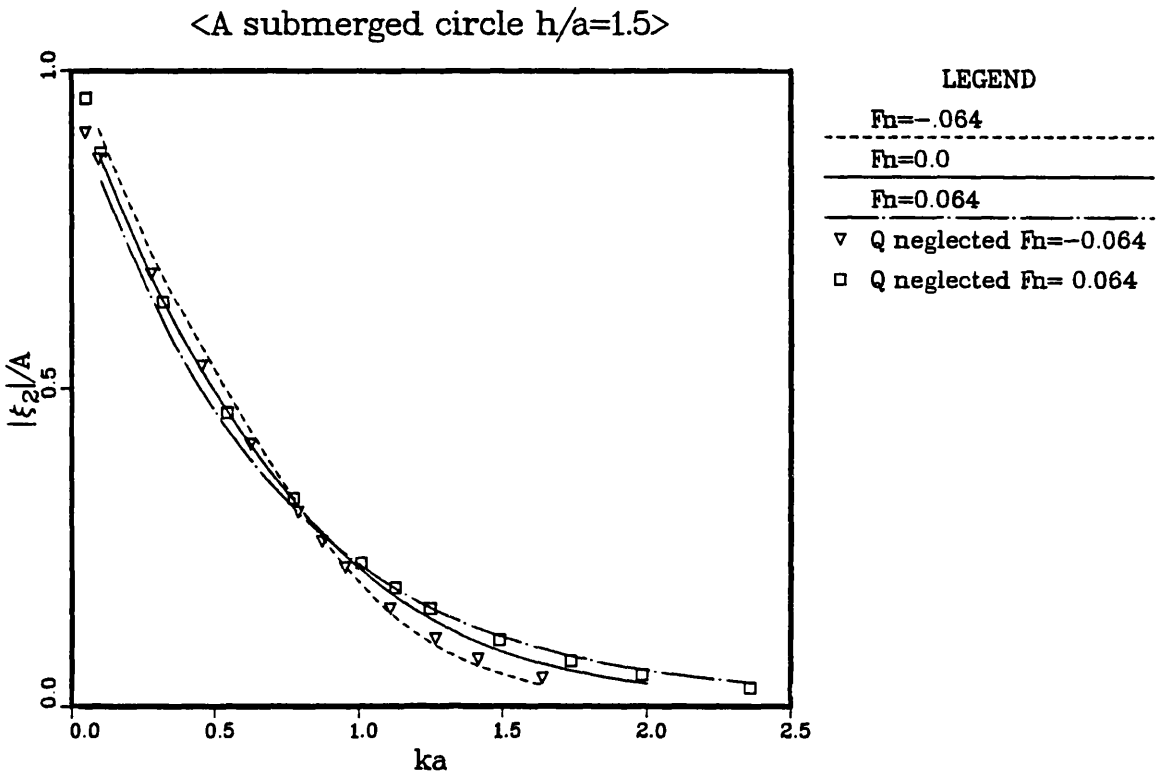

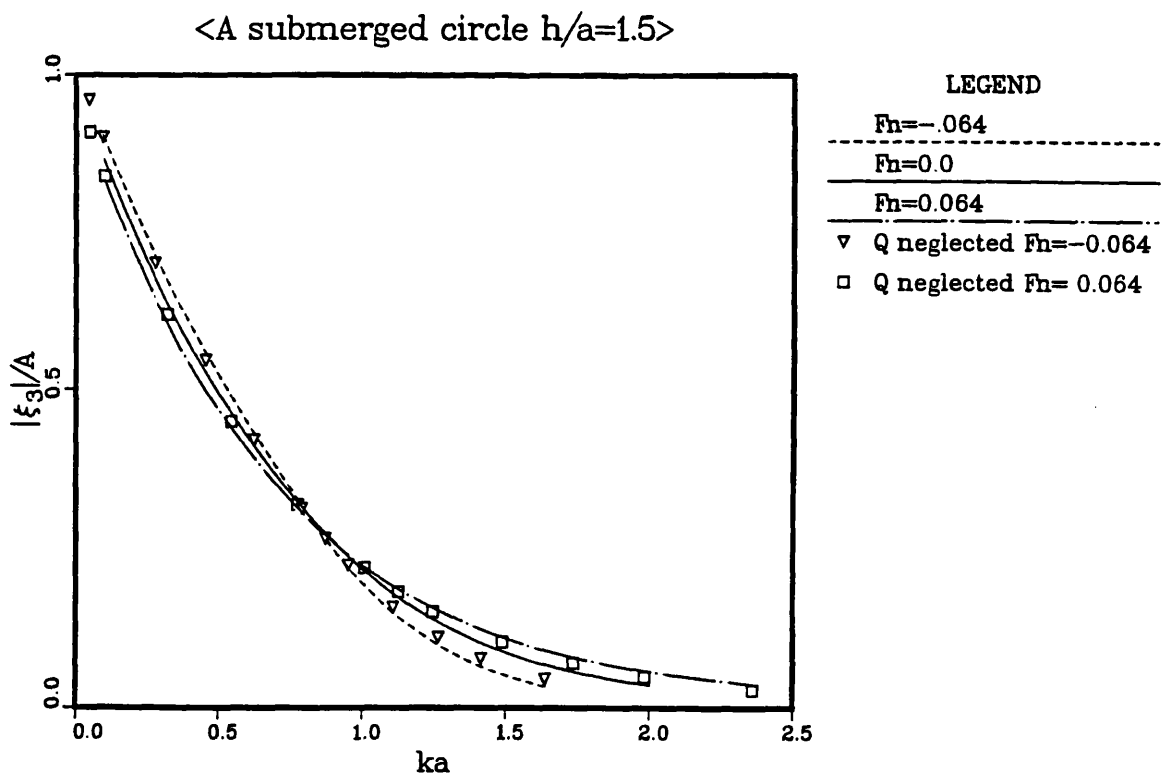

Figure 6.38 Dynamic responses of a submerged circular cylinder at forward speed: h/a=1.5

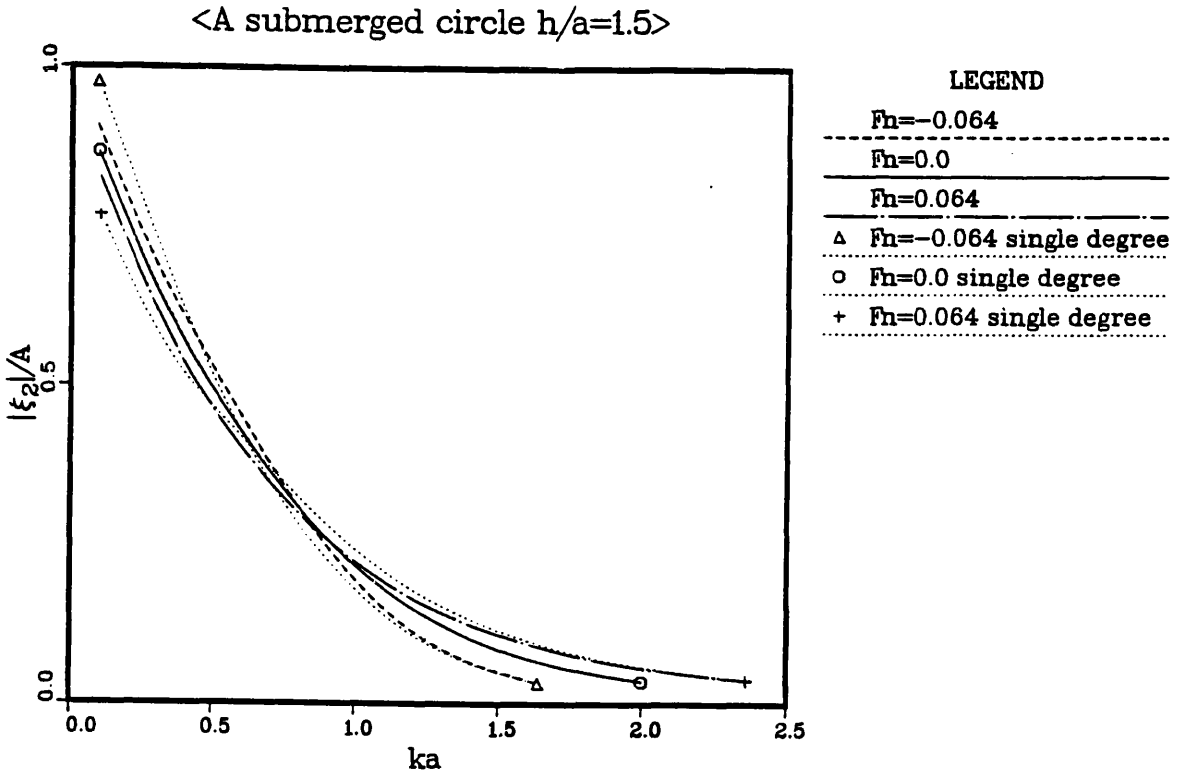

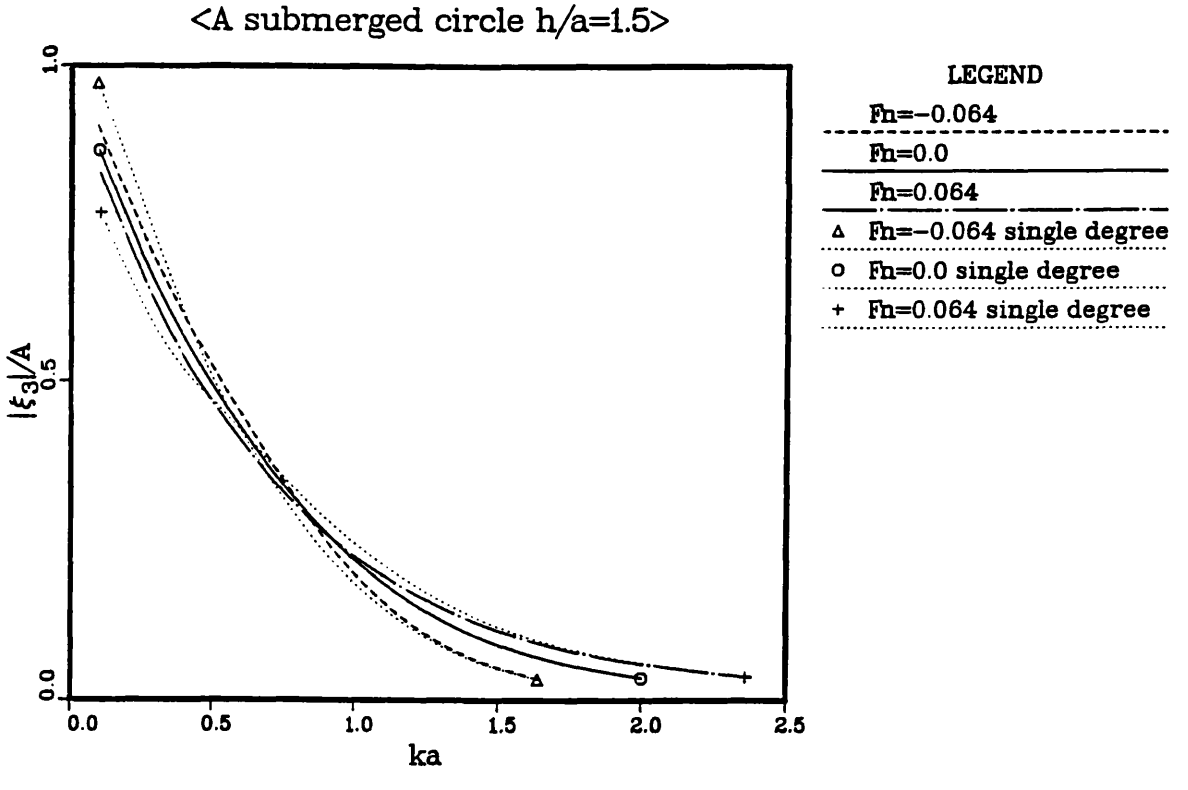

Figure 6.39 Coupling effects of responses of a submerged circular cylinder at forward speed: h/a=1.5

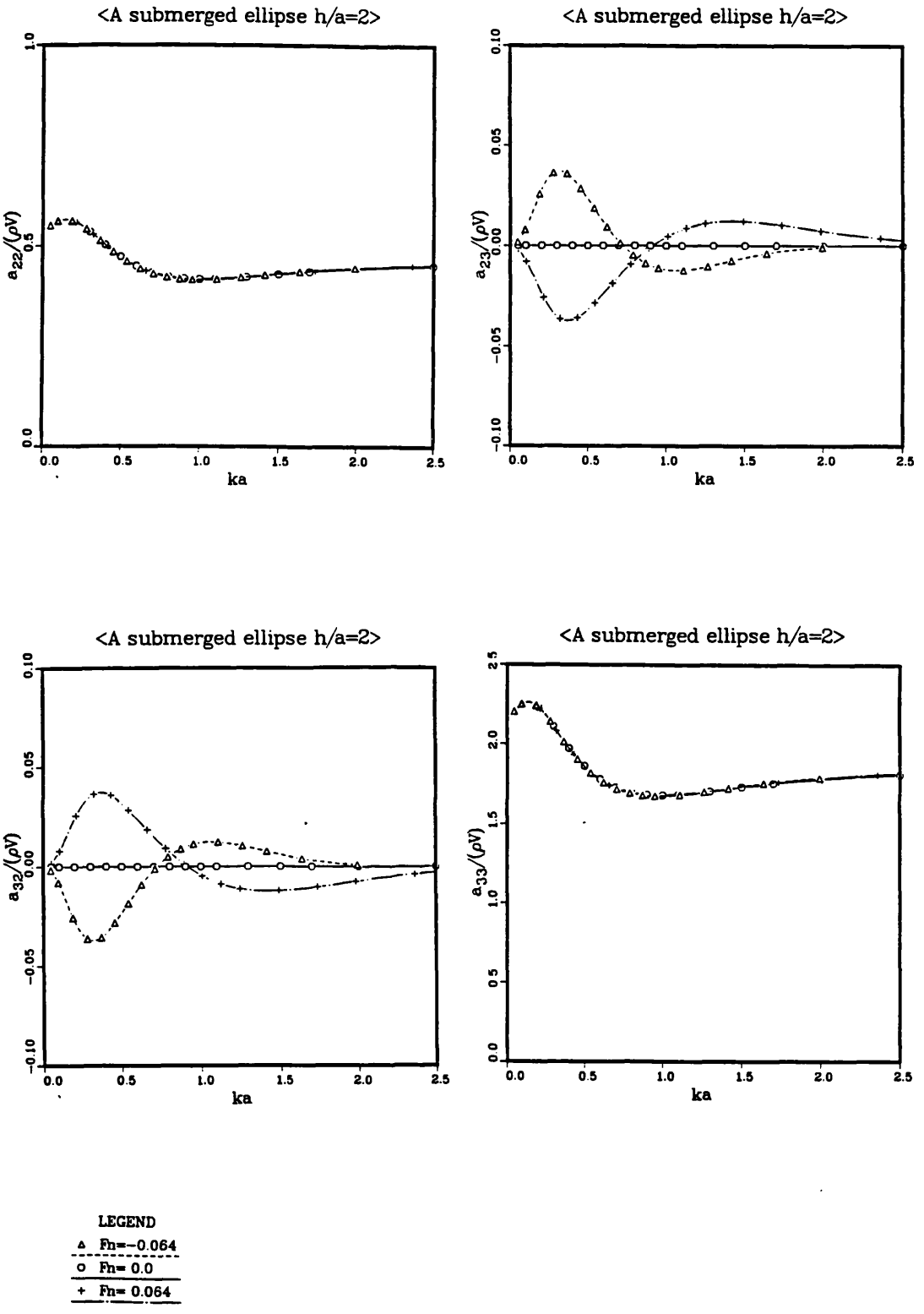

Figure 6.40 Added mass for a submerged elliptic cylinder at forward speed: b/a=0.5, h/a=2.0

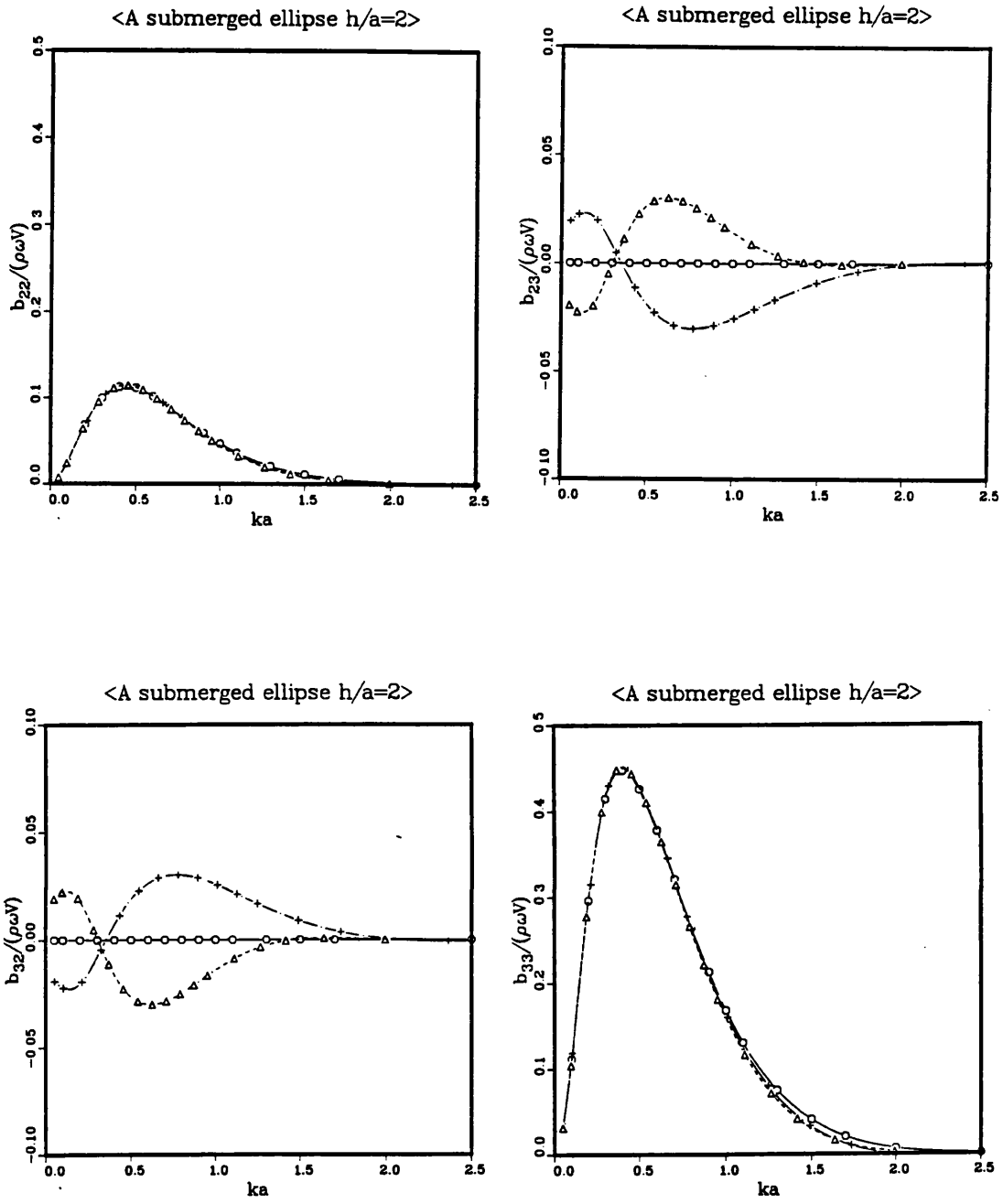

Figure 6.41 Radiation damping for a submerged elliptic cylinder at forward speed: b/a=0.5, h/a=2.0

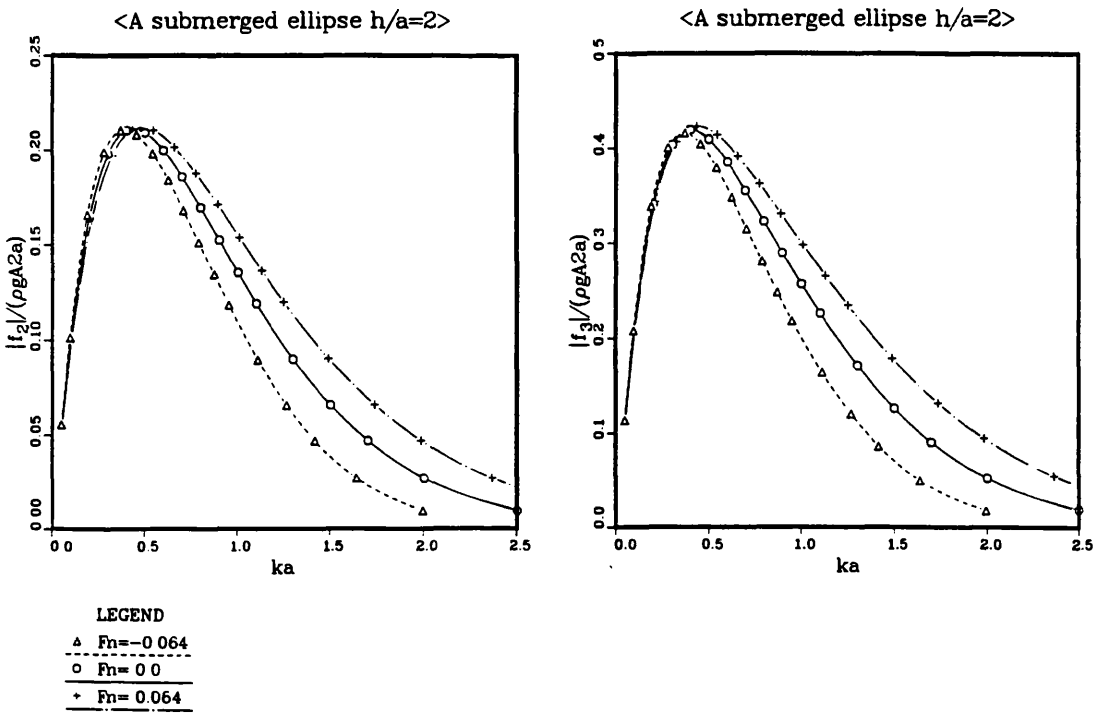

Figure 6.42 Exciting forces for a submerged elliptic cylinder at forward speed: b/a=0.5, h/a=2.0

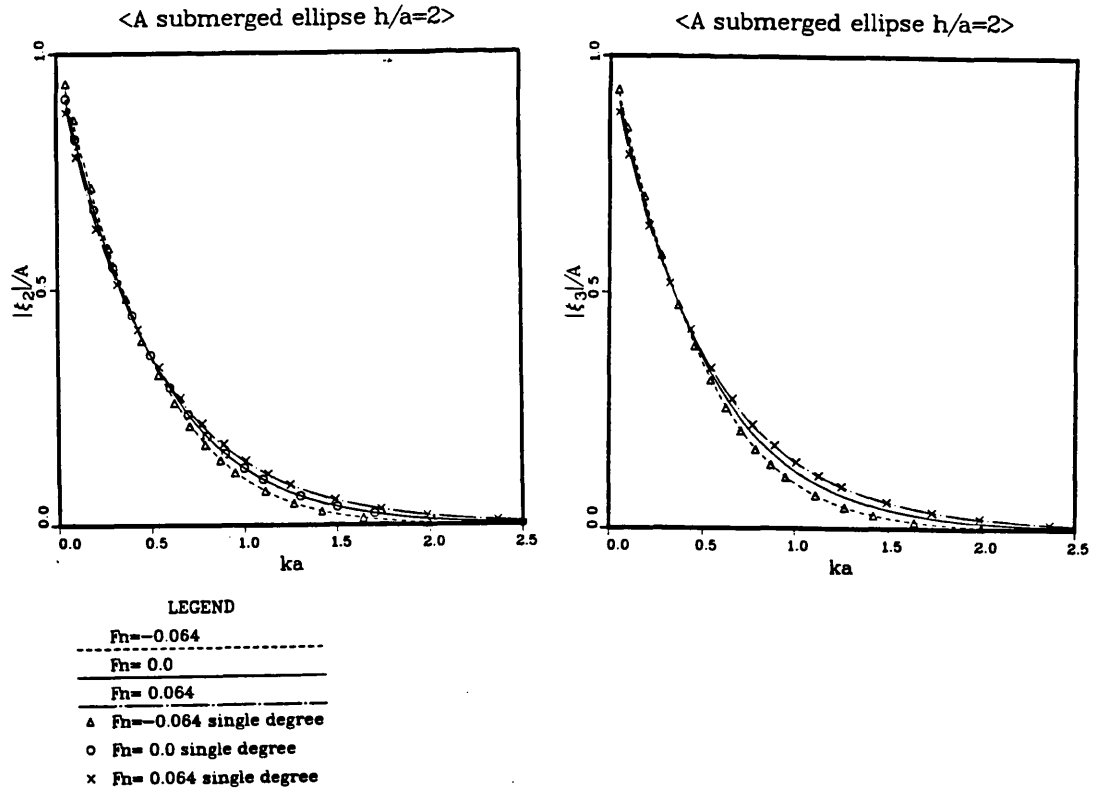

Figure 6.43 Dynamic responses of a submerged elliptic cylinder at forward speed: b/a=0.5, h/a=2.0

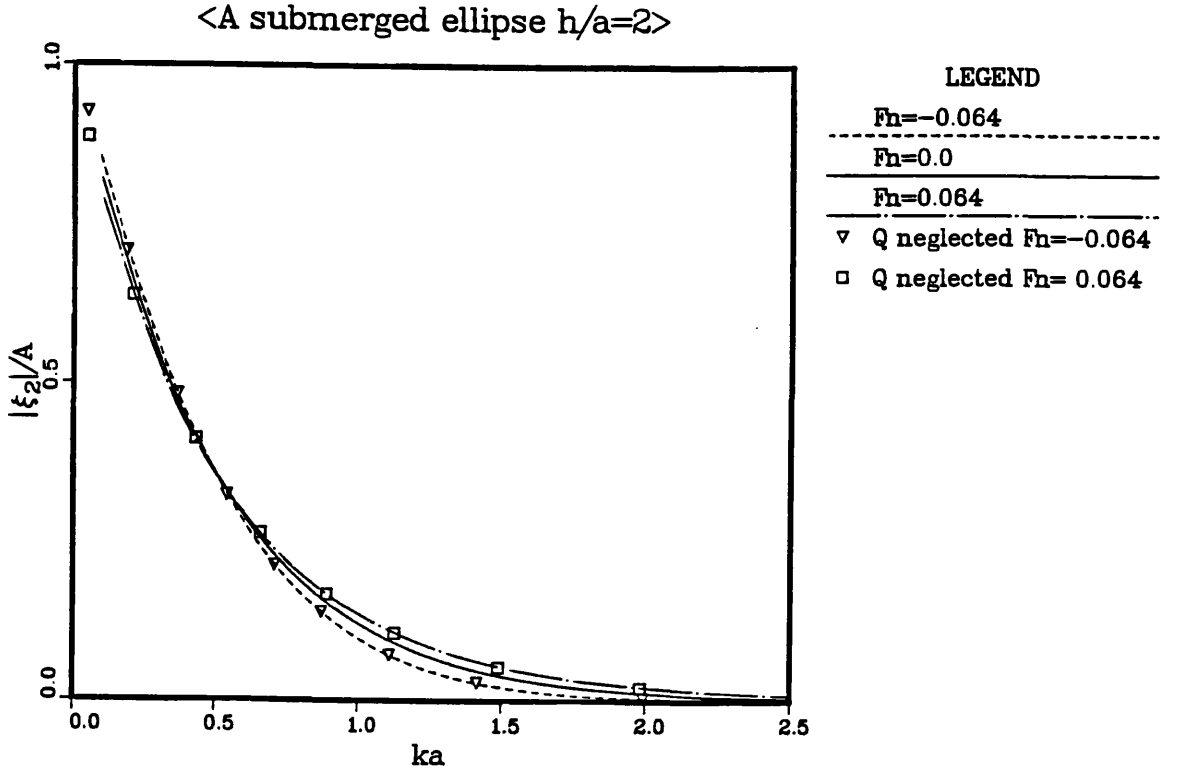

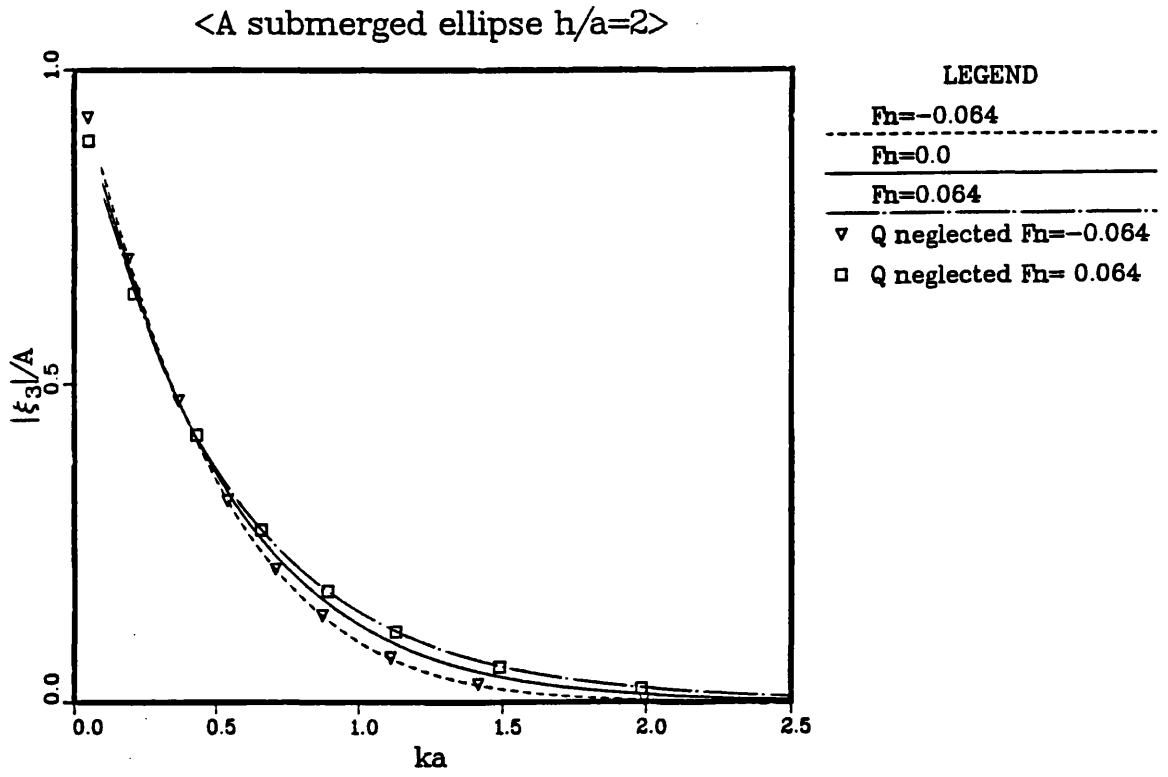

Figure 6.44 Influence of Q term on the responses of a submerged elliptic cylinder at forward speed: h/a=2

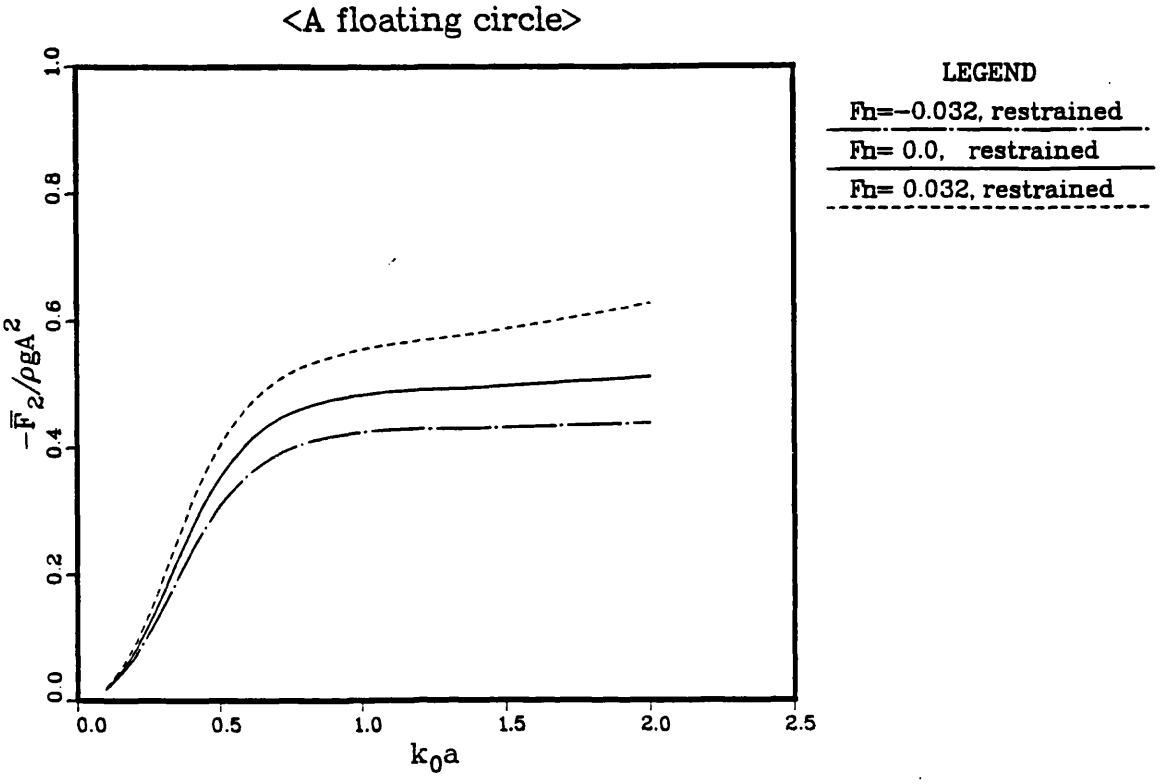

Figure 6.45 Horizontal mean drift force on a floating ciruclar cylinder: restrained from responses

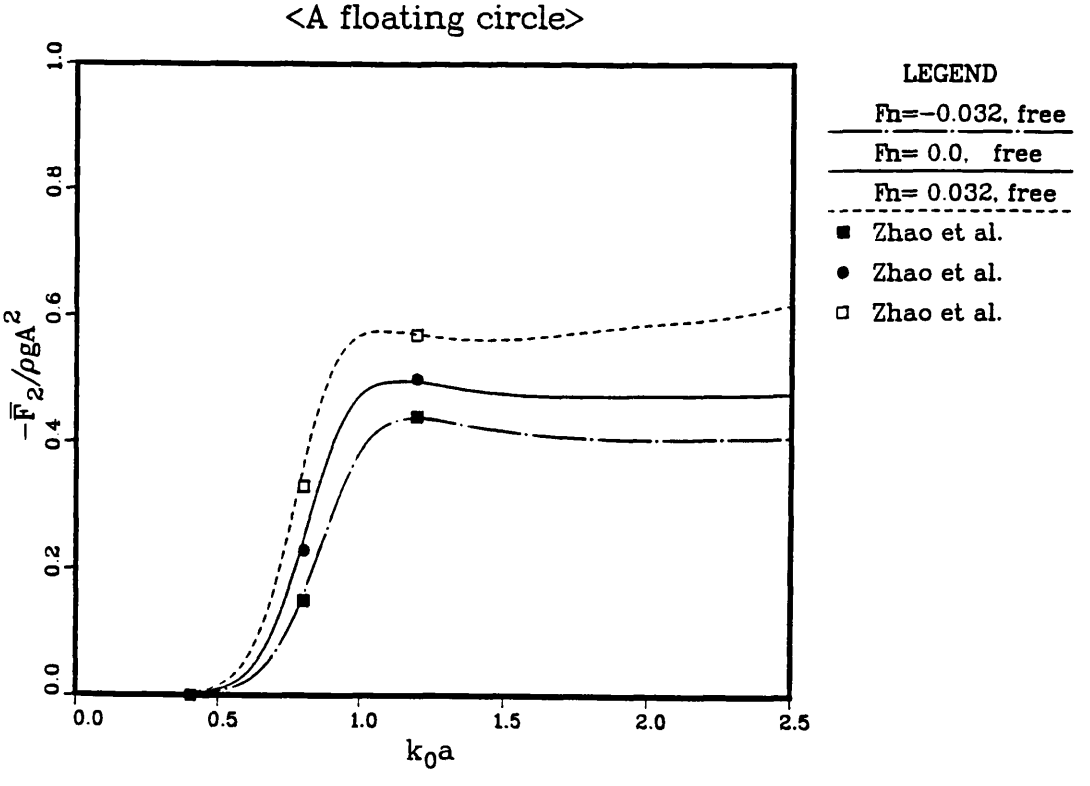

Figure 6.46 Horizontal mean drift force on a floating circular cylinder: free to respond in sway and heave

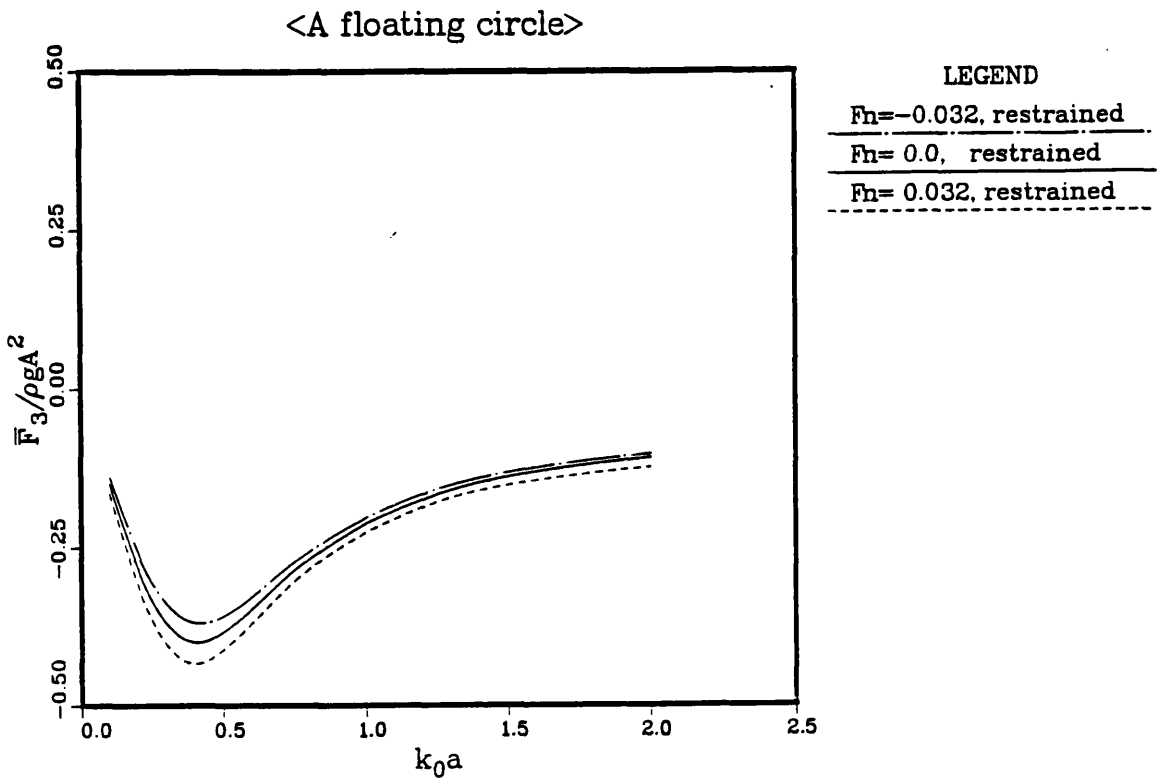

Figure 6.47 Vertical mean drift force on a floating circular cylinder: restrained from responses

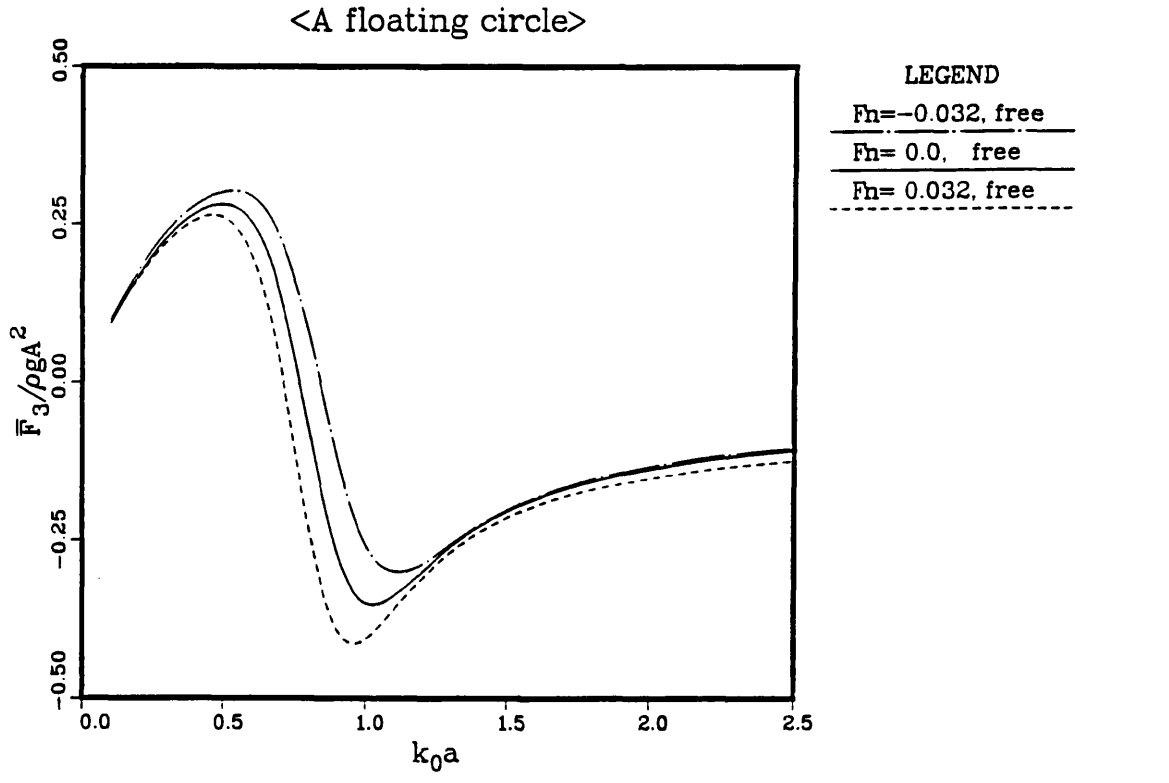

Figure 6.48 Vertical mean drift force on a floating circular cylinder: free to respond in sway and heave

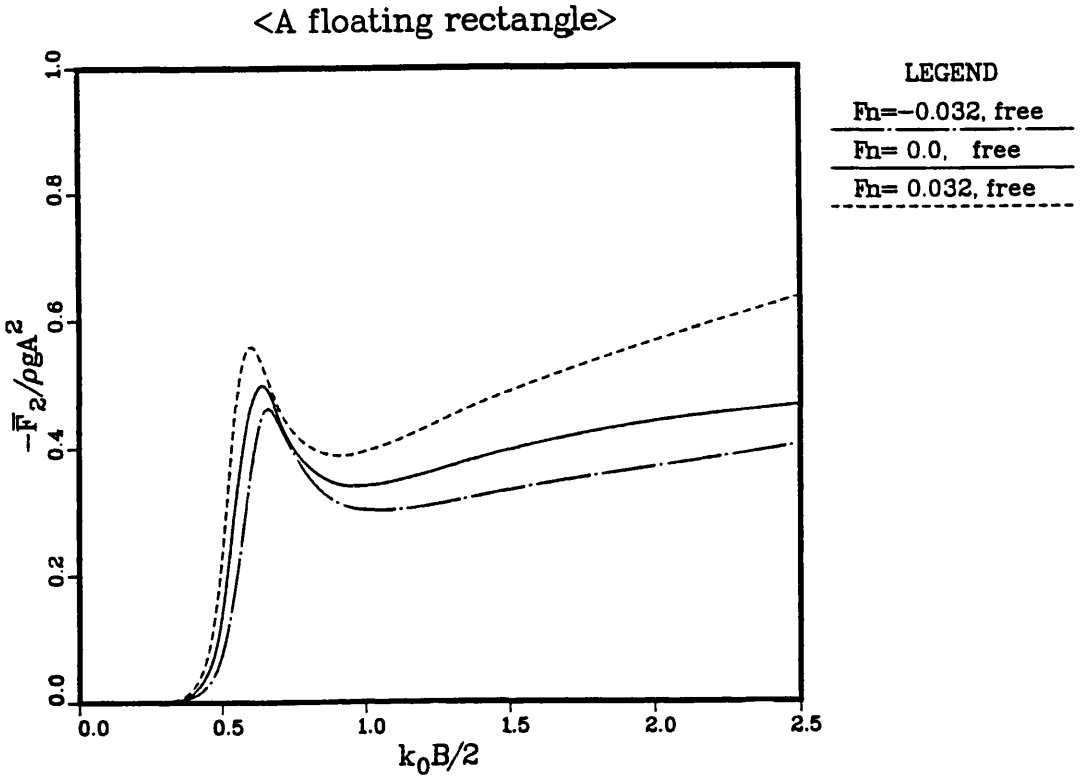

Figure 6.49 Horizontal mean drift force on a floating rectangular cylinder: free to respond in sway and heave

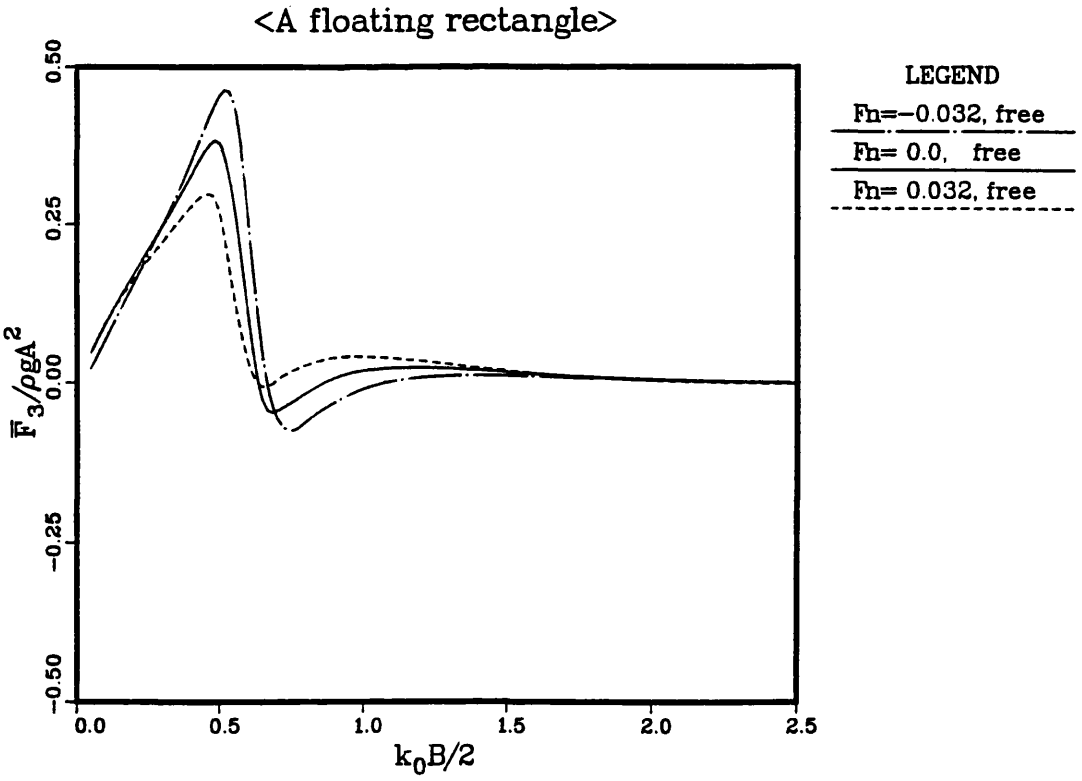

Figure 6.50 Vertical mean drift force on a floating rectangular cylinder: free to respond in sway and heave

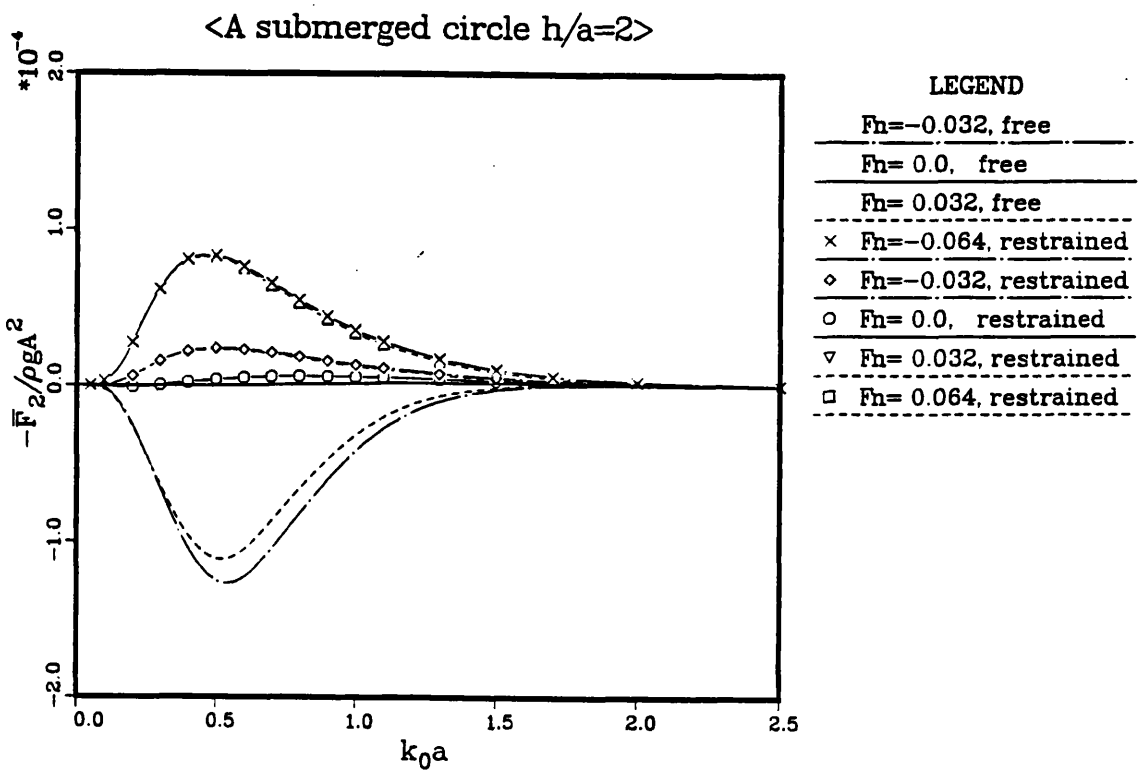

Figure 6.51 Horizontal mean drift force on a submerged circular cylinder: h/a=2.0

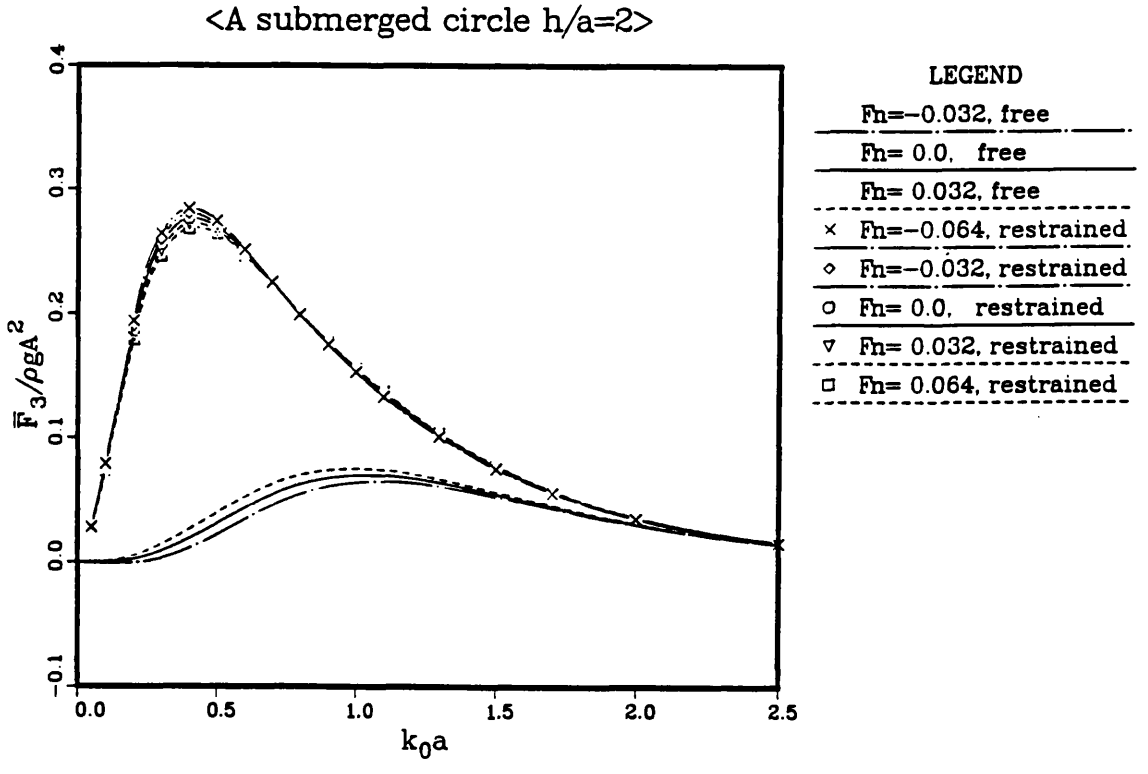

Figure 6.52 Vertical mean drift force on a submerged circular cylinder: h/a=2.0

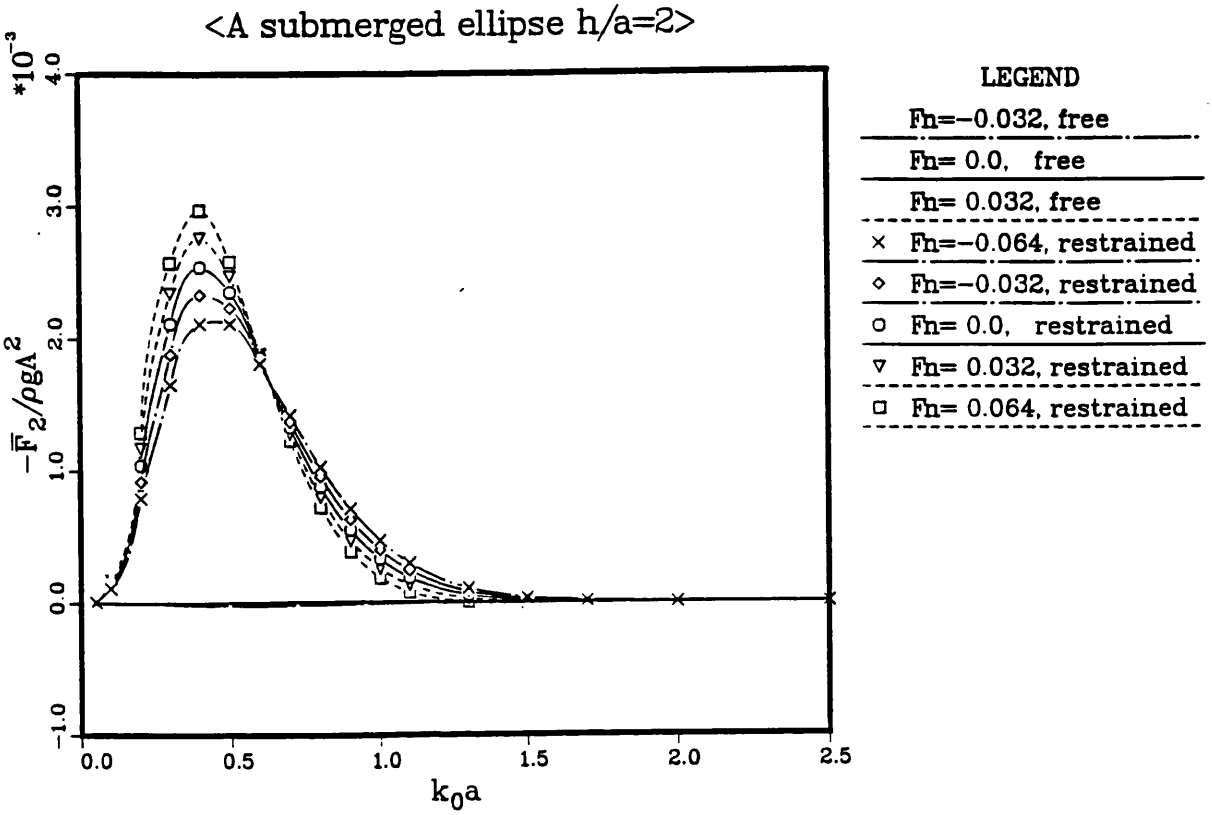

Figure 6.53 Horizontal mean drift force on a submerged elliptic cylinder: b/a=0.5, h/a=2.0

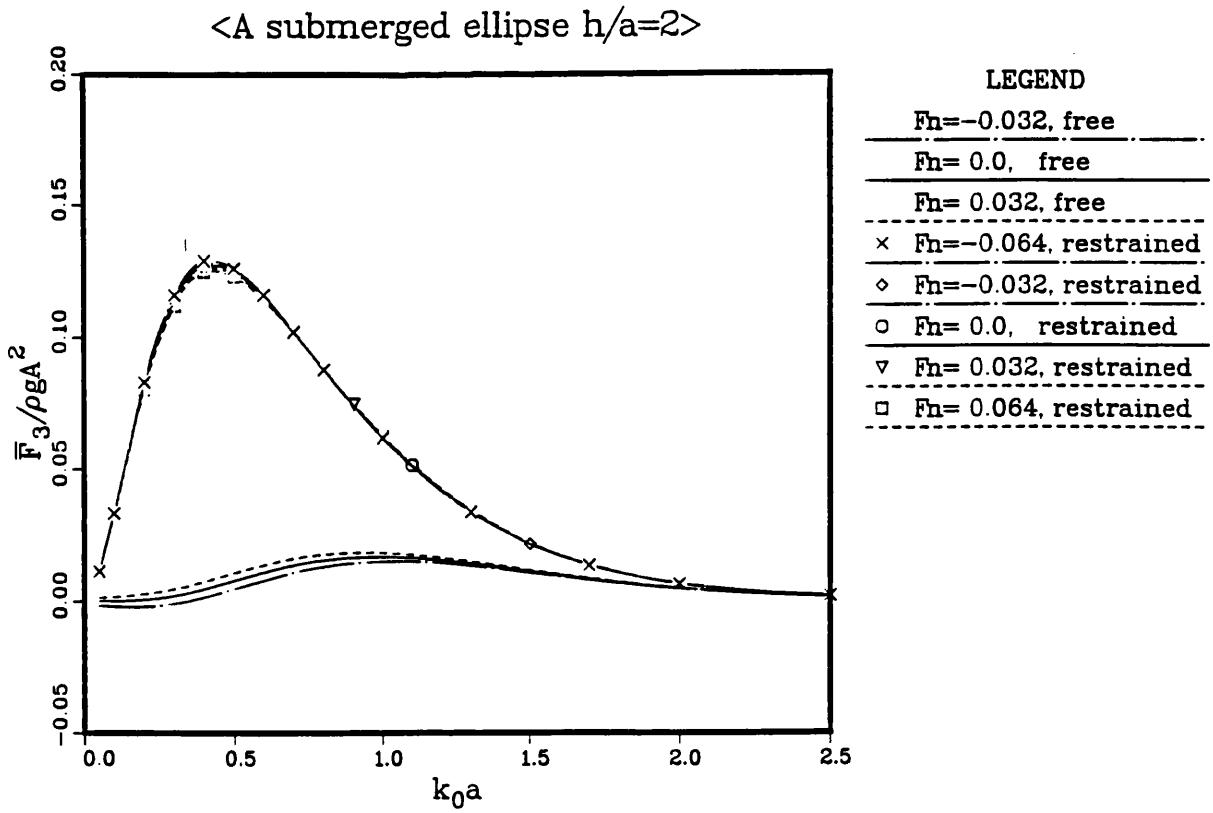

Figure 6.54 Vertical mean drift force on a submerged elliptic cylinder: b/a=0.5, h/a=2.0

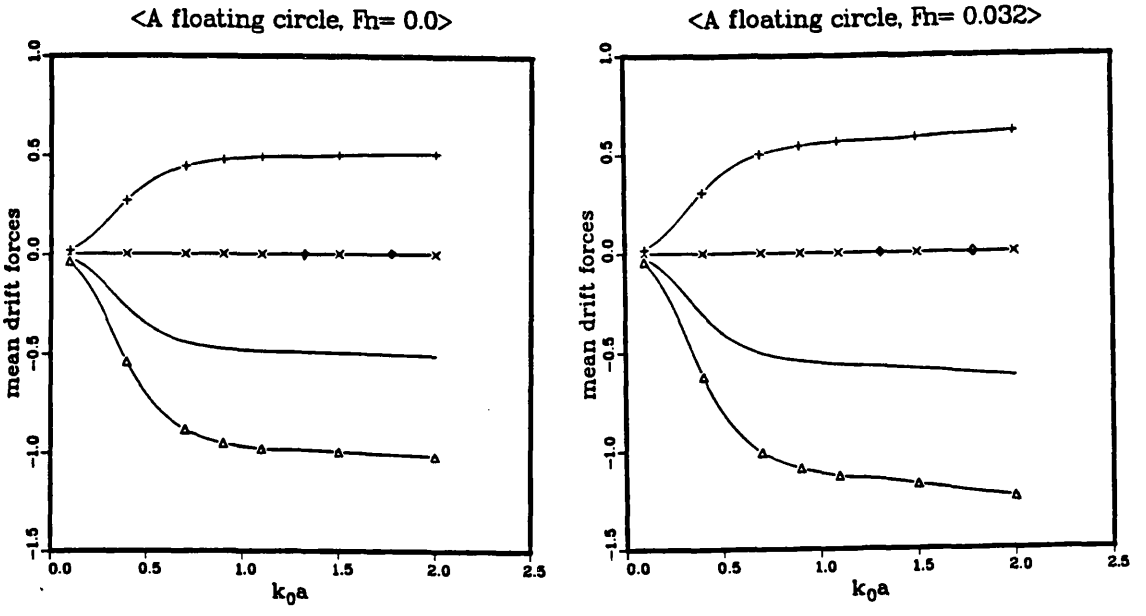

Figure 6.55 Components of the horizontal mean drift force on a floating circular cylinder: restrained

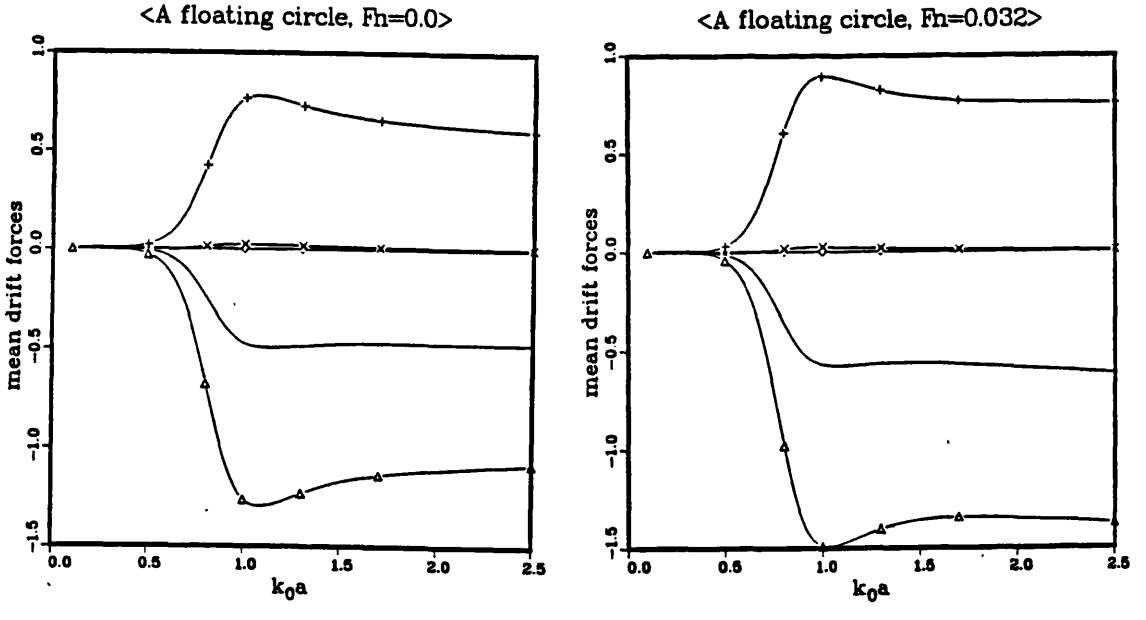

Figure 6.56 Components of the horizontal mean drift force on a floating circular cylinder: free to respond in sway and heave

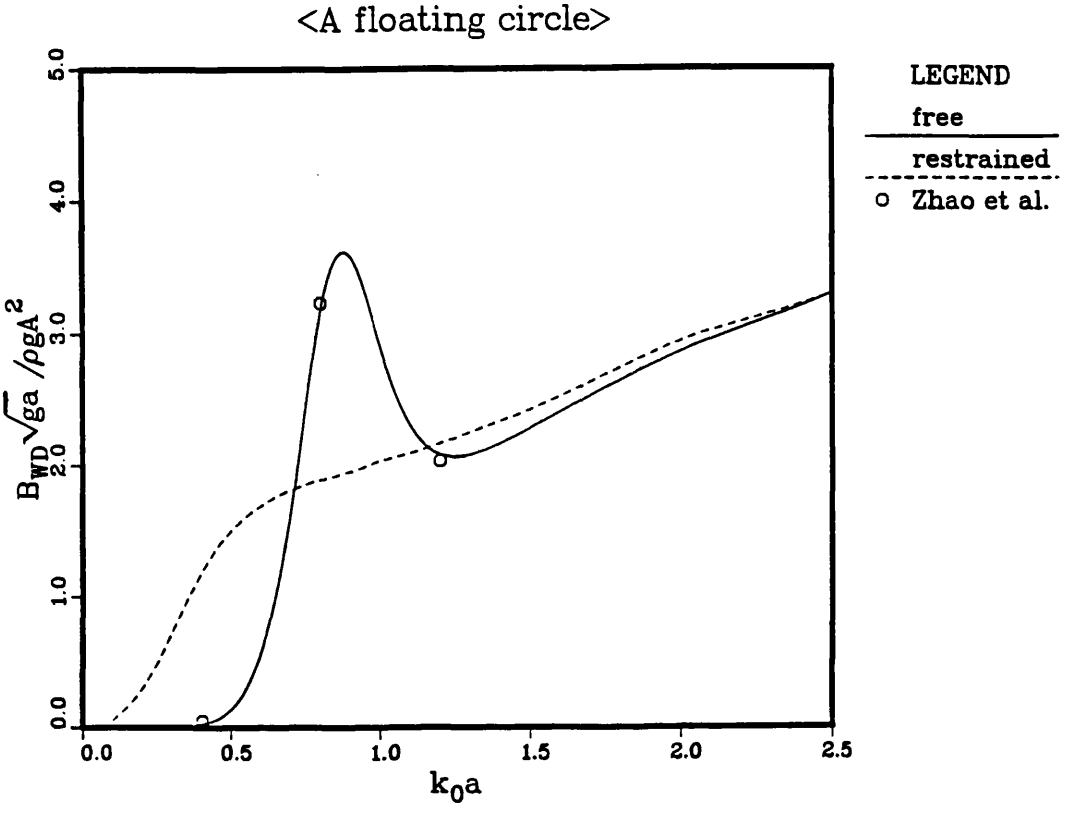

Figure 6.57 Wave drift damping for a floating circular cylinder

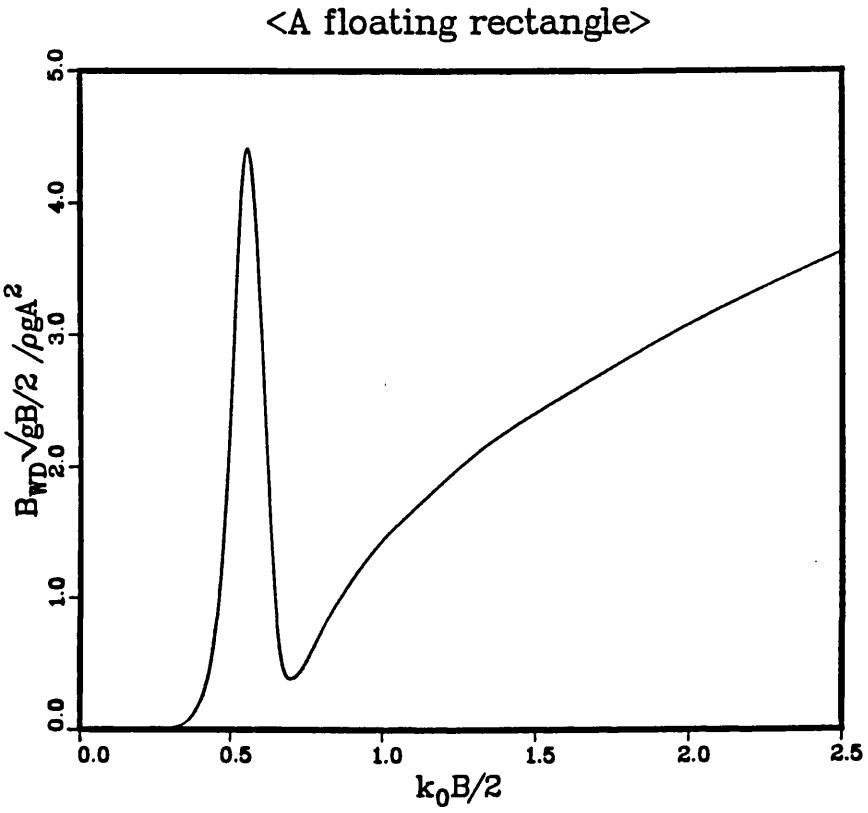

Figure 6.58 Wave drift damping for a floating rectangular cylinder